U.PORTO

DOUTORAMENTO
BIOLOGIA MOLECULAR E CELULAR

Extracellular polymeric substances (EPS) from the cyanobacterium *Synechocystis* sp. PCC 6803: from genes to polymer application as antitumor agent

Carlos Eduardo de Bento Flores

D 2019

U.PORTO

Carlos Eduardo de Bento Flores. Extracellular polymeric substances (EPS) from the cyanobacterium *Synechocystis* sp. PCC 6803: from genes to polymer application as antitumor agent

D.ICBAS **2019**

Unveiling Extracellular polymeric substances (EPS) from the cyanobacterium *Synechocystis* sp. PCC 6803: from genes to polymer application as antitumor agent

Carlos Eduardo de Bento Flores

SEDE ADMINISTRATIVA INSTITUTO DE CIÊNCIAS BIOMÉDICAS ABEL SALAZAR
FACULDADE DE CIÊNCIAS

CARLOS EDUARDO DE BENTO FLORES

Extracellular polymeric substances (EPS) from the cyanobacterium *Synechocystis* sp. PCC 6803: from genes to polymer application as antitumor agent

Tese de Candidatura ao grau de Doutor em Biologia Molecular e Celular;
Programa Doutoral da Universidade do Porto (Instituto de Ciências Biomédicas de Abel Salazar e Faculdade de Ciências)

Orientador:
Paula Tamagnini
Professora Associada
Faculdade de Ciências,
i3S - Instituto de Investigação e Inovação em Saúde,
IBMC - Instituto de Biologia Molecular e Celular,
Universidade do Porto, Portugal.

Co-orientador:
Roberto De Philippis
Associate Professor
DAGRI - Department of Agriculture, Food, Environment and Forestry,
University of Florence, Italy.

Co-orientador:
Paula Soares
Professora Auxiliar
Faculdade de Medicina,
i3S - Instituto de Investigação e Inovação em Saúde,
IPATIMUP – Instituto de Patologia e Imunologia Molecular da Universidade do Porto,
Universidade do Porto, Portugal.

Acknowledgments / Agradecimentos

Firstly, I would like to thank all the people that contributed directly or indirectly to this work, either in a scientific and technical context, or through important conversations/advices that made me improve as a person who wants to be scientist.

To my supervisor, Prof. Dr. Paula Tamagnini, I have to thank the opportunity to work in the Bioengineering & Synthetic Microbiology (BSM) group, and all the time, patience and money invested in me as well as the freedom to follow my own way in the framework of my PhD.

I would like to express my deepest gratitude to my both amazing co-supervisors, Prof. Dr. Roberto De Philippis and Prof. Dr. Paula Soares, that always believed in me an opened the doors of completely distinct scientific fields far away from my comfort zone, teaching me from the scratch and letting me go to explore not so conventional paths.

To Prof. Dr. Cláudio Sunkel and the scientific committee of the Doctoral Program in Molecular and Cell Biology, I thank you all the logistical support and advices.

To all collaborators and technical staff from the different institutions, that helped me to achieve my goals and overcome technical/logistical challenges, such as Frederico Silva, Fátima Fonseca, Hugo Osório, Rui Fernandes, Emília Cardoso, Paula Magalhães, Tânia Meireles, Paula Esteves, Catarina Carona, Isabel Menezes, Aureliana Sousa, Frederico Rossi, Phillip Wright and Narciso Couto. Joana Correia, Bárbara Amorim and Pedro Martins you are fantastic partners (with or without *picanha*!). Thank you all also for the kindness!

To Prof. Martin Hagemann (University of Rostock), for all the comments, help, and kindness, as well as for all the strains and social + “scientific” time spent in conferences.

To Prof. Pedro Moradas Ferreira that has always a nice word and wise comment to me.

A special thanks to all the post-docs that were my “lab Gurus”, and that I had the pleasure to become closer at the personal level, allowing not only the share of knowledge but also life experiences that put everything into perspective: Paulo Oliveira and Catarina Pacheco (“lab stepparents”), Sara Pereira (“lab EPS consultant”), Raquel Lima (“lab eukaryotic cell partner and mentor”) and Alessandra Adessi (cannoli time!!). You were AWESOME!!

To the other “EPS team” members, Marina Santos and Rita Mota, I have to thank the constant share of knowledge and experience. In particular, I thank Marina that become a crucial colleague and friend throughout this long journey, many thanks for the partnership.

To other members/former members from the BSM, Cancer Signalling & Metabolism, Yeast Signalling Networks groups (i3S) and the DAGRI (University of Florence) that were also very important for my PhD work with crucial pieces of great moments, fruitful discussions, fun and solidarity, namely Prof. Vítor Costa, Clara Pereira, Rita Vilaça, Inês (the Lisbon one), D. Helena, Marta Mendes, Pedro Albuquerque, Filipe Pinto, Sílvia Pires (show de bola!), Susana Duarte, João Rodrigues, Cátia Gonçalves, José Pedro (the music), Steeve Lima (the jokes); Roberta Rizzo, Zé Ferreira and Sónia Chamizo (the Italy).

To Eunice Ferreira, Ângela Brito and Rute Oliveira, that were wonderful and essential “lab shoulders”, as well as crazy enough to listen to me. Thank you for the motivation and spectacular good/bad mood!

To all my colleagues from the 1st year of the MCbiology, you were always supportive and wonderful buddies.

To my amazing friends “4Life” and “Malta do costume” that provided great funny moments and necessary distractions to maintain the bright side of the life. Thank you for all the support you gave me and friendship.

To the one that makes everything remarkable and has the superpower to understand me… Marina Silva. Thank you for everything in all the languages of the World, for every single piece of your friendship and much more. Thank you for the “Map that we have inside us”.

Finalmente, mas também especialmente, agradeço a toda a minha enorme (em quantidade e qualidade) família que esteve do meu lado, sempre! E cujos agradecimentos merecidos encheriam todas as páginas da minha tese. Embora não vos nomeie a todos, vocês sabem que têm sempre um lugar no meu coração. Um enorme beijo e abraço aos meus tios/padrinhos Tia Bela e Tio Miguel, bem como as minhas primas, obrigado por todos os momentos! Um UNIVERSO de obrigados aos meus pais, Carlos e Maria da Conceição, e às minhas manas Vânia e Catarina, que me deram as “armas” para enfrentar o mundo, todo o Amor necessário que faz a vida valer a pena, todo o apoio fundamental para a conclusão desta etapa e para ser quem sou hoje, não só como pessoa, mas também como cientista!

Financial support

This work was financed by FEDER - Fundo Europeu de Desenvolvimento Regional funds through the COMPETE 2020 - Operacional Programme for Competitiveness and Internationalisation (POCI), Portugal 2020, and by Portuguese funds through FCT - Fundação para a Ciência e a Tecnologia/Ministério da Ciência, Tecnologia e Ensino Superior in the framework of the PhD grant SFRH/BD/99715/2014, and the projects POCI-01-0145-FEDER-028779 (PTDC/BIA-MIC/28779/2017), POCI-01-0145-FEDER-031520 (PTDC/MEC-ONC/31520/2017) and POCI-01-0145-FEDER-029540 (PTDC/BIA-OUT/29540/2017). Further funding was obtained from the projects “Structured Programme on Bioengeneering Therapies for Infectious Diseases and Tissue Regeneration”, NORTE-01-0145-FEDER-000012 and “Advancing cancer research: from basic knowledge to application”, NORTE-01- 0145-FEDER-000029: “Projetos Estruturados de I & D”, supported by NORTE 2020 – Programa Operacional Regional do Norte under the Portugal 2020 Partnership Agreement.

Part of the work from Chapters III and V was awarded by funds of the Portuguese Society of Microbiology (SPM) and the Federation of European Microbiological Society (FEMS).

I hope you have dreams…
having an unplanned life in Science is not easy, but it's worthy!

Alexandre Quintanilha

Table of Contents

List of Publications

This dissertation is based on some unpublished results and the following publications:

FLORES, C., Lima, R. T., Adessi, A., Sousa, A., Pereira, S. B., Granja, P. L., De Philippis, R., Soares, P., & Tamagnini, P. (2019). Characterization and antitumor activity of the extracellular carbohydrate polymer from the cyanobacterium *Synechocystis* Δ*sigF* mutant. *International Journal of Biological Macromolecules*, 136: 1219-1227.

FLORES, C., & Tamagnini, P. (2019). Looking Outwards: Isolation of Cyanobacterial Released Carbohydrate Polymers and Proteins. *JoVE - Journal of visualized experiments*, 147: e59590.

FLORES, C., Santos, M., Pereira, S. B., Mota, R., Rossi, F., De Philippis, R., Couto, N., Karunakaran, E., Wright, P. C., Oliveira, P., & Tamagnini, P. (2019). The alternative sigma factor SigF is a key player in the control of secretion mechanisms in *Synechocystis* sp. PCC 6803. *Environmental Microbiology*, 21: 343–359.

Other publications:

Mota, R., Vidal, R., Pandeirada, C., **FLORES, C.**, Adessi, A., De Philippis, R., Nunes, C., Coimbra, M. A., & Tamagnini, P. (2019). Cyanoflan: a cyanobacterial sulfated carbohydrate polymer with emulsifying properties. *Carbohydrate Polymers* (*in press*), https://doi.org/10.1016/j.carbpol.2019.115525.

Pereira, S. B., Santos, M., Leite, J. P., **FLORES, C.**, Eisfeld, C., Büttel, Z., Mota, R., Rossi, F., De Philippis, Roberto., Gales, L., Morais-Cabral, J. H., & Tamagnini, P. (2019). The role of the tyrosine kinase Wzc (Sll0923) and the phosphatase Wzb (Slr0328) in the production of extracellular polymeric substances (EPS) by *Synechocystis* PCC 6803. *MicrobiologyOpen*, 8: e753.

List of Abbreviations

Ab	Antibody
ANOVA	Analysis of variance
ApcA	Allophycocyanin alpha chain
ATP	Adenosine triphosphate
ATPase	ATP synthase
BCA	Bicinchoninic acid assay
BLAST	Basic local alignment search tool
bp	Base pairs
C	Carbon
cAMP	Cyclic adenosine monophosphate
Car	Carotenoids
CAZyme	Carbohydrate-active enzyme
CcmK	Carbon dioxide-concentrating mechanism protein
c-di-GMP	Cyclic diguanylate monophosphate
cDNA	Complementary DNA
Chl *a*	Chlorophyll *a*
Ci	Inorganic carbon
Cl	Chlorine
CO_2	Carbon dioxide
Cpc	Phycocyanin subunit
CPD	Disodium 2-chloro-5-(4-methoxyspiro[1,2-dioxetane-3,2′-(5-chlorotricyclo[3.3.1.13.7]decan])-4-yl]-1-phenyl phosphate
CPS	Capsular polysaccharides
CX	Carotenoid index
DIG	Digoxigenin
DNA	Deoxyribonucleic acid
DW	Dry weight
ECF	Sigma factor of extracytoplasmic function
EDTA	Ethylenediaminetetraacetic acid
EPS	Extracellular polymeric substances
FACS	Fluorescence-activated cell sorting
FBS	Fetal bovine serum
FTIR	Fourier-transform infrared spectroscopy

GH	Glycoside hydrolase
GO	Gene ontology
GT	Glycosyltransferase
H_2DCF-DA	2',7'-dichlorodihydrofluorescein diacetate
H_2O_2	Hydrogen peroxide
HCl	Hydrogen chloride
HlyA	Hemolysin A
HPLC	High-performance liquid chromatography
IM	Inner membrane
iTRAQ	Isobaric tags for relative and absolute quantitation
KDO	Keto-deoxyoctulosonate
KEGG	Kyoto encyclopedia of genes and genomes
KOH	Potassium hydroxide
LPS	Lipopolysaccharides
m/z	Mass-to-charge ratio
Mg	Magnesium
MTT	Thiazolyl blue tetrazolium bromide
MW	Molecular weight
N	Nitrogen
Na	Sodium
NADH	Nicotinamide adenine dinucleotide (reduced form)
NCBI	National center for biotechnology information, US
ncRNA	Non-coding RNA
OD	Optical density
OM	Outer membrane
OMVs	Outer membrane vesicles
PAGE	Polyacrylamide gel electrophoresis
PBS	Phosphate-buffered saline
PC	Phycocyanin index
PCC	Pasteur culture collection
PCC-M	Pasteur culture collection Moscow substrain
PCR	Polymerase chain reaction
PG	Peptidoglycan
PHB	Polyhydroxybutyrate

PI	Propidium iodide
PilA	Pilin protein
PMF	Peptide mass fingerprinting
PPI	Protein-protein interaction
PrC	Carboxyl-terminal protease
PrK	Phosphoribulokinase
r.p.m.	Revolutions per minute
RbcL	Ribulose bisphosphate carboxylase large chain
RBS	Ribosome binding site
RNA	Ribonucleic acid
RND	Resistance-nodulation-cell division
ROS	Reactive oxygen species
RPS	Released polysaccharides
RT-PCR	Reverse transcription polymerase chain reaction
RuBisCO	Ribulose-1,5-bisphosphate carboxylase/oxygenase
S	Sulfur
SbpA	Sulfate-binding protein
SDS	Sodium dodecyl sulfate
SEC	Size-exclusion chromatography
SecA	Protein translocase subunit
SEM	Scanning electron microscopy
SigF, G, H, I, J	Alternative sigma factor F, G, H, I, J
SOD	Superoxide dismutase
sRNA	Small RNA
T1SS	Type 1 secretion system
TCA	Tricarboxylic acid
TEM	Transmission electron microscopy
TFA	Trifluoroacetic acid
TFBS	Transcription factor binding site
TSS	Transcription starting site
TU	Transcriptional unit
UV	Ultraviolet
wt	Wild-type
Zn	Zinc

Abstract

Cyanobacteria are a very particular group of photoautotrophic organisms with major ecological significance in the carbon and nitrogen cycles. Furthermore, their long evolutionary road allowed the development of a wide range of cell survival strategies and a high metabolic plasticity, which are also important assets for biotechnological applications, e.g. regarding the cost-effective production of industrially relevant biomolecules, such as biopolymers. However, compared to other biopolymers, the research on the production of cyanobacterial extracellular polymeric substances (EPS) is still at an early stage. Cyanobacterial EPS are mainly composed of heteropolysaccharides that can remain attached to cell surface or be released into the extracellular environment, as released polysaccharides (RPS). They frequently have distinct features compared to other bacterial EPS, which make them suitable for application in several fields, namely in biomedicine. However, very little is known about the antitumor activity of cyanobacterial EPS and the polymer properties involved. This lack of information, together with the limited knowledge about the mechanisms underlying EPS production in cyanobacteria, hinders the implementation of industrial systems based on these organisms and the application of cyanobacterial polymers as antitumor agents.

In this study, a comprehensive approach was followed, from the study of genes/proteins involved in EPS production of the model cyanobacterium *Synechocystis* sp. PCC 6803, to the characterization of the produced polymers, evaluation of their antitumor activity and manipulation of their features. Initially, key players putatively involved in EPS production as well as in its regulation were identified *in silico*, revealing promising targets for further studies. A Group 3 alternative sigma factor (SigF) was shown to be involved in the control of EPS production/export and several secretion mechanisms (transporter-mediated and vesiculation). A *Synechocystis* knockout mutant on this factor (Δ*sigF*) displayed up to 4-fold higher production of RPS compared to the wild-type, accompanied by a 2-fold increase in the total carbohydrate content. After optimization of the isolation method of the produced polymer, it was possible to obtain a yield of 80 mg of polymer per g of culture dry weight (also 4-fold higher than for the wild-type). Both polymers, from *Synechocystis* wild-type and Δ*sigF*, displayed typical features of cyanobacterial EPS, such as the high number of different monosaccharides (with predominance of glucose), the presence of uronic acids, unusual EPS sugars (two amino-sugars), high sulfate content (≈12% w/w), peptides and high molecular weight polysaccharide fractions, an amorphous nature and a non-Newtonian fluid behavior. These polymers have also low viscosity even in highly concentrated aqueous solutions. However, some differences were also observed between them, namely the Δ*sigF* polymer has a higher protein content.

Moreover, although both polymers strongly reduced the viability of different tumor cell lines in a time- and concentration-dependent manner, this effect was more evident in cells treated with the Δ*sigF* polymer. The study of possible molecular mechanisms underlying the antitumor mode of action revealed that the Δ*sigF* polymer induces high rates of apoptosis (up to 40%), through the stimulation of the mitochondrial-mediated apoptotic pathway via p53 and activation of caspase-3. Furthermore, preliminary results suggested that the sulfate content and particularly the high molecular weight polysaccharide fractions are important for the Δ*sigF* polymer potent antitumor activity.

Overall, *Synechocystis* emerged as a promising platform to study and manipulate EPS production, and the produced polymers are valuable natural products that can be easily tailored for biomedical application, namely as antitumor agents.

Keywords: cyanobacteria, *Synechocystis*, extracellular polymeric substances (EPS), released polysaccharides (RPS), sigma factor, secretion, antitumor activity, apoptosis.

Resumo

As cianobactérias são um grupo muito particular de organismos fotoautotróficos com elevada importância ecológica nos ciclos do carbon e azoto. Além disso, o seu longo percurso evolutivo permitiu o desenvolvimento de uma ampla gama de estratégias de sobrevivência e uma alta plasticidade metabólica, que constituem aspectos importantes para aplicações biotecnológicas, como por exemplo, considerando a produção rentável de biomoléculas industrialmente relevantes, como os biopolímeros. No entanto, em comparação com outros biopolímeros, a investigação acerca da produção de substâncias poliméricas extracelulares (EPS) cianobacterianas ainda está numa fase inicial. As EPS cianobacterianas são compostas principalmente de heteropolissacarídeos que podem permanecer ligados à superfície celular, ou serem libertados para o ambiente extracelular, como polissacarídeos libertados (RPS). Elas geralmente têm características distintas em comparação com outras EPS bacterianas, que as tornam adequadas para aplicação em vários campos, nomeadamente na biomedicina. Contudo, muito pouco se sabe acerca da atividade antitumoral de EPS cianobacterianas e das propriedades do polímero que estão envolvidas. Esta falta de informação, juntamente com o conhecimento limitado sobre os mechanismos subjacentes à produção de EPS em cianobactérias, dificulta a implementação de sistemas industriais baseados nestes organismos, bem como a aplicação de polímeros cianobacterianos como agentes antitumorais.

Neste trabalho, seguiu-se uma abordagem abrangente, desde o estudo de genes/proteínas envolvidos na produção de EPS da cianobactéria modelo *Synechocystis* sp. PCC 6803, até à caracterização dos polímeros produzidos, avaliação da sua atividade antitumoral e manipulação das suas características. Inicialmente, intervenientes-chave que podem estar envolvidos na produção de EPS, bem como na sua regulação, foram identificados *in silico*, o que revelou alvos promissores para estudos futuros. Foi demonstrado que um fator sigma alternativo do Grupo 3 (SigF) está envolvido no controlo da produção/exportação de EPS e de vários mecanismos de secreção (mediados por transportadores e vesiculação). Um mutante *knockout* de *Synechocystis* neste fator (Δ*sigF*) teve uma produção até 4 vezes superior de RPS em comparação com a estirpe selvagem, acompanhada por um aumento de 2 vezes no teor total de hidratos de carbono. Após otimização do método de isolamento do polímero produzido, foi possível obter um rendimento de 80 mg de polímero por g de peso seco de cultura (também 4 vezes superior ao obtido para a estirpe selvagem). Ambos os polímeros, da estirpe selvagem e do Δ*sigF*, apresentaram características típicas de EPS cianobacterianas, tais como o elevado número de diferentes monossacarídeos (com

predominância de glucose), a presença de ácidos urónicos, açúcares raros de EPS (dois amino açúcares), alto teor de sulfato (≈12% p/p), péptidos e frações polissacarídicas de alto peso molecular, uma natureza amorfa e um comportamento de fluido não newtoniano. Estes polímeros têm também reduzida viscosidade mesmo em soluções aquosas altamente concentradas. Contudo, foram observadas também algumas diferenças entre eles, nomeadamente, o polímero de Δ*sigF* possui um maior teor peptídico. Para além disso, embora ambos os polímeros reduzam extremamente a viabilidade de diferentes linhas de células tumorais num modo dependente do tempo e da concentração, este efeito foi mais evidente nas células tratadas com o polímero de Δ*sigF*. O estudo de possíveis mecanismos moleculares subjacentes ao modo de ação antitumoral revelou que o polímero de Δ*sigF* induz elevadas taxas de apoptose (até 40%), através da estimulação da via apoptótica mitocondrial, via p53 e ativação da caspase-3. Além disso, resultados preliminares indicaram que o conteúdo em sulfato e particularmente as frações polissacarídicas de alto peso molecular são importantes para a atividade antitumoral do polímero de Δ*sigF*.

No geral, *Synechocystis* surgiu como uma plataforma promissora para estudar e manipular a produção de EPS, e os polímeros produzidos são produtos naturais valiosos que podem ser facilmente modificados para aplicação biomédica, nomeadamente como agentes antitumorais.

Palavras-chave: cianobactérias, *Synechocystis*, substâncias poliméricas extracelulares (EPS), polissacarídeos libertados (RPS), fator sigma, secreção, atividade antitumoral, apoptose.

CHAPTER I

General Introduction

General Introduction

1. Cyanobacteria

1.1. Evolutionary and ecological significance

The origin of cyanobacteria dates back to the Pre-Cambrian, during the Proterozoic, and the beginning of Phanerozoic Eon, with the emergence of the first marine cyanobacterial ancestors (Sánchez-Baracaldo, 2015). These bacteria have transformed the geochemistry of our planet 2.5 billion years ago, with the widespread oxygenation of the oceans (Soo et al., 2017). They are believed to be the first group of photoautotrophs able to produce molecular oxygen through water oxidation, triggering the transition from the primitive anaerobic state of Earth's atmosphere to its aerobic condition (Schopf, 2000). In addition, the study of ancient cyanobacterial strains supported that aerobic respiration evolved after oxygenic photosynthesis through independent acquisition of aerobic respiratory complexes by these organisms (Soo et al., 2017). Later on, cyanobacteria have been involved in the origin of the first plastids around 1.5 billion years ago (Ochoa de Alda et al., 2014; Dyall et al., 2004). Phylogenetic, structural and biochemical analyses supports that this occurred via endosymbiosis of a cyanobacterium by the ancestors of Archaeplastida (eukaryotic organisms), which led to the birth of primitive eukaryotic photoautotrophs (Archibald, 2009; Dyall et al., 2004). Although still under debate, the most recent studies strongly support that this endosymbiotic event involved early-branching cyanobacterial lineages and took place in terrestrial-freshwater settings instead of oceans (Ponce-Toledo et al., 2017). These plastids further evolved into semiautonomous organelles (well-known as chloroplasts), representing a critical step in the evolution and diversification of algae and higher plants (Maréchal, 2018; Dyall et al., 2004). Moreover, cyanobacteria were not only essential for the establishment of the current nitrogen and carbon cycles, due to their metabolic capabilities and particular enzymes, but they also represent crucial players in these cycles as primary producers in the modern days (Raven et al., 2012; Canfield et al., 2010; Savage et al., 2010; Galloway et al. 2004).

1.2. Environmental adaptation and phenotypic diversity

As a result of a long evolutionary process, very distinct cyanobacterial strains can be found nowadays, regarding their morphology and genetic background (Fig. 1). Cyanobacteria is now broadly considered a monophyletic group, that can be subdivided into five main subsections with a wide range of lineages, although a recent classification system proposed its division in 8 major subsections (Komárek et al., 2014). This group of organisms includes unicellular, colonial, and filamentous forms (Tomitani et al., 2006; Castenholz et al., 2001; Rippka et al., 1979). Some strains may even display a higher degree of

morphological complexity, being capable of cell differentiation (Castenholz et al., 2001). Some filamentous strains may display heterocysts (cells specialized in nitrogen fixation), akinetes (resting cells for survival under stress conditions), or motile hormogonia (small filaments, essential for short-distance dispersal and host infection). Regarding the unicellular ones, small and easily dispersible cells called baeocytes may be formed by some strains when cell division occurs by multiple fission (Castenholz et al., 2001).

The long cyanobacteria's evolutionary road and their high metabolic plasticity allowed also the development of different tools and strategies for survival. Currently, cyanobacteria are considered a ubiquitous bacterial group, with wide geographical distribution and presence in a broad spectrum of environmental conditions. Their simple nutritional requirements, namely the ability to live autotrophycally and/or diazotrophycally, allowed a successful colonization of diverse habitats, from fresh and salt water to soil and extreme environments, such as hot springs, polar regions and hypersaline areas (Whitton, 2012). Additionally, these bacteria managed to adapt their living-styles according to the metabolic necessities, being able to live as planktonic free-living cells, in biofilms, aggregates and complex mats, or even in symbiosis with a wide range of eukaryotic hosts (providing them combined nitrogen and/or carbon).

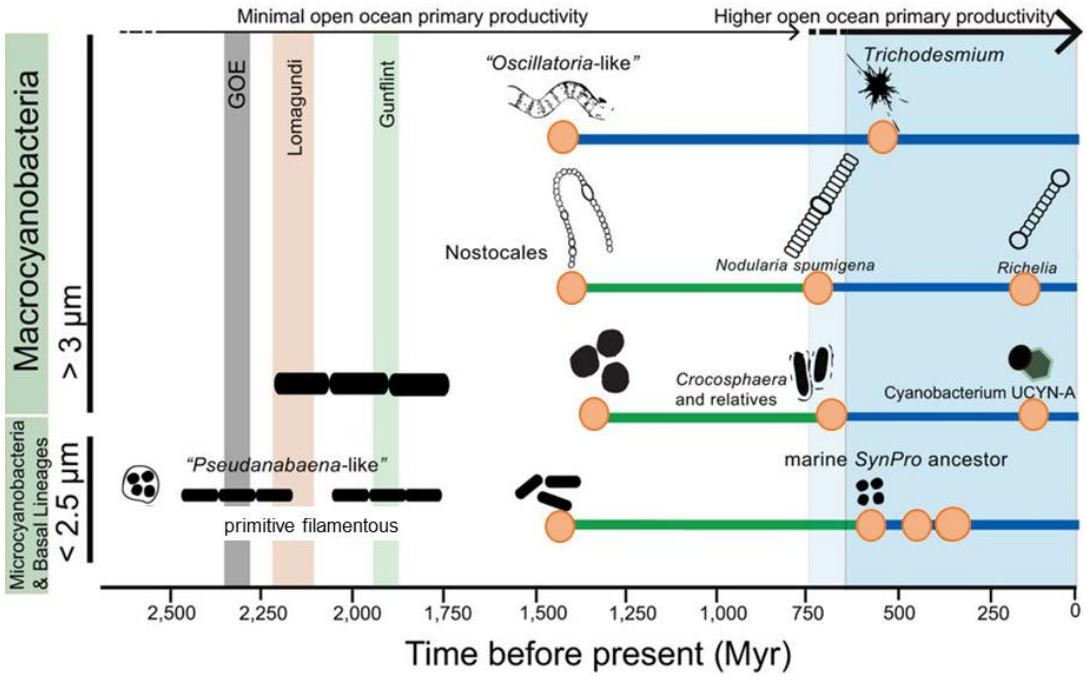

Figure 1. Cyanobacterial evolutionary course (*adapted from* Sánchez-Baracaldo, *2015*). The morphological diversity is depicted in the different cyanobacterial lineages. Orange nodes represent the major cell differentiation events occurred in freshwater (green lines) or marine (blue lines) lineages, based on Bayesian inference of character evolution. Taxa with smaller cell diameter are shown at the bottom and with larger cell diameter at the top. GOE, "Great Oxygenation Event"; Lomagundi, *Lomagundi–Jatuli* carbon isotope excursion; Gunflint, Gunflint iron formation; Myr, million years.

1.3. Cyanobacteria as prolific sources of biotechnological relevant biomolecules

The high metabolic plasticity of cyanobacteria, that is on the basis of their successful colonization and adaptation to challenging environments, allows also the production of a vast array of biomacromolecules and other metabolites by these bacteria. The nature and composition of these products may vary dramatically depending on the cyanobacterial strain, ranging from simple lipids, proteins and polysaccharides to complex polymers, pigments, compatible solutes or toxins (Brito et al., 2015; Dittmann et al., 2015; Kehr & Dittmann, 2015). Several of them can even be actively secreted (e.g. scytonemin, microcystin, biopolymers), while others are accumulated inside the cells (e.g. PHB, glycogen, phycocyanin) (Fig. 2).

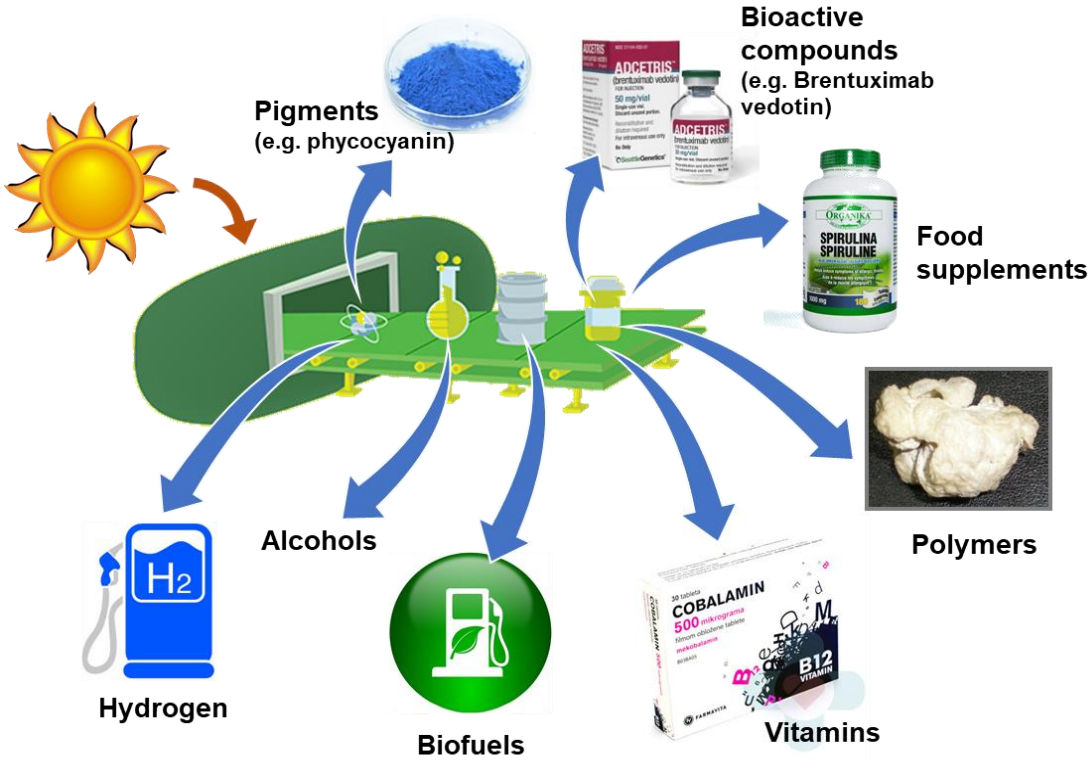

Figure 2. Schematic representation of cyanobacteria as microbial cell factories for the production of commodity products (background image: Cyanobacteria Bio-Factory, Washington University in St. Louis, https://www.eurekalert.org/pub_releases/2015-02/wuis-cfi020115.php).

Importantly, the vast majority of these biomacromolecules can be (or are envisaged to be) applied as cosmetics, bioplastics, emulsifiers, drugs, food supplements, additives, etc., due to their particular properties in terms of structure, composition and/or biological activity (Markl et al., 2018; Dittmann et al., 2015; Liu et al., 2012; Kanekiyo et al., 2005). Therefore, cyanobacteria have been emerged as powerful platforms for the development of green catalysts, utilizing renewable feedstock (CO_2) and sunlight (energy source) to produce added-value products (Knoot et al., 2018; Branco dos Santos et al., 2016). The

cyanobacterial simple nutritional requirements associated to their higher growth rates, compared to other photosynthetic organisms, make their industrial use simple and cost-effective. Moreover, in the recent years, a big effort has been made in order to maximize and customize the production of added-value compounds by cyanobacteria (e.g. biofuels and commodity chemicals), using genetic/metabolic engineering (Carroll et al., 2018; Hagemann & Hess, 2018; Knoot et al., 2018; Luan & Lu, 2018). In this framework, some cyanobacterial strains emerge as promising microbial cell factories, since they can be easily genetically manipulated and there is an increasing amount of synthetic biology tools available for their manipulation, such as for *Synechococcus* sp. PCC 7002, *Anabaena* sp. PCC 7120, and particularly *Synechocystis* sp. PCC 6803 (Carroll et al., 2018; Ferreira et al., 2018; Hagemann & Hess, 2018; Luan & Lu, 2018; Liu & Pakrasi, 2018; Yu et al., 2013; Wang et al., 2012a).

2. Extracellular polymeric substances (EPS)

2.1. Main features and physiological roles

Extracellular polymeric substances (EPS) are one of the oldest studied biomacromolecules and are produced by species from all the three life domains. The discovery of bacterial EPS might have occurred when Pasteur (around 1861) identified a viscous microbial product (dextran) during wine fermentation experiments (Pasteur, 1861). However, the first reference in the literature of the so-called EPS was most likely in 1870, when Thomas Henry Huxley reported the discovery of an albuminous slime, forming a “continuous mat of living protoplasm” (although this is still controversial, Flemming, 2016). He named it as *Bathybius Haeckelii*, since he believed that it was the “primordial slime”, postulated by Ernst Haeckel in 1868 as being the origin of life. Further studies proved that this material resulted from the chemical precipitation of components present in the Atlantic seafloor mud sample that Huxley was studying, due to its long preservation in alcohol.

In the following years, bacterial EPS were studied increasingly, and nowadays their study gained even more attention, not only due to their roles for crucial bacterial physiological processes, but also due to their biotechnological potential. They are mainly composed by polysaccharides, but frequently enclose nucleic acids, proteins, lipids, glycoconjugates, non-carbohydrate constituents (phosphate, lactate, acetate, pyruvate, succinate and glycerol) and/or other minor components, e.g. pigments (Gunn et al., 2016; Flemming & Wingender, 2010). Their production is a widespread feature among the different bacterial groups, from the common Gram-negative and Gram-positive bacteria to more complex and particular groups, such as mycobacteria or cyanobacteria. Fundamentally, this represents an important process for the maintenance of bacterial cell homeostasis, either as a sink of carbon/energy and other molecules, or as a response to

environmental stimuli, being also an adaptative advantage (Flemming, 2016). Therefore, bacterial EPS can play a wide range of physiological roles depending on the producer strain and its habitat, such as in cell-cell communication (either as vehicles of compounds or as quorum sensing molecules), in motility (either through cell sequestration or as gliding facilitators), in biofilm matrix (as scaffold), in cell protection (from UV radiation, heavy metals, etc.), in infection, in nutrient/water entrapment, and many others (extensively reviewed in Flemming, 2016; Donot et al., 2012; Flemming & Wingender, 2010). However, in some cases, the production of EPS may also bring some drawbacks to the producer, namely higher grazing susceptibility (Liu & Buskey, 2000) and growth impairment, due to redirection of nutrients and energy for EPS production. Furthermore, in an industrial context, it may lead to some problems of cultivation and cell harvesting, due to cell adhesion to the bioreactors, or the impairment of culture mixing/aeration (Freitas et al., 2011).

2.2. Biosynthesis

The intricate machinery underlying bacterial EPS biosynthesis have been extensively studied in the last two decades, mainly in pathogenic Gram-negative and lactic acid Gram-positive bacteria (Low & Howell, 2018; Kawaharada et al., 2015; Schmid et al., 2015; Whitfield et al., 2015; Rehm, 2010; Pereira et al., 2009). In general, bacteria may display either intra or extracellular EPS biosynthetic pathways (Schmid, 2018).

Studies in both Gram-negative and Gram-positive bacteria indicate that the intracellular EPS biosynthetic pathways rely on 4 major steps (Rossi & Philippis, 2016; Freitas et al., 2011; Rehm, 2010): i) in cytoplasm, primary metabolites, mainly from glycolysis, are used for the synthesis of energy-rich monosaccharides (or activated monosaccharides), derived from phosphorylated sugars; ii) at the plasma membrane, glycosyltransferases assemble these sugars as repeating units onto a carrier (generally lipidic), which will define the composition of the polysaccharide backbone; iii) proteins in the plasma membrane, periplasmic space and outer layers continue the assembly and/or polymerization of the repeating units (controlling both EPS composition and chain length); iv) the polymer is exported to the cell surface/extracellular space. This is a challenging process for the bacterium, since these large and usual hydrophilic molecules have to cross the cell envelope without compromising the critical barrier properties. The group of enzymes working in steps i) and ii) is the most diverse and highly heterogeneous, varying significantly between strains. Furthermore, the majority of these proteins are not exclusively dedicated to EPS production, being important players in the general (carbohydrate) metabolism. In contrast, and in spite of the diversity of EPS producers and of the produced polymers, the proteins involved in steps iii) and iv) are relatively well-conserved among bacteria. In fact, the mechanisms of assembly and export of bacterial EPS (designated also as the final steps

of EPS production) can be resumed to 3 main types (recently reviewed in Schmid, 2018, 2015; Whitney & Howell, 2013): Wzy-, ABC transporter- and Synthase-dependent pathways (Fig. 3). The genes encoding proteins involved in these pathways are usually in large gene clusters in both Gram-positive and Gram-negative bacteria, nearby genes encoding sugar activation/modification enzymes and glycosyltransferases (Rehm, 2010; Schmid et al., 2015).

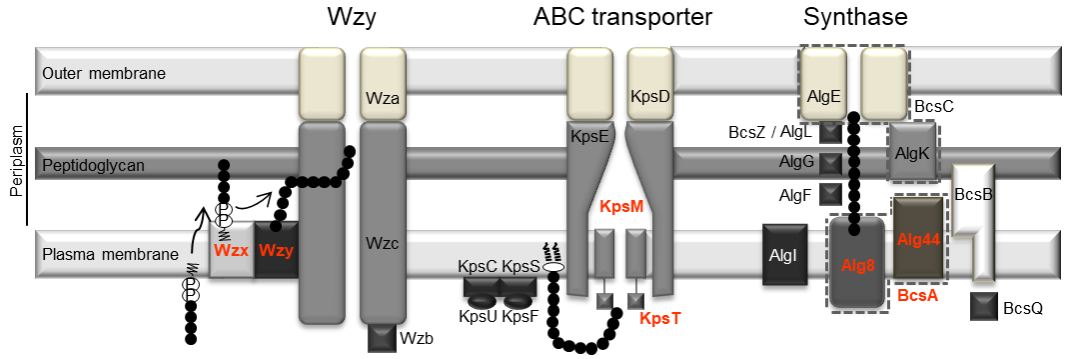

Figure 3. Representation of the three main bacterial EPS assembly and export mechanisms (*adapted from* Pereira et al., 2015). Hallmark proteins from each pathway are indicated in orange and bold.

In the Wzy-dependent pathway, oligosaccharide repeating units (linked to the lipid carrier) are flipped across the plasma membrane by Wzx (Islam & Lam, 2013). Then, Wzy continues the polymerization task at the periplasmic face of the membrane. Both enzymes cooperate in order to control the polymer chain length (Whitfield & Larue, 2008). Subsequently, the translocation process of the polymer through the cell envelope is performed by the complex Wza/Wzc, which forms a transmembrane channel (Cuthbertson et al., 2010; Collins et al., 2007). Wzc also works as copolymerization unit in collaboration with Wzy, being implicated in the chain length control, and its activity is regulated by phosphorylation/dephosphorylation cycles, usually controlled by a Wzb phosphatase (Paiment et al., 2002).

In the case of the ABC transporter-dependent pathway, the polysaccharide is fully polymerized at the cytoplasmic face of the plasma membrane. The KpsC/KpsS, KpsF and KpsU are usually involved in the synthesis of the 3-deoxy-D-manno-oct-2-ulosonic acid (KDO) linker or its activated donor, that connect the polysaccharide to a terminal lipid in the membrane (Willis & Whitfield, 2013). After that, the polymer is translocated across the plasma membrane by an ABC transporter complex formed by the KpsM and KpsT subunits (Cuthbertson et al., 2010). Finally, the export of the polymer is accomplished by the activity of the transmembrane complex KpsE/KpsD. KpsE and KpsD may form an analogous transenvelope system to Wzc and Wza, belonging to the same protein families, the

polysaccharide copolymerase (PCP) and the outer membrane polysaccharide export protein (OPX), respectively (Cuthbertson et al., 2009).

Regarding the molecular machinery involved in Synthase-dependent pathways, it may differ significantly depending on the polymer produced (Low & Howell, 2018). In general, a polysaccharide synthase embedded in the plasma membrane (e.g. Alg8 or BcsA) is responsible for the simultaneous polymerization and export of the polysaccharide, which may be facilitated by a membrane-embedded glycosyltransferase. This process occurs in the presence or absence of a lipid acceptor molecule and it is controlled by the secondary messenger c-di-GMP. Meanwhile, other proteins in the periplasm may modify the polymer (e.g. AlgI, AlgF, AlgG) or even degrade polymer surplus (e.g. AlgL or BscZ) (Whitfield et al., 2015). The polymer is then guided and protected from degradation by a periplasmic tetratricopeptide repeat (TPR)-containing scaffold lipoprotein through a β-barrel porin, which will export it. This step can be performed by two independent proteins (e.g. AlgK and AlgE) or a single protein that combines both functions (e.g. BcsC).

Players from the different biosynthetic pathways, namely Wzx, Wzy, Wzc/KpsE, KpsM and KpsT, might be involved in the production of very specific polysaccharides, such as the O-antigen of lipopolysaccharides (LPS) or S-layer glycans (Whitfield & Trent, 2014; Ristl et al., 2011).

There is still another group of very peculiar bacterial EPS biosynthetic mechanisms, that is dependent on extracellular sucrases. Their encoding genes are expressed constitutively in some strains, and these enzymes are secreted and anchored to the bacterial cell wall (Schwab et al., 2007). Furthermore, they belong to the class of transglucosidases (glycosyl hydrolase family), using sucrose to transfer glucose, fructose or maltose onto a growing chain oligosaccharide (Lombard et al., 2014; Díez-Municio et al., 2013; Vujicic-Zagar et al., 2010). In this pathway, the polysaccharide chain initiation and elongation processes are still debatable, but regardless the scenario, EPS biosynthesis occurs entirely outside the cell. The polymers produced are frequently branched to different degrees, since they have possible branching points at all hydroxyl groups. In general, these extracellular EPS biosynthetic pathways are particularly well-described for the production of some commercially exploited bacterial EPS, such as dextran, levan and their derivatives, through the action of glucansucrases or levansucrases, respectively (Tian et al., 2014; Robyt et al., 2008).

2.3. EPS production by cyanobacteria

Many cyanobacteria are able to produce EPS, mainly formed by heteropolysaccharides (Fig. 4). These polymers may remain attached to the cell surface and depending on their thickness, consistency and degree of cell association are frequently

named as capsules (thick and slimy layer intimately associated with the cell surface), sheaths (thin and dense layer loosely surrounding cells) or slimes (mucilaginous material dispersed around the cells); or may be released into the extracellular environment, as released polysaccharides (RPS) (Rossi & De Philippis, 2016). In general, cyanobacterial EPS seem to play similar roles to the ones described for other bacteria, for example regarding protection against environmental stresses (Jittawuttipoka et al., 2013), motility (Ursell et al., 2013), biofilm formation (Rossi & De Philippis, 2015) or creation of a hydration shell that prevents cell desiccation and sequesters water, minerals and nutrients (Mager & Thomas, 2011). However, specific EPS roles have also been reported for some cyanobacteria, such as protection of heterocysts, through the formation of an heterocyst envelope polysaccharide (HEP) layer (Muro-Pastor & Hess, 2012), or involvement in the gliding motility of hormogonia (Khayatan et al., 2015) in filamentous strains.

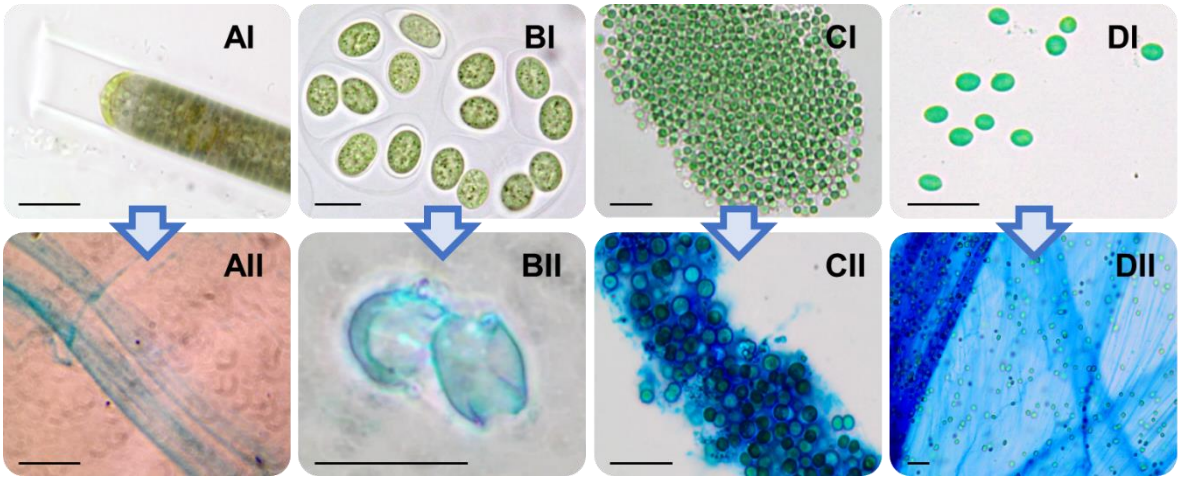

Figure 4. Extracellular polymeric substances (EPS) from morphologically distinct cyanobacteria. Light micrographs of the filamentous *Lyngbya majuscula* CCAP 1446/4 (AI) an its isolated sheath (AII); the colonial *Gloeothece* sp. PCC 6909 (BI) and its isolated sheath (BII); *Geminobacterium atlanticum* LEGE 07459 (CI) and respective slime (CII); unicellular *Cyanothece* sp. CCY 0110 (DI) and released polysaccharides (DII). EPS were stained with Alcian blue (lower panel micrographs). Some images were kindly provided by Sara Pereira (AI, AII, BI, BII, DI) and Ângela Brito (CI, CII). Scale bars: 15 µm.

Several environmental factors may influence cyanobacterial EPS production, affecting the amount of EPS produced, their composition, structure and consequently physiochemical and functional properties. The influence of each factor is strongly strain-dependent, and frequently intimately related to the cell growth (Mota et al., 2013; Pereira et al., 2009). In contrast to their bacterial counterparts, light (intensity and quality) is most probably the main factor coordinating EPS production by cyanobacteria. For some strains, the culture exposure to continuous light or high-light intensities enhances EPS production (Khattar et al., 2010). In other cases, specific light wavelengths stimulates production, such

as UV radiation for *Nostoc commune* (Ehling-Schulz et al., 1997), or red light for *Nostoc flagelliforme*, which also changes significantly the monosaccharide composition of their capsular polysaccharides (CPS) and RPS (Han et al., 2015, 2014). Light may also cause temperature fluctuations (e.g. due to heat generation), resulting in alterations of EPS productivity. Although only a very few studies addressed the impact of temperature in cyanobacterial EPS production (and often in combination with changes in light intensity), it seems that the production tends to be higher under slightly higher temperatures than the ones used for optimal cell growth (Trabelsi et al., 2009; Moreno et al., 1998). However, in other cases, no effect or even slight reductions in EPS production were also detected (Otero & Vincenzini, 2004; Nicolaus et al., 1999). Moreover, higher temperatures compared to the ones used for optimal cell growth also altered the monosaccharide composition of the CPS bulk from a biofilm formed by the cyanobacterium *Synechocystis* and algae *Chlorococcum* (Di Pippo et al., 2012).

Nutrient availability (namely carbon, nitrogen, phosphate and sulfate) and its cell ratio (e.g. C:N) are also highly important for cyanobacterial EPS production. In general, higher availability of carbon and/or nitrogen leads to higher production (Otero & Vincenzini, 2003; De Philippis et al., 1996; Lama et al., 1996). However, N starvation may also lead to higher production due to the increase of C:N ratio (Otero and Vincenzini, 2004; De Philippis et al., 1998, 1993), and the availability of different N sources may affect EPS composition and/or cyanobacterial productivity (Shah et al., 1999; De Philippis & Vincenzini, 1998). In agreement, the starvation or limiting availability of other nutrients such as sulfur or phosphorus, and even of manganese or potassium, triggered carbohydrate synthesis and accumulation in several cyanobacteria and microalgae (Markou et al., 2012; Cade-Menun & Paytan, 2010; Lama et al., 1996). In phosphorous-limiting conditions was even reported the stimulation of cyanobacterial EPS production (Huang et al., 2007; De Philippis et al., 1993).

Two other factors are frequently described as enhancers of EPS production by cyanobacteria: aeration and salt stress. Aeration seems to provide a better nutrient and light availability for the cells (Su et al., 2008, 2007; Moreno et al., 1998), while salt stress is a common stimulator of carbohydrate synthesis, mainly for production of compatible solutes, but in some cases also for EPS production, enhancing salt stress tolerance (Bemal & Anil, 2018; Yoshimura et al., 2012; Ozturk & Aslim, 2010; Shah et al., 1999). In addition, a few studies reported that salt stress alters the monosaccharide composition of EPS produced by some cyanobacterial strains (Yoshimura et al., 2012; Li et al., 2001).

Although some key environmental factors that affect cyanobacterial EPS production have been revealed, the way they trigger changes in the production, and the molecular machinery they activate and/or repress is still largely unknown. In fact, only a few

genes/proteins were undoubtedly related to EPS production in cyanobacteria (Fisher et al., 2013; Jittawuttipoka et al., 2013; Shi et al., 2013; Simkovsky et al., 2012; Yoshimura et al., 2007; Huang et al., 2005; Nobles et al., 2001), but recent studies suggested that this process is much more complex compared to the common bacterial scenario (Pereira et al., 2015). In cyanobacteria, more players might be involved, homologs belonging to the well-conserved bacterial pathways (*see section 2.2*) cooperate and/or display redundant functions, and EPS production may not follow a single pathway, being the full picture far from being elucidated. Furthermore, an intricate regulatory network should operate in order to control the various players involved. As occur in other bacteria, regulation of gene transcription is expected to be one of the most important steps for the control of cyanobacterial EPS production (Schmid et al., 2015), particularly considering that a higher number of genes are involved and some of them may encode proteins with redundant function. So far, only two cyanobacterial regulatory elements were associated to the control of EPS production, and were both described for *Anabaena* sp. PCC 7120. The nitrogen-control transcription factor (NtcA) was shown to be a key player in the regulation of the transport of glycosides in this cyanobacterium, which has an indirect influence in the distribution of the building blocks for EPS biosynthesis (López-Igual et al., 2012). Another global regulator, the alternative sigma factor SigJ was specifically associated with the control of EPS production, in particular for the formation of the heterocyst HEP-layer (Yoshimura et al., 2007). In fact, alternative sigma factors represent very promising candidates for the control of cyanobacterial EPS production, since they can help the RNA polymerase initiating the transcription of specific cyanobacterial gene sets involved in cell acclimation processes and survival in particular conditions (Imamura & Asayama, 2009). Furthermore, cyanobacteria have orthologs to other bacterial sigma factors that control cell envelope maintenance processes and other physiological mechanisms intrinsically dependent on EPS production (e.g. motility, biofilm formation) (Zhao et al., 2007; Rachid et al., 2002).

2.4. The distinct cyanobacterial EPS

In agreement with the intricate cyanobacterial EPS biosynthetic pathways, the EPS produced are also very complex, having distinct features compared to the ones from other bacterial sources (with nearly 150 cyanobacterial strains screened in Rossi & De Philippis, 2016), such as the presence of:

i) **higher number of different monosaccharides** (up to 13), with usual predominance of glucose, but having also other hexoses (galactose, mannose and fructose), deoxyhexoses (fucose and rhamnose), **frequently 2 acidic hexoses/uronic acids** (glucuronic and galacturonic acids) and pentoses (ribose, xylose and arabinose). This

leads to polymers with complex repeating units and structure, allowing a wide range of conformational possibilities.

ii) **different polysaccharidic fractions** with hydrophilic and/or hydrophobic properties, determining the rheological behavior and jellification ability of the polymer. The hydrophobic fractions enhance the capacity of cell adhesion, while the hydrophilic ones are involved in entrapment of minerals, nutrients and water (allowing the stabilization of the cell membrane during desiccation).

iii) **sulfate**, which is extremely rare in EPS from bacteria, but common among EPS from algae and some archaea. The sulfate groups are involved in cell protection in harmful habitats (under pH, temperature and salinity stresses). In addition, together with uronic acids and ketal-linked pyruvate groups, they confer a strong anionic charge and "gluey" behavior to the polymer.

iv) **peptides**, enriched in glycine, alanine, valine, leucine, isoleucine and phenylalanine, but also with aspartic and glutamic acids in some cases. They stabilize the polymer through the creation of hydrogen bonds, and confer hydrophobicity (together with deoxysugars and ester-linked acetyl groups).

v) **unusual EPS sugars**, such as methyl, acetyl and amino-sugars. They are expected to contribute to polymers' biological activity, most probably involved in cell recognition, adhesion and protection (together with sulfate and other functional groups).

Other non-carbohydrate constituents, such as pyruvate and acetate, have also been found in cyanobacterial EPS, namely from some *Nostoc* (De Philippis et al., 2000) and *Cyanothece* (De Philippis et al., 1998) strains. However, the search for these type of components in cyanobacterial EPS is not common. Another interesting feature of many cyanobacterial EPS is the presence of high-molecular weight fractions, reaching values ≥ 2 MDa in some cases. This feature has a crucial importance in the polymers' rheological behavior in solution (e.g. viscosity) and influences directly an envisaged application of the polymer (Xu & Zhang, 2016).

The complexity associated to cyanobacterial EPS hinders the solving of their structure (successfully achieved only in a very few cases: Volk et al., 2007; Helm et al., 2000; Shah et al., 2000; Gloaguen et al., 1999; Garozzo et al., 1998), but at the same time makes these polymers more versatile and particularly attractive for biotechnological application.

2.5. Biotechnological application of cyanobacterial EPS

The development and biotechnological application of added-value products based on cyanobacterial and other bacterial EPS is increasingly attractive, since there is a constant implementation of restrictive regulation in the polymer industry to promote environmental preservation. This led to an increase in the global market demand for

products with a lower ecological footprint (“green materials”), even considering the production costs, downstream processing and some batch inconsistency in quantity/quality of the final product (Roca et al., 2015; Freitas et al., 2011). These natural polymers are derived from renewable resources and by definition, they present several competitive advantages compared to the recalcitrant petroleum/oil-based products, such as biodegradability, eco-friendliness, and often biocompatibility (Donot et al., 2012; Rehm, 2010). Furthermore, the industrial production of bacterial EPS presents important advantages compared to the production of biopolymers using other natural sources: i) they are generally actively secreted by the cells, being easy to extract and usually do not need a challenging purification process, which reduces the production costs; ii) their manufacturing is not ruled by the stringent environmental measures applied in the production of polymers using animals or plants (e.g. ethics and animal protection, or deforestation preventive measures); iii) the strains used have usually high growth rates, which accelerates the production process; iv) in some cases, the polymers and/or the producing strain can be easily engineered/functionalized to obtain a product with the desired properties and/or enhanced performance. Additionally, EPS production by cyanobacteria brings also two other major advantages, even compared to the production of bacterial EPS that are currently being commercially exploited: i) cyanobacteria have extremely simple nutritional requirements, since their growth and EPS production do not depend on the addition of expensive EPS precursors or substrates (Rütering et al., 2016; Freitas et al., 2011; Rehm, 2010). This allows a better control of growth/production, a lower variability of the final product and a reduction in the costs of production (Raposo et al., 2013); ii) the cyanobacterial EPS are more complex, which make them more versatile and with a broader-spectrum of potential application fields. In fact, some polymers showed potential to be used in completely distinct fields, such as the EPS from *Nostoc flageliforme*, which are promising emulsifying and flocculating agents that could be used in cosmetics and food industry (Han et al., 2014b), and since they have a potent antiviral activity, they could be also applied in the biomedical field (Kanekiyo et al., 2005). Currently, the main areas of possible application for cyanobacterial EPS are the bioremediation, food, cosmetics and painting industry (as bio flocculants or emulsifiers), biomedicine and tissue engineering, pharmaceutics, and soil stabilization, namely when inoculated with the producing strain (reviewed in Singh et al., 2019).

The advent of high-throughput genome sequencing, functional genomics, protein engineering, synthetic biology and new bioinformatic tools may allow the implementation of strategies for optimization of industrial systems based on cyanobacterial cell factories for EPS production, similar to the ones that have been created using other bacterial strains (Schmid, 2018; Rehm, 2015). These approaches are extremely important to fully

understand and to manipulate the mechanisms underlying cyanobacterial EPS biosynthesis. Currently, the manipulation of cyanobacterial EPS production has two main goals: the maximization of productivity/polymer yields cost-effectively, and the creation of tailor-made polymer variants with desirable properties. So far, the strategies that have been developed to achieve these purposes are mainly based on modification of culture growth conditions and feeding (Tiwari et al., 2015; Jindal et al., 2013; Mota et al., 2013; Singh & Das, 2011; Yu, 2012). Furthermore, several patents have been filled to protect the knowledge/use related to methods of cyanobacterial EPS production in large-scale, their extraction and/or downstream processing, as well as the use of the polymers (pure or combined in formulae) in specific fields (compiled in Borowitzka, 2014; Sekar & Paulraj, 2007). However, these strategies are still far behind compared to the ones established for production of other added-value products by cyanobacteria, such as biofuels, food supplements (biomass-based), bio alcohols, intracellular biopolymers, bioplastics and bioactive secondary metabolites (Kitchener & Grunden, 2018; Knoot et al., 2018; Luan & Lu, 2018; Hays & Ducat, 2015; Abed et al., 2009). In fact, some of these products have been already commercially exploited. Regarding cyanobacterial EPS, although some efforts have been made, more work is needed in order to improve the yields and determine the biosynthetic mechanism(s) underlying their production (Chentir et al., 2017; Depraetere et al., 2014; Singh & Das, 2011). These two factors are the main bottlenecks that hinder the implementation of cyanobacterial-based industrial systems for EPS production. Nevertheless, cyanobacteria have been emerging as promising “feedstock” for development of more, novel and tailor-made valuable materials based on EPS, extending their application to new fields.

2.5.1. Biological activities and biomedical application of cyanobacterial EPS

A wide range of different biological activities is described for cyanobacterial EPS, which make them very attractive for researches in the development of innovative natural products, suitable for application in the medical industry as drugs, food supplements, nanocarriers, coatings or scaffolds (Table 1). Moreover, different biological activities (e.g. immunostimulatory, cytotoxic, pro-inflammatory and antimicrobial) were also found for entire cyanobacterial crude extracts containing EPS and EPS from mats/consortia with cyanobacteria (Angelis et al., 2012; Hayashi et al., 2006; Hernández-Corona et al., 2002), as well as for cyanobacterial LPS (Klemm et al., 2018; Parages et al., 2012).

In general, the study of cyanobacterial EPS bioactivities has been focused on marine strains. On the top of the list are the EPS from *Arthrospira platensis*, well-known as *Spirulina*, for which were found at least 9 well-described biological activities and were published several patents. However, these bioactive properties are described for different

types of *A. platensis* EPS (Table 1), which vary in composition and/or structure depending on the extraction method, culture conditions and the substrain (Phélippé et al., 2019).

The vast array of bioactivities found for cyanobacterial EPS may be related to several compositional and/or structural features, namely the presence/accessibility of uronic acids, amino-sugars, sulfate and other functional groups, low molecular weight fractions, polymer hydrophobic nature and structure conformation. However, only very few polymer properties were clearly associated with its bioactivity and in the majority of the cases this association is inferred based on other compositionally similar bioactive polymers, from eukaryotic (mainly macroalgae) or other bacterial sources (Flamm & Blaschek, 2014; Gacheva et al., 2013; Okajima-kaneko et al., 2007; Kanekiyo et al., 2005; Yamamoto et al., 2003).

Table 1. Main biological activities and/or biomedical applications described for cyanobacterial EPS.

Strain	Extracellular polymer	Biological activity / Biomedical application	References
Arthrospira platensis	Immulina (EPS)	Immunostimulatory, Pro-inflammatory	Løbner et al., 2008; Pugh et al., 2001
	Calcium-spirulan (EPS)	Antiviral, Stimulation of fibrinolysis (tissue remodeling and migration), Antithrombin, Anti-atherogenic, Delay in vascular endothelium repair, Stimulation of anticoagulant proteoglycan secretion, Antitumor	Mader et al., 2016; Kaji et al., 2002a, 2002c; Hayakawa et al., 2000, 1996, 1997; Mishima et al., 1998; Hayashi et al., 1996
	Sodium-spirulan (EPS)	Antithrombin, Anti-atherogenic, Inhibition of cell proliferation, Stimulation of anticoagulant proteoglycan secretion, Modulation of fibrinolysis (tissue remodeling and migration)	Kaji et al., 2004, 2002b, 2002c; Yamamoto et al., 2003
	EPS	Antimicrobial (bactericidal, bacteriostatic), Antioxidant, Bacterial anti-adhesive, Antiviral	Reichert et al., 2017; Kurd & Samavati, 2015; Chaiklahan et al., 2013; Challouf et al., 2011; Loke et al., 2007
Cyanothece sp. CCY 0110	RPS	Controlled drug delivery	Estevinho et al., 2019; Leite et al., 2016
Synechocystis sp.; *Gloeocapsa* sp.	EPS	Antifungal, Antibacterial	Najdenski et al., 2013
Aphanothece sacrum	Sacran (EPS)	Scaffold (hydrogel-like behavior)	Okajima et al., 2018
Nostoc commune	EPS	Antioxidant, Inhibition of human complement, Biomaterial in coatings and membranes, Capping agent of silver nanoparticles (bactericidal)	Rodriguez et al., 2017; Morsy et al., 2014; Wang et al., 2014; Li et al., 2011a; Brull et al., 2000
Nostoc flagelliforme	Nostoflan (EPS)	Antiviral, Antitumor	Yue et al., 2011; Kanekiyo et al., 2005
Aphanothece halophytica	EPS	Antitumor, Immunomodulatory, Antiviral, Cytolytic	Ou et al., 2014; Zheng et al., 2006
Anabaena variabilis; A. anomala; A. oryzae; Tolypothrix tenuis	EPS	Hemostatic blood clotting agent, Wound dressing/healing, Antibacterial Antioxidant, Iron-chelating agent	Bhatnagar et al., 2014, 2012; Parwani et al., 2014
Oscillatoria sp.; Phormidium sp.	EPS	Antibiofilm	Arunkumar et al., 2018
Phormidium sp. (8 substrains)	CPS	Anti-inflammatory	Garbacki et al., 2000

The lack of knowledge about the mode of action of bioactive cyanobacterial EPS, and the scarce information available regarding their mechanisms of production, hinders the approval of these polymers as qualified commodity materials by the policy agencies worldwide. These agencies are responsible for the control and supervision of biopharmaceuticals, food, personal care products and medical devices, being this process more restrictive for products with biological activity and to use in biomedicine. So far, only *Arthrospira* (namely *A. platensis* and *A. maxima*), regarding its entire biomass, successfully accomplished the high-quality criteria to be commercialized as dietary supplement and cosmetic product (Marles et al., 2011). It was firstly approved in 1981 by the Food and Drug Administration (FDA, United States), and after that it was assigned with the Generally Recognized as Safe (GRAS) status, considered by the World Health Organization (WHO) one of the greatest superfood, and approved with class A safety rating by Pharmacopoeial conventions globally (e.g. in European Union, United States and Japan).

2.6. Antitumor activity of EPS

Cancer is a leading cause of death worldwide and topic of intensive research not only in the medical field, but also in biotechnology. Nowadays, the discovery of new and less expensive drugs and therapeutics based on natural resources represent a huge demand, especially because the current clinical practices are still based on the use of very toxic chemotherapy and radiotherapy agents, having many and aggressive side effects (Cragg & Newman, 2018). Furthermore, there are several cancer types completely insensitive or that are even able to develop resistance to the actual treatments. Additionally, the advent of personalized medicine stimulated the search for novel compounds, with high specificity for a certain cancer genotype/phenotype, and taking into consideration the patient characteristics (metabolism, age, etc.) (Pauli et al., 2017). This becomes particularly important with the recent understanding that the specific features of each cancer may allow a better cancer classification and treatment rather than the use of the well-established cancer hallmarks, which describe common traits and have been the guidelines for drug design during the last decades (Pavlova & Thompson, 2016).

In this framework, biopolymers of polysaccharidic nature, namely EPS from different producing sources, have been shown to be valuable antitumor agents (reviewed in Khan et al., 2019; Zong et al., 2012): i) preventing tumorigenesis or tumor development; ii) presenting a direct antitumor effect, impairing tumor growth, proliferation, progression, invasion and/or adhesion; iii) inhibiting tumor metastasis and/or angiogenesis; iv) in immunomodulation, promoting antigen-specific cancer immunotherapy by stimulation of the immune response to reject the tumor, or as adjuvants in vaccine-induced protection. Moreover, several studies demonstrated that these macromolecules may act in combination

with conventional anticancer drugs, improving their activity through the enhancement of both tumor sensitivity and patient immune response (Moscovici, 2015; Zong et al., 2012).

The molecular mechanisms that these natural polymers may trigger can be divided into 5 five main types (Fig. 5) (Khan et al., 2019; Zong et al., 2012): i) cell cycle arrest; ii) depolarization of mitochondrial membrane (mitochondrial-mediated apoptotic pathway); iii) stimulation of nitric oxide (NO) production and activation of NO pathway; iv) immunomodulatory mechanisms; v) other few specific mechanisms, such as inhibition of galectin 3, topoisomerases, etc. Furthermore, there are several studies showing cytotoxicity/inhibition of tumor cell growth after treatment with EPS and other natural polysaccharides, but without association to a molecular mechanism. Nevertheless, these mechanisms are not mutually exclusive, so one polymer may act through multiple pathways.

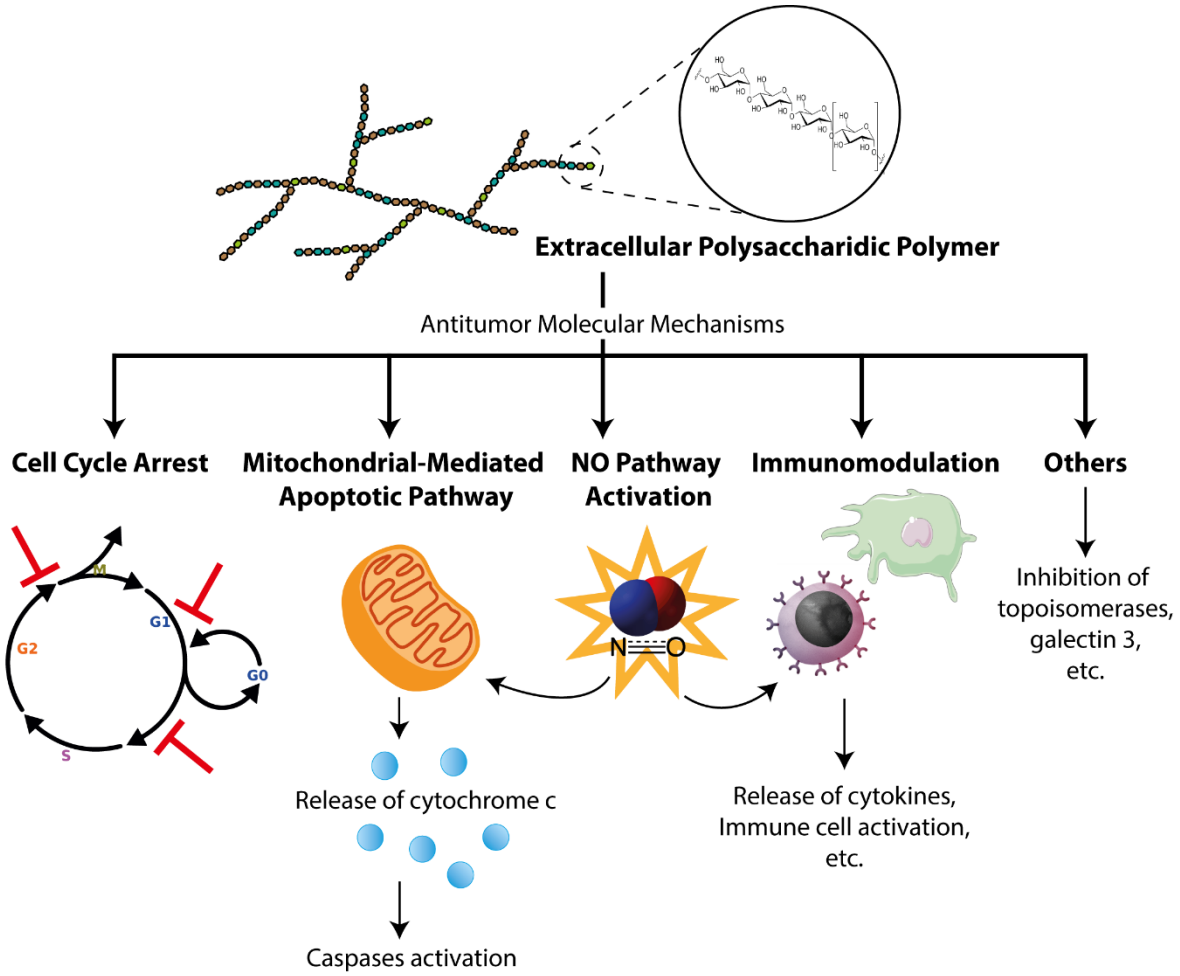

Figure 5. Schematic representation of the main molecular mechanisms described for the antitumor mode of action of polysaccharidic biopolymers. NO, nitric oxide.

The first studies revealing EPS antitumor efficacy were performed in the 1940s, showing that the injection of “toxin preparations” (essentially bacterial EPS) in patients induced remission of different cancer types (Nauts et al., 1946; Hartwell et al., 1943).

Currently, the majority of the studies are being performed with cancer cell lines and mouse models, using not only polysaccharides from bacteria but also from other sources (Zong et al., 2012). Indeed, only very few polymers have been clinically tested in humans (e.g. fungi extracellular β-glucans, such as the well-described lentinan), and even those still show lack of consistency regarding their efficacy (Oba et al., 2009; Yang et al., 2008). Moreover, the repurposing of bacterial EPS that are already in the market has been explored in order to allow the delivery and accumulation of anticancer drugs specifically in tumor cells (Moscovici, 2015), using them as carriers in nanoparticle conjugates (Tran et al., 2014; Gao et al., 2010; Choi et al., 2009), or as scaffolds in emulsion and hydrogels (Koop et al., 2015; D'Arrigo et al., 2014; Gao et al., 2014; Vandamme et al., 2002).

2.6.1. Cyanobacterial EPS as antitumor agents

Some cyanobacterial EPS and cell crude extracts containing EPS have previously been described to have antitumor activity (Czerwonka et al., 2018; Li et al., 2018; Hernandez et al., 2017; Ou et al., 2014). However, most of these studies are based on antioxidant and ROS scavenging assays, which may be correlated to antitumor potential, but are not sufficient to define an antitumor biological activity (Kurd & Samavati, 2015). In addition, antioxidants may also protect tumor cells from ROS induced cell death, being considered mostly advantageous for cancer prevention in healthy individuals (Sznarkowska et al., 2017). Therefore, those studies cannot be considered *per se* as antitumor activity assessments. The remaining studies, aiming to evaluate the antitumor potential of cyanobacterial EPS, are still very preliminary and mainly based on the well-known "cytotoxicity MTT assays" using tumor cell lines, which indirectly access cytotoxicity through the evaluation of tumor cell metabolic activity (Li et al., 2018, 2011b; Ou et al., 2014; Gacheva et al., 2013; Yue et al., 2011; Zheng et al. 1994). Only two of these studies tested also the effect of EPS *in vivo*, using tumor cell-transplanted mice (Mishima et al., 1998; Zheng et al., 1994).

Remarkably, only two very recent studies attempted to unveil the molecular mechanisms underlying the antitumor activity of cyanobacterial EPS, from *Nostoc sphaeroides* (Li et al., 2018) and *Aphanothece halophytica* (Ou et al., 2014). Both studies suggested the involvement of the mitochondrial-mediated apoptotic pathway, particularly through the activation of the executioner caspase-3. In addition, Ou et al., 2014 proposed that this mechanism occurs via p53-survivin signaling. Moreover, other studies indicate that the antitumor activity of cyanobacterial EPS is intrinsically related to other polymer properties, associated to antioxidant (Li et al., 2018) or immunostimulatory (Zheng et al. 1994) activities.

In spite of the recent attempts to unveil the molecular mechanisms behind cyanobacterial EPS antitumor activity, and the extensive characterization of some of the polymers, it is still unclear which compositional/structural features are relevant for their bioactivity. Although a few studies have suggested putative key players, none was unequivocally assigned as playing an antitumor role yet. For example, Mishima et al., 1998 suggested that the high amount of rhamnose in Calcium-Spirulan (EPS from *Arthrospira platensis*) may be associated to its strong antiadhesive activity towards lung metastatic tumors. These tumor cells usually have surface receptors capable of recognizing rhamnose residues, and the binding of Calcium-Spirulan will mask them as well as other proteins (e.g. integrins) that are essential for tumor adhesion to extracellular matrix components and consequent invasion. The authors also suggested that Calcium-Spirulan may inactivate essential enzymes for tumor invasion, such as heparanases. In contrast, the antiproliferative activity of EPS extracted from *Gloeocapsa* sp. cultures, were not only associated with the polymer monosaccharide composition, but also with its protein content (Gacheva et al., 2013). In this case, the EPS from cultures grown under suboptimal conditions (e.g. low temperature) and from old cultures presented lower protein content (higher protease activity in some cases) and also enhanced bioactivity.

One of the most promising candidates expected to be involved in antitumor activity of cyanobacterial EPS is their sulfate content. This feature was previously associated with other cyanobacterial EPS biological activities, such as antiviral (Radonić et al., 2010), antioxidant (Parwani et al., 2014), anticoagulant (Majdoub et al., 2009) and antimicrobial (Loke et al., 2007). Furthermore, sulfate groups were considered key players for the antitumor activity of several natural polysaccharides, specially from algae (e.g. fucoidans and carrageenans), but also from a few plants and bacteria (Zong et al., 2012; Ruiz-Ruiz et al., 2011). Although the exact mode(s) of action are not fully understood yet, sulfated polysaccharides are able to interfere with a wide range of tumor cell physiological processes (reviewed in Wang & Zhao, 2017; Li et al., 2008).

Altogether, the particular features of cyanobacterial EPS, namely their high sulfate content, monosaccharide composition and common presence of peptides and rare bacterial EPS sugars, make them promising antitumor agents. They also emerge as good candidates for economic and new therapeutic approaches, such as the envisaged but still unexplored use of functionalized EPS as antitumor drug carriers to cross the blood-brain barrier (Moscovici, 2015). So far, only one cyanobacterial carbohydrate-based polymer with antitumor activity is in clinical trials: a peptidoglycan complex from *A. platensis* (*Spirulina*), which reached the phase I in December 2016. Its antitumor activity is being tested in patients with advanced pancreatic cancer in order to increase the tolerance of monotherapy, but the results of this study are still not currently available (Khan et al., 2019).

Nevertheless, although very promising *in vitro* results have been obtained testing cyanobacterial EPS towards tumor cell lines, more comprehensive studies are needed to confirm these results *in vivo*, as well as to fully understand the mechanisms and the EPS features associated with their antitumor activity.

3. Main aims

The major aim of this study was to improve the knowledge about cyanobacterial EPS, their biosynthetic pathways and regulatory mechanisms, and evaluate the antitumor activity of cyanobacterial polymers. For this purpose, the unicellular cyanobacterium *Synechocystis* sp. PCC 6803 was used as a model to:

i) study genes/proteins putatively involved in EPS production, mainly through an extensive bioinformatic analysis (Chapter II).
ii) identify regulatory elements underlying EPS production (Chapters II and III).
iii) optimize isolation methods for cyanobacterial secreted products: EPS and proteins (Chapter IV).
iv) characterize the produced polymers, to evaluate their performance as antitumor agents and to have an insight on the molecular mechanisms that are involved (Chapters V).
v) manipulate polymer features (e.g. sulfate content and molecular weight) in order to unveil their relationship with the polymer antitumor activity (Chapter VI).

CHAPTER II

Uncovering key EPS-related genes/proteins and regulatory factors in *Synechocystis* sp. PCC 6803

Uncovering key EPS-related genes/proteins and regulatory factors in *Synechocystis* sp. PCC 6803

Abstract

Following up a previous study that identified several *Synechocystis* genes/proteins putatively involved in EPS assembly and export, a blueprint of these genes was elaborated. These genes are either isolated or in small clusters throughout *Synechocystis* chromosome, and in a particular region of the pSYSM plasmid. An in-depth *in silico* analysis revealed that nine genes (out of 31) might play a more prominent role in EPS production. Three of the identified clusters contain not only genes putatively involved in EPS assembly/export but also genes encoding a high diversity of proteins involved (or predicted to be involved) in the first steps of EPS production/residues' modification. Additionally, several regulatory factors, both global transcriptional regulators and a few stress-related regulators were identified as candidates to control the EPS biosynthesis.

1. Introduction

Bacterial extracellular polymeric substances (EPS) not only play crucial roles for the maintenance of cell homeostasis (Rossi & De Philippis, 2016), but have also been shown as attractive biomolecules in terms of biotechnological application (Freitas et al., 2011; Rehm, 2010). The use of bacterial strains that can be easily manipulated and produce EPS with biotechnological potential is therefore of extreme interest, in order to allow a comprehensive study of the EPS production mechanisms and the polymer tailoring (Sengupta et al., 2018; Hays & Ducat, 2015). In this context, the model cyanobacterium *Synechocystis* sp. PCC 6803 (hereafter *Synechocystis*) fulfils both requirements. This organism can be easily genetically manipulated and since it is one of the best studied cyanobacteria, there is a large amount of genomic, transcriptomic and proteomic data available, which allowed the conception of metabolic models (Sebesta et al., 2019; Branco dos Santos et al., 2014). In addition, a few studies have also revealed that *Synechocystis* is able to produce both capsular and released polysaccharides - RPS (Fisher et al., 2013; Jittawuttipoka et al., 2013; Planchon et al., 2013; Panoff et al., 1988). Some of these studies also reported a few genes that might be involved in EPS production, mainly based on characterization of *Synechocystis* knockout mutants. Recently, a different approach based on a phylum-wide analysis revealed a broad set of cyanobacterial homologs of genes/proteins involved in the conventional bacterial mechanisms of assembly and export of EPS (EPS-related genes/proteins): the Wzy-, ABC transporter- or Synthase-dependent pathways, but often there is not a complete set defining one pathway (Pereira et al., 2015).

This analysis indicated also that crosstalk between the different pathways may occur. In *Synechocystis*, the EPS-related genes identified, include several putative gene copies, such as for *wzy* (5 copies), *wzx* (4 copies), *kpsM*/*kpsT* (3 copies each) and *alg8* (4 copies). This not only supports that *Synechocystis* EPS production follows a more complex scenario compared to other bacteria, but also raises the question if all of the gene copies are fully dedicated to EPS production or if there is any cell preference for some of them. Furthermore, it is still not known how the cells can regulate such intricate network.

The main aim of this study was to improve the knowledge about the previous reported group of *Synechocystis* EPS-related genes, in order to have an insight on their importance for EPS production and to highlight putative key players, as well as to identify possible regulators. For this purpose, a comprehensive study was carried out, mainly based on *in silico* analysis of genomic, transcriptomic and proteomic data.

2. Material and Methods

2.1. Physical organization and genomic context of *Synechocystis* EPS-related genes

The putative EPS-related genes previously reported in Pereira et al., 2015 were mapped throughout the *Synechocystis* sp. PCC 6803 genome using the genomic data and respective base pair coordinates deposited by Kazusa DNA Research Institute (Japan) at NCBI database (National Library of Medicine, National Center for Biotechnology Information, US), with RefSeq assembly accession: GCF_000009725.1, available from https://www.ncbi.nlm.nih.gov/refseq/ (Tatusova et al., 2016). Physical maps were created using the schematic representations of the *Synechocystis* chromosome and plasmid pSYSM available in CyanoBase (http://genome.microbedb.jp/cyanobase, Fujisawa et al., 2017). For the identification and representation of the genomic clusters, the same genomic information was analyzed in Vector NTI software (Thermo Fisher Scientific).

2.2. Computational analysis of transcriptional profiles

Genome-wide expression data from 722 microarrays (31 independent studies) were retrieved from CyanoEXpress database v. 2.3 (Hernández-Prieto et al., 2016). Datasets were obtained from *Synechocystis* wild-type cultures growing with or without environmental perturbations, including variations in light intensity and quality, temperature, availability of nutrients, concentration of atmospheric O_2, osmotic and induced oxidative stresses. More information about the studies, data processing and normalizations can be found at http://cyanoexpress.sysbiolab.eu. Co-expression analysis was based on the correlation values (c) of the integrated expression data provided in the database (with a minimum c=0.4). For hierarchical two-way clustering (with simultaneous clustering of genes and samples), the open source clustering software Cluster 3.063 was used (de Hoon et al.,

2004) considering complete linkage and Spearman's rank correlation as similarity measure. Differential expression was displayed as heat maps using Java TreeView v. 3.0 software (Saldanha, 2004). A dendrogram attached to the heat map was displayed, with the length of the branches representing a measure of similarity between the gene's expression profiles. Analyses of co-expressed genes and ncRNAs were also performed using the RNA-seq high-throughput data from Kopf et al., 2014 (deposited in CyanoEXpress database).

2.3. Description of promoter regions and identification of putative transcriptional regulators

The promoter regions of the putative EPS-related genes were depicted in 5'-3' based on the data available in Kopf et al., 2014, the BPROM prediction software (Softberry, Salamov & Bachinsky, 2011) and genome mining. The following elements were identified up to 1000 bp upstream of the genes (Supplementary data S1): i) genomic coordinates and sense or antisense strand; ii) transcription starting sites (TSS), including the alternative and internal ones; iii) regions -10 and -35; iv) transcriptional units (TU); v) co-transcribed genes; vi) transcription factor binding sites (TFBS) and respective transcriptional regulators (TF). The search for TFs was also performed using the RegPrecise v. 3.0 database (Novichkov et al., 2013).

2.4. Pull-down assays and mass spectrometry

Synechocystis sp. PCC 6803 cultures were grown in Erlenmeyer flasks with BG11 media (Rippka et al., 1979). Axenic cultures were incubated at 30 ºC under a 12 h light (50 μE m^{-2} s^{-1})/12 h dark regimen or continuous light (25 μE m^{-2} s^{-1}), with orbital shaking at 150 r.p.m. DNA and protein extractions were performed as previously described in Tamagnini et al., 1997 and Oliveira et al., 2015, respectively. The protein concentration was measured using the BCA™ Protein Assay Kit (Pierce Biotechnology) and the iMark Microplate Absorbance Reader (Bio-Rad) according to the manufacturer's instructions. The DNA fragments corresponding to the promoter regions of *sll0737* (*wzy*), *sll5049* (*wzx*) and *slr2107* (*kpsM*) were amplified by PCR using oligonucleotides labelled with biotin (Table S1) and following standard protocols (Sambrook & Russell, 2001). DNA-protein affinity assays were performed as described elsewhere (Oliveira & Lindblad, 2005; Drewett et al., 2001), using 5 μg of biotinylated DNA and 100 to 600 μg of protein. Streptavidin-coated magnetic beads (Dynabeads M-280®, Invitrogen, Life Technologies) were used to separate biotinylated DNA-protein complexes, following manufacturer's instructions. Samples were separated by electrophoresis on SDS-polyacrylamide gels (Bio-Rad) and visualized with colloidal Coomassie brilliant blue (Sigma). 6 ug of total protein extracts were used as loading controls. Stained bands of interest were excised and processed for mass spectrometry

analysis as previously described (Gomes et al., 2013; Osório & Reis, 2013). Peptide mass spectra were acquired in reflector positive mode in the mass range of m/z 700–5000. Proteins were identified by Peptide Mass Fingerprint (PMF) approach with the Mascot software v. 2.5.1 (Matrix Science) using the UniProt protein sequence database (http://www.uniprot.org/) for the taxonomic selection *Synechocystis* (accessed in September 2014).

2.5. Protein domains and predicted protein subcellular localization

Protein query sequences in FASTA format from the *Synechocystis* EPS-related proteins were obtained from CyanoBase. Specific functional domains of these proteins were identified using: i) the Simple Modular Architecture Research Tool (SMART), for prediction of conserved domains, low complexity domains (SEG domains) and areas that may adopt a coiled-coil conformation (Letunic & Bork, 2018); ii) the TMHMM Server v.2.0 (DTU Bioinformatics, Krogh et al., 2001) and SOSUI v.1.11 (Hirokawa et al., 1998) software for prediction of transmembrane helices. These domains and the ones used by Pereira et al., 2015 for the phylum-wide analysis were sorted throughout the protein primary structure and compared between proteins from the same putative family. The subcellular localization of EPS-related proteins was predicted using CELLO v.2.5 (Yu et al., 2006), PSORTb v.3.0 (Yu et al., 2010) and QuickGo (EMBL-EBI, available from https://www.ebi.ac.uk/QuickGO/) tools.

2.6. Prediction of protein-protein interactions (PPIs)

Possible PPIs involving EPS-related proteins were identified using the IntAct Molecular Interaction database (EMBL-EBI, Orchard et al., 2014), considering fundamentally experimental data. For a broader analysis, the STRING v.11 database (Szklarczyk et al., 2018) was used, since it predicts PPIs based on data from metabolic pathway databases, textmining, gene neighborhood, gene fusion, gene cooccurrence, co-expression and protein-protein interaction experiments. The scores retrieved by this database for each PPI (from 0-1) represent a degree of confidence that considers also the information available regarding protein homologs. A manual curated analysis of the hits obtained was performed, excluding the interactors that were predicted only based on textmining and the ones that are not involved (or predicted to be involved) in polysaccharide metabolism and/or EPS production.

2.7. Identification of Carbohydrate-Active enzymes (CAZymes)

The identification of proteins from *Synechocystis* with structurally-related catalytic and carbohydrate-binding modules, or other functional domains that degrade, modify or

create glycosidic bonds (CAZymes) was based on the information available in CAZy database (http://www.cazy.org/, Lombard et al., 2013). The data was manually curated in order to remove duplicates and categorize the proteins according to their CAZyme family and biological function (using the Uniprot database).

3. Results and Discussion

3.1. The *Synechocystis* sp. PCC 6803 EPS-related genes

Previously, Pereira et al., 2015, 2013 reported the presence of several putative EPS-related genes/proteins in *Synechocystis* sp. PCC 6803, however, these studies were mainly based on the similarity of their protein domains to bacterial homologs. For a more comprehensive study, an extensive search in the literature was performed (information compiled in Table S2). Although some of these genes/proteins have been directly or indirectly implicated in EPS production, namely *sll1581* (*wza*/*kpsD*), *slr0328* (*wzb*), *sll0923* and *sll5052* (*wzc* copies), *sll0574* and *slr0977* (*kpsM* copies), *sll0575* and *slr0982* (*kpsT* copies), *sll1377* (*alg8*) and *slr1875* (*exoD*), others have been studied in completely different contexts, such as photosynthesis - *slr0067* (*wzc*/*kpsE*) and *slr2111* (*kpsF*), metal or multidrug tolerance mechanisms - *slr0946* (*wzb*), *slr0896* and *slr1543* (*wzx* copies), *sll1181* (*alg44*), and bicarbonate transport - *slr1515* (*wzy*). For the remaining genes, *sll0737*, *sll5047*, *slr0728* and *slr1074* (*wzy* copies), *sll5049* and *slr0488* (*wzx* copies), *slr2115* (*kpsC/kpsS*), *slr2107* (*kpsM*), *slr2108* (*kpsT*), *slr2122* (*kpsU*), *sll1004*, *slr1566* and *slr5056* (*alg8* copies) and *sll1481* (*alg44*), there is still very limited information about the function of their encoded proteins or the metabolic pathways in which they might be involved. In general, the majority of the information available about these *Synechocystis* putative EPS-related genes was obtained from the characterization of knockout mutants (Table S3), a very small amount from *in silico* analysis, and even less from functional studies of the EPS-related proteins and their molecular interactions (Table S2). Therefore, the limited knowledge about these genes/proteins, particularly in an EPS production context, guided our analysis towards fundamental aspects such as the genes' localization in *Synechocystis* genome and respective genomic context.

3.1.1. Organization and genomic context of the EPS-related genes

The putative EPS-related genes are scattered throughout the chromosome of *Synechocystis* either isolated or in small clusters, and in a particular region at the pSYSM plasmid (Fig. 1), being the location of the genes that define a putative ABC transporter-dependent pathway limited to the chromosome. This is a completely different scenario compared to the distribution of EPS-related genes in other bacteria, in which they are often in large clusters, in specific regions and as single gene copies (Rehm, 2010). Overall, 3

main clusters were found in *Synechocystis* (Fig. 1 and 2): i) Cluster 1 contains genes encoding a putative ABC transporter, *kpsM* (*slr0977*)/*kpsT* (*slr0982*), one *wzc*/*kpsE* copy (*slr0923*) and one *wzy* copy (*slr1074*); ii) Cluster 2 also contains genes encoding a putative ABC transporter, *kpsM* (*slr2107*)/*kpsT* (*slr2108*), plus other gene set that may be involved in an ABC transporter-dependent pathway (for detailed description of the pathways see *Chapter I, section 2.2.*), *kpsF* (*slr2111*), *kpsU* (*slr2122*) and *kpsC*/*kpsS* (*slr2115*); iii) Cluster 3 includes the 4 EPS-related genes that are in the plasmid pSYSM - *sll5047* (*wzy*), *sll5049* (*wzx*), *sll5052* (*wzc*/*kpsE*) and *slr5056* (*alg8*/*bcsA*).

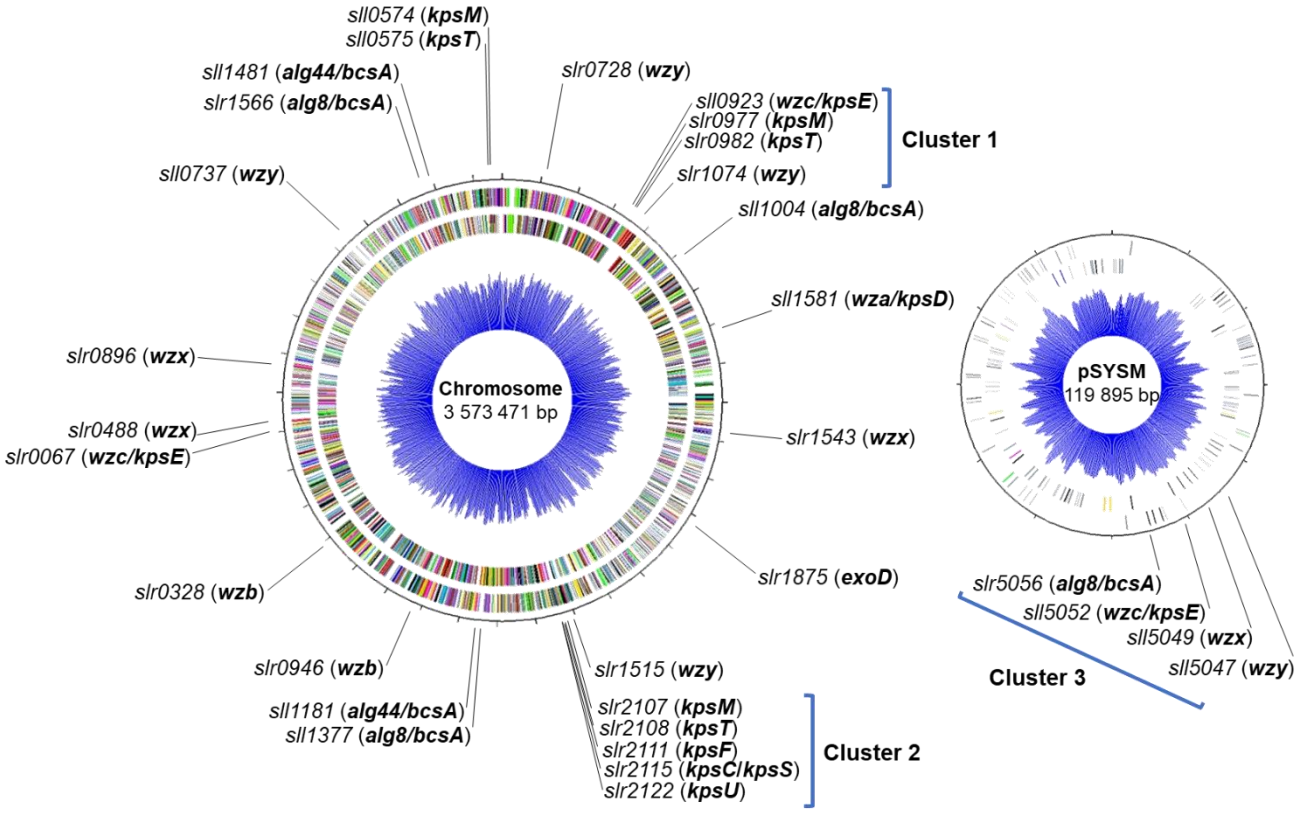

Figure 1. Physical map of putative EPS-related genes distributed throughout *Synechocystis* sp. PCC 6803 chromosome and pSYSM plasmid, with the clustered ones highlighted. Colored bars indicate protein coding sequences and the blue spectra corresponds to the GC content along the genome (retrieved from CyanoBase, http://genome.microbedb.jp/cyanobase).

Some of the *Synechocystis* putative EPS-related genes in Fig. 1 are in a highly relevant genomic context in terms of EPS production, i.e. nearby genes encoding proteins that are most probably relevant for the first steps of EPS production (e.g. glycosyltransferases) and/or responsible for EPS modifications (e.g. methyltransferases, sulfotransferases). This is particularly evident for the genes present in the 3 clusters aforementioned (Fig. 2), and is in agreement with the scenario that has been described for

the large EPS-related gene clusters from other bacteria (Whitney & Howell, 2013; Janczarek, 2011; Rehm, 2010).

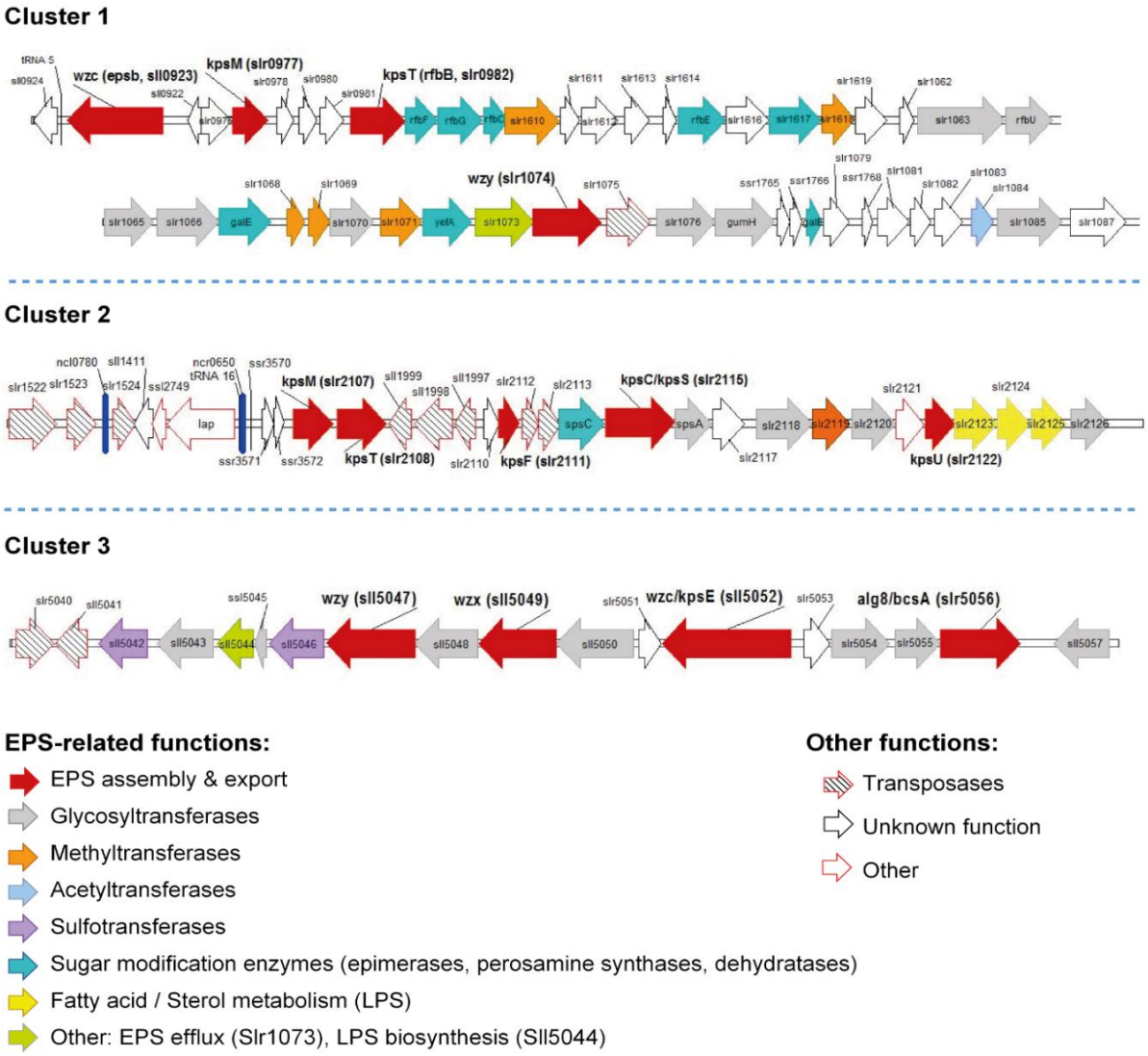

Figure 2. Genomic context of the EPS-related genes in the 3 clusters identified in *Synechocystis* sp. PCC 6803 chromosome (Cluster 1 and 2) and plasmid pSYSM (Cluster 3). The putative function of the encoded proteins is represented by different colors.

Previously, Fisher et al., 2013 described a smaller part of the Cluster 1 as being the "*slr0977* gene cluster" and suggested that was important for EPS production due to its relevant genomic context. Later on, the comparative genomic analysis of Kopf et al., 2014 revealed that this cluster covers a larger genomic region and named it as the "*rfb*-gene cluster" or "glycosyltransferase gene cluster", essential for cell wall biosynthesis and modification of cell surface properties. In addition, Kopf et al., 2014 found that this region is a genomic island well-conserved across different *Synechocystis* strains, and consists in a flexible gene pool that might be laterally transferred between different bacterial groups to confer certain fitness advantages. Moreover, in this cluster, there is a gene encoding a

putative acetyltransferase, suggesting that acetylated EPS could be formed, as observed in some *Synechocystis* strains and other cyanobacteria (Flamm & Blaschek, 2010, 2014; Pereira et al., 2009).

Remarkably, Cluster 2 contains genes that might be involved in the production of lipopolysaccharides (LPS), peculiar extracellular polysaccharides formed by a polysaccharide backbone linked to a lipidic part (Greenfield & Whitfield, 2012; Simkovsky et al., 2012, 2016), as well as a EPS-related gene set that define a ABC transporter-dependent pathway, that was previously proposed to be preferentially used for LPS assembly/export in cyanobacteria (Simkovsky et al., 2016). In Clusters 1 and 2, the presence of genes encoding methyltransferases nearby genes encoding putative KpsM/KpsT ABC transporters is also particularly relevant, since methylated carbohydrate residues are important recognition signals for these type of transporters in order to allow the export of the polysaccharides (Cuthbertson et al., 2010).

In contrast to the gene clusters, the majority of the isolated *Synechocystis* EPS-related genes are not in a particular relevant genomic context in terms of EPS production. The exceptions are the *slr0728* (*wzy*) that is upstream to a gene encoding a glycosyltransferase (*slr0729*), and the genes *sll0574* (*kpsM*) and *sll0575* (*kpsT*), which are nearby and upstream of a gene encoding a sugar epimerase (*sll0576*). Moreover, some of the remaining putative EPS-related genes were even associated with other metabolic pathways based on their genomic context, such as *slr0896* (*wzx*), part of a cluster involved in mitigation of oxidative stress triggered by chemical agents (Babykin et al., 2003; Khan et al., 2016; Nefedova et al., 2003), and *slr0946* (*wzb*), which belongs to an operon involved in arsenate and cadmium tolerance in *Synechocystis* (Houot et al., 2007; Li et al., 2003; López-Maury et al., 2003).

Regarding the genes that might be related to the Synthase-dependent pathway, only homologs to *alg8* or *alg44* were identified in *Synechocystis* genome. The presence of an incomplete gene set related to this pathway is common among cyanobacteria (Pereira et al., 2013), even in *Synechococcus* sp. PCC 7002, that needs a Synthase-dependent pathway to produce cellulose for the cell envelope (Zhao et al., 2015). Therefore, this corroborates the hypothesis that cyanobacteria may not have a conventional Synthase-dependent pathway, or that different partners from the ones detected in other bacteria may complement it. The *alg8* and *alg44 Synechocystis* homologs are located nearby, in chromosomic regions, such as the pairs *sll1566* (*alg8*)/*sll1481* (*alg44*) and *sll1377* (*alg8*)/*sll1181* (*alg44*), or isolated, such as the other *alg8* copies (*sll1004* in the chromosome and *slr5056* in pSYSM). This organization is in agreement with the possibility of the Alg8 homologs work independently, as polymerization units, or cooperating with Alg44, a c-di-GMP-binding subunit (Whitney & Howell, 2013).

The *slr1875* (*exoD*) gene was also included in our *in silico* analyses, since previous studies showed that its knockout impaired EPS production in *Synechocystis* (Jittawuttipoka et al., 2013; Planchon et al., 2013a). This gene is isolated in *Synechocystis* chromosome, which is in agreement with what was previously observed for homologs in rhizobia (Janczarek, 2011; Skorupska et al., 2006). However, it is still unclear whether ExoD cooperates with the conventional EPS assembly/export pathways.

3.2. The transcription of EPS-related genes

3.2.1. Analysis of transcriptional profiles of EPS-related genes

In spite of the lack of studies addressing specifically the transcription of EPS-related genes in cyanobacteria, a large amount of high-throughput data is available regarding the whole *Synechocystis* transcriptome, obtained mainly by Microarrays (Hernández-Prieto et al., 2016; Mitschke et al., 2011), but also by a still smaller number of RNA-seq studies (Kopf et al., 2014). Therefore, the putative EPS-related genes were grouped according to the similarity of their transcriptional profiles (Fig. 3), obtained from 722 Microarray experiments and deposited in CyanoEXpress 2.3 (Hernández-Prieto et al., 2016). The genes that are in the plasmid pSYSM were excluded from the analysis, since no data was available in the database. In general, 3 main groups were detected, being *slr0067* (*wzc*/*kpsE*) separated from these groups.

Taking into account the results obtained from the genomic context analysis (Fig. 2), the co-expression data from CyanoEXpress 2.3 and the information available in the literature (Table S2), some similarities between the members of each group were found: i) Group 1 includes putative EPS-related genes previously experimentally associated with EPS production, or nearby and/or co-expressed with genes involved (or predicted to be involved) in EPS production/modification; ii) Group 2 includes genes that after being knocked out did not cause alterations in EPS production, and/or that were shown to be involved or co-expressed with genes involved in non-EPS related pathways; iii) Group 3 includes two genes, *slr0328* (*wzb*) and *sll1481* (*alg44*), which are most probably involved in a wide range of metabolic pathways. The *slr0328* (*wzb*) gene encodes a phosphatase envisaged to be important for the regulation of Sll0923 (Wzc) activity, and consequently, EPS export (Pereira et al., 2019), but it might also interact with many other targets (Lescop et al., 2006), such as proteins involved in photosynthesis (Mukhopadhyay & Kennelly, 2011). In the case of *sll1481* (*alg44*), it is likely that the encoded protein either is part of or interacts with several non-EPS related ABC transporters (Gonçalves et al., 2018; Kwon et al., 2010; Huang et al., 2002b), e.g. for the secretion of butanol (Zhu et al., 2013).

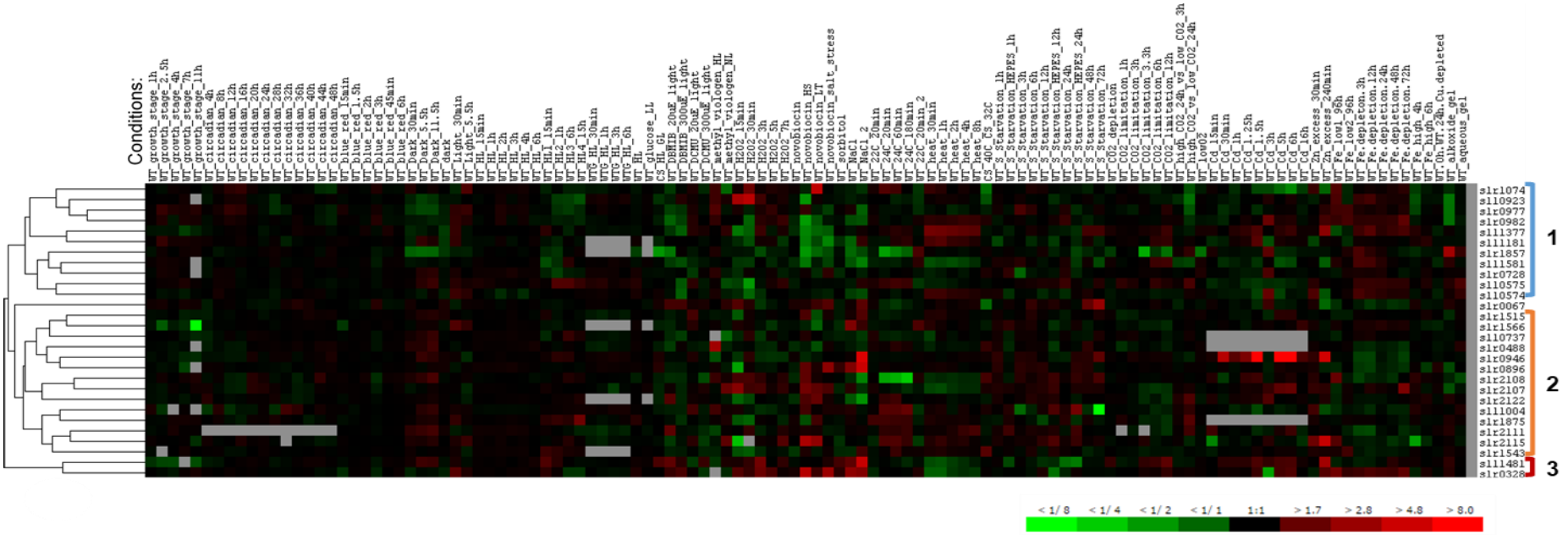

Group	Putative EPS-related genes	Description
1	*slr1074, sll0923, slr0977, slr0982, sll1377, sll1181, sll1581, slr1875, slr0728, sll0575, sll0574*	Genes in relevant genomic context, previously associated to EPS production, and/or co-expressed with genes important for EPS production or modification
2	*slr1515, slr1566, sll0737, slr0488, slr0946, slr0896, slr2108, slr2107, slr2122, sll1004, slr2111, slr2115, slr1543, slr1875*	Genes associated or co-expressed with genes involved in non-EPS related pathways, and/or their knockout does not affect EPS production
3	*slr0328, sll1481*	Others

Figure 3. Hierarchical clustering of *Synechocystis* EPS-related genes using expression data from 722 microarrays (31 independent studies, data from CyanoEXpress v.2.3.). Clustering was based on complete linkage, using Spearman's rank correlation as similarity measure. Differential expression was displayed as heat maps, using the color range from green to red, with shades of green or red indicating negative or positive expression changes in relation to the reference sample. No differences in expression are indicated by black, while grey represents missing data. The dendrogram attached to the heat map display the cluster structure, with the length of the branches used as a measure of the similarity between genes, based on their expression. The table below the heat maps indicates the 3 main groups observed.

Overall, our analyses suggested that the best candidate genes to study and manipulate EPS assembly and export in *Synechocystis* are in Group 1. Nevertheless, some of the putative EPS-related genes from Group 2 might: i) play a redundant role under certain conditions, or ii) be dedicated to the production of particular types of polysaccharides, such as the O-antigen of LPS. For example, the single gene copies *slr2111* (*kpsF*), *slr2122* (*kpsU*) and *slr2115* (*kpsC/kpsS*) are homologs of genes associated to the synthesis of the oligosaccharide 3-deoxy-d-manno-oct-2-ulosonic acid (KDO), which is usually found in LPS or specific bacterial EPS exported by the ABC transporter-dependent pathway (Willis & Whitfield, 2013), but predicted to be unessential for the formation of the majority of cyanobacterial polysaccharides (Gemma et al., 2016; Durai et al., 2015).

The analysis of Microarray data of the putative EPS-related genes allowed also the identification of other genes showing significantly similar transcriptional profiles to the ones putatively involved in Wzy- and ABC-dependent pathways (list of co-expressed genes in Tables S4 and S5). The majority of the genes co-expressed with two or three of the EPS-related genes in Group 1, encode proteins that can be related to EPS/LPS production, based on their function/predicted function (Table S5). Moreover, a network was created connecting the putative EPS-related genes that share at least two co-expressed genes (Fig. 4).

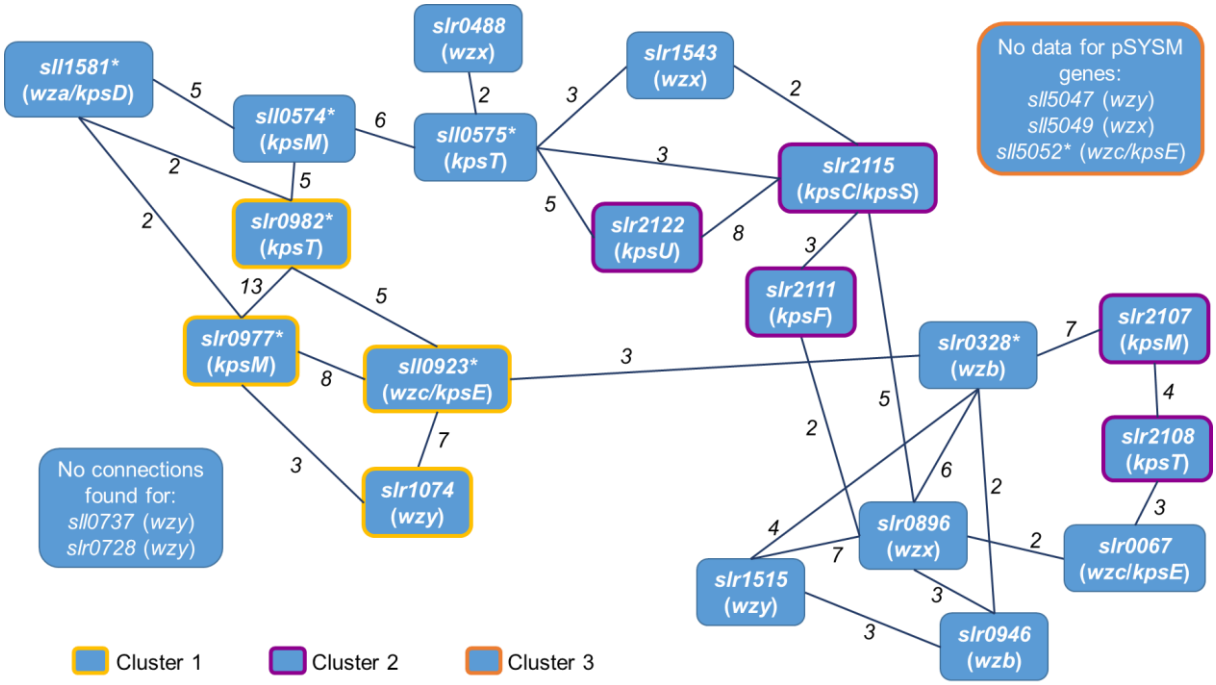

Figure 4. Number of *Synechocystis* genes that can be co-expressed with the EPS-related genes (represented by blue boxes). Transcriptional profiles were analyzed using CyanoEXpress v.2.3, considering Microarray data from experiments with wild-type cultures exposed to environmental perturbations. Numbers next to the lines represent the number of co-expressed genes (≥2) with Pearson correlation coefficient higher than 0.4. Genes from the 3 genomic clusters (see Fig. 1) are highlighted by different colored outlined boxes. *, indicates genes associated to EPS production (experimentally). Detailed list of the co-expressed genes is available in Table S5.

The genes *slr0982* (*kpsT*) and *slr0977* (*kpsM*) share the highest number of co-expressed genes (13), and only *slr0728* and *sll0737* (*wzy* gene copies) do not have a connection to other EPS-related gene. In addition, and in agreement with the envisaged interaction between their encoded proteins (Pereira et al., 2019), *slr0923* (*wzc*) is connected to *slr0328* (*wzb*), in spite of *slr0923* shares a higher number of co-expressed genes with other members from the Cluster 1. Moreover, the single gene copy *slr2115* (*kpsC/kpsS*) is connected to the other EPS-related genes putatively involved in KDO synthesis and the ABC transporter-dependent mechanism, *slr2122* (*kpsU*) and *slr2111* (*kpsF*). However, none of these three genes is connected with *slr2107* (*kpsM*) or *slr2108* (*kpsT*), that are in the same genomic cluster and are predicted to be involved in the same pathway. In contrast, *slr2122* (*kpsU*) and *slr2115* (*kpsC/kpsS*) are connected to *sll0575* (*kpsT*). These results support previous findings from Fisher et al., 2013, suggesting that different KpsM/KpsT complexes can cooperate with the other components of the ABC transporter-dependent mechanisms, since different KpsT proteins might encode proteins with affinity for different substrates.

Altogether, our results indicated also that the *Synechocystis* putative EPS-related genes are not usually transcribed as operons, even in the case of the genes that are in clusters. This scenario have been also previously observed for other *Synechocystis* gene sets involved in same biosynthetic pathways (Kaneko & Tabata, 1997). Moreover, this is in agreement with the presence of redundant EPS-related gene copies that may be expressed only in specific conditions, and/or with the presence of alternative routes to the conventional bacterial EPS assembly/export pathways. In fact, the hypothesis of functional gene redundancy and crosstalk between the different pathways was also further supported after the characterization of knockout mutants in some of the putative EPS-related genes (Pereira et al., 2019). These mutants slightly decreased (Δ*sll0923-wzc*, Δ*slr0328-wzb*) or even maintained EPS production (Δ*sll0737-wzy*, Δ*sll5049-wzx* and Δ*slr2107-kpsM*) compared to the wild-type, and maintained or increased the transcription levels of other gene copies (Fig. 5).

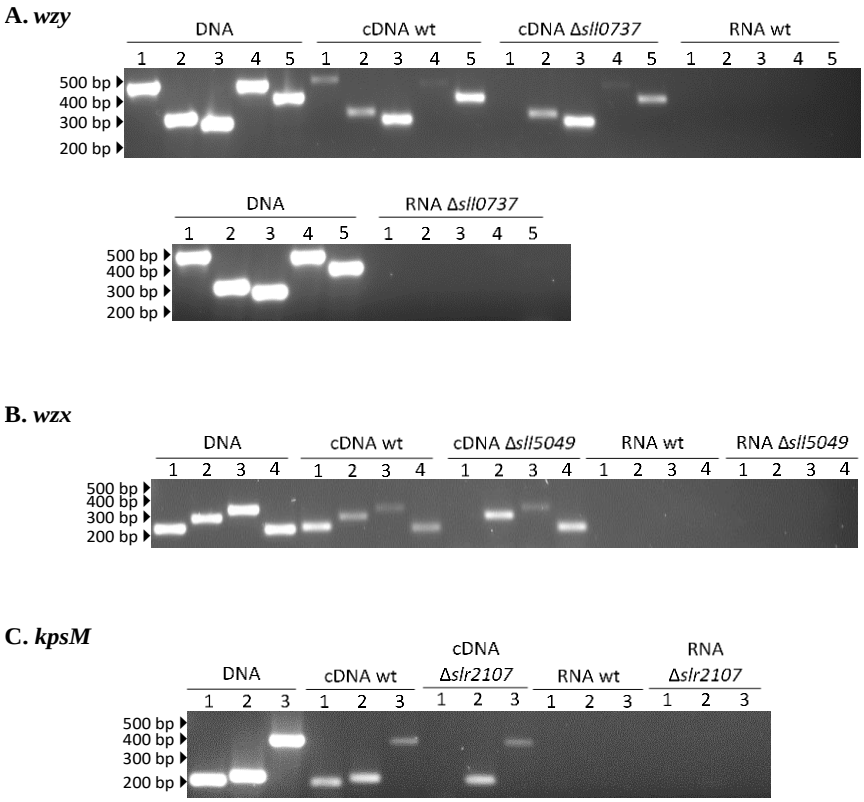

Figure 5. Transcription profiles evaluated by RT-PCR of the putative *wzy* (A), *wzx* (B) and *kpsM* (C) gene copies in *Synechocystis* sp. PCC 6803 wild-type (wt) and Δ*sll0737* (*wzy*), Δ*sll5049* (*wzx*) and Δ*slr2107* (*kpsM*) mutants, respectively. Samples for RNA extraction were collected 6h into the light period of the 12h light (50 µE m^{-2} s^{-1})/12h dark growth regimen at 30 ºC. The cDNAs were produced with random primers and used in PCR amplifications with specific primer pairs. Expected size of PCR products: *wzy*: 1 – *sll0737* (465 bp); 2 – *slr0728* (288 bp); 3 – *slr1515* (256 bp); 4 – *sll5074* (440 bp); 5 – *slr1074* (368 bp); *wzx*: 1 – *sll5049* (223 bp); 2 – *slr0488* (274 bp); 3 – slr0896(323 bp); 4- *slr1543* (208 bp); *kpsM*: 1 – *slr2107* (203 bp); 2 – *slr0977* (220 bp); 3 – *sll0564* (396 bp). Amplification of the housekeeping gene *rnpb* was used as control (*adapted from* Pereira et al., 2019).

An analysis of genes that may be co-expressed with the *Synechocystis* putative EPS-related genes was also performed using the RNA-seq data from Kopf et al., 2014, showing similar results to the ones obtained using the Microarray data (Table S6). In addition, since the study of Kopf et al., 2014 included also the transcriptional profiles from non-coding RNAs (ncRNAs), it was possible to identify several ncRNAs co-expressed with the putative *Synechocystis* EPS-related genes (Table S6). Six ncRNAs are co-expressed with 2 or more EPS-related genes, and other two are even located immediately upstream the gene and in the same transcriptional unit, SyR5 is upstream *sll0737* (*wzy*) and ncr0050 is upstream *slr0728* (*wzy*). Therefore, they emerged as the first ncRNA candidates that may be involved in the regulation of EPS production in cyanobacteria, although other ones were previously shown to control the production of other *Synechocystis* polysaccharidic polymers, such as glycogen (de Porcellinis et al., 2016) and murein, the fundamental part

of peptidoglycan (Georg et al., 2009). In agreement, previous studies have reported the involvement of ncRNAs in the regulation of EPS production in a few bacteria, such as *E. coli* (Wang et al., 2005), *Klebsiella* (Huang et al., 2012) or *Streptococcus* (Mao et al., 2016).

3.2.2. Identification of EPS-related genes' promoter regions and possible transcriptional regulators

Transcriptional regulation is one of the most essential and extensive regulatory steps in the entire bacterial EPS production process, involving two-component signaling, transduction pathways, quorum sensing, alternative RNA polymerase σ-factors and anti-σ-factors, as well as integration host factor (IHF)-dependent and secondary messengers (recently reviewed in Schmid et al., 2015). However, in cyanobacteria, only very few studies addressed this issue, and mainly in filamentous strains (Gonzalez et al. 2019; Campbell et al., 2015; López-Igual et al., 2012; Yoshimura et al., 2007).

Initially, the search for transcriptional regulators of the *Synechocystis* EPS-related genes was performed using the RegPrecise 3.0 database. However, the only hit retrieved was the transcription factor Sll1957 (ArsR), which regulates the transcription of *slr0946* (*wzb*) and other genes in the same operon, dedicated to arsenate tolerance (Li et al., 2003; López-Maury et al., 2003). This operon can be also indirectly regulated by Slr1738 in order to promote cadmium tolerance (Houot et al., 2007). Moreover, there is only one more regulatory network described in the literature involving a putative *Synechocystis* EPS-related gene, the *slr0896* (*wzx*), which is regulated by Slr0895 (PrqR), playing a role in multidrug efflux (Babykin et al., 2003; Nefedova et al., 2003).

To perform a more comprehensive prediction of possible transcriptional factors (TFs) regulating the putative EPS-related genes, their promoter regions were defined (for more details see *Material and Methods section 2.3.* and Supplementary data S1) and used to identify transcription factor binding sites (TFBS). In total, 27 different types of TFs were found (Table 1), and several global transcription regulators (e.g. RpoD-like, LexA or Lrp regulators) were predicted to bind to these promoter regions.

The RpoD transcription regulators represent a large group of sigma factors from σ^{70} family, since they are similar to the sigma factor 70 from *E. coli* (Feklístov et al., 2014). Although *Synechocystis* has 9 different sigma factors from this family, the ones belonging to Group(s) 3/4 (SigF, SigG, SigH, SigI) are the best candidates to control EPS production, since they are usually dedicated to the expression of regulons assigned to the survival under stress and to the maintenance/modification of the cell envelope (Imamura & Asayama, 2009). SigF, in particular, is the most similar protein to the only transcriptional regulator undoubtedly related to EPS production in cyanobacteria, the *Anabaena*'s SigJ

(Yoshimura et al., 2007), which controls the transcription of genes involved in the first steps of EPS production (e.g. glycosyltransferases), as well as in EPS assembly/export.

Table 1. Transcription factors predicted by BPROM software to bind to the promoter regions of *Synechocystis* EPS-related genes, and their respective binding sites (TFBS).

Transcription factor type	TFBS	EPS-related genes
Lrp (leucine-responsive global regulator)	TTTCTTTT	*sll1581, sll5050*
	TTGACAAT	*slr0328*
	ATTTATTA	*slr1074*
	ATTTTTTT TATTTTTT	*slr0982*
RpoD15 (RNA polymerase sigma factor)	CCTCTCCC	*slr0728*
ArcA (aerobic respiration control regulator)	TTAATTAA	*slr0946, slr2115*
	AATAAAAA	*slr1074*
GcvA (glycine cleavage activator)	AACTAATT	*slr0946*
RpoD17 (RNA polymerase sigma factor)	CTAAACCA	*sll0923*
	ACTTTTGT	*slr1515*
	AAAAATAG	*slr0728*
	TTTATAAT	*slr1074*
	TTTGTTTT	*slr0896*
	TTTTCCTT	*slr0977*
	CGTTGTAA	*sll0574*
Fnr (fumarate/nitrate reduction regulator)	ATTTGTTT	*slr0896*
Crp (cAMP-regulatory protein)	ATCACAAA	*sll5047*
	TCACACTT	*slr0977*
OxyR (oxidative stress regulatory protein)	GATTAATT	*sll0737, slr0328*
TyrR (aromatic amino acid biosynthesis and transport regulon regulator)	TAAATAAA	*sll0923, sll0574*
Ihf (integration host factor)	AAATAAAA	*sll0923, sll0574*
	TTTTATTT	*slr0977*
PhoB (pho regulon activator under phosphate limitation)	TGTCATCA	*slr1875*
	TTTTCATA	*slr0896*
	TTTAATTA	*slr0896, slr2115*
LexA (transcriptional repressor of SOS regulon)	ATAGATAA	*slr0728*
Hns (heat-stable nucleoid-structuring protein repressor)	TAATTTAA	*slr0728*
RpoD16 (RNA polymerase sigma factor)	TTTTTATA	*slr1074*
OmpR (osmolarity response regulator)	TTCTTTTT	*sll0737*
	TCATATTT	*slr0896*
	GTTACATA	*slr2107*
ArgR (arginine biosynthesis repressor)	TTATAATT ATAAAAAT	*slr1074*
	TAATTCAT	*slr2111*
Fur (ferric iron uptake repressor)	ATAATTGT	*slr1074*
	TAATGCTT	*slr2108*
RpoD18 (RNA polymerase sigma factor)	TTAATTTT	*slr2107, sll0575*
Fis (factor for inversion stimulation regulator)	AATTATTT	*slr0896, slr0982*
	TTATCTAA	*slr2107*
	ACAATTAT	*slr0982*
MetR (methionine biosynthesis regulator)	TTTTTTCA	*slr0896*
	CAAATTTT ATTTTTCC	*slr0977*
CpxR (transcription of stress-combative genes activator)	GTAAATTA	*slr0488*
AraC (arabinose metabolism regulator)	TCCTTGTT	*slr0977*
ArgR2 (arginine catabolic regulator)	TTTATTTT TTTTTATT	*slr0977*
RpoD19 (RNA polymerase sigma factor)	TTTCATAT	*slr0896*
NagC (N-acetylglucosamine-inducible nag divergent operon repressor)	TTTAATTT	*slr2107, sll0575*
DeoR (deoxyribose-5-phosphate-inducible deoxyribose operon repressor)	AATTTTAT	*sll0575*
Tus (inhibitor of replication at Ter - terminator protein)	TAGTATGT	*slr1875*

Some TFs controlling adaptative responses to stress conditions (e.g. OxyR, CpxR, PhoB or Fur) were also predicted to bind to the EPS-related genes' promoter regions, which supports that EPS production in *Synechocystis* might be modulated by environmental stresses as it occurs in several cyanobacteria (Chakraborty & Pal, 2014; Chen et al., 2009; Ozturk and Aslim, 2010; Tamaru et al., 2005). Moreover, the indication that Crp and Fnr transcription factors may regulate some of these genes suggests that the secondary messengers cAMP and c-di-GMP (the main modulators of Crp/Fnr activity) might also be involved, similarly to what was found for other bacteria (Jenal et al., 2017; O'Toole & Wong, 2016). In agreement, cAMP and c-di-GMP control cell motility in *Synechocystis* (Savakis et al. 2012; Yoshimura et al., 2002) and other processes intrinsically dependent on EPS production in other cyanobacteria, e.g biofilm formation (Enomoto et al. 2014; Ohmori et al., 1992) and heterocyst differentiation (Neunuebel & Golden, 2008; Imashimizu et al., 2005).

Using the previous defined promoter regions (Supplementary data S1), DNA-protein affinity assays were performed to pull-down TFs binding to 3 *Synechocystis* putative EPS-related genes: *sll0737* (*wzy*), *sll5049* (*wzx*) and *slr2107* (*kpsM*). However, LexA was the only regulator that was consistently found binding to the promoter regions tested, even using protein extracts from cells growing under different light regimens (Fig. 6).

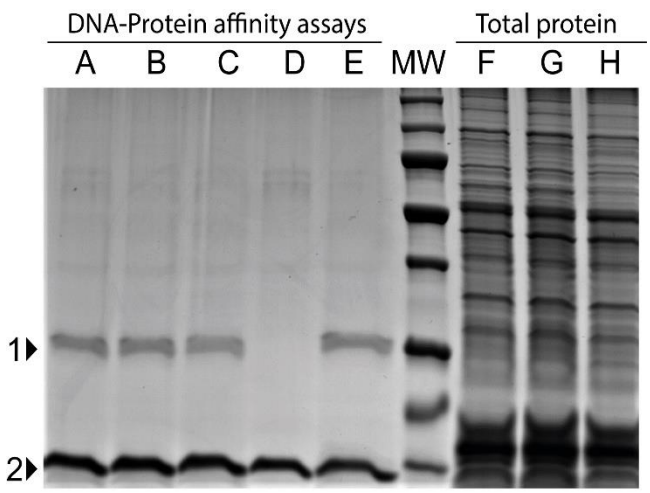

Figure 6. DNA-protein affinity assays using the promoter region of *sll5049* (*wzx*) of *Synechocystis* sp. PCC 6803 (A-D). Samples for protein extraction were collected 6 h into the light phase (A, F) and 6 h into the dark phase (B, G) of the growth regimen, or from cells growing at continuous light (C, H). Assays performed without protein extract (D) and with the promoter region of *hox* gene - binding region of LexA (E) were used as controls. Total protein extracts (F, G, H). MW, Precision Plus Protein™ All Blue Standards (BioRad); 1, LexA protein (≈25 kDa); 2, Streptavidin band from Dynabeads (Invitrogen).

LexA is a well-known bacterial transcription factor that controls stress-oxidative responses and DNA repairing mechanisms (Butala et al., 2009). However, in *Synechocystis* and other freshwater cyanobacteria, LexA is described as a global regulator dedicated to the control of other physiological processes, such as carbon metabolism (Domain et al., 2004), fatty acid biosynthesis (Kizawa et al., 2017), cell motility and glucosylglycerol metabolism (Kizawa et al., 2016), and the expression of the bidirectional hydrogenase (Oliveira & Lindblad, 2005). Furthermore, the proteomic analysis from Kizawa et al., 2016

of a *Synehocystis* Δ*lexA* mutant also suggested that LexA may be directly or indirectly involved in the control of EPS production, since the mutant showed altered levels of enzymes involved in sugar activation/modification (e.g. glycosyltransferases), cell envelope maintenance, secretion systems, as well as of several transcriptional regulators and sensory mechanisms.

Altogether, our results suggested that a complex net of transcriptional factors must regulate the *Synechocystis* EPS-related genes, namely global regulators such as LexA and alternative sigma factors.

3.3. *In silico* analysis of the EPS-related proteins

3.3.1. Protein domain organization and protein subcellular localization

In previous studies, Pereira et al., 2015, 2013 described *Synechocystis* putative EPS-related proteins based on the identification of specific sequence domains similar to the ones found in other bacterial proteins. Using this information and data from *in silico* tools (SMART, TMHM and SOSUI), the main structural/functional domains of the *Synechocystis* putative EPS-related proteins were organized according to their protein primary structure (Fig. 7). In spite of the majority of the proteins from the same EPS-related protein family (i.e. Wza, Wzb, Wzc, etc..) have a similar domain organization, a few of them are clearly distinct, such as Slr0067 (Wzc/KpsE) and Sll0737 (Wzy). The Slr0067 (Wzc/KpsE) does not have a Wzz domain associated to the correct function of a Wzc/KpsE protein (Cuthbertson et al., 2009), which supports our previous results (*section 3.2.1.*) indicating that this protein may not be involved in EPS-production. Moreover, in the Wzx family, two distinct subgroups can be depicted in terms of domain organization, one including Sll5049 and Slr0488 and another with Slr1543 and Slr0896, suggesting that they have different functions. Since Slr1543 and Slr0896 seem to be mainly involved in the multidrug efflux/tolerance (Ongley et al., 2016; Pengelly, 2008), Sll5049 and Slr0488 represent the best Wzx candidates for EPS production in *Synechocystis*. Another interesting observation was that Slr1074 (Wzy) is the only protein in the Wzy family having the exact Wzy_C sequence domain, which could be particularly relevant for the correct function of a Wzy protein and supports that *slr1074* is the most important *wzy* gene copy in terms of EPS production in *Synechocystis* (since it belongs to the aforementioned Group 1, *section 3.2.1.*).

Regarding the proteins putatively involved in Synthase-dependent pathways, each protein family (Alg8/BscA and Alg44/BscA) display an identical protein domain organization and high aminoacidic sequence homology. Furthermore, their coding sequences are also similar to the ones found for cellulose synthases from plants, which was also previously observed for other cyanobacteria (Nobles et al., 2001).

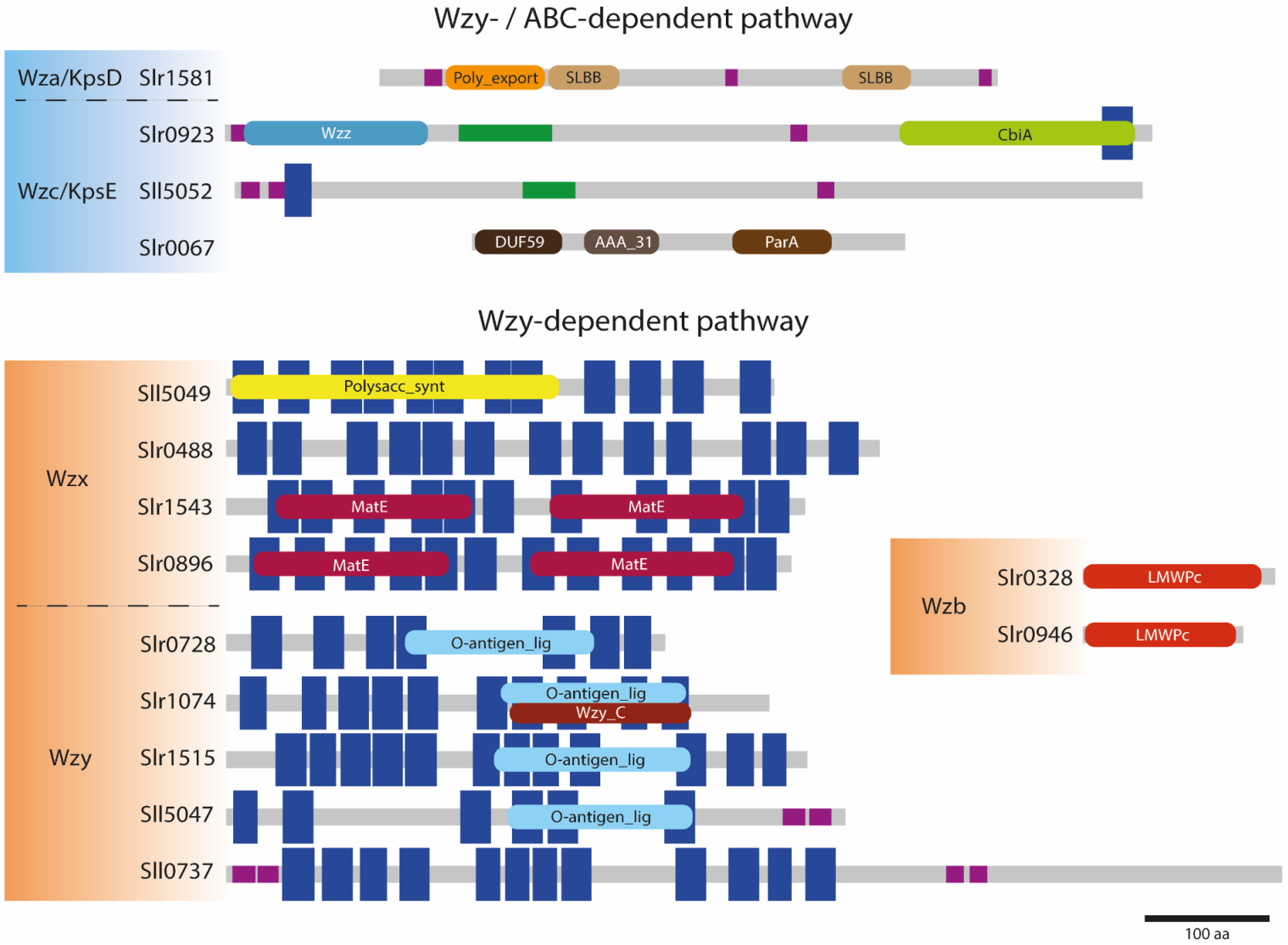

(Figure 7. continued)

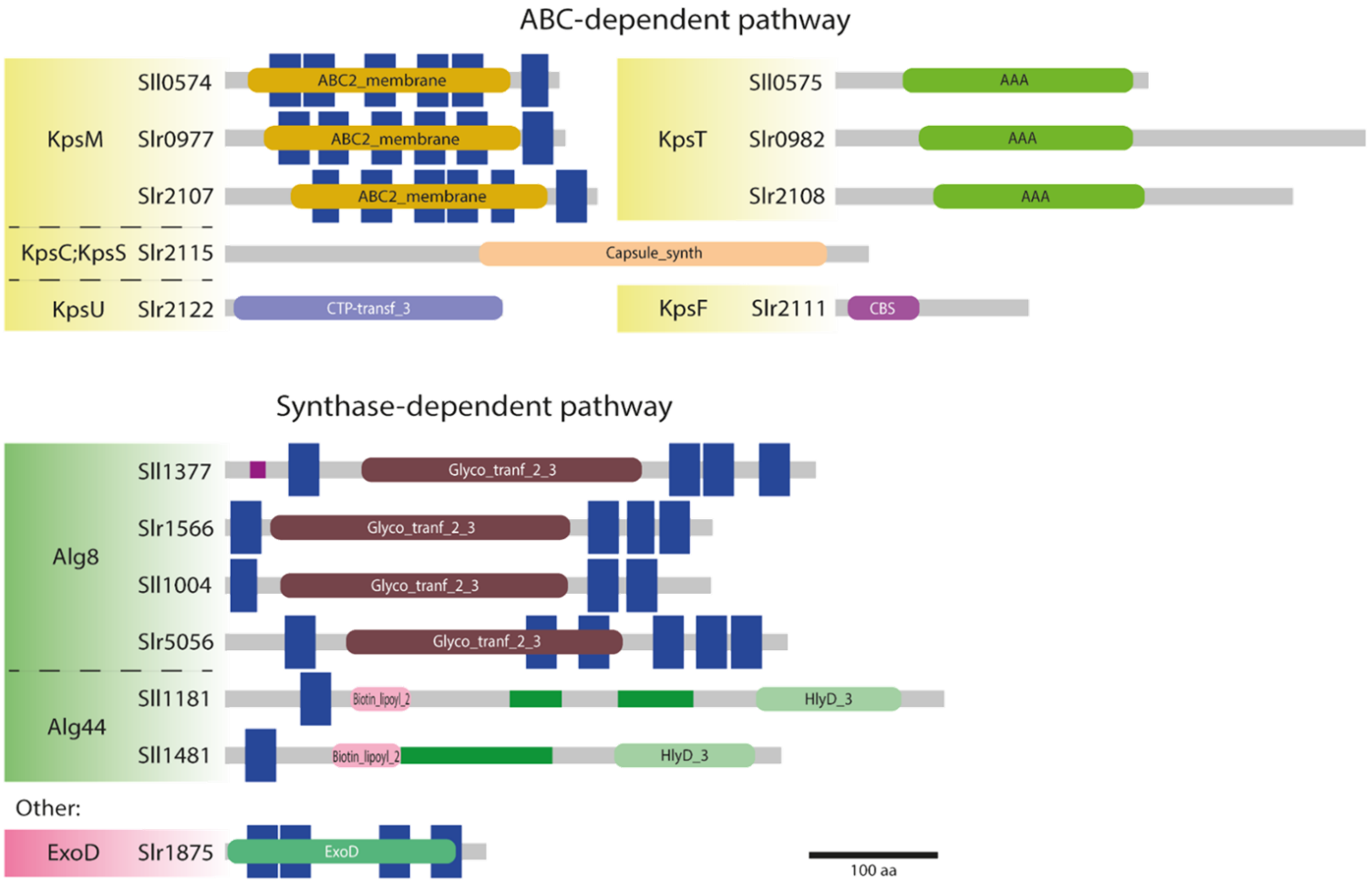

Figure 7. Protein domain organization of the putative EPS-related proteins from *Synechocystis* sp. PCC 6803. Proteins are grouped according to the EPS-related pathway(s) that they are expected to be involved: Wzy- or/and ABC-dependent (blue), Wzy-dependent (orange), ABC-dependent (yellow), Synthase-dependent (green) and Other (pink). Blue squares represent transmembrane domains, dark pink squares represent low complexity domains and green areas are prone to adopt a coiled-coil conformation (data obtained from SMART and TMHMM tools). Other protein functional domains are highlighted in different colored boxes.

The subcellular localization of the putative EPS-related proteins was predicted using the most 3 popular platforms for this purpose, CELLO, PSORTb, and QuickGO (Table 2). In general, their predicted location was in agreement with the common schematic model described for the conventional bacterial EPS-related pathways (see *Chapter I, section 2.2.*) and with experimental data previously reported for some of the proteins (Table S2).

Table 2. Subcellular localization of the EPS-related proteins according to CELLO (Yu et al., 2006), PSORTb 3.0 (Yu et al., 2010) and QuickGO (EMBL-EBI) predictions. Grey shades highlight proteins predicted to be located in agreement with Pereira et al., 2015.

EPS-related protein	CELLO	PSORTb	QuickGO
Sll1581 (Wza/KpsD)	Outer membrane	Periplasmic	Membrane
Slr0328 (Wzb)	Cytoplasmic	Cytoplasmic	Unknown
Slr0946 (Wzb)	Cytoplasmic	Cytoplasmic	Unknown
Sll0923 (Wzc/KpsE)	Outer membrane	Inner membrane	Inner membrane
Sll5052 (Wzc/KpsE)	Inner membrane	Inner membrane	Inner membrane
Slr0067 (Wzc/KpsE)	Periplasmic / Inner or Outer membrane	Inner membrane	Unknown
Sll0737 (Wzy)	Inner membrane	Inner membrane	Membrane
Sll5047 (Wzy)	Inner membrane	Inner membrane	Membrane
Slr0728 (Wzy)	Inner membrane	Inner membrane	Membrane
Slr1074 (Wzy)	Inner membrane	Inner membrane	Membrane
Slr1515 (Wzy)	Inner membrane	Inner membrane	Membrane
Sll5049 (Wzx)	Inner membrane	Inner membrane	Membrane
Slr0488 (Wzx)	Inner membrane	Inner membrane	Inner membrane
Slr0896 (Wzx)	Inner membrane	Inner membrane	Inner membrane
Slr1543 (Wzx)	Inner membrane	Inner membrane	Inner membrane
Slr2115 (KpsC/KpsS)	Cytoplasmic/Inner membrane	Inner membrane	Unknown
Slr2111 (KpsF)	Cytoplasmic	Unknown	Unknown
Sll0574 (KpsM)	Inner membrane	Inner membrane	Inner membrane
Slr0977 (KpsM)	Inner membrane	Inner membrane	Inner membrane
Slr2107 (KpsM)	Inner membrane	Inner membrane	Membrane
Sll0575 (KpsT)	Cytoplasmic	Inner membrane	Unknown
Slr0982 (KpsT)	Cytoplasmic	Inner membrane	Unknown
Slr2108 (KpsT)	Cytoplasmic	Inner membrane	Unknown
Slr2122 (KpsU)	Cytoplasmic	Cytoplasmic	Unknown
Sll1004 (Alg8/BcsA)	Inner membrane	Inner membrane	Membrane
Sll1377 (Alg8/BcsA)	Inner membrane	Inner membrane	Inner membrane
Slr1566 (Alg8/BcsA)	Inner membrane	Inner membrane	Membrane
Slr5056 (Alg8/BcsA)	Inner membrane	Inner membrane	Membrane
Sll1181 (Alg44/BcsA)	Outer membrane	Inner membrane	Membrane
Sll1481 (Alg44/BcsA)	Outer membrane	Cytoplasmic	Membrane
Slr1875 (ExoD)	Inner membrane	Inner membrane	Inner membrane

The most incomplete prediction was obtained using QuickGO (EMBL-EBI), mainly because the gene ontology (GO) term corresponding to “cytoplasm location” is not assigned to the majority of *Synechocystis* cytoplasmic proteins in the database. In contrast, the protein sorting was particularly accurate using the PSORTb software, with the exception of the three KpsT proteins and the Sll1481 (Alg44). In the case of KpsT proteins, they are expected to be located at the cytoplasm, which is in agreement with the results obtained using CELLO but not with PSORTb or QuickGO. However, since these proteins have a

small aminoacidic sequence that can be highly variable, inaccurate *in silico* predictions are expected, frequently leading to the use of the *kpsM* gene for more robust analyses, since it is usually immediately downstream of *kpsT* and encodes the other subunit of the ABC-transporter complex (Pereira et al., 2015; Cuthbertson et al., 2010). Regarding Sll1481 (Alg44), previous studies placed this protein at the plasma membrane, through either gel-based or shotgun proteomics of isolated membrane fractions (Pisareva et al., 2011; Huang et al., 2002a), clearly contradicting the *in silico* predictions.

3.3.2. Putative EPS-related protein-protein interactions (PPIs)

Protein-protein interactions (PPIs) involving *Synechocystis* putative EPS-related proteins were firstly predicted using the InAct database (EMBL-EBI, Orchard et al., 2014). However, only very few PPIs were detected and only for 9 out of the 31 EPS-related proteins (Table 3), most probably due to the stringent prediction method of the database, mainly based on experimental data available in the literature. Therefore, all PPIs found were the ones described in the large-scale yeast two-hybrid assay performed by Sato et al., 2007, which only addressed PPIs involving 28% of the *Synechocystis* proteome, considering 3 very specific protein groups (two-component signal transducers, *Arabidopsis thaliana* homologs and proteins assigned with unknown function), which includes only very few membrane-associated proteins.

Table 3. Predicted protein-protein interactions involving EPS-related proteins, based on the data from IntAct database (EMBL-EBI, Orchard et al., 2014).

EPS-related protein	Interactors	Interactor function
Sll5052 (Wzc/KpsE)	Slr0848	Unknown
	Slr0020	ATP-dependent DNA helicase
Slr0067 (Wzc/KpsE)	Slr0008	Carboxyl-terminal-processing protease
Sll0737 (Wzy)	Slr1232	Unknown
	Slr1391	Unknown
Slr1074 (Wzy)	Slr1618	Methyltransferase
Slr2115 (KpsC/kpsS)	Sll0861	N-acetylmuramic acid 6-phosphate etherase
Slr2111 (KpsF)	Slr0514	Unknown
	Slr1393	Sensory transduction histidine kinase
Slr0977 (KpsM)	Sll1446	Unknown
Slr2122 (KpsU)	Slr0020	ATP-dependent DNA helicase
	Sll0252	Unknown (formation of a cellular spore)
Slr1566 (Alg8/BcsA)	Slr2099	Hybrid sensory kinase
	Sll1967	Methyltransferase

To perform a broader analysis, the STRING database of known and predicted PPI networks was used, considering direct (physical) and indirect (functional) associations of the *Synechocystis* putative EPS-related proteins and respective homologs (Supplementary data S2). In this case, a larger number of PPIs were found, and several of them including other proteins involved (or predicted to be involved) in EPS/LPS biosynthesis (Fig. 8), with the exception of the PPIs identified for Sll0737 (Wzy), Slr0896 and Slr1543 (both Wzx),

Sll1181 and Sll1481 (both Alg44/BscA), and Slr1875 (ExoD). No data was available for the 3 proteins encoded by genes in pSYSM.

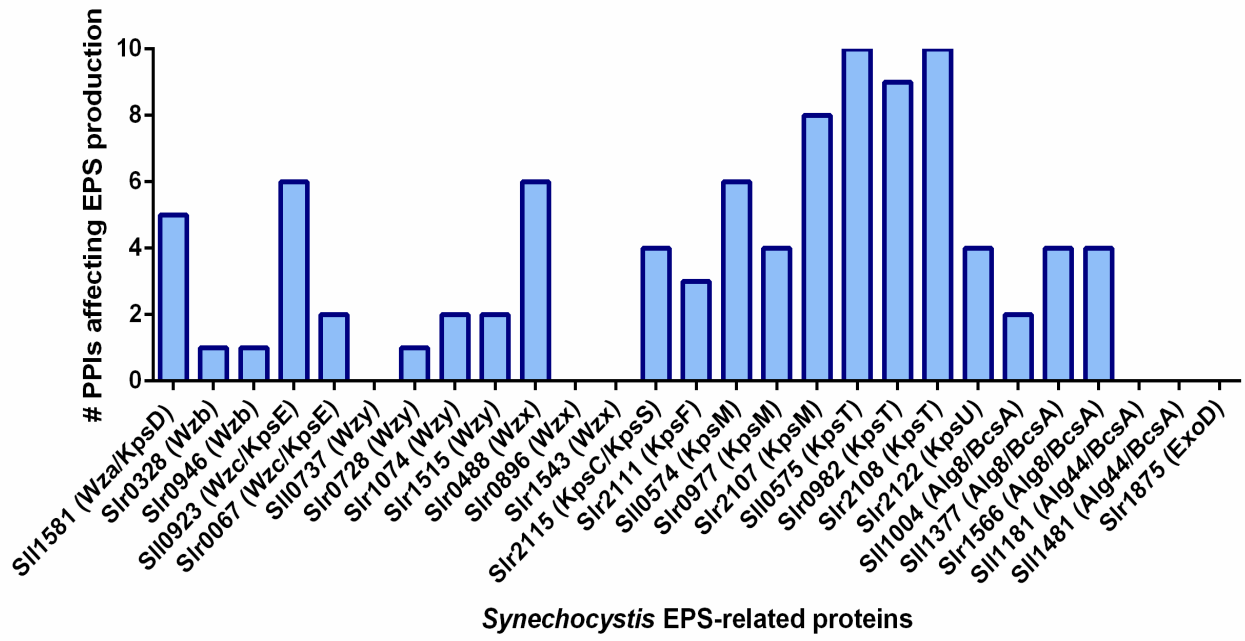

Figure 8. Number of predicted protein-protein interactions (PPIs) involving the *Synechocystis* putative EPS-related proteins and other proteins that are involved (or predicted to be involved) in EPS production, based on the data from STRING database (Szklarczyk et al., 2018). Detailed description of the interactors is available in Supplementary data S2.

As expected, some of the putative EPS-related proteins associated to one of the conventional EPS-related pathways are usually in the same PPI network, such as the KpsM and KpsT proteins (from ABC transporter-dependent pathway), or the Wza, Wzb and Wzc proteins (from Wzy-dependent pathway). In agreement, we demonstrated *in vitro* that Slr0328 (Wzb) can interact to and dephosphorylate Sll0923 (Wzc) (Pereira et al., 2019). Moreover, a PPI network was also observed between Slr2115 (KpsC/KpsS), Slr2122 (KpsU) and Slr2111 (KpsF), which is in agreement with the results obtained from the transcriptional profile analysis indicating that they are involved in a same pathway (*section 3.2.1.*). However, although previous studies showed *in vivo* and *in vitro* an interaction between Slr2111 (KpsF) and the photoreceptor Slr1393, involved in chromophorylation (He et al., 2018; Chen et al., 2012), this PPI was not found in our *in silico* analysis. Nevertheless, distinct PPI networks were found for the different gene copies encoding putative Wzc, Wzy and Wzx proteins. In general, Sll0923 (Wzc), Slr1074 (Wzy) and Slr0488 (Wzx) have a higher number of predicted PPIs involving proteins related (or predicted to be related) to EPS production compared to their counterparts, which in turn have a vast portfolio of interactors, but none or very few associated with EPS production. These findings support that Sll0923 (Wzc), Slr1074 (Wzy) and Slr0488 (Wzx) are among the most promising candidates to be involved in *Synechocystis* EPS production.

Regarding the proteins putatively involved in the Synthase-dependent pathway, Alg8 and Alg44 homologs were not found together in the same PPI network, and they also do not share the same interactors (Supplementary data S2). In addition, putative Alg8 proteins are in PPI networks with proteins involved (or predicted to be involved) in EPS production, while the interactors of Alg44 proteins are mainly involved in non-EPS related transport systems (with ABC-type and other transporters). Altogether, these results suggested that the *Synechocystis* putative Alg8 and Alg44 may function as independent units, being Alg8 homologs the ones most probably involved in EPS production.

3.3.3. Other proteins involved in EPS production

As aforementioned in the previous sections, a wide range of players are expected to be involved in *Synechocystis* EPS production, namely enzymes with functional domains that degrade, modify, or create glycosidic bonds on glycoconjugates, oligo- and/or polysaccharides, well-known as Carbohydrate-Active enzymes (CAZymes, Lombard et al., 2014). In *Synechocystis* sp. PCC 6803, a total of 103 CAZymes were identified (Table S7), belonging to 4 families (Fig. 9): i) glycosyltransferases (GTs), responsible for the formation of glycosidic bonds from phosphor-activated sugar donors to specific acceptor molecules; ii) glycosyl hydrolases (GHs), that catalyze the hydrolysis of glycosidic bonds in O-, N- and S-linked glycosides; iii) carbohydrate esterases (CEs), that hydrolyze carbohydrate esters by diacylation and may facilitate GHs action on complex sugars; and iv) carbohydrate-binding modules (CBMs), that can be catalytic or non-catalytic sugar binding proteins.

CAZyme family	Protein classes																
Glycoside hydrolase	**3**	**9**	**13**	**23**	**38**	**57**	**77**	**100**	**102**	**104**	**116**	**nc**					
Number of sequences	1	1	4	1	1	2	1	1	1	2	1	2					
Glycosyltransferase	**1**	**2**	**4**	**5**	**9**	**19**	**20**	**21**	**25**	**26**	**28**	**35**	**39**	**41**	**51**	**83**	**nc**
Number of sequences	2	23	25	2	1	1	1	1	1	3	1	2	1	1	3	3	4
Carbohydrate esterase	**11**																
Number of sequences	1																
Carbohydrate-binding module	**2**	**42**	**48**	**50**													
Number of sequences	2	1	3	3													

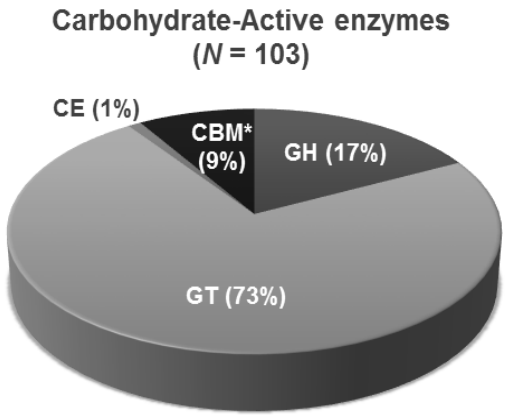

Figure 9. Carbohydrate-Active enzymes (CAZymes) found in *Synechocystis* sp. PCC 6803 (*N* = 103), based on the data from CAZy database (http://www.cazy.org/). In the table above are the number of different *Synechocystis* CAZymes and their respective classes (numbers highlighted in bold). The chart on the left shows the relative amount of the different CAZyme families. GT, glycosyltranferases; GH, glycoside hydrolases; CBM*, Carbohydrate-binding modules (50% GHs + 50% others); CE, carbohydrate esterases; nc, enzymes not yet classified in classes.

The prevalence and higher diversity of GTs, followed by GHs, is notorious in *Synechocystis* and it is in agreement with previous findings in other cyanobacteria (Rossi & De Philippis, 2016). In contrast, no enzymes belonging to other two CAZyme families were identified (enzymes with auxiliary activities and polysaccharide lyases). This is particularly relevant since several studies reported the presence of uronic acids in *Synechocystis* EPS (Pereira et al., 2019; Miranda et al., 2017; Panoff et al., 1988), and polysaccharide lyases are CAZymes that cleave the glycosidic bonds of uronic acid-containing polysaccharides.

Remarkably, the genes encoding the *Synechocystis* CAZymes are restricted to the chromosome and the plasmid pSYSM (Table S7), in agreement with the scenario depicted for the *Synechocystis* putative EPS-related genes. In addition, several of them (e.g. encoding glycosyltransferases and epimerases) are even in the genomic context of these EPS-related genes and may be co-expressed with them (see Table S5), while some CAZymes are also putative interactors of the EPS-related proteins (Supplementary data S2). However, so far, only very few studies showed experimentally that some of these CAZymes are associated to the production of EPS, such as the glycosyltransferases Sll1722, Sll1723 and Sll1724 (Foster et al., 2009).

In addition to CAZymes, only a very small number of other proteins were associated to EPS production in *Synechocystis*, such as the monooxygenase Sll1783, shown to be involved in EPS degradation and uptake (Miranda et al., 2017), and the Slr1670 (GghA, a glucosylglycerol-degrading enzyme), in this case, the inhibition of its activity was shown to stimulate EPS production (Kirsch et al., 2017).

Overall, the huge variety of *Synechocystis* sp. PCC 6803 enzymes that are able to act on polysaccharides is in agreement with an intricate mechanism(s) underlying EPS biosynthesis in this cyanobacterium as well as with the complex polymers that can be produced. In fact, although no structure of *Synechocystis* EPS was solved yet, a few studies have been reporting the high EPS complexity regarding the number and type of monosaccharides (Pereira et al., 2019; Miranda et al., 2017; Panoff et al., 1988). Moreover, some of the above mentioned CAZymes (e.g. epimerases, glycosyl-, sulfo- and methyltransferases) represent promising candidates to tailor the composition and structure of the *Synechocystis* EPS.

4. Conclusions

In brief, this study allowed to identify putative key players in the production of EPS by *Synechocystis*, as well as in its regulation. We showed that among the *Synechocystis* putative EPS-related genes previously identified by Pereira et al., 2015, some may play a more prominent role in EPS production, such as the genes *sll0923* (*wzc/kpsE*), *slr1074* (*wzy*), *slr0982* (*kpsT*), *slr0977* (*kpsM*), *sll1581* (*wza/kpsD*), *sll0575* (*kpsT*) and *sll0574*

(*kpsM*), *sll1377* (*alg8*), *slr1875* (*exoD*). In addition, Sll5049 and Slr0488 are the most promising candidates to function as Wzx flippases. In contrast, the majority of the putative EPS-related genes are most probably not involved in EPS production (e.g. *slr0067-wzc*/*kpsE* and *slr0946-wzb*), play a secondary/redundant role, or are responsible for the production of very specific polysaccharides (e.g. *slr2115* (*kpsC/kpsS*), *slr2111* (*kpsF*), *slr2122* (*kpsU*)). Moreover, our results support that an intricate network of different players operates in *Synechocystis*, and suggested that this network is tightly controlled through the action of several transcriptional regulators, namely global regulators, such as alternative sigma factors and LexA. Overall, this work represents a valuable blueprint for the study and manipulation of EPS production in *Synechocystis*, envisaging the tailoring and biotechnological application of the polymers produced.

5. References

Babykin, M.M., Sidoruk, K.V, Zinchenko, V.V, Nefedova, L.N., Cerff, R., and Shestakov, S.V. (2003). On the Involvement of the Regulatory Gene *prqR* in the Development of Resistance to Methyl Viologen in Cyanobacterium *Synechocystis* sp. PCC 6803. *Russ. J. Genet.* 39(1), 18–24.

Branco dos Santos, F., Du, W., and Hellingwerf, K.J. (2016). *Synechocystis*: not just a plug-bug for CO_2, but a green *E. coli*. *Front. Bioeng. Biotechnol.* 2, 36.

Butala, M., Žgur-Bertok, D., and Busby, S.J.W. (2009). The bacterial LexA transcriptional repressor. *Cell. Mol. Life Sci.* 66(1), 82–93.

Campbell, E.L., Hagen, K. D., Chen, R., Risser, D.D., Ferreira, D.P., and Meeks, J.C. (2015). Genetic analysis reveals the identity of the photoreceptor for phototaxis in hormogonium filaments of *Nostoc punctiforme*. *J. Bacteriol.* 197(4), 782-791.

Chakraborty, T., and Pal, R. (2014). An Overview of Cyanobacterial Exopolysaccharides: Features, Composition and Effects of Stress Exposure. *Int. J. Life Sci.* 8(4), 1–9.

Chen, L., Li, P., Liu, Z., and Jiao, Q. (2009). The released polysaccharide of the cyanobacterium *Aphanothece halophytica* inhibits flocculation of the alga with ferric chloride. *J. Appl. Phycol.* 21(3), 327–331.

Chen, Y., Zhang, J., Luo, J., Tu, J., Zeng, X., Xie, J., et al. (2012). Photophysical diversity of two novel cyanobacteriochromes with phycocyanobilin chromophores: photochemistry and dark reversion kinetics. *FEBS J.* 279(1), 40–54.

Cuthbertson, L., Mainprize, I.L., Naismith, J.H., and Whitfield, C. (2009). Pivotal roles of the outer membrane polysaccharide export and polysaccharide copolymerase protein families in export of extracellular polysaccharides in gram-negative bacteria. *Microbiol. Mol. Biol. Rev.* 73(1), 155–177.

Cuthbertson, L., Kos, V., and Whitfield, C. (2010). ABC transporters involved in export of cell surface glycoconjugates. *Microbiol. Mol. Biol. Rev.* 74(3), 341–362.

Domain, F., Houot, L., Chauvat, F., and Cassier-Chauvat, C. (2004). Function and regulation of the cyanobacterial genes *lexA*, *recA* and *ruvB*: LexA is critical to the survival of cells facing inorganic carbon starvation. *Mol. Microbiol.* 53(1), 65–80.

Drewett, V., Molina, H., Millar, A., Muller, S., Hesler, F. von, and Shaw, P.E. (2001). DNA-bound transcription factor complexes analysed by mass-spectrometry: binding of novel proteins to the human c-fos SRE and related sequences. *Nucleic Acids Res.* 29(2), 479–487.

Durai, P., Batool, M., and Choi, S. (2015). Structure and effects of cyanobacterial lipopolysaccharides. *Mar. Drugs* 13(7), 4217–4230.

Feklístov, A., Sharon, B.D., Darst, S.A., and Gross, C.A. (2014). Bacterial Sigma Factors: A Historical, Structural, and Genomic Perspective. *Annu. Rev. Microbiol.* 68(1), 357–376.

Fisher, M.L., Allen, R., Luo, Y., and Iii, R.C. (2013). Export of Extracellular Polysaccharides Modulates Adherence of the Cyanobacterium *Synechocystis*. *PloS one* 8(9), e74514.

Flamm, D., and Blaschek, W. (2010). Rare amino sugars in exopolysaccharides (EPS) from cyanobacteria of the genus Synechocystis. *Planta Med.* 76(12), P165.

Flamm, D., and Blaschek, W. (2014). Exopolysaccharides of *Synechocystis aquatilis* are sulfated arabinofucans containing N-acetyl-fucosamine. *Carbohydr. Polym.* 101, 301–306.

Foster, J.S., Havemann, S.A., Singh, A.K., and Sherman, L.A. (2009). Role of *mrgA* in peroxide and light stress in the cyanobacterium. *FEMS Microbiol. Lett.* 293(2), 298–304.
Freitas, F., Alves, V.D., and Reis, M.A.M. (2011). Advances in bacterial exopolysaccharides: From production to biotechnological applications. *Trends Biotechnol.* 29(8), 388–398.
Fujisawa, T., Narikawa, R., Maeda, S., Watanabe, S., Kanesaki, Y., Kobayashi, K., et al. (2017). CyanoBase: a large-scale update on its 20th anniversary. *Nucleic Acids Res.* 45(D1), D551–D554.
Gemma, S., Molteni, M., and Rossetti, C. (2016). Lipopolysaccharides in Cyanobacteria: A Brief Overview. *Adv. Microbiol.* 06(05), 391–397.
Georg, J., Voß, B., Scholz, I., Mitschke, J., Wilde, A., and Hess, W.R. (2009). Evidence for a major role of antisense RNAs in cyanobacterial gene regulation. *Mol. Syst. Biol.* 5, 305.
Gomes, C., Almeida, A., Ferreira, J.A., Silva, L., Santos-Sousa, H., Pinto-de-Sousa, J., et al. (2013). Glycoproteomic Analysis of Serum from Patients with Gastric Precancerous Lesions. *J. Proteome Res.* 12(3), 1454–1466.
Gonçalves, C.F., Pacheco, C.C., Tamagnini, P., and Oliveira, P. (2018). Identification of inner membrane translocase components of TolC-mediated secretion in the cyanobacterium *Synechocystis* sp. PCC 6803. *Environ. Microbiol.* 20(7), 2354–2369.
Gonzalez, A., Riley, K.W., Harwood, T.V., Zuniga, E.G., Risser, D.D., and Ellermeier, C.D. (2019). A Tripartite, Hierarchical Sigma Factor Cascade Promotes Hormogonium Development in the Filamentous Cyanobacterium *Nostoc punctiforme*. *mSphere* 4(3), e00231-19.
Greenfield, L.K., and Whitfield, C. (2012). Synthesis of lipopolysaccharide O-antigens by ABC transporter-dependent pathways. *Carbohydr. Res.* 356, 12–24.
Hays, S.G., and Ducat, D.C. (2015). Engineering cyanobacteria as photosynthetic feedstock factories. *Photosynth. Res.* 123(3), 285–295.
He, Q., Tang, Q., Sun, Y., Zhou, M., Gärtner, W., and Zhao, K.H. (2018). Chromophorylation of cyanobacteriochrome Slr1393 from *Synechocystis* sp. PCC 6803 is regulated by protein Slr2111 through allosteric interaction. *J. Biol. Chem.* 293(46), 17705-17715.
Hernández-Prieto, M.A., Semeniuk, T.A., Giner-Lamia, J., and Futschik, M.E. (2016). The Transcriptional Landscape of the Photosynthetic Model Cyanobacterium *Synechocystis* sp. PCC6803. *Sci. Rep.* 6(1), 22168.
Hirokawa, T., Boon-Chieng, S., and Mitaku, S. (1998). SOSUI: classification and secondary structure prediction system for membrane proteins. *Bioinformatics* 14(4), 378–379.
de Hoon, M.J.L., Imoto, S., Nolan, J., and Miyano, S. (2004). Open source clustering software. *Bioinformatics* 20(9), 1453–1454.
Houot, L., Floutier, M., Marteyn, B., Michaut, M., Picciocchi, A., Legrain, P., et al. (2007). Cadmium triggers an integrated reprogramming of the metabolism of *Synechocystis* PCC6803, under the control of the Slr1738 regulator. *BMC Genomics* 8(1), 350.
Huang, F., Parmryd, I., Nilsson, F., Persson, A.L., Pakrasi, H.B., Andersson, B., et al. (2002a). Proteomics of *Synechocystis* sp. strain PCC 6803: identification of plasma membrane proteins. *Mol. Cell Proteomics* 1(12), 956-966.
Huang, L., Mccluskey, M.P., Ni, H., and Larossa, R.A. (2002b). Global Gene Expression Profiles of the Cyanobacterium *Synechocystis* sp. Strain PCC 6803 in Response to Irradiation with UV-B and White Light. *J. Bacteriol.* 184(24), 6845–6858.
Huang, S., Wang, C., Peng, H., Wu, C., Chen, Y., Hong, Y., et al. (2012). Role of the small RNA RyhB in the Fur regulon in mediating the capsular polysaccharide biosynthesis and iron acquisition systems in *Klebsiella pneumoniae*. *BMC Microbiol.* 12(1), 148.
Imamura, S., and Asayama, M. (2009). Sigma factors for cyanobacterial transcription. *Gene Regul. Syst. Bio.* 3, 65–87.
Imashimizu, M., Yoshimura, H., Katoh, H., Ehira, S., and Ohmori, M. (2005). NaCl enhances cellular cAMP and upregulates genes related to heterocyst development in the cyanobacterium, *Anabaena* sp. strain PCC 7120. *FEMS Microbiol. Lett.* 252(1), 97–103.
Janczarek, M. (2011). Environmental Signals and Regulatory Pathways That Influence Exopolysaccharide Production in Rhizobia. *Int. J. Mol. Sci.* 12(11), 7898–7933.
Jenal, U., Reinders, A., and Lori, C. (2017). Cyclic di-GMP: Second messenger extraordinaire. *Nat. Rev. Microbiol.* 15(5), 271–284.
Jittawuttipoka, T., Planchon, M., Spalla, O., Benzerara, K., Guyot, F., Cassier-Chauvat, C., et al. (2013). Multidisciplinary Evidences that *Synechocystis* PCC6803 Exopolysaccharides Operate in Cell Sedimentation and Protection against Salt and Metal Stresses. *PLoS One* 8(2), e55564.
Kaneko, T., and Tabata, S. (1997). Complete Genome Structure of the Unicellular Cyanobacterium *Synechocystis* sp. PCC6803. *Plant Cell Physiol.* 38(11), 1171–1176.
Khan, R.I., Wang, Y., Afrin, S., Wang, B., Liu, Y., and Zhang, X. (2016). Transcriptional regulator

PrqR plays a negative role in glucose metabolism and oxidative stress acclimation in *Synechocystis* sp. PCC 6803. *Sci. Rep.* 6, 32507.

Kirsch, F., Pade, N., Klähn, S., Hess, W.R., and Hagemann, M. (2017). The glucosylglycerol-degrading enzyme GghA is involved in acclimation to fluctuating salinities by the cyanobacterium *Synechocystis* sp. strain PCC 6803. *Microbiology* 163(9), 1319-1328.

Kizawa, A., Kawahara, A., Takimura, Y., Nishiyama, Y., and Hihara, Y. (2016). RNA-seq Profiling Reveals Novel Target Genes of LexA in the Cyanobacterium *Synechocystis* sp. PCC 6803. *Front. Microbiol.* 7, 193.

Kizawa, A., Kawahara, A., Takashima, K., Takimura, Y., Nishiyama, Y., and Hihara, Y. (2017). The LexA transcription factor regulates fatty acid biosynthetic genes in the cyanobacterium *Synechocystis* sp. PCC 6803. *Plant J.* 92(2), 189–198.

Kopf, M., Klähn, S., Scholz, I., Matthiessen, J.K.F., Hess, W.R., and Voß, B. (2014). Comparative Analysis of the Primary Transcriptome of *Synechocystis* sp. PCC 6803. *DNA Res.* 21(5), 527–539.

Krogh, A., Larsson, B., von Heijne, G., and Sonnhammer, E.L.. (2001). Predicting transmembrane protein topology with a hidden markov model: application to complete genomes. *J. Mol. Biol.* 305(3), 567–580.

Kwon, J., Oh, J., Park, C., Cho, K., Il, S., Kim, S., et al. (2010). Systematic cyanobacterial membrane proteome analysis by combining acid hydrolysis and digestive enzymes with nano-liquid chromatography–Fourier transform mass spectrometry. *J. Chromatogr. A* 1217(3), 285–293.

Lescop, E., Hu, Y., Xu, H., Hu, W., Chen, J., Xia, B., et al. (2006). The Solution Structure of *Escherichia coli* Wzb Reveals a Novel Substrate Recognition Mechanism of Prokaryotic Low Molecular Weight Protein-tyrosine Phosphatases. *J. Biol. Chem.* 281(28), 19570–19577.

Letunic, I., and Bork, P. (2018). 20 years of the SMART protein domain annotation resource. *Nucleic Acids Res.* 46(D1), D493–D496.

Li, R., Haile, J.D., Kennelly, P.J., Li, R., Haile, J.D., and Kennelly, P.J. (2003). An arsenate reductase from *Synechocystis* sp. strain PCC 6803 exhibits a novel combination of catalytic characteristics. *J. Bacteriol.* 185(23), 6780-6789.

Lombard, V., Golaconda Ramulu, H., Drula, E., Coutinho, P.M., and Henrissat, B. (2014). The carbohydrate-active enzymes database (CAZy) in 2013. *Nucleic Acids Res.* 42(1), 490–495.

López-Igual, R., Lechno-Yossef, S., Fan, Q., Herrero, A., Flores, E., and Wolk, C.P. (2012). A Major Facilitator Superfamily Protein, HepP, Is Involved in Formation of the Heterocyst Envelope Polysaccharide in the Cyanobacterium *Anabaena* sp. Strain PCC 7120. *J. Bacteriol.* 194(17), 4677–4687.

López-Maury, L., Florencio, F.J., and Reyes, J.C. (2003). Arsenic sensing and resistance system in the cyanobacterium Synechocystis sp. strain PCC 6803. *J. Bacteriol.* 185(18), 5363–5371.

Mao, M., Yang, Y., Li, K., Lei, L., Li, M., Yang, Y., et al. (2016). The rnc Gene Promotes Exopolysaccharide Synthesis and Represses the vicRKX Gene Expressions via MicroRNA-Size Small RNAs in *Streptococcus mutans*. *Front. Microbiol.* 7, 687.

Miranda, H., Immerzeel, P., Gerber, L., Hörnaeus, K., Lind, S.B., Pattanaik, B., et al. (2017). Sll1783, a monooxygenase associated with polysaccharide processing in the unicellular cyanobacterium *Synechocystis* PCC 6803. *Physiol. Plant.* 161(2), 182–195.

Mitschke, J., Georg, J., Scholz, I., Sharma, C.M., Dienst, D., Bantscheff, J., et al. (2011). An experimentally anchored map of transcriptional start sites in the model cyanobacterium *Synechocystis* sp. PCC6803. *Proc. Natl. Acad. Sci. U. S. A.* 108(5), 2124–2129.

Mukhopadhyay, A., and Kennelly, P.J. (2011). A low molecular weight protein tyrosine phosphatase from *Synechocystis* sp. strain PCC 6803: enzymatic characterization and identification of its potential substrates. *J. Biochem.* 149(5), 551–562.

Nefedova, L.N., Fantin, Y.S., Zinchenko, V. V., and Babykin, M.M. (2003). The prqA and mvrA Genes Encoding Drug Efflux Proteins Control Resistance to Methyl Viologen in the Cyanobacterium *Synechocystis* sp. PCC 6803. *Russ. J. Genet.* 39(3), 264–268.

Nobles, D.R., Romanovicz, D.K., and Brown, R.M. (2001). Cellulose in cyanobacteria. Origin of vascular plant cellulose synthase? *Plant Physiol.* 127(2), 529–542.

Novichkov, P.S., Kazakov, A.E., Ravcheev, D.A., Leyn, S.A., Kovaleva, G.Y., Sutormin, R.A., et al. (2013). RegPrecise 3.0 – A resource for genome-scale exploration of transcriptional regulation in bacteria. *BMC Genomics* 14(1), 745.

O'Toole, G.A., and Wong, G.C.L. (2016). Sensational biofilms: Surface sensing in bacteria. *Curr. Opin. Microbiol.* 30(1999), 139–146.

Ohmori, K., Hirose, M., and Ohmori, M. (1992). Function of cAMP as a mat-forming factor in the cyanobacterium *Spirulina platensis*. *Plant Cell Physiol.* 33(1), 21–25.

Oliveira, P., and Lindblad, P. (2005). LexA, a transcription regulator binding in the promoter region

of the bidirectional hydrogenase in the cyanobacterium *Synechocystis* sp. PCC 6803. *FEMS Microbiol. Lett.* 251(1), 59–66.
Oliveira, P., Martins, N., Santos, M., Couto, N., Wright, P., Tamagnini, P., et al. (2015). The *Anabaena* sp. PCC 7120 Exoproteome: Taking a Peek outside the Box. *Life* 5(1), 130–163.
Ongley, S.E., Pengelly, J.J.L., and Neilan, B.A. (2016). A multidrug efflux response to methyl viologen and acriflavine toxicity in the cyanobacterium *Synechocystis* sp. PCC6803. *J. Appl. Phycol.* 28(5), 2793–2803.
Orchard, S., Ammari, M., Aranda, B., Breuza, L., Briganti, L., Broackes-Carter, F., et al. (2014). The MIntAct project—IntAct as a common curation platform for 11 molecular interaction databases. *Nucleic Acids Res.* 42(D1), D358–D363.
Osório, H., and Reis, C.A. (2013). Mass Spectrometry Methods for Studying Glycosylation in Cancer. In *Mass spectrometry data analysis in proteomics* (Humana Press, Totowa, NJ), pp. 301–316.
Ozturk, S., and Aslim, B. (2010). Modification of exopolysaccharide composition and production by three cyanobacterial isolates under salt stress. *Environ. Sci. Pollut. Res.* 17(3), 595–602.
Panoff, J.M., Priem, B., Morvan, H., and Joset, F. (1988). Sulphated exopolysaccharides produced by two unicellular strains of cyanobacteria, *Synechocystis* PCC 6803 and 6714. *Arch. Microbiol.* 150(6), 558–563.
Pengelly, J.J.L. (2008). Molecular characterisation of membrane transporters associated with saxitoxin biosynthesis in cyanobacteria*. Doctoral dissertation*, UNSW, School of Biotechnology and Biomolecular Sciences.
Pereira, S., Zille, A., Micheletti, E., Moradas-Ferreira, P., De Philippis, R., and Tamagnini, P. (2009). Complexity of cyanobacterial exopolysaccharides: composition, structures, inducing factors and putative genes involved in their biosynthesis and assembly. *FEMS Microbiol. Rev.* 33(5), 917–941.
Pereira, S.B., Mota, R., Santos, C.L., De Philippis, R., and Tamagnini, P. (2013). Assembly and export of extracellular polymeric substances (EPS) in cyanobacteria: a phylogenomic approach. In *Advances in Botanical Research* (Academic Press), pp. 235-279.
Pereira, S.B., Mota, R., Vieira, C.P., Vieira, J., and Tamagnini, P. (2015). Phylum-wide analysis of genes/proteins related to the last steps of assembly and export of extracellular polymeric substances (EPS) in cyanobacteria. *Sci. Rep.* 5, 14835.
Pereira, S.B., Santos, M., Leite, J.P., Flores, C., Eisfeld, C., Büttel, Z., et al. (2019). The role of the tyrosine kinase Wzc (Sll0923) and the phosphatase Wzb (Slr0328) in the production of extracellular polymeric substances (EPS) by *Synechocystis* PCC 6803. *Microbiologyopen* 8, e753.
Pisareva, T., Kwon, J., Oh, J., Kim, S., Ge, C., Wieslander, Å., et al. (2011). Model for Membrane Organization and Protein Sorting in the Cyanobacterium *Synechocystis* sp . PCC 6803 Inferred from Proteomics and Multivariate Sequence Analyses. *J. Proteome Res.* 10(8), 3617–3631.
Planchon, M., Jittawuttipoka, T., Cassier-chauvat, C., Guyot, F., Gelabert, A., Benedetti, M.F., et al. (2013). Exopolysaccharides protect *Synechocystis* against the deleterious effects of Titanium dioxide nanoparticles in natural and artificial waters. *J. Colloid Interface Sci.* 405, 35–43.
de Porcellinis, A.J., Klähn, S., Rosgaard, L., Kirsch, R., Gutekunst, K., Georg, J., et al. (2016). The Non-Coding RNA Ncr0700/PmgR1 is Required for Photomixotrophic Growth and the Regulation of Glycogen Accumulation in the Cyanobacterium *Synechocystis* sp. PCC 6803. *Plant Cell Physiol.* 57(10), 2091–2103.
Rehm, B.H.A. (2010). Bacterial polymers: Biosynthesis, modifications and applications. *Nat. Rev. Microbiol.* 8(8), 578–592.
Rippka, E., Deruelles, J., and Waterbury, N.B. (1979). Generic Assignments, Strain Histories and Properties of Pure Cultures of Cyanobacteria. *Microbiology* 111(1), 1-61.
Rossi, F., and De Philippis, R. (2016). Exocellular Polysaccharides in Microalgae and Cyanobacteria: Chemical Features, Role and Enzymes and Genes Involved in Their Biosynthesis. In *The Physiology of Microalgae* (Cham: Springer International Publishing), pp. 565–590.
Salamov, A., and Bachinsky, A. (2011). Automatic Annotation of Bacterial Community Sequences and Application to Infections Diagnostic. In *Bioinformatics*, pp. 346-353.
Saldanha, A.J. (2004). Java Treeview--extensible visualization of microarray data. *Bioinformatics* 20(17), 3246–3248.
Sato, S., Shimoda, Y., Muraki, A., Kohara, M., Nakamura, Y., and Tabata, S. (2007). A large-scale protein–protein interaction analysis in *Synechocystis* sp. PCC6803. *DNA Res.* 14(5), 207-216.
Schmid, J., Sieber, V., and Rehm, B. (2015). Bacterial exopolysaccharides: biosynthesis pathways and engineering strategies. *Front. Microbiol.* 6, 496.
Sebesta, J., Werner, A., and Peebles, C.A.M. (2019). Genetic Engineering of Cyanobacteria: Design, Implementation, and Characterization of Recombinant *Synechocystis* sp. PCC 6803. In *Microbial Metabolic Engineering* (Humana Press, New York, NY), pp. 139–154.

Sengupta, D., Datta, S., and Biswas, D. (2018). Towards a better production of bacterial exopolysaccharides by controlling genetic as well as physico-chemical parameters. *Appl. Microbiol. Biotechnol.* 102(4), 1587–1598.

Simkovsky, R., Daniels, E.F., Tang, K., Huynh, S.C., Golden, S.S., and Brahamsha, B. (2012). Impairment of O-antigen production confers resistance to grazing in a model amoeba – cyanobacterium predator – prey system. *Proc. Natl. Acad. Sci. U. S. A.* 109(41), 16678-16683.

Simkovsky, R., Effner, E.E., Iglesias-Sánchez, M.J., and Golden, S.S. (2016). Mutations in Novel Lipopolysaccharide Biogenesis Genes Confer Resistance to Amoebal Grazing in *Synechococcus elongatus. Appl. Environ. Microbiol.* 82(9), 2738–2750.

Skorupska, A., Janczarek, M., Marczak, M., Mazur, A., and Król, J. (2006). Rhizobial exopolysaccharides: genetic control and symbiotic functions. *Microb. Cell Fact.* 5(1), 7.

Szklarczyk, D., Gable, A.L., Lyon, D., Junge, A., Wyder, S., Huerta-Cepas, J., et al. (2019). STRING v11: protein–protein association networks with increased coverage, supporting functional discovery in genome-wide experimental datasets. *Nucleic Acids Res.* 47(D1), D607–D613.

Tamagnini, P., Troshina, O., Oxelfelt, F., Salema, R., and Lindblad, P. (1997). Hydrogenases in *Nostoc* sp. Strain PCC 73102, a Strain Lacking a Bidirectional Enzyme. *Appl. Environ. Microbiol.* 63(5), 1801–1807.

Tamaru, Y., Takani, Y., Yoshida, T., and Sakamoto, T. (2005). Crucial role of extracellular polysaccharides in desiccation and freezing tolerance in the terrestrial cyanobacterium *Nostoc commune*. *Appl. Environ. Microbiol.* 71(11), 7327–7333.

Tatusova, T., DiCuccio, M., Badretdin, A., Chetvernin, V., Nawrocki, E.P., Zaslavsky, L., et al. (2016). NCBI prokaryotic genome annotation pipeline. *Nucleic Acids Res.* 44(14), 6614–6624.

Wang, X., Dubey, A.K., Suzuki, K., Baker, C.S., Babitzke, P., and Romeo, T. (2005). CsrA post-transcriptionally represses *pgaABCD*, responsible for synthesis of a biofilm polysaccharide adhesin of *Escherichia coli*. *Mol. Microbiol.* 56(6), 1648–1663.

Whitney, J.C., and Howell, P.L. (2013). Synthase-dependent exopolysaccharide secretion in Gram-negative bacteria. *Trends Microbiol.* 21(2), 63–72.

Willis, L.M., and Whitfield, C. (2013). KpsC and KpsS are retaining 3-deoxy-D-manno-oct-2-ulosonic acid (Kdo) transferases involved in synthesis of bacterial capsules. *Proc. Natl. Acad. Sci. U. S. A.* 110(51), 20753–20758.

Yoshimura, H., Yoshihara, S., Okamoto, S., Ikeuchi, M., and Ohmori, M. (2002). A cAMP Receptor Protein, SYCRP1, is Responsible for the Cell Motility of *Synechocystis* sp. PCC 6803. *Plant Cell Physiol.* 43(4), 460–463.

Yoshimura, H., Okamoto, S., Tsumuraya, Y., and Ohmori, M. (2007). Group 3 sigma factor gene, sigJ, a key regulator of desiccation tolerance, regulates the synthesis of extracellular polysaccharide in cyanobacterium *Anabaena* sp. strain PCC 7120. *DNA Res.* 14(1), 13–24.

Yu, C.-S., Chen, Y.-C., Lu, C.-H., and Hwang, J.-K. (2006). Prediction of protein subcellular localization. *Proteins Struct. Funct. Bioinforma.* 64(3), 643–651.

Yu, N.Y., Wagner, J.R., Laird, M.R., Melli, G., Rey, S., Lo, R., et al. (2010). PSORTb 3.0: improved protein subcellular localization prediction with refined localization subcategories and predictive capabilities for all prokaryotes. *Bioinformatics* 26(13), 1608–1615.

Zhao, C., Li, Z., Li, T., Zhang, Y., Bryant, D.A., and Zhao, J. (2015). High-yield production of extracellular type-I cellulose by the cyanobacterium *Synechococcus* sp. PCC 7002. *Cell Discov.* 1, 15004.

Zhu, H., Ren, X., Wang, J., Song, Z., Shi, M., Qiao, J., et al. (2013). Integrated OMICS guided engineering of biofuel butanol-tolerance in photosynthetic *Synechocystis* sp. PCC 6803. *Biotechnol. Biofuels* 6(1), 106.

6. Supplementary Material

Supplementary material to this chapter can be found in two separate files:

Chapter II. Supplementary Material I – Supplementary data S1; Tables S1, S2, S3.

Chapter II. Supplementary Material II – Tables S4, S5, S6, S7;
Supplementary data S2.

CHAPTER III

The alternative sigma factor SigF is a key player in the control of secretion mechanisms in *Synechocystis* sp. PCC 6803

Work published in: ***FLORES, C.***, *Santos, M., Pereira, S. B., Mota, R., Rossi, F., De Philippis, R., Couto, N., Karunakaran, E., Wright, P. C., Oliveira, P., & Tamagnini, P. (2019). The alternative sigma factor SigF is a key player in the control of secretion mechanisms in* Synechocystis *sp. PCC 6803. Environmental Microbiology, 21: 343–359.*

environmental microbiology

Environmental Microbiology (2019) **21**(1), 343–359 doi:10.1111/1462-2920.14465

The alternative sigma factor SigF is a key player in the control of secretion mechanisms in *Synechocystis* sp. PCC 6803

Carlos Flores,[1,2,3] Marina Santos,[1,2,3] Sara B. Pereira,[1,2] Rita Mota,[1,2] Federico Rossi,[4] Roberto De Philippis,[4] Narciso Couto,[5‡] Esther Karunakaran,[5] Phillip C. Wright,[5†] Paulo Oliveira [1,2] and Paula Tamagnini [1,2,6*]

[1]*Bioengineering and Synthetic Microbiology Group, i3S – Instituto de Investigação e Inovação em Saúde, Universidade do Porto, Porto, Portugal.*

[2]*Bioengineering and Synthetic Microbiology Group, IBMC – Instituto de Biologia Celular e Molecular, Universidade do Porto, Porto, Portugal.*

[3]*Departamento de Biologia Molecular, ICBAS – Instituto de Ciências Biomédicas Abel Salazar, Porto, Portugal.*

[4]*Department of Agrifood Production and Environmental Sciences, University of Florence, Florence, Italy.*

[5]*Department of Chemical and Biological Engineering, ChELSI Institute, University of Sheffield, Sheffield, UK.*

[6]*Faculdade de Ciências, Departamento de Biologia, Universidade do Porto, Porto, Portugal.*

Summary

Cyanobacterial alternative sigma factors are crucial players in environmental adaptation processes, which may involve bacterial responses related to maintenance of cell envelope and control of secretion pathways. Here, we show that the Group 3 alternative sigma factor F (SigF) plays a pleiotropic role in *Synechocystis* sp. PCC 6803 physiology, with a major impact on growth and secretion mechanisms, such as the production of extracellular polysaccharides, vesiculation and protein secretion. Although Δ*sigF* growth was significantly impaired, the production of released polysaccharides (RPS) increased threefold to fourfold compared with the wild-type. Δ*sigF* exhibits also impairment in formation of outer-membrane vesicles (OMVs) and pili, as well as several other cell envelope alterations. Similarly, the exoproteome composition of Δ*sigF* differs from the wild-type both in amount and type of proteins identified. Quantitative proteomics (iTRAQ) and an *in silico* analysis of SigF binding motifs revealed possible targets/pathways under SigF control. Besides changes in protein levels involved in secretion mechanisms, our results indicated that photosynthesis, central carbon metabolism and protein folding/degradation mechanisms are altered in Δ*sigF*. Overall, this work provided new evidences about the role of SigF on *Synechocystis* physiology and associates this regulatory element with classical and non-classical secretion pathways.

Received 17 July, 2018; revised 14 September, 2018; accepted 31 October, 2018. *For correspondence. E-mail pmtamagn@ibmc.up.pt; Tel. +351 220 408 800; Fax +351 220408848. Present addresses: †Centre for Applied Pharmacokinetic Research, University of Manchester, Manchester, UK; ‡Faculty of Science, Agriculture & Engineering, Newcastle University, Newcastle, UK.

Introduction

RNA polymerase sigma factors play a major role in the regulation of bacterial acclimation processes and cell survival (Gruber and Gross, 2003; Feklístov *et al*., 2014). This regulation occurs after perception of environmental signals and subsequent orchestration of the replacement of one sigma factor by another in the RNA polymerase holoenzyme (Österberg *et al*., 2011). These events trigger a change in gene expression pattern, producing multiple cellular responses and allowing the adaptation of the bacterial cell. Therefore, bacterial sigma factors have been emerging as new targets to engineer a wide range of microorganisms (Tripathi *et al*., 2014; Stensjö *et al*., 2017). The vast majority of bacterial sigma factors belong to the so-called σ^{70} family, due to their similarities with the sigma factor 70 from *E. coli* (Feklístov *et al*., 2014; Paget, 2015), but some members of a second family (σ^{54}) have also been identified in a restricted number of bacteria. Sigma factors belonging to the σ^{70} family are commonly divided in four different groups: (i) Group 1-sigma factors, which are essential to cell viability and mainly related with the transcription of housekeeping genes; (ii) Group 2-sigma factors, structurally similar to those of group 1, but considered non-essential in near optimal growth conditions; (iii) Group 3-sigma factors,

responsible for the expression of regulons assigned to the survival under stress and (iv) Group 4-sigma factors, also named as sigma factors of extracytoplasmic function (ECFs), as they respond to signals that are generated outside of the cell or in the cell wall. The Groups 3 and 4 are the most diverse and they comprise sigma factors that coordinate processes responsible for the maintenance or modification of the cell envelope, through sporulation (Hilbert *et al*., 2004), motility (Zhao *et al*., 2007), adhesion (Claret *et al*., 2007), protein secretion (Eichelberg and Galán, 2000), quorum sensing (Schuster *et al*., 2004), formation of biofilm matrices (Rachid *et al*., 2000) and others. These processes seem to be intrinsically related with the secretion capacity of the microorganism, which can be achieved through pathways dependent on membrane transporters (Costa *et al*., 2015) or mediated by vesicles (Schwechheimer and Kuehn, 2015; Roier *et al*., 2016). These mechanisms need to be tightly regulated in order to provide the most appropriate bacterial response, and to be rapidly remodelled when cells are exposed to different environmental conditions (Marx *et al*., 2009; Christie-Oleza *et al*., 2015; Donia and Fischbach, 2015). Despite the available knowledge on the influence of sigma factors and the regulatory networks behind secretion in pathogenic bacteria (see for e.g. Vilches *et al*., 2009; Rutherford and Bassler, 2012), information about these complex mechanisms is still limited for other bacteria.

In cyanobacteria, all sigma factors described until now belong to the σ^{70} family, being divided in three main groups according to Imamura and Asayama (2009). In these organisms, the ECF sigma factors are either categorized as an additional group (Bell *et al*., 2017) or as a subset of Group 3 (Imamura and Asayama, 2009). Cyanobacterial Group 3 sigma factors generally occur at relatively low levels at optimal physiological conditions, but they are crucial players in environmental adaptation (Imamura *et al*., 2003). They seem to perform similar roles to their orthologues in other bacteria, regulating pathways that involve repair of the cell envelope (Bell *et al*., 2017), production and secretion of polysaccharides (Yoshimura *et al*., 2007) and other acclimation processes (Inoue-Sakamoto *et al*., 2007; Srivastava *et al*., 2017). The study of cyanobacterial sigma factors has been mostly performed using the model unicellular cyanobacterium *Synechocystis* sp. PCC 6803 (hereafter *Synechocystis*). *Synechocystis´* Group 3 alternative sigma factors comprise a subgroup of three ECF sigma factors (SigG - Slr1545; SigH - Sll0856; SigI - Sll0687) and SigF (Slr1564), being the latter the most phylogenetically divergent protein (Imamura *et al*., 2003). In contrast with its counterparts, the physiological importance of SigF has been poorly understood. Previous studies reported that SigF is important for *Synechocystis* motility through the regulation of pili formation (Bhaya *et al*., 1999) and in adaptive responses to salt stress conditions (Marin *et al*., 2002). Furthermore, Asayama and Imamura (2008) suggested that SigF may display stringent promoter recognition, being able to auto-regulate its gene expression.

The main goal of this study was to evaluate the impact of SigF on *Synechocystis* sp. PCC 6803 physiology, unveiling possible targets and biosynthetic pathways that may be under the control of this Group 3 sigma factor, which is the only one that is not categorized as having an extracytoplasmic function.

Results

Synechocystis ΔsigF *mutant exhibits growth impairment and clumping phenotype*

In this work, we started by characterizing *Synechocystis* wild-type (substrain PCC-M; Huckauf *et al*., 2000) and its Δ*sigF* mutant, kindly provided by Prof. Martin Hagemann (University of Rostock, Germany). The growth of Δ*sigF* mutant was compared with that of the wild-type strain by measuring the OD_{730nm}, the content in chlorophyll *a* (chl *a*) and by cell counting. The growth curves based on chl *a* measurements revealed a growth impairment of approximately 50% of the mutant compared with the wild-type. This result was corroborated by counting the number of cells (being the μg of chl *a* per cell similar for both strains: wild-type $3.11 \pm 0.12 \times 10^{-2}$ and Δ*sigF* $3.26 \pm 0.26 \times 10^{-2}$) (Fig. 1), but not by the OD_{730nm} measurements (Supporting Information Fig. S1). This is most probably due to the higher turbidity of the medium derived from the accumulation of secreted products in the Δ*sigF* culture. The Δ*sigF* growth impairment could be partially rescued

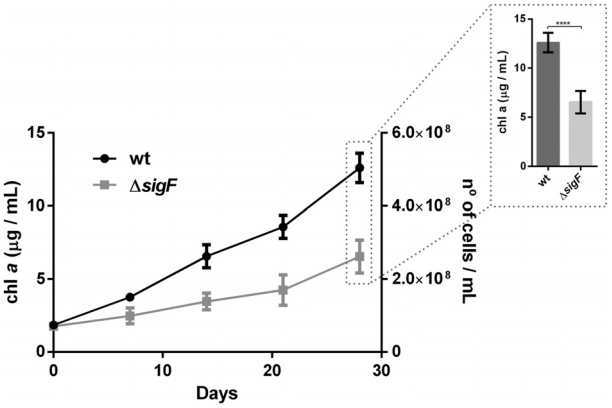

Fig. 1. Growth curves of *Synechocystis* sp. PCC 6803 wild-type (wt) and Δ*sigF* mutant. Growth was monitored by measuring the chlorophyll *a* (chl *a*) content and by counting the number of cells. Cells were grown in BG11 at 30 °C under a 12 h light (50 μE m^{-2} s^{-1})/12 h dark regimen, with orbital shaking at 150 r.p.m. Experiments were made in triplicate and statistical analysis is presented for the last time point (**** *p* value ≤0.0001).

(about 40%) by complementation (Supporting Information Fig. S2). This partial rescue is most probably due to altered *sigF* expression levels, that can be explained by the use of a replicative plasmid (pSEVA351) containing the native *sigF* gene under the control of different regulatory elements (the P_{rbcL} promotor and the B0032 or the RBS found upstream of *rbcL*; for more details see Supporting Information Experimental Procedures).

Besides the obvious impairment in growth, Δ*sigF* exhibited a striking macroscopic phenotype with the cells clumping under mild orbital shaking and sedimenting spontaneously without agitation at a much faster rate than the wild-type – overnight for the mutant and about 3 weeks for the wild-type (Fig. 2A and B). Moreover, after centrifugation a much thicker layer of extracellular material could be observed above the pellet of Δ*sigF* (Fig. 2C). This extracellular material stained with Alcian Blue, a specific dye for acidic polysaccharides. Therefore, the Δ*sigF* mutant seems to be overproducing extracellular polymeric substances (EPS).

The ΔsigF *mutant produces more and distinct EPS*

As it was possible to observe that the Δ*sigF* mutant produces more EPS than the wild-type, we pursued the characterization by measuring the amount of total carbohydrates, capsular polysaccharides – CPS and polysaccharides released to the extracellular medium – RPS. The amount of total carbohydrates in the culture and the amount of RPS are approximately 2-fold and 3.5-fold higher in the Δ*sigF* culture compared with the wild-type respectively (Fig. 3). For the complemented mutant, the amount of total carbohydrates is approximately 1.5-fold higher compared with the wild-type whereas the production of RPS increases only by 0.8-fold (Supporting Information Fig. S2). No significant differences were observed in terms of CPS.

The RPS were isolated from both the wild-type and the Δ*sigF* cultures (Fig. 4) and the differences observed were not limited to the amount of polymer produced, but also encompassed the monosaccharidic composition (Table 1).

Eleven different monosaccharides were detected in wild-type in contrast with ten in Δ*sigF* RPS, with the prevalence of glucose in both cases. In general, the isolated RPS are composed by three hexoses (glucose, mannose and galactose), two deoxyhexoses (rhamnose and fucose), three pentoses (xylose, arabinose and ribose), two amino sugars (glucosamine and galactosamine) and two acidic hexoses/uronic acids (glucuronic and galacturonic acids). Considerable differences were observed in the amount of almost all monosaccharides, with the exception of mannose, rhamnose and xylose. *Synechocystis* Δ*sigF* mutant secretes a polymer enriched in hexoses compared with the wild-type. On the other hand, the amount of the other sugars decreases in Δ*sigF* RPS,

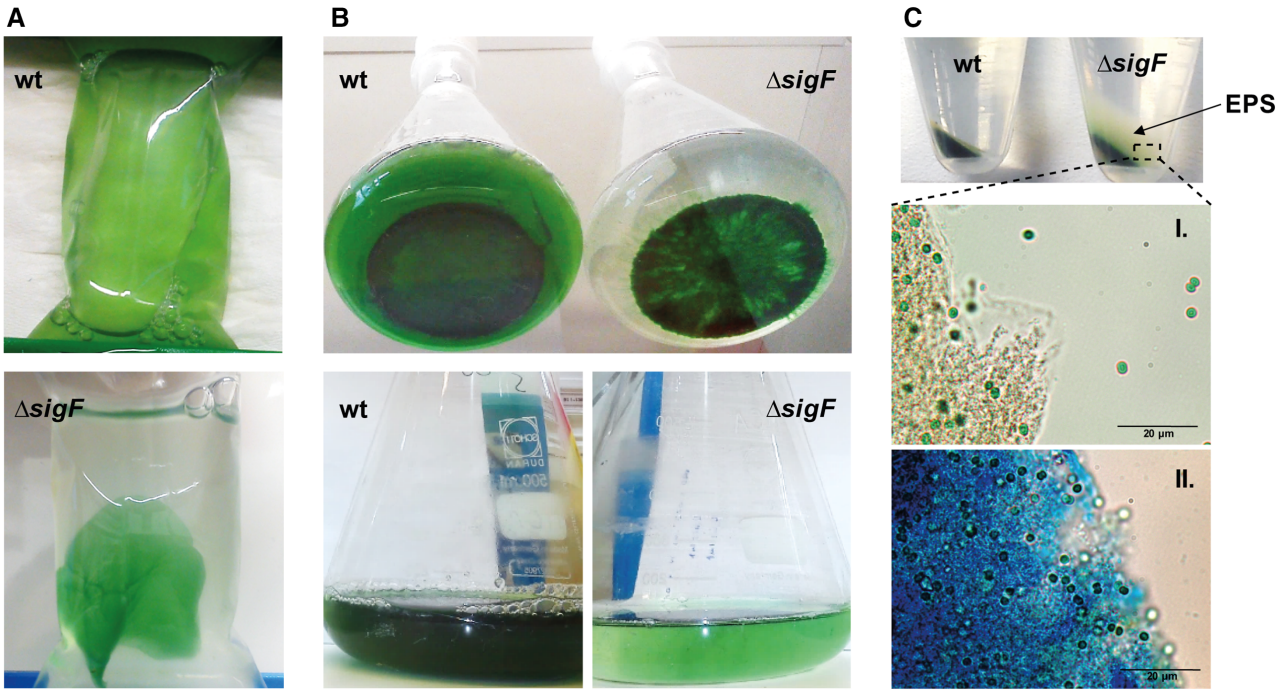

Fig. 2. *Synechocystis* sp. PCC 6803 wild-type (wt) and Δ*sigF* mutant phenotypes.
A. Cultures after dialysis, showing the clumping of the mutant cells.
B. Batch cultures depicting the higher rate of spontaneous sedimentation of Δ*sigF*.
C. Centrifuged cultures where it is possible to observe the higher amount of EPS produced by the Δ*sigF* mutant compared with the wt, and light micrographs from the Δ*sigF* culture (**I** and **II**), with the EPS stained with Alcian Blue (**II**).

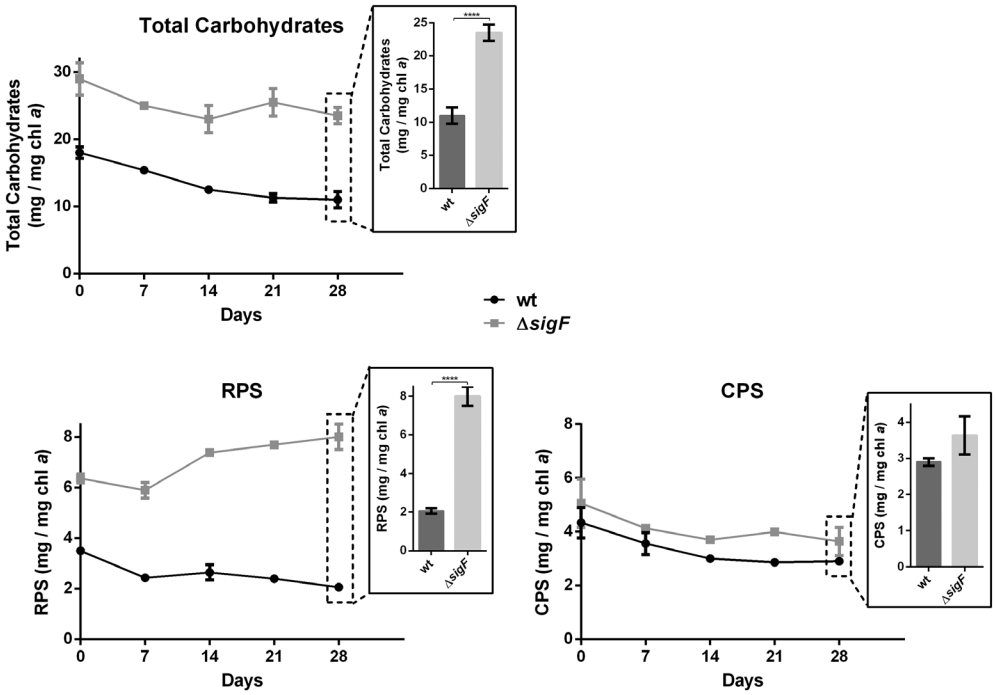

Fig. 3. Total carbohydrates, released and capsular polysaccharides of *Synechocystis* wild-type and Δ*sigF*. The values are expressed as mg of carbohydrates per mg of chlorophyll *a* (chl *a*). Cultures were grown in BG11 at 30 °C under a 12 h light (50 μE m^{-2} s^{-1})/12 h dark regimen, with orbital shaking at 150 r.p.m. Experiments were made in triplicate and the statistical analysis is presented for the last time point (**** *p* value ≤0.0001). RPS: released polysaccharides, CPS: capsular polysaccharides.

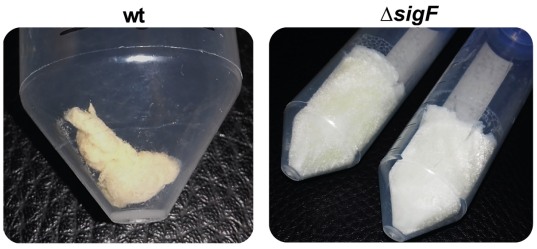

Fig. 4. Purified lyophilized RPS obtained from *Synechocystis* wild-type and Δ*sigF* cultures. [Color figure can be viewed at wileyonlinelibrary.com]

Table 1. Monosaccharidic composition of the RPS obtained from *Synechocystis* wild-type and Δ*sigF* cultures expressed as molar %.

	wt		Δ*sigF*	
Monosaccharide	Mean	SD	Mean	SD
Glucose	18.54	0.94	33.87	1.50
Mannose	17.74	0.70	20.29	0.45
Galactose	2.53	0.53	5.03	0.60
Rhamnose	14.24	1.56	17.23	0.35
Fucose	10.28	0.16	3.89	0.41
Xylose	6.05	0.11	5.73	0.52
Arabinose	1.83	0.57	Traces	–
Ribose	1.35	0.02	Traces	–
Glucosamine	12.42	1.36	5.17	0.43
Galactosamine	9.34	0.78	4.13	0.15
Glucuronic acid	4.16	0.74	1.35	0.22
Galacturonic acid	Traces	–	1.76	0.04

with the exception of rhamnose. Furthermore, two uronic acids were detected in Δ*sigF* RPS, whereas in the RPS from the wild-type only glucuronic acid was detected but in higher amount than in Δ*sigF*.

The cell envelope and vesiculation capacity are altered in the ΔsigF *mutant*

During the isolation of the polymers, a difference in pigmentation of the RPS produced by the wild-type and the Δ*sigF* mutant was observed (Fig. 4). Therefore, we decided to analyse the composition of the extracellular medium. The absorption spectra of the concentrated samples showed the characteristic absorption peaks of carotenoids for both strains, but the absorption levels were significantly higher for the wild-type (Fig. 5A). As carotenoids are lipophilic molecules and thus embedded in lipid structures, the presence of lipopolysaccharides (LPS) and lipids were also investigated. In agreement with the previous results, the medium from *Synechocystis* wild-type culture contains larger amounts of lipids, as well as LPS compared with the Δ*sigF* mutant (Fig. 5B). Altogether, these observations suggest the presence of outer membrane vesicles (OMVs) in the extracellular medium, predominantly in the wild-type culture. These results were confirmed by negative staining transmission electron microscopy, with the micrographs of the Δ*sigF* mutant clearly showing an impaired vesiculation capacity compared with the wild-type (Fig. 6).

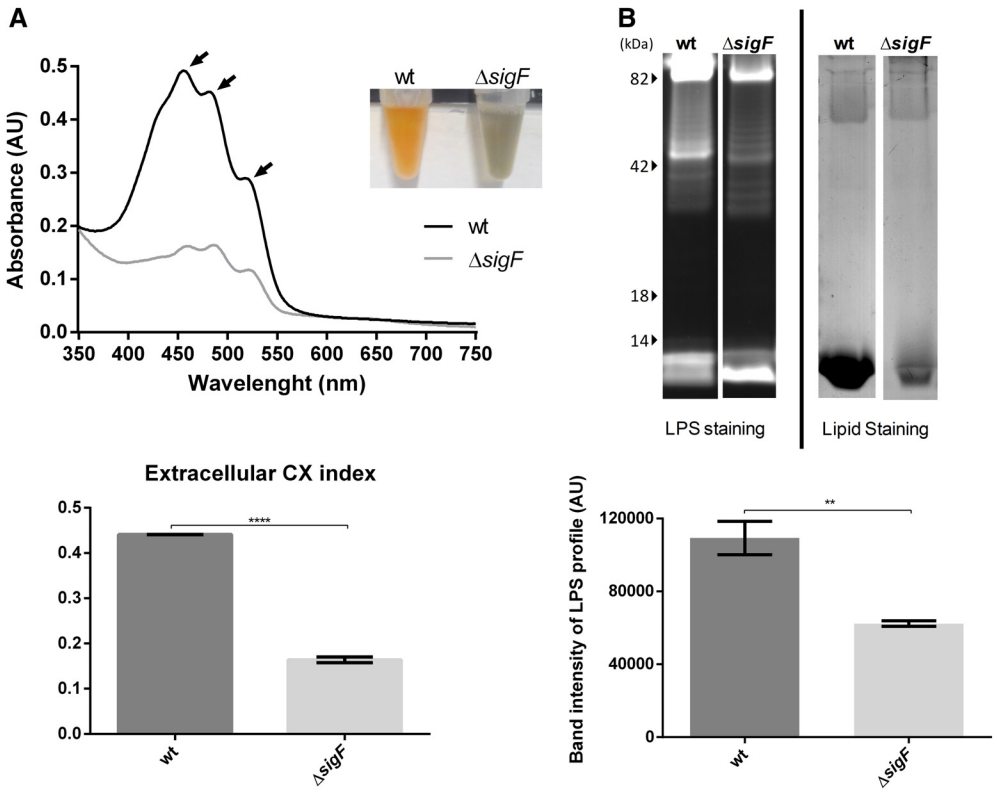

Fig. 5. Analysis of concentrated medium from *Synechocystis* wild-type (wt) and Δ*sigF* cultures.
A. Absorption spectra of the 500× concentrated medium, with arrows indicating the characteristic carotenoids peaks (upper panel) and quantification of the relative abundance of carotenoids - CX index (lower panel) (**** p value ≤ 0.0001).
B. Lipopolysaccharides (LPS) profile analysed by SDS-polyacrylamide gel electrophoresis and stained with Pro-Q® Emerald 300 lipopolysaccharide (upper left panel). The gel was subsequently stained with Sudan Black B solution for lipids visualization (upper right panel). Comparison between the intensity of the bands observed in the LPS profiles of the wt and the Δ*sigF* mutant (lower panel) (** p value ≤ 0.01). [Color figure can be viewed at wileyonlinelibrary.com]

Moreover, impairment in pili formation was also observed in these micrographs (Fig. 6A), and this observation is in agreement with the absence of phototactic motility by Δ*sigF* (Fig. 6C). Furthermore, a dense amorphous layer, probably consisting of crippled EPS and/or LPS, was detected by transmission electron microscopy surrounding Δ*sigF* cells (Fig. 6A and Supporting Information Fig. S3), containing structures that resemble protein aggregates (Fig. 6A and B).

Still regarding the cell envelope ultrastructure, other alterations could be detected in Δ*sigF*, namely the thickness of the peptidoglycan layer (Supporting Information Fig. S3) that is considerably thicker (10.9 ± 0.3 nm), compared with the wild-type (6.5 ± 0.4 nm). Additionally, the LPS profile of the outer membrane isolated from Δ*sigF* cells is distinct compared with the wild-type (Supporting Information Fig. S4).

The ΔsigF *exoproteome differs from the wild-type*

As critical differences in the cell envelope and secretion of *Synechocystis* wild-type and Δ*sigF* were observed, their exoproteomes were also analysed by SDS-polyacrylamide gel electrophoresis. Overall, the exoproteome of the Δ*sigF* mutant is remarkably different from the wild-type with proteins of lower molecular weight accumulating in higher amounts in Δ*sigF* (Fig. 7). Coomassie stained bands and/or gel portions were subjected to in-gel trypsin digestion followed by peptide identification by mass spectrometry. Peptides from 21 different proteins and belonging to the following four functional categories were detected (Table 2 and Supporting Information Table S2): 'Carbon metabolism' (5 proteins), 'Secretion & Membrane transporters' (4 proteins), 'Photosynthesis' (3 proteins) and 'Protein folding & degradation' (1 protein). The remaining proteins (about half of the ones identified) are categorized as 'unknown'. The predicted protein localization revealed that nearly half of the proteins identified are expected to be functionally active in the outer membrane or in the periplasmic space (Supporting Information Table S2). However, three proteins are predicted to be located in the cytoplasm: Sll1525 (PrK), Sll1029 (CcmK1) and Sll1028 (CcmK2), which are proteins involved in the CO_2 fixation mechanism in *Synechocystis*. Furthermore, three proteins associated with thylakoid membranes were also detected in the exoproteomes: the phycobiliproteins, Sll1577 and

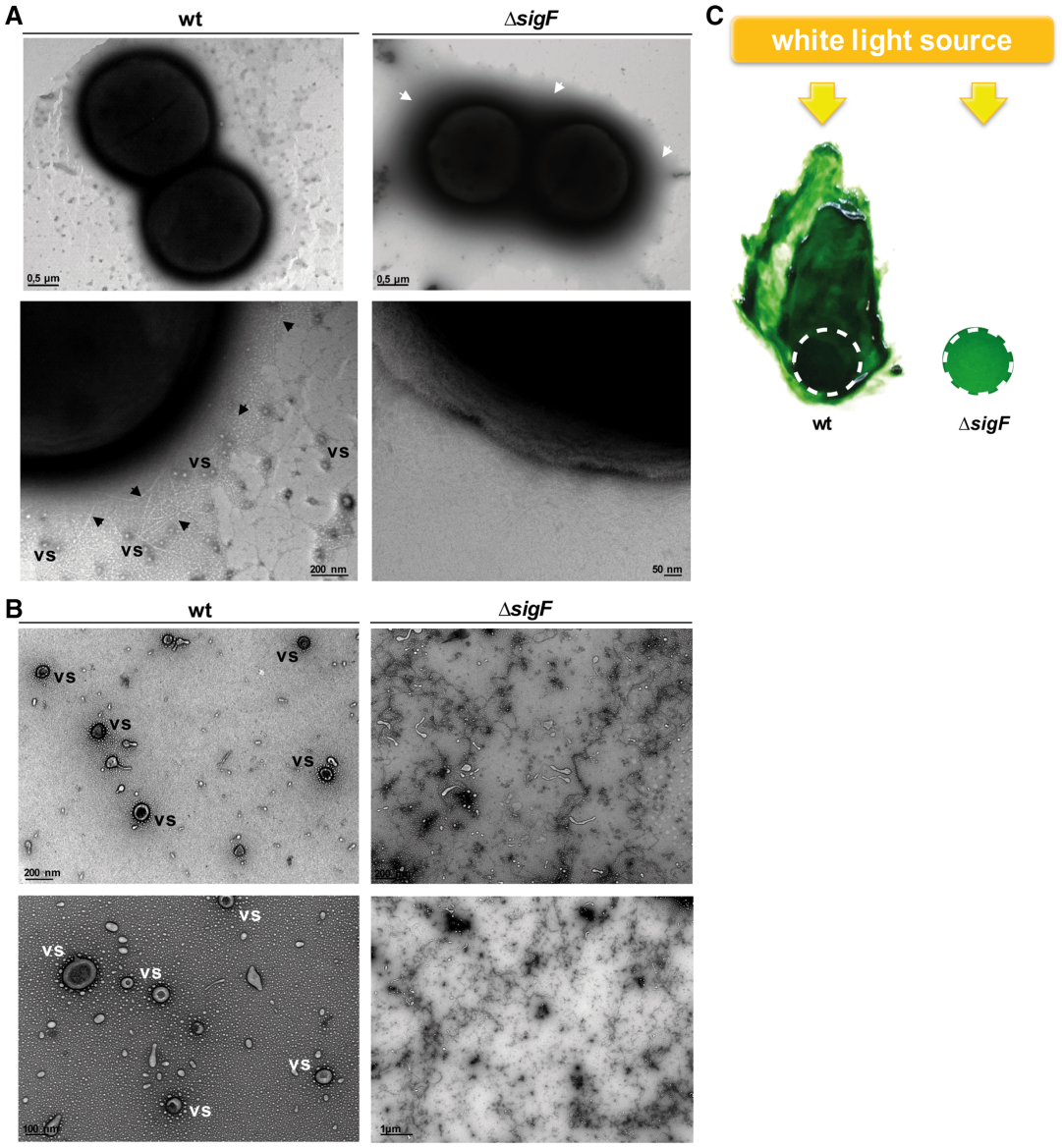

Fig. 6. Negatively stained transmission electron micrographs of *Synechocystis* wild-type and Δ*sigF*.
A. Cells.
B. 500× concentrated cell-free media. The presence of vesicles (vs) and pili (black arrowheads) is depicted for the wt, whereas for Δ*sigF* a dense layer surrounding the cell (white arrowheads).
C. Directional motility agar assay showing the phototaxis of wt and the non-motile phenotype of Δ*sigF*. Dashed circles indicate the place where cell culture was spotted. [Color figure can be viewed at wileyonlinelibrary.com]

Sll1578 (CpcA and CpcB phycocyanin subunits respectively) and the allophycocyanin Slr2067 (ApcA). These three proteins accumulate in higher amounts in Δ*sigF* exoproteome. On the other hand, Sll1009 is accumulating in higher abundance in the wild-type exoproteome. This protein was shown to be glycosylated (data not shown), and although is being annotated as a FrpC, its exact function remains to be elucidated. The proteins Slr0191 (SpoIID), Slr1751 (PrC) and Sll1525 (PrK) accumulated exclusively in the exoproteome of Δ*sigF*. In contrast, the Slr1452 (SbpA), involved in the sulfate transport, appeared only in the wild-type exoproteome.

SigF has a pleiotropic action on Synechocystis *physiology*

To obtain a holistic perspective about the impact of SigF in *Synechocystis* physiology and to investigate the putative pathways and possible targets under the control of SigF, two different approaches were implemented: (i) The

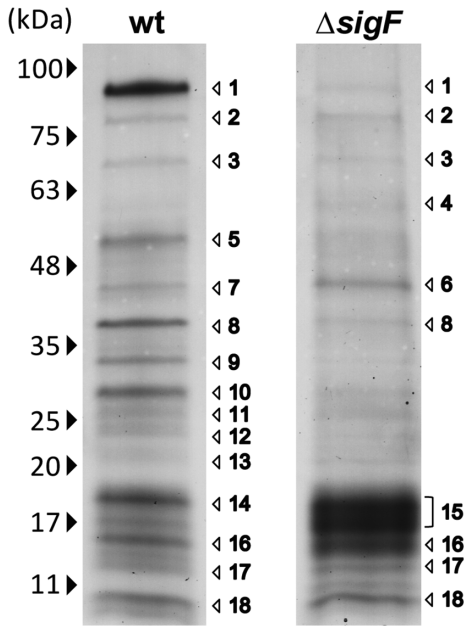

Fig. 7. Exoproteomes of *Synechocystis* wild-type and Δ*sigF* separated by SDS-PAGE/stained with Coomassie Blue. Numbers to the right highlight the bands/gel region observed across at least three biological replicates and excised for protein identification (Table 2).

Table 2. List of proteins identified in the exoproteomes of *Synechocystis* sp. PCC 6803 wild-type (wt) and Δ*sigF* mutant by mass spectrometry.

Band	Protein	Description
1	**Sll1009,** FrpC	Protein with calcium ion binding motifs
2	**Slr0168**	Unknown
3	**Slr1841**	Porin (carbohydrate selective)
4	**Slr0191,** SpoIID	Amidase enhancer, role at murein and peptidoglycan
5	**Slr0447,** AmiC and **Slr1940**	ABC transporter (urea) and Protein involved in extracellular connection structures
6	**Slr1751,** PrC and **Sll1525,** PrK	Protease (PSII repair) and CO_2 fixation
7	**Slr1452** SbpA	Sulfate transport
8	**Slr0513,** FutA	Iron uptake (PSII protection from ROS)
9	**Slr1410** and **Sll1491**	WD proteins
10	**Sll0314**	Lipoprotein (signalling)
11, 12, 13	**Slr1704**	Unknown
14	**Sll1577,** CpcB	C-phycocyanin beta chain
15	**Sll1578,** CpcA and **Slr2067,** ApcA and **Sll1577**	C-phycocyanin alpha chain and Allophycocyanin alpha chain
16	**Slr0518**	Carbohydrate binding protein (arabinofuranidase)
17	**Sll0470**	Unknown
18	**Sll1029** and **Sll1028**	CCMK (CO_2 concentrating mechanism)

in silico analysis of putative SigF binding sites in *Synechocystis* gene promoter regions (Fig. 8) and (ii) A quantitative proteomic analysis (iTRAQ) of cell extracts from *Synechocystis* wild-type and Δ*sigF* (Fig. 9). The complete description of the genes or proteins obtained in both analyses is listed in Supporting Information Table S3 and Table S4 respectively.

For the analysis of the putative SigF binding sites (Fig. 8), the consensus sequences GGGTAAG and [C/T] AGGC [N10-30] GGGT[A/G][A/G][A/G] previously reported by Asayama and Imamura (2008) were searched in the whole genome of the *Synechocystis* substrain understudy, which was deposited by Trautmann and colleagues (2012). The hits retrieved were manually curated (see Experimental procedures) and a total of 110 genes were found with promoter regions displaying a putative SigF binding site. Nearly half of the genes identified encode proteins with unknown function. The majority of the remaining genes encode proteins involved in the central carbon metabolism, including glycosyltransferases and proteins involved in CO_2 fixation and glycolysis. Furthermore, genes encoding proteins responsible for energy production and conversion (photosynthesis and oxidative phosphorylation), and proteins involved in secretion pathways (including the ones related to pilin secretion) are highly represented. Several genes encoding proteins important for sensing environmental stimuli and coordinating stress-related responses were also identified, namely kinases (e.g. Sll1770, Sll1525), sensors of two-component systems (e.g. Slr0302, Sll1672), other regulators (e.g. Slr1305, Slr1416), as well as proteins involved in protein folding and degradation (e.g. Slr0093, Sll1063, Sll0055). Moreover, various promoter regions of genes that encode oxidoreductases were identified as harbouring putative SigF binding sites.

Regarding the quantitative proteomic analysis (iTRAQ), a total of 313 proteins (out of the 1654 identified and quantified) had significant fold changes in the *Synechocystis* Δ*sigF* cell extracts compared with the wild-type. In general, the distribution of these proteins by functional

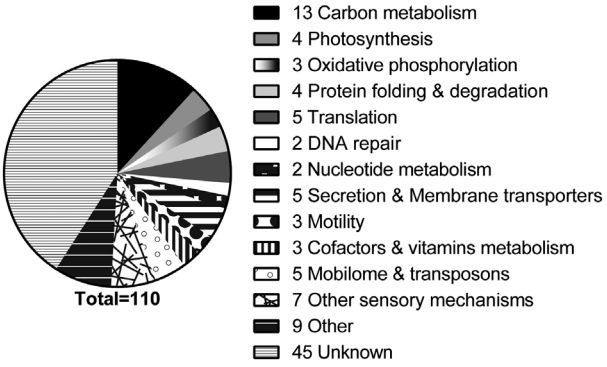

Fig. 8. Functional groups of proteins encoded by genes with putative SigF binding motifs in the promoters. See annotated list of genes in Supporting Information Table S3.

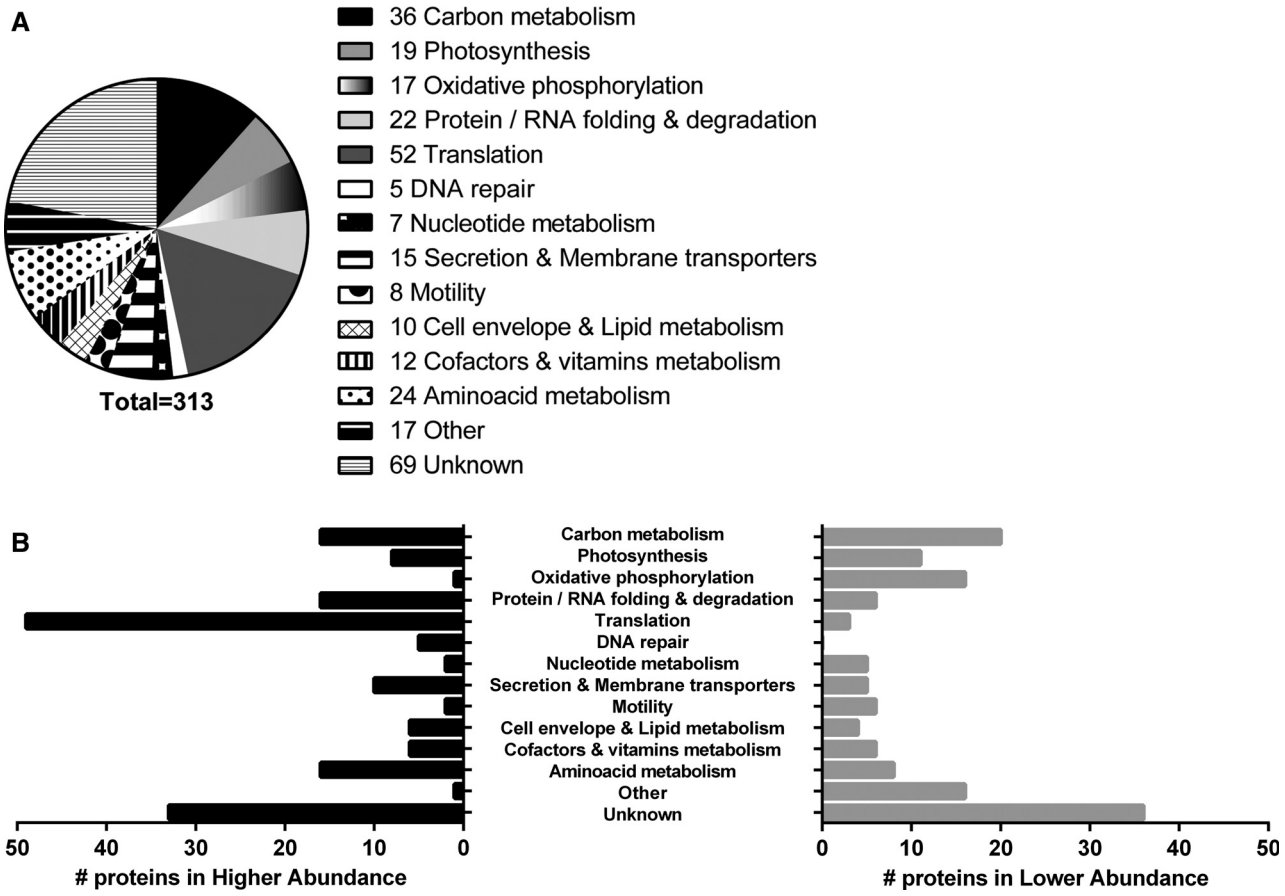

Fig. 9. Functional groups of proteins with significant fold changes in *Synechocystis* Δ*sigF vs.* wild-type.
A. Distribution by functional categories of the total number of proteins quantified in the iTRAQ analysis.
B. Number of proteins in each functional category with significant higher or lower abundance in Δ*sigF* compared with the wild-type. See annotated list of proteins in Supporting Information Table S4.

groups is similar to the distribution of the proteins encoded by genes retrieved in the analysis of putative SigF binding sites (Fig. 9A). Both analyses have 12 hits in common, which embody the most promising candidates of being directly regulated by SigF (Table 3). In the iTRAQ analysis, only 22% of the proteins identified are categorized as 'unknown function', and several proteins are associated to cell envelope maintenance, in contrast to the SigF binding sites analysis. The mechanisms related with the basal energy production and conversion, mainly through photosynthesis and oxidative phosphorylation, seem to be strongly affected in the Δ*sigF* mutant. The levels of the main players in light harvesting, the antenna proteins from phycobilissomes, are higher in the mutant, which is corroborated by the higher amount of phycocyanin content in Δ*sigF* cell extracts detected by absorption spectra analysis (Supporting Information Fig. S5). In contrast, the Psa proteins that constitute the photosystem I are in lower abundance in Δ*sigF.* Remarkably, plastocyanin has one of the lowest levels and cytochrome c6 the highest level in the entire iTRAQ analysis, which clearly shows that cytochrome c6 is a preferential route for the photosynthetic electron transport in Δ*sigF.* In terms of oxidative phosphorylation, the different subunits from the main players in this process are less abundant in Δ*sigF*, for e.g. the NADH dehydrogenase, succinate dehydrogenase/fumarate reductase and ATP synthetase (ATPase). Therefore, the photosynthetic activity of Δ*sigF* was evaluated to understand how changes in protein levels related to the main mechanisms of energy production and conversion could affect primary metabolism (Supporting Information Fig. S6). These changes seem to be responsible for a higher photosynthetic rate in Δ*sigF*, which increases when cells are exposed to high-light intensity. In addition, the respiratory activity during the dark period of Δ*sigF* growth is also significantly higher compared with the wild-type (Supporting Information Fig. S6).

In agreement with our previous results, a wide range of proteins involved in the carbon metabolism were differentially expressed in Δ*sigF* mutant, in processes such as glycolysis, pentose phosphate pathway and CO_2 fixation. The two subunits of RuBisCO, the major enzyme responsible for CO_2 fixation in *Synechocystis,* are in lower

Table 3. List of proteins displaying significant fold changes in *Synechocystis* Δ*sigF* compared with the wild-type (A and B are the two iTRAQ studies), encoded by genes displaying putative SigF binding motifs in their promoter regions.

Protein name	Uniprot ID	Description	Functional Category	Fold changes (mt: wt)	
				A	B
Slr1301	P72839	Predicted ABC transporter	Unknown	2.05	2.06
Sll1127, MenB	P73495	DHNA-CoA synthase	Cofactors and vitamins metabolism	1.12	–
Sll1812, RpsE, Rps5	P73304	30S ribosomal protein S5	Translation	1.28	1.23
Sll1837	P73107	Predicted UDP-dehydrogenase	Unknown	–	1.16
Sll1654	P72817	Universal stress protein	Unknown	–	1.22
Slr1338	P74074	Hypothetical protein	Unknown	1.30	1.22
Sll0634, BtpA	P72966	Protein involved in PSI biogenesis	Photosynthesis	1.20	1.18
Sll1525, PrK, Ptk	P37101	Phosphoribulokinase	Carbon metabolism	2.00	2.16
Slr0884, Gap1	P49433	Glyceraldehyde-3-phosphate dehydrogenase 1 (GAPDH 1)	Carbon metabolism	−1.50	−1.60
Sll0837	P73762	Periplasmic protein similar to TadD (Pilus assembly protein)	Unknown	−1.35	–
Sll1694, HofG	P73704	General secretion pathway protein G	Motility	−2.27	−2.39
Ssl3093, CpcD	P73202	Phycobilisome rod-linker polypeptide	Photosynthesis	−1.34	−1.40

levels in Δ*sigF.* This was confirmed by Western blot using antibodies against its large subunit (RbcL), which revealed a significant reduction in the levels of RbcL of approximately 75% in Δ*sigF* compared with the wild-type (Supporting Information Fig. S6). Other proteins described to be involved in the inorganic carbon (Ci) uptake are also in lower abundance in Δ*sigF* (Supporting Information Table S4). However, several proteins involved in the reactions immediately after CO_2 fixation or Ci uptake are in higher abundance.

Translation was the functional category with the highest number of proteins in higher abundance in Δ*sigF*, which indicates a deregulation of translational mechanisms (Fig. 9B). Remarkably, Δ*sigF* displays a higher number of chaperones, proteases, heat-shock proteins and folding catalysts that may help the mutant to cope with abnormal translational events. Additionally, the number and abundance of this type of proteins in the mutant suggests that Δ*sigF* cells may be under stress. Following up on these observations, the redox defences were also investigated (Supporting Information Fig. S7). Although the levels of ROS were slightly higher in Δ*sigF*, they were not statistically significant. The activity of the superoxide dismutase (SOD) was significantly higher in the mutant, but the catalase activity decreased approximately 50%, either detected by zymography or measured by spectrophotometric assays. The reduction of catalase activity is in agreement with the lower catalase abundance in Δ*sigF,* detected in the iTRAQ. Additionally, the spectrophotometric analysis of carotenoids revealed a reduction in the levels of these pigments of about 50% in the mutant (Supporting Information Fig. S5). However, a protein that binds specifically to carotenoids (Slr1963) is in higher abundance in Δ*sigF* (Supporting Information Table S4).

Regarding proteins that play a role in the biosynthesis of cell envelope components, Slr0776 (LpxD), one of the few proteins described as being involved in LPS biosynthesis, shows lower levels in the Δ*sigF* mutant. Moreover, other proteins that are known to be involved in lipid biosynthesis and with altered abundance in Δ*sigF*, are also expected to affect not only LPS formation but also vesiculation.

Alterations were also observed for several membrane transporters and proteins involved/or predicted to be involved in secretory pathways (e.g. Sll0616 – SecA). In the case of cell motility, not only the pilin and the pilin export and assembly machinery are in lower levels in Δ*sigF* but also other proteins involved in cell phototaxis and chemotaxis are also affected. The abundance of some regulators (e.g. Sll1626 - LexA) is also negatively affected in Δ*sigF*, reflecting the importance of the indirect regulation and cross-talk between regulatory networks in the pleiotropic role of SigF.

Discussion

The results of the extensive characterization of the Δ*sigF* (*slr1564*) knockout mutant presented here clearly show that this Group 3 sigma factor F has a remarkable pleiotropic effect on the physiology of this *Synechocystis* substrain (PCC-M) under the conditions tested. We show, for the first time, a strong growth impairment and conspicuous phenotype for the Δ*sigF* mutant (Figs 1 and 2). Earlier, this was not observed by Huckauf and colleagues (2000) but it is important to notice that the cells where grown in very different conditions, namely (i) the presence of NaCl, which induces the production of compatible solutes and generally reduces EPS production (Kirsch *et al*., 2017), and (ii) aeration with CO_2-enriched air, which provides an additional inorganic carbon supply and it is widely used to optimize cyanobacterial fitness (Zhang *et al*., 2002; Kim *et al*., 2010).

We also showed that the knockout of *sigF* leads to higher RPS production and total carbohydrate content (Fig. 3). The overproduction of RPS, strongly suggests a re-direction of energy and carbon fluxes towards RPS production, with a negative impact on the growth rate, as commonly observed for *Synechocystis* overproducing other carbon-rich compounds (Yoo *et al*., 2007; Carpine *et al*., 2017). In addition, no increase in the storage of other carbon reserves (e.g. glycogen) could be observed on the electron transmission micrographs of Δ*sigF* (Supporting Information Fig. S3). Earlier, another sigma factor (SigJ) was shown to be important for EPS production by the cyanobacterium *Anabaena* sp. PCC 7120, but in this strain the increase occurred only when *sigJ* was overexpressed (Yoshimura *et al*., 2007). *Synechocystis* does not have J-type sigma factors, but a BLASTp® analysis (NCBI database) revealed that *Synechocystis* SigF besides being closely related to *Anabaena´* SigF shares some similarity with *Anabaena´* SigJ, which is in agreement with the phylogenetic proximity between F and J sigma factor subtypes in cyanobacteria (Imamura *et al*., 2003; Yoshimura *et al*., 2007). The higher amount of RPS produced most probably play an important role in the establishment of the clumping phenotype displayed by the Δ*sigF* cells (Fig. 2). This has been reported for other bacterial and cyanobacterial strains in which EPS promote aggregation and embedment of the cells, which may work as a mechanism of self-shading with the polymers acting as protective molecules against light stress (Miranda *et al*., 2017; Quijano *et al*., 2017). Furthermore, according to Trautmann and colleagues (2012), this *Synechocystis* substrain has already the predisposition to exhibit a stress-induced clumping phenotype due to the truncation of genes encoding the proteins Sll1951 (hemolysin HlyA) and Slr1753 (surface protein), and here, we show that this feature can be exacerbated by the absence of SigF.

Although the RPS produced by both *Synechocystis* wild-type and Δ*sigF* display features commonly found in other cyanobacterial RPS, such as the high number of monosaccharides and the prevalence of glucose (Pereira *et al*., 2009; Rossi and De Philippis, 2016), our results show that the quality of the polymer produced by Δ*sigF* is also distinct from the wild-type (Table 1). These differences may have an impact on the physical–chemical properties of the extracellular polymer such as the hydrophobicity (due to the lower amount of deoxyhexoses/pentoses in Δ*sigF*) or the anionic nature (due to the absence of galacturonic acid in the wild-type). These alterations also suggest that the basic steps of RPS production and central carbon metabolism are under SigF control, as reinforced by the altered levels of a high number of proteins involved in the photosynthesis and central carbon metabolism in Δ*sigF* compared with the wild-type (Fig. 9 and Supporting Information Table S4).

In contrast with the increase of RPS in Δ*sigF* cultures, other components of the extracellular milieu were found in lower levels, namely carotenoids, LPS and lipids (Fig. 5) These results suggest impaired vesiculation ability, which was further confirmed by TEM analysis (Fig. 6A and B). Several studies have reported an increase in the formation of bacterial outer membrane vesicles (OMVs) as a result of cell stress, being a mechanism of releasing damaged cellular material into the extracellular space and/or promote communication among neighbour cells, similar to a warning (McBroom and Kuehn, 2007, Gonçalves *et al*., 2018). Although *Synechocystis* SigF is phylogenetically closest to *E. coli* FliA, in *E. coli* these events rely on different pathways regulated by SigE (Uniprot accession id P0AGB6; McBroom and Kuehn, 2007). Despite the decrease of OMVs formation, our results indicate that Δ*sigF* is under higher stress compared with the wild-type, as confirmed by the higher abundance of folding catalysts, chaperones and heat-shock proteins, which play a crucial role in protein quality control, maintenance of cell redox status and repair of cellular damages (Fig. 9 and Supporting Information Table S4). These proteins most probably function in alternative pathways to vesiculation in order to cope with accumulated damaged material. It is likely that the light intensity used here is one of the stress factors, as previous studies reported that SigF is crucial for light acclimation responses in *Synechocystis* (Huckauf *et al*., 2000; Ogawa *et al*., 2018). Furthermore, this hypothesis agrees with the higher amount of RPS and the strong clumping phenotype of the mutant, which are usual responses to light-induced stress (Miranda *et al*., 2017; Quijano *et al*., 2017). On the other hand, the lower levels/activities of some stress oxidative defences in Δ*sigF* are either due to regulatory adjustments or to the energetic burden that they represent (Supporting Information Fig. S5 and S7). For example, it is likely that the reduction of carotenoid levels is related to the redirection of carbon skeletons to RPS overproduction, similar to what occurs in *Synechocystis* mutants overproducing other carbon reserves such as glycogen or polyhydroxybutyrate - PHB (Antal *et al*., 2016; Tokumaru *et al*., 2018).

An absence of pili and of phototactic motility was also observed for Δ*sigF* (Fig. 6). This is in agreement with previous reports, describing SigF as the only sigma factor that regulates *pilA1* gene expression and consequent formation of pilin-like polypeptides in *Synechocystis* (Bhaya *et al*., 1999; Asayama and Imamura, 2008). Bhaya and colleagues (1999) also described a 'cell-surface aberration' surrounding Δ*sigF* cells, formed by the accumulation of extracellular material enclosing protein aggregates,

namely the main protein component of S-layer (HlyA). This structure is similar to the amorphous layer observed in our study and that is most likely formed by crippled EPS/LPS and other material resembling protein aggregates (Fig. 6A). In addition, other modifications were observed in sugar-rich cell envelope components of Δ*sigF* cells, such as a thicker peptidoglycan layer and alteration in the LPS profile on the O-antigen region (Supporting Information Figs S3 and S4). These results can be explained by alterations in the sugar amount/type of saccharides linked to these structures, as previously reported for *Synechocystis* mutants with an altered central carbon metabolism (Mohamed *et al*., 2005). The SigF importance in cell envelope maintenance was also reinforced by the iTRAQ results, showing that crucial proteins, such as Deg proteases, are in lower abundance in Δ*sigF* (Supporting Information Table S4). In addition, reduced levels of these proteins can increase cell sensitivity to light and oxidative stress, as well as result in protein secretion alterations (Barker *et al*., 2006; Cheregi *et al*., 2015). Indeed, the exoproteome of *Synechocystis* Δ*sigF* is remarkably different from the wild-type (Fig. 7 and Table 2). Among the 21 proteins identified, 13 were previously detected in *Synechocystis*' exoproteomes (Supporting Information Table S2). The variation in exoproteome composition among different studies may happen not only due to the growth conditions and method of isolation but also depending on the substrain. Here, we describe the first exoproteome of a *Synechocystis* substrain without a S-layer due to the truncation of the HlyA protein (Trautmann *et al*., 2012). In other *Synechocystis* substrains, HlyA accumulates extracellularly in such high amount that may hinder the identification of other proteins in the exoproteome samples. The phycocyanin subunits CpcA and CpcB are among the proteins that stand out in Δ*sigF* exoproteome suggesting possible cell lysis. Although CpcA is predicted to be secreted, these proteins (commonly found in thylakoids) are expected to be in lower abundance in the extracellular environment (Katoh, 1988; Gao *et al*., 2014). In contrast, Sll1009 (unknown function) was found in higher abundance in the wild-type exoproteome. This protein is also predicted to be secreted and prone to suffer glycosylation (Gao *et al*., 2014), as confirmed by us experimentally (data not shown). As Δ*sigF* has an altered carbon metabolism, secretion alterations are expected for glycosylated proteins, that are usually predominant at the bacterial cell surface and in the extracellular space (Nothaft and Szymanski, 2010; Gao *et al*., 2014). Moreover, we verified that the levels of several proteins involved in secretion mechanisms are altered in Δ*sigF* (Supporting Information Table S4). Among these, several components recently described as belonging to the TolC-mediated secretion mechanisms (Gonçalves *et al*., 2018) are in higher abundance in Δ*sigF.* In contrast, proteins of the type 4 secretion system which are responsible for pilin assembly and secretion, are in lower abundance, indicating that the requirement of SigF for *Synechocystis* motility may not be exclusively due to the regulation of the *pilA* gene.

Regarding translation mechanisms, the higher levels of the different ribosome subunits in Δ*sigF* clearly indicate an overproduction of the ribosomal machinery, which was also recently observed in a Δ*sigBCDE* strain of *Synechocystis* sp. PCC 6803 lacking all Group 2 sigma factors (Koskinen *et al*., 2018).

The two holistic approaches used to evaluate the impact of SigF on *Synechocystis* physiology, namely the iTRAQ quantitative proteomic analysis and the *in silico* search for SigF binding sites, confirmed the pleiotropic role of this sigma factor and a list of 12 gene candidates to be regulated by SigF emerged for further studies (Table 3). Two of these genes, *sll1694* (*hofG*/*pilA1*) and *sll0837* (*tadD*-like), were already reported as being SigF targets (Asayama and Imamura, 2008), which also reported that SigF regulates *sll0041* (*pixJ1*) expression (besides *sigF* autoregulation). In agreement, the proteins encoded by these three genes were found in lower abundance in Δ*sigF* (Supporting Information Table S4). Additionally, our results indicate that SigF can be indirectly controlling different pathways, as other regulators or proteins from sensory mechanisms have altered levels, and/or their encoding-genes present putative SigF binding motifs (Figs 8 and 9; Supporting Information Tables S3 and S4). Our perspective is reinforced by the fact that several SigF bacterial orthologues were associated with the regulation of various processes that are intrinsically dependent on secretion pathways, such as motility (Ohnishi *et al*., 1990; Claret *et al*., 2007), quorum sensing (Schuster *et al*., 2004) and morphological differentiation (Potuckova *et al*., 1995). Nevertheless, it is important to notice that the list of genes that are putatively regulated by SigF was generated by *in silico* analysis. Therefore, experimental validation studies are needed to confirm SigF specific binding and regulation.

In conclusion, the work presented here provides new evidences about the versatile role of SigF on *Synechocystis* physiology and its importance for environmental adaptation. The diversity of pathways and targets that are/could be under SigF influence also highlights how much is unknown about the regulatory networks involving alternative sigma factors. Nevertheless, SigF seems to have a particular importance in terms of cell envelope maintenance and control of classical and non-classical secretion pathways, being the first regulatory element associated with secretion in *Synechocystis* (for a brief summary see Fig. 10). Moreover, *Synechocystis* Δ*sigF* emerges as a promising platform to study/manipulate EPS production and to obtain higher amounts of RPS.

Interestingly, Δ*sigF* culture also presents the fastest *Synechocystis* spontaneous cell sedimentation described up to now, which is an important feature for industrial applications as it facilitates the harvesting of biomass and/or the recovery of secreted products.

Experimental procedures

Bacterial strains and culture conditions

Synechocystis sp. PCC 6803 (substrain PCC-M, for details see Huckauf *et al*., 2000; Trautmann *et al*., 2012), henceforth referred to as *Synechocystis* wild-type and the respective knockout mutant Δ*sigF* (both kindly provided by Prof. Martin Hagemann, University of Rostock, Germany) were grown in Erlenmeyer flasks containing BG11 media (Rippka *et al*., 1979). Axenic cultures were incubated at 30 °C under a 12 h light (50 μE m^{-2} s^{-1})/12 h dark regimen, with orbital shaking at 150 r.p.m. Cultures of Δ*sigF* mutant were maintained in BG11 medium supplemented with kanamycin (100 μg ml^{-1}), while all experiments were performed in the absence of selective pressure.

DNA extraction and confirmation of mutant segregation

Cyanobacterial genomic DNA was extracted using a phenol/chloroform method (Tamagnini *et al*., 1997). Complete segregation of the mutants was confirmed by agarose gel electrophoresis of PCR amplification products using standard protocols (Sambrook and Russell, 2001) and Southern blot (oligonucleotides in Supporting Information Table S1). Southern blots were performed after digestion of genomic DNA with AseI (Thermo Scientific). The DNA fragments were separated by electrophoresis on 1% agarose gel and blotted onto Amersham HybondTM-N membrane (GE Healthcare). Probes were amplified by PCR and labelled using DIG DNA labeling kit (Roche Diagnostics GmbH) according to manufacturer's instructions. Hybridization was done overnight at 60 °C and digoxigenin labelled probes were detected by chemiluminescence using CPD-star (Roche Diagnostics GmbH) in a Chemi DocTM XRS+ Imager (Bio-Rad).

Growth assessment

Growth measurements were performed by monitoring the chlorophyll *a* content in cyanobacterial cultures as

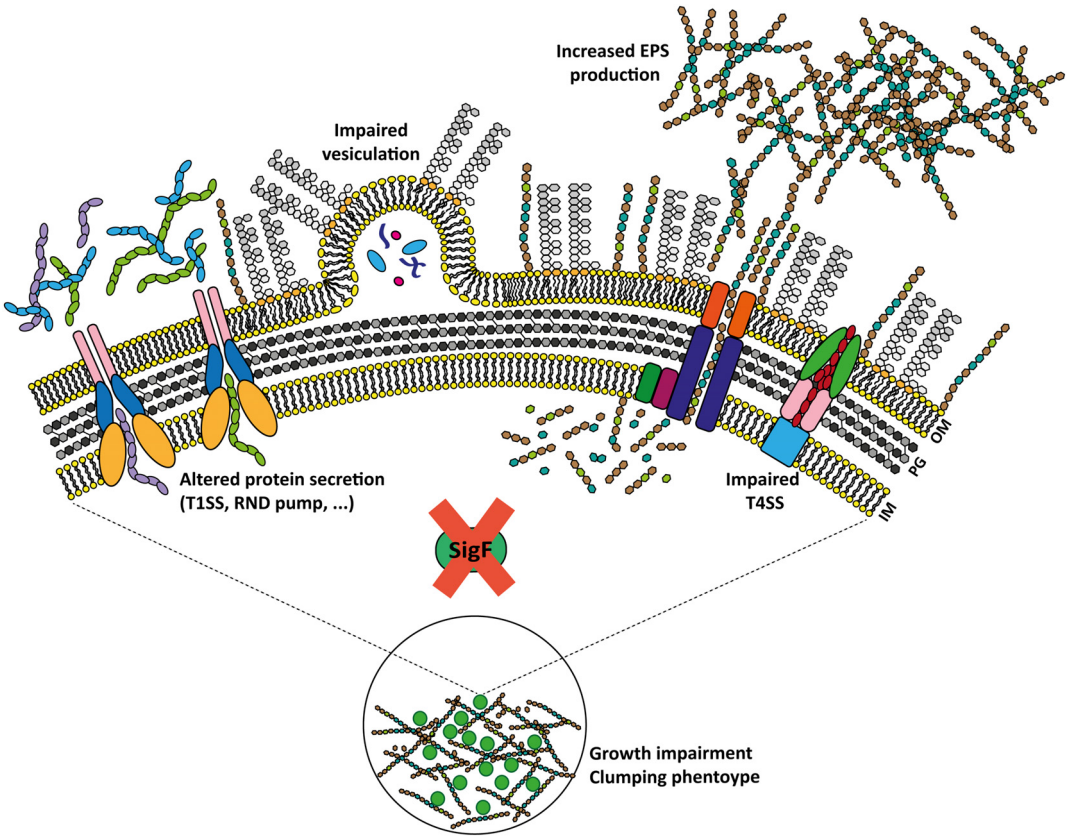

Fig. 10. Schematic representation of *Synechocystis* Δ*sigF* phenotype/genotype. Both classical and non-classical secretion pathways are altered in the mutant. EPS: extracellular polymeric substances, OM: outer membrane, PG: peptidoglycan, IM: inner membrane, T4SS: type 4 secretion system, T1SS: type 1 secretion system, RND pump: resistance-nodulation-division pump.

described by Meeks and Castenholz (1971) and by cell counting using Neubauer Chamber (Superior Marienfeld). Optical Density (OD) at 730 nm was also monitored spectrophotometrically (Shimadzu UVmini-1240, Shimadzu Corporation). All experiments were performed with three technical and three biological triplicates.

Determination of total carbohydrate content, RPS and CPS

The amount of total carbohydrates and released polysaccharides (RPS) in the cyanobacterial cultures were determined as previously reported in Mota and colleagues (2013). To isolate capsular polysaccharides (CPS), 5 ml of culture was centrifuged at 3857 *g* for 15 min, the pellet resuspended in 5 ml deionized water and boiled at 95 °C during 15 min. The suspension was centrifuged at 3857 *g* and the supernatant used for CPS quantification using the phenol-sulfuric acid assay described in Dubois and colleagues (1956). All experiments were performed with three technical and three biological triplicates.

RPS isolation and determination of monosaccharide composition

For RPS isolation, cultures were dialysed (12–14 kDa of molecular weight cut-off; Medicell International) against a minimum of 10 volumes of deionized water for 24 h with continuous stirring. The cells were removed by centrifugation at 12 000 *g* during 15 min at 4 °C and the RPS were precipitated from the supernatant with two volumes of 96% cold ethanol. The suspension was centrifuged at 10 000 *g* for 20 min at 15 °C, the pellet was resuspended in deionized water and lyophilized. The dried polymer was resuspended in deionized water and lyophilized again. To determine the monosaccharide composition, 5 mg of isolated RPS were hydrolysed with 1 ml of 2 M trifluoroacetic acid (TFA) at 120 °C for 1 h. Subsequently, samples were analysed by ion exchange chromatography using an ICS-2500 ion chromatograph (Dionex Corporation) as described in Mota and colleagues (2013).

Light and transmission electron microscopy (TEM)

For light microscopy, cells were observed directly using an Olympus X31 light microscope (Olympus). Micrographs were acquired with an Olympus DP25 camera using the Cell B image software (Olympus). Staining with 0.5% (w/v) Alcian Blue in 3% (v/v) acetic acid was performed in 1:1 (culture:dye) ratio. For TEM, cells were collected, centrifuged and processed as described by Seabra and colleagues (2009), with the exception of the resin used that was EMBed-812 resin (Electron Microscopy Sciences). Ultrathin sections were examined using a JEM-1400Plus (Jeol). Negative staining was performed in 10 μl of cells or 500× concentrated media (diluted 1:100), mounted on formvar/carbon film coated mesh nickel grids (Electron Microscopy Sciences) and left standing for 2 min. The liquid in excess was removed with filter paper and 5 μl of 1% uranyl acetate was added on to the grids, and left standing for 10 s, after which liquid in excess was removed with filter paper.

Motility assays

Phototactic movement was examined on BG11 0.5% (w/v) agar plates (Bacto agar, Difco) supplemented with 10 mM TES and 10 mM glucose, where 15 μl of cell culture was spotted. The plates were half covered and exposed to unidirectional white light source.

Outer membrane isolation and lipopolysaccharide (LPS) staining

Outer membranes were isolated as described by Simkovsky and colleagues (2012). The pellet was resuspended in 100 μl of 10 mM Tris–HCl, pH 8.0. Protease digested LPS samples were separated by electrophoresis on 12% SDS-PAGE (Bio-Rad) and stained using Pro-Q® Emerald 300 Lipopolysaccharide Gel Stain Kit (Molecular Probes) according to the manufacturer's instructions.

Concentration and analysis of extracellular medium

The medium from *Synechocystis* wild-type and Δ*sigF* cultures was isolated and concentrated as described in Oliveira and colleagues (2016). Concentrated samples were saved at −20 °C until further analysis. For the analysis of the pigments present in the medium, samples were diluted in 1:100 ratio and the absorption spectra in the visible light range of the extracts were measured at room temperature from 350 to 750 nm using Shimadzu UV-2401 PC spectrophotometer (Shimadzu Corporation). The relative abundance of carotenoids (CX index) was determined using carotenoids absorbance at 487 nm to the chl *a* absorbance at 663 nm ratio (Yang *et al*., 2010). For LPS detection, concentrated medium samples were separated by gel electrophoresis on 12% SDS-polyacrylamide gels, which were stained as aforementioned. Subsequently, gels were incubated overnight with Sudan Black B solution [0.5% (w/v) Sudan Black B in 17% (v/v) acetone and 12.5% (v/v) acetic acid] for lipids visualization.

Exoproteome analysis

The analysis of the exoproteomes was performed using concentrated medium samples. The protein concentration

was measured using the BCA™ Protein Assay Kit (Pierce Biotechnology) and the iMark Microplate Absorbance Reader (Bio-Rad) according to the manufacturer's instructions, and 6 μg of protein were separated by electrophoresis on gradient 4%–15% SDS-polyacrylamide gels (Bio-Rad) and visualized with colloidal Coomassie brilliant blue (Sigma). Stained bands or gel regions observed consistently across at least three biological replicates were further excised and processed for mass spectrometry analysis as previously described (Gomes *et al*., 2013; Osório and Reis, 2013). Peptide mass spectra were acquired in reflector positive mode in the mass range of *m/z* 700–5000. Proteins were identified by Peptide Mass Fingerprint (PMF) approach with the Mascot software (v2.5.1, Matrix Science) using the UniProt protein sequence database for the taxonomic selection *Synechocystis* (2017_01 release). The predicted localization of the identified proteins was based on the ontology of their encoding-genes (GO annotations, EMBL-EBI database https://www.ebi.ac.uk/QuickGO/) and the PSORTb online tool (http://www.psort.org/psortb/).

In silico *consensus binding motif analysis*

Identification of putative gene promoter regions recognized by SigF was performed searching for the consensus binding motifs GGGTAAG, GGGT[A/G], [C/G]GGT [A/G][A/G/T], [C/T]AGGC [N10-30] GGGT[A/G][A/G][A/G] previously reported by Asayama and Imamura (2008), in *Synechocystis* sp. PCC-M genome deposited by Trautmann and colleagues (2012). The sequences GGGT [A/G] and [C/G]GGT[A/G][A/G/T] are highly unspecific and retrieved a large number of hits, that were not considered for further analysis. For the remaining hits, a manual curation was performed in order to select only promoter regions that present a SigF binding motif within 300 bp upstream of the coding sequence. Description of the proteins encoded by the genes identified and their distribution into functional categories was based on CyanoBase (http://genome.microbedb.jp/cyanobase, Fujisawa *et al*., 2016), Uniprot (http://www.uniprot.org/) and KEGG (Kyoto Encyclopedia of Genes and Genomes, http://www.genome.jp/kegg/) databases and complemented with the information available in the literature.

iTRAQ experiment

The proteomes of *Synechocystis* wild-type and Δ*sigF* were analysed by 8-plex isobaric tags for relative and absolute quantification (iTRAQ), using two biological and two technical replicates. The detailed description of the procedure can be found in the Supporting Information Experimental Procedures. The distribution into functional categories of the identified proteins was performed as described above.

Statistical analysis

Data were statistically analysed in GraphPad Prism v7 (GraphPad Software) using an analysis of variance (ANOVA), followed by Bonferroni's multiple comparisons test.

Acknowledgements

This work was financed by FEDER - Fundo Europeu de Desenvolvimento Regional funds through the COMPETE 2020 - Operational Programme for Competitiveness and Internationalization (POCI); projects NORTE-01-0145-FEDER-000012 - Structured Programme on Bioengineering Therapies for Infectious Diseases and Tissue Regeneration, supported by Norte Portugal Regional Operational Programme (NORTE 2020), under the PORTUGAL 2020 Partnership Agreement; and by Portuguese funds through FCT – Fundação para a Ciência e a Tecnologia/Ministério da Ciência, Tecnologia e Ensino Superior in the framework of the project 'Institute for Research and Innovation in Health Sciences' (POCI-01-0145-FEDER-007274) and grants SFRH/BD/99715/2014 (CF) and SFRH/BD/119920/2016 (MS). The authors thank Rui Fernandes, Francisco Figueiredo and Hugo Osório for their technical assistance. PCW and NC acknowledge the financial support from the European Union Seventh Framework Programme (FP7/2007-2013) under grant agreement number 308518 (CyanoFactory) and from BBSRC under grant number [BB/M012166/1]. PO was supported by Fundo Social Europeu and Programa Operacional Potencial Humano through the FCT Investigator grant IF/00256/2015, and by the POCI/FEDER-FCT grant POCI-01-0145-FEDER-029540.

The authors have no conflict of interest to declare.

References

Antal, T., Kurkela, J., Parikainen, M., Kårlund, A., Hakkila, K., Tyystjärvi, E., and Tyystjärvi, T. (2016) Roles of group 2 sigma factors in acclimation of the cyanobacterium *Synechocystis* sp. PCC 6803 to nitrogen deficiency. *Plant Cell Physiol* **57**: 1309–1318.

Asayama, M., and Imamura, S. (2008) Stringent promoter recognition and autoregulation by the group 3 σ-factor SigF in the cyanobacterium *Synechocystis* sp. strain PCC 6803. *Nucleic Acids Res* **36**: 5297–5305.

Barker, M., de Vries, R., Nield, J., Komenda, J., and Nixon, P. J. (2006) The deg proteases protect *Synechocystis* sp. PCC 6803 during heat and light stresses but are not essential for removal of damaged D1 protein during the photosystem two repair cycle. *J Biol Chem* **281**: 30347–30355.

Bell, N., Lee, J. J., and Summers, M. L. (2017) Characterization and in vivo regulon determination of an ECF sigma factor and its cognate anti-sigma factor in *Nostoc punctiforme*. *Mol Microbiol* **104**: 179–194.

Bhaya, D., Watanabe, N., Ogawa, T., and Grossman, A. R. (1999) The role of an alternative sigma factor in motility and pilus formation in the cyanobacterium *Synechocystis* sp. strain PCC6803. *Proc Natl Acad Sci USA* **96**: 3188–3193.

Carpine, R., Du, W., Olivieri, G., Pollio, A., Hellingwerf, K. J., Marzocchella, A., and dos Santos, F. B. (2017) Genetic engineering of *Synechocystis* sp. PCC6803 for poly-β-hydroxybutyrate overproduction. *Algal Res* **25**: 117–127.

Cheregi, O., Miranda, H., Gröbner, G., and Funk, C. (2015) Inactivation of the Deg protease family in the cyanobacterium *Synechocystis* sp. PCC 6803 has impact on the outer cell layers. *J Photochem Photobiol B* **152**: 383–394.

Christie-Oleza, J. A., Armengaud, J., Guerin, P., and Scanlan, D. J. (2015) Functional distinctness in the exoproteomes of marine *Synechococcus*. *Environ Microbiol* **17**: 3781–3794.

Claret, L., Miquel, S., Vieille, N., Ryjenkov, D. A., Gomelsky, M., and Darfeuille-Michaud, A. (2007) The flagellar sigma factor FliA regulates adhesion and invasion of Crohn disease-associated *Escherichia coli* via a cyclic dimeric GMP-dependent pathway. *J Biol Chem* **282**: 33275–33283.

Costa, T. R., Felisberto-Rodrigues, C., Meir, A., Prevost, M. S., Redzej, A., Trokter, M., and Waksman, G. (2015) Secretion systems in gram-negative bacteria: structural and mechanistic insights. *Nat Rev Microbiol* **13**: 343–359.

Donia, M. S., and Fischbach, M. A. (2015) Small molecules from the human microbiota. *Science* **349**: 1254766.

Dubois, M., Gilles, K. A., Hamilton, J. K., Rebers, P. A., and Smith, F. (1956) Colorimetric method for determination of sugars and related substances. *Anal Chem* **28**: 350–356.

Eichelberg, K., and Galán, J. E. (2000) The Flagellar sigma factor FliA (σ^{28}) regulates the expression of *Salmonella* genes associated with the centisome 63 type III secretion system. *Infect Immun* **68**: 2735–2743.

Feklístov, A., Sharon, B. D., Darst, S. A., and Gross, C. A. (2014) Bacterial sigma factors: a historical, structural, and genomic perspective. *Annu Rev Microbiol* **68**: 357–376.

Fujisawa, T., Narikawa, R., Maeda, S. I., Watanabe, S., Kanesaki, Y., Kobayashi, K., *et al*. (2016) CyanoBase: a large-scale update on its 20th anniversary. *Nucleic Acids Res* **45**: D551–D554.

Gao, L., Huang, X., Ge, H., Zhang, Y., Kang, Y., Fang, L., *et al*. (2014) Profiling and compositional analysis of the exoproteome of *Synechocystis* sp. PCC 6803. *J Metabol Sys Biol* **1**: 8.

Gomes, C., Almeida, A., Ferreira, J. A., Silva, L., Santos-Sousa, H., Pinto-de-Sousa, J., *et al*. (2013) Glycoproteomic analysis of serum from patients with gastric precancerous lesions. *J Proteome Res* **12**: 1454–1466.

Gonçalves, C. F., Pacheco, C. C., Tamagnini, P., and Oliveira, P. (2018) Identification of inner membrane translocase components of TolC-mediated secretion in the cyanobacterium *Synechocystis* sp. PCC 6803. *Environ Microbiol* **20**: 2354–2369.

Gruber, T. M., and Gross, C. A. (2003) Multiple sigma subunits and the partitioning of bacterial transcription space. *Annu Rev Microbiol* **57**: 441–466.

Hilbert, D. W., Chary, V. K., and Piggot, P. J. (2004) Contrasting effects of σ^{E} on compartmentalization of σ^{F} activity during sporulation of *Bacillus subtilis*. *J Bacteriol* **186**: 1983–1990.

Huckauf, J., Nomura, C., Forchhammer, K., and Hagemann, M. (2000) Stress responses of *Synechocystis* sp. strain PCC 6803 mutants impaired in genes encoding putative alternative sigma factors. *Microbiology* **146**: 2877–2889.

Imamura, S., and Asayama, M. (2009) Sigma factors for cyanobacterial transcription. *Gene Regul Syst Bio* **3**: 65–87.

Imamura, S., Yoshihara, S., Nakano, S., Shiozaki, N., Yamada, A., Tanaka, K., *et al*. (2003) Purification, characterization, and gene expression of all sigma factors of RNA polymerase in a cyanobacterium. *J Mol Biol* **325**: 857–872.

Inoue-Sakamoto, K., Gruber, T. M., Christensen, S. K., Arima, H., Sakamoto, T., and Bryant, D. A. (2007) Group 3 sigma factors in the marine cyanobacterium *Synechococcus* sp. strain PCC 7002 are required for growth at low temperature. *J Gen Appl Microbiol* **53**: 89–104.

Katoh, T. (1988) Phycobilisome stability. In *Methods in Enzymology*. San Diego, CA: Academic Press, pp. 313–318.

Kim, H. W., Vannela, R., Zhou, C., Harto, C., and Rittmann, B. E. (2010) Photoautotrophic nutrient utilization and limitation during semi-continuous growth of *Synechocystis* sp. PCC6803. *Biotechnol Bioeng* **106**: 553–563.

Kirsch, F., Pade, N., Klähn, S., Hess, W. R., and Hagemann, M. (2017) The glucosylglycerol-degrading enzyme GghA is involved in acclimation to fluctuating salinities by the cyanobacterium *Synechocystis* sp. strain PCC 6803. *Microbiology* **163**: 1319–1328.

Koskinen, S., Hakkila, K., Kurkela, J., Tyystjärvi, E., and Tyystjärvi, T. (2018) Inactivation of group 2 σ factors upregulates production of transcription and translation machineries in the cyanobacterium *Synechocystis* sp. PCC 6803. *Sci Rep* **8**: 10305.

Marin, K., Huckauf, J., Fulda, S., and Hagemann, M. (2002) Salt-dependent expression of glucosylglycerol-phosphate synthase, involved in osmolyte synthesis in the cyanobacterium *Synechocystis* sp. strain PCC 6803. *J Bacteriol* **184**: 2870–2877.

Marx, J. G., Carpenter, S. D., and Deming, J. W. (2009) Production of cryoprotectant extracellular polysaccharide substances (EPS) by the marine psychrophilic bacterium *Colwellia psychrerythraea* strain 34H under extreme conditions. *Can J Microbiol* **55**: 63–72.

McBroom, A. J., and Kuehn, M. J. (2007) Release of outer membrane vesicles by gram-negative bacteria is a novel envelope stress response. *Mol Microbiol* **63**: 545–558.

Meeks, J. C., and Castenholz, R. W. (1971) Growth and photosynthesis in an extreme thermophile, *Synechococcus lividus* (Cyanophyta). *Arch Mikrobiol* **78**: 25–41.

Miranda, H., Immerzeel, P., Gerber, L., Hörnaeus, K., Lind, S. B., Pattanaik, B., *et al*. (2017) Sll1783, a monooxygenase associated with polysaccharide processing in the unicellular cyanobacterium *Synechocystis* PCC 6803. *Physiol Plant* **161**: 182–195.

Mohamed, H. E., Van De Meene, A. M., Roberson, R. W., and Vermaas, W. F. (2005) Myxoxanthophyll is required for normal cell wall structure and thylakoid organization in the cyanobacterium *Synechocystis* sp. strain PCC 6803. *J Bacteriol* **187**: 6883–6892.

Mota, R., Guimarães, R., Büttel, Z., Rossi, F., Colica, G., Silva, C. J., *et al*. (2013) Production and characterization of extracellular carbohydrate polymer from *Cyanothece* sp. CCY 0110. *Carbohydr Polym* **92**: 1408–1415.

Nothaft, H., and Szymanski, C. M. (2010) Protein glycosylation in bacteria: sweeter than ever. *Nat Rev Microbiol* **8**: 765–778.

Ogawa, K., Yoshikawa, K., Matsuda, F., Toya, Y., and Shimizu, H. (2018) Transcriptome analysis of the cyanobacterium *Synechocystis* sp. PCC 6803 and mechanisms of photoinhibition tolerance under extreme high light conditions. *J Biosci Bioeng* **126**: 596–602.

Ohnishi, K., Kutsukake, K., Suzuki, H., and Iino, T. (1990) Gene fliA encodes an alternative sigma factor specific for flagellar operons in *Salmonella typhimurium*. *Mol Gen Genet* **221**: 139–147.

Oliveira, P., Martins, N. M., Santos, M., Pinto, F., Büttel, Z., Couto, N. A., *et al*. (2016) The versatile TolC-like Slr1270 in the cyanobacterium *Synechocystis* sp. PCC 6803. *Environ Microbiol* **18**: 486–502.

Osório, H., and Reis, C. A. (2013) Mass spectrometry methods for studying glycosylation in cancer. In *Mass Spectrometry Data Analysis in Proteomics*, Matthiesen, R. (ed). Totowa, NJ: Humana Press, pp. 301–316.

Österberg, S., Peso-Santos, T. D., and Shingler, V. (2011) Regulation of alternative sigma factor use. *Annu Rev Microbiol* **65**: 37–55.

Paget, M. S. (2015) Bacterial sigma factors and anti-sigma factors: structure, function and distribution. *Biomolecules* **5**: 1245–1265.

Pereira, S., Zille, A., Micheletti, E., Moradas-Ferreira, P., De Philippis, R., and Tamagnini, P. (2009) Complexity of cyanobacterial exopolysaccharides: composition, structures, inducing factors and putative genes involved in their biosynthesis and assembly. *FEMS Microbiol Rev* **33**: 917–941.

Potuckova, L., Kelemen, G. H., Findlay, K. C., Lonetto, M. A., Buttner, M. J., and Kormanec, J. (1995) A new RNA polymerase sigma factor, sigma F, is required for the late stages of morphological differentiation in *Streptomyces* spp. *Mol Microbiol* **17**: 37–48.

Quijano, G., Arcila, J. S., and Buitrón, G. (2017) Microalgal-bacterial aggregates: applications and perspectives for wastewater treatment. *Biotechnol Adv* **35**: 772–781.

Rachid, S., Ohlsen, K., Wallner, U., Hacker, J., Hecker, M., and Ziebuhr, W. (2000) Alternative transcription factor σ^B is involved in regulation of biofilm expression in a *Staphylococcus aureus* mucosal isolate. *J Bacteriol* **182**: 6824–6826.

Rippka, R., Deruelles, J., Waterbury, J. B., Herdman, M., and Stanier, R. Y. (1979) Generic assignments, strain histories and properties of pure cultures of cyanobacteria. *Microbiology* **111**: 1–61.

Roier, S., Zingl, F. G., Cakar, F., and Schild, S. (2016) Bacterial outer membrane vesicle biogenesis: a new mechanism and its implications. *Microb Cell* **3**: 257–259.

Rossi, F., and De Philippis, R. (2016) Exocellular polysaccharides in microalgae and cyanobacteria: chemical features, role and enzymes and genes involved in their biosynthesis. In *The Physiology of Microalgae*, Borowitzka, M. A., Beardall, J., and Raven, J. A. (eds). Cham, Switzerland: Springer, pp. 565–590.

Rutherford, S. T., and Bassler, B. L. (2012) Bacterial quorum sensing: its role in virulence and possibilities for its control. *Cold Spring Harb Perspect Med* **2**: a012427.

Sambrook, J., and Russell, D. W. (2001) *Molecular Cloning: A Laboratory Manual*, 3rd ed. New York, NY: Cold Spring Harbor Laboratory Press.

Schuster, M., Hawkins, A. C., Harwood, C. S., and Greenberg, E. P. (2004) The *Pseudomonas aeruginosa* RpoS regulon and its relationship to quorum sensing. *Mol Microbiol* **51**: 973–985.

Schwechheimer, C., and Kuehn, M. J. (2015) Outer-membrane vesicles from gram-negative bacteria: biogenesis and functions. *Nat Rev Microbiol* **13**: 605–619.

Seabra, R., Santos, A., Pereira, S., Moradas-Ferreira, P., and Tamagnini, P. (2009) Immunolocalization of the uptake hydrogenase in the marine cyanobacterium *Lyngbya majuscula* CCAP 1446/4 and two *Nostoc* strains. *FEMS Microbiol Lett* **292**: 57–62.

Simkovsky, R., Daniels, E. F., Tang, K., Huynh, S. C., Golden, S. S., and Brahamsha, B. (2012) Impairment of O-antigen production confers resistance to grazing in a model amoeba–cyanobacterium predator–prey system. *Proc Natl Acad Sci USA* **109**: 16678–16683.

Srivastava, A., Brilisauer, K., Rai, A. K., Ballal, A., Forchhammer, K., and Tripathi, A. K. (2017) Down-regulation of the alternative sigma factor SigJ confers a Photoprotective phenotype to *Anabaena* PCC 7120. *Plant Cell Physiol* **58**: 287–297.

Stensjö, K., Vavitsas, K., and Tyystjärvi, T. (2017) Harnessing transcription for bioproduction in cyanobacteria. *Physiol Plant* **162**: 148–155.

Tamagnini, P., Troshina, O., Oxelfelt, F., Salema, R., and Lindblad, P. (1997) Hydrogenases in *Nostoc* sp. strain PCC 73102, a strain lacking a bidirectional enzyme. *Appl Environ Microbiol* **63**: 1801–1807.

Tokumaru, Y., Uebayashi, K., Toyoshima, M., Osanai, T., Matsuda, F., and Shimizu, H. (2018) Comparative targeted proteomics of the central metabolism and photosystems in SigE mutant strains of *Synechocystis* sp. PCC 6803. *Molecules* **23**: 1051.

Trautmann, D., Voß, B., Wilde, A., Al-Babili, S., and Hess, W. R. (2012) Microevolution in cyanobacteria: re-sequencing a motile substrain of *Synechocystis* sp. PCC 6803. *DNA Res* **19**: 435–448.

Tripathi, L., Zhang, Y., and Lin, Z. (2014) Bacterial sigma factors as targets for engineered or synthetic transcriptional control. *Front Bioeng Biotechnol* **2**: 33.

Vilches, S., Jimenez, N., Tomás, J. M., and Merino, S. (2009) *Aeromonas hydrophila* AH-3 type III secretion system expression and regulatory network. *Appl Environ Microbiol* **75**: 6382–6392.

Yang, D., Qing, Y., and Min, C. (2010) Incorporation of the chlorophyll d-binding light-harvesting protein from *Acaryochloris marina* and its localization within the photosynthetic apparatus of *Synechocystis* sp. PCC6803. *Biochim Biophys Acta* **1797**: 204–211.

Yoo, S. H., Keppel, C., Spalding, M., and Jane, J. L. (2007) Effects of growth condition on the structure of glycogen

produced in cyanobacterium *Synechocystis* sp. PCC6803. *Int J Biol Macromol* **40**: 498–504.

Yoshimura, H., Okamoto, S., Tsumuraya, Y., and Ohmori, M. (2007) Group 3 sigma factor gene, *sigJ*, a key regulator of desiccation tolerance, regulates the synthesis of extracellular polysaccharide in cyanobacterium *Anabaena* sp. strain PCC 7120. *DNA Res* **14**: 13–24.

Zhang, K., Kurano, N., and Miyachi, S. (2002) Optimized aeration by carbon dioxide gas for microalgal production and mass transfer characterization in a vertical flat-plate photobioreactor. *Bioprocess Biosyst Eng* **25**: 97–101.

Zhao, K., Liu, M., and Burgess, R. R. (2007) Adaptation in bacterial flagellar and motility systems: from regulon members to 'foraging'-like behavior in *E. coli*. *Nucleic Acids Res* **35**: 4441–4452.

Supporting Information

Additional Supporting Information may be found in the online version of this article at the publisher's web-site:

Fig. S1. Growth curves of *Synechocystis* sp. PCC 6803 wild-type (wt) and Δ*sigF* mutant. Growth was monitored by measuring optical density at 730 nm. Cells were grown in BG11 at 30 °C under a 12 h light (50 μE m^{-2} s^{-1})/12 h dark regimen, with orbital shaking at 150 r.p.m.

Fig. S2. Characterization of *Synechocystis* sp. PCC 6803 wild-type (wt), Δ*sigF* and complementation mutants Δ*sigF* pS351B*sigF* and Δ*sigF* pS351R*sigF* in terms of growth (chlorophyll *a*), total carbohydrates content, and production of released polysaccharides (RPS). Cultures were grown in BG11 at 30 °C under a 12 h light (50 μE m^{-2} s^{-1})/12 h dark regimen, with orbital shaking at 150 r.p.m. Experiments were made in triplicate and the statistical analysis is presented for the last time point comparing Δ*sigF* to the complemented mutants (**** p value ≤ 0.0001).

Fig. S3. Transmission electron micrographs of *Synechocystis* sp. PCC 6803 wild-type (wt) and Δ*sigF* mutant highlighting differences in the cell envelope. In the left panel, it is possible to observe the vesiculation capacity of the wt (vs), while in the right panel the ticker peptidoglycan layer and the presence of amorphous material surrounding the cells of Δ*sigF* can be noticed (star) amorphous layer; (black arrowhead) outer membrane; (white arrowhead) peptidoglycan; (white arrow) cytoplasmic membrane. The measurements of the peptidoglycan thickness are presented below the micrographs (**** p value ≤ 0.0001).

Fig. S4. Lipopolysaccharides profile from outer membrane preparations of *Synechocystis* sp. PCC 6803 wild-type (wt) and Δ*sigF.* Samples were resolved in SDS-polyacrylamide gels and visualized using Pro-Q® Emerald 300 Lipopolysaccharide Gel Stain Kit (Life Technologies). White arrowheads highlight the differences between the profiles.

Fig. S5. Absorption spectra of cell-free extracts of *Synechocystis* PCC 6803 wild-type (wt) and Δ*sigF* mutant (upper panel). Arrows indicate the characteristic absorption peaks of the different pigments – Car, carotenoids; Chl *a*, chlorophyll *a*; PC, phycocyanin. Quantification of the relative abundance of carotenoids – CX index and phycocyanin – PC index (lower panel) (**** p value ≤ 0.0001).

Fig. S6. A. Oxygen evolution rates from cultures of *Synechocystis* sp. strain PCC 6803 wild-type (wt) and Δ*sigF.* The photosynthetic activity was measured during the light period, and the respiration rate during the dark period of the 12 h light/12 h dark growth regimen as described at the Experimental procedures section (** p value ≤ 0.01; **** p value ≤ 0.0001). **B.** Quantification of the RbcL (large subunit of RuBisCO) relative abundance after Western blot. 100 μg of total protein from each strain were separated by SDS-polyacrylamide electrophoresis prior to blot transfer. Quantification of the bands intensity according to the Image J software (Rueden *et al*., 2017) (** p value ≤ 0.01).

Fig. S7. *In vivo* detection of reactive oxygen species (ROS) and assessment of superoxide dismutase and catalase activities from *Synechocystis* sp. PCC 6803 wild-type (wt) and Δ*sigF.* **A**. Relative levels of ROS are expressed as intensity of the fluorescent probe H2DCF-DA per amount of chlorophyll *a.* **B.** and **C.** Protein extracts from *Synechocystis* wt and Δ*sigF* were separated by electrophoresis on native-polyacrylamide gels and stained for specific detection of SOD (**B**) or catalase activities (C**I**). Total catalase activity was further quantified *in vitro* by spectrophotometry (C**II**), measuring absorbance at 240 nm as an indication of H_2O_2 dissociation. Catalase activity is expressed as units per mg of total protein, defining a unit as the amount of enzyme that catalyses the dissociation of 1 μmol of H_2O_2 per minute at pH 7.0 at 25 °C. (* p value ≤ 0.05; *** p ≤ 0.001).

Table S1. List of organisms, plasmids and oligonucleotides used in this work.

Table S2. List of proteins identified in the exoproteomes of *Synechocystis* sp PCC 6803 wild-type and Δ*sigF.* Legend: E – Extracellular, OM – Outer membrane, P – Periplasmic, CM – Cytoplasmic membrane, TM – Thylakoid membrane, C – Cytoplasmic, U – Unknown.

Table S3. List of genes with putative SigF binding motifs in their promoter regions (*in silico* predicted).

Table S4. Distribution by functional categories of the proteins quantified in the two iTRAQ analysis (A and B) with significant fold changes in *Synechocystis* Δ*sigF vs.* wild-type.

Supporting Information

Supporting Tables

Table S1. List of organisms, plasmids and oligonucleotides used in this work.

Organisms	Description	Source
Escherichia coli DH5α	Transformation / Cloning strain	Invitrogen
Synechocystis sp. PCC 6803	Wild-type substrain PCC-M (Moscow State University, Russia)	Huckauf *et al.*, 2000
Synechocystis Δ*sigF*	*Synechocystis* mutant with a kanamycin resistance cassette inserted in the restriction site StuI on the *sigF* (*slr1564*) gene	Huckauf *et al.*, 2000
Δ*sigF* pS351B*sigF*	*Synechocystis* Δ*sigF* mutant complemented with the replicative plasmid pS351B*sigF*	This work
Δ*sigF* pS351R*sigF*	*Synechocystis* Δ*sigF* mutant complemented with the replicative plasmid pS351R*sigF*	This work

Plasmid	Description	Source
psb1A3	Shuttle vector for *E. coli* transformation	Registry of Standard Biological Parts (http://parts.igem.org)
psbP$_{rbcL}$	psb1A3 with the promotor region of *rbcL*	This work
psbB*sigF*	psb1A3 with *slr1564* downstream the synthetic RBS BBa_B0032 under the control of P$_{rbcL}$	This work
psbR*sigF*	psb1A3 with *slr1564* downstream the native RBS of *rbcL* under the control of P$_{rbcL}$	This work
pSEVA351	Replicative shuttle vector for *Synechocystis* transformation.	SEVA database (Silva-Rocha *et al.*, 2012)
pS351B*sigF*	psb1A3 with *slr1564* downstream the synthetic RBS BBa_B0032 under the control of P$_{rbcL}$	This work
pS351R*sigF*	pSEVA351 with *slr1564* downstream the native RBS of *rbcL* under the control of P$_{rbcL}$	This work

Primer name	Sequence (5' – 3')	Purpose	Reference
slr1564F	TATTGGCGTGCGTAATCGGA	Δ*sigF* segregation confirmation by PCR	This work
KmR2Rev	CGCAATCACGAATGAATAACGGT	Δ*sigF* segregation confirmation by PCR	This work
slr1564.5O	GGGTGGTTATCAACAGCAAGCCCAGCAAAT	Δ*sigF* segregation confirmation	This work

Table S1 (continued)

slr1564.3O	GAGATTGTGGAGGTAACCTGCACTCTGGCT	Δ*sigF* segregation confirmation	This work
slr1564F_SB	GCGTGGGTTCCTATGCCATA	Southern blot probe amplification	This work
slr1564R_SB	GGGAATGGCAAAGGAGCTAA	Southern blot probe amplification	This work
rbcL_sigF_fwd	TCTAGAATGGAGGACTGACCTAGATGACCAATGCCACCAGCGAAAGC	Amplification of *sigF* introducing XbaI restriction site and native RBS of *rbcL*	This work
BBa_B0032	TCACACAGGAAAG	Synthetic RBS	Registry of Standard Biological Parts (http://parts.igem.org)
B0032_sigF_fwd	TCTAGATCACACAGGAAAGACTAGATGACCAATGCCACCAGCGAAAGC	Amplification of *sigF* introducing XbaI Restriction site and BBa_B0032	This work
sigF_rev	GCACTAGTCTACTGGAGATAGACTCTAAACAG	Amplification of *sigF* introducing SpeI restriction site	This work
PrbcL_fwd	GTTTCTTCGAATTCGCGGCCGCTTCTAGAGCTAATTAGAAAGTCCAAAAATTGTAAT	Amplification of P_{rbcL} introducing EcoRI and XbaI	This work
PrbcL_rev	GTTTCTTCCTGCAGCGGCCGCTACTAGTAAAACATTGAATAGCCTAGCTTTCTCC	Amplification of P_{rbcL} introducing SpeI and PstI	This work
PS1	AGGGCGGCGGATTTGTCC	Sequencing and Amplification of the insert in the cloning site of pSEVA351	SEVA database (Silva-Rocha *et al.*, 2012)
PS2	GCGGCAACCGAGCGTTC		
VF2	TGCCACCTGACGTCTAAGAA	Sequencing and Amplification of the insert in the cloning site of psb1A3	Registry of Standard Biological Parts (http://parts.igem.org)
VR	ATTACCGCCTTTGAGTGAGC		

Table S2. List of proteins identified in the exoproteomes of *Synechocystis* sp PCC 6803 wild-type and Δ*sigF*. Legend: E – Extracellular, OM – Outer membrane, P – Periplasmic, CM – Cytoplasmic membrane, TM – Thylakoid membrane, C – Cytoplasmic, U – Unknown

Band / Region	Uniprot ID	Cyanobase ORF	Description / Functional category	PSORTb	GO terms	Previously identified in exoproteomes
1	P73019	**Sll1009**	FrpC - Protein with calcium ion binding motifs (Iron-regulated protein) / Unknown	E	U	Chiregi *et al.*, 2015; Gao *et al.*, 2014; Oliveira *et al.*, 2016
2	Q55549	**Slr0168**	Unknown / Unknown	OM	U	Sergeyenko and Los, 2000
3	P73409	**Slr1841**	Porin (carbohydrate selective) / Unknown	OM	OM	Oliveira *et al.*, 2016
4	Q55763	**Slr0191**	SpoIID - Amidase enhancer, role at murein and peptidoglycan / Unknown	U	OM	
5	P74390	**Slr0447**	AmiC - ABC Transporter (urea) / Secretion & Membrane transporters	C	OM	Oliveira *et al.*, 2016
	P74500	**Slr1940**	Protein putatively involved in extracellular connection structures / Unknown	U	OM	
6	P73458	**Slr1751**	Prc - Protease (photosystem II repair) / Protein folding & degradation	CM	OM	Chiregi *et al.*, 2015, Oliveira *et al.*, 2016
	P37101	**Sll1525**	PrK – Phosphoribulokinase (protein involved in the CO_2 fixation mechanism) / Carbon metab.	C	C	
7	Q01903	**Slr1452**	SbpA - Sulfate transport / Secretion & Membrane transp.	P	P	
8	Q55835	**Slr0513**	FutA - Iron uptake (photosystem II protection from ROS) / Secretion & Membrane transporters	P	P / OM	Chiregi *et al.*, 2015; Gao *et al.*, 2014; Oliveira *et al.*, 2016
9	P74598	**Slr1410**	WD proteins / Unknown	U	OM	Oliveira *et al.*, 2016
	P73595	**Sll1491**		CM	OM	Oliveira *et al.*, 2016
10	Q55648	**Sll0314**	Lipoprotein (signaling) / Unknown	U	OM	Oliveira *et al.*, 2016
11, 12, 13	P73207	**Slr1704**	Unknown / Unknown	CM	U	
14	Q54714	**Sll1577**	CpcB - C-phycocyanin beta chain / Photosynthesis	U	TM	Gao *et al.*, 2014; Oliveira *et al.*, 2016
	Q54714	**Sll1577**		U	TM	
15	Q54715	**Sll1578**	CpcA - C-phycocyanin alpha chain / Photosynthesis	U	TM	Gao *et al.*, 2014; Oliveira *et al.*, 2016
	Q01951	**Slr2067**	ApcA - Allophycocyanin alpha chain / Photosynthesis	U	TM	
16	Q55841	**Slr0518**	Carbohydrate binding protein (arabinofuranidase) / Carbon metabolism	U	U	
17	Q55847	**Sll0470**	Unknown / Carbon metabolism	U	U	Oliveira *et al.*, 2016
18	P72760	**Sll1029**	CCMK (CO_2 concentrating mechanism) / Carbon metabolism	C	U	
	P72761	**Sll1028**		C	U	

Table S3. List of genes with putative SigF binding motifs in their promoter regions (*in silico* predicted).

Binding motif: 5'- GGGTAAG - 3'				
Gene	**Motif distance***	**Location**	**Strand**	**Encoded protein / protein function**
slr1123, gmK	260 bp	Chromosome	+	guanylate kinase, Purine ribonucleotide biosynthesis
rnpB	69 bp	Chromosome	+	RNA subunit B of RNaseP
slr0249	246 bp	Chromosome	+	Hypothetical protein
slr1416, morR	152 bp	Chromosome	+	Regulatory functions
slr1100	274 bp	Chromosome	+	Hypothetical protein
slr1787	198 bp	Chromosome	+	thiamine-monophosphate kinase, thiamin biosynthetic process
slr1795, msrA	112 bp	Chromosome	+	peptide methionine sulfoxide reductase, Protein modification and translation factors
ssr2142, ycf19	119 bp	Chromosome	+	cell membrane component, function unknown
slr1301	109 bp	Chromosome	+	Hypothetical protein
slr1305	65 bp	Chromosome	+	two-component response regulator, Regulatory functions
slr1611	213 bp	Chromosome	+	Hypothetical protein
slr1074	279 bp	Chromosome	+	Hypothetical protein
ssr2711	225 bp	Chromosome	+	Hypothetical protein
slr2005	293 bp	Chromosome	+	periplasmic protein, function unknown
slr1228, prfC	213 bp	Chromosome	+	peptide-chain-release factor 3, Protein modification and translation factors
slr1440	62 bp	Chromosome	+	Hypothetical protein
slr0884, gap1	252 bp	Chromosome	+	glyceraldehyde 3-phosphate dehydrogenase 1, Glycolysis
slr1743, ndh	277 bp	Chromosome	+	type 2 NADH dehydrogenase, oxidoreductase activity
slr1723, lacG	47 bp 11 bp	Chromosome	+	permease protein of sugar ABC transporter, Transport and binding proteins
ssr2227	302 bp	Chromosome	+	transposase
slr0806	182 bp	Chromosome	+	oxidoreductase activity, photorespiration
slr1674	110 bp	Chromosome	+	Hypothetical protein
slr1635	117 bp	Chromosome	+	transposase
slr0145	228 bp	Chromosome	+	Hypothetical protein
slr0344, rfbW	230 bp	Chromosome	+	Glycosyltransferase - Surface polysaccharides, lipopolysaccharides
slr0014, mgtC	25 bp	Chromosome	+	Mg2+ transport ATPase
slr0899, cynS	318 bp	Chromosome	+	cyanate lyase, Glutamate family / Nitrogen assimilation
slr0920	65 bp	Chromosome	+	mutator MutT protein, DNA replication, restriction, modification, recombination, and repair
slr0573	268 bp	Chromosome	+	Hypothetical protein
slr0845	37 bp	Chromosome	+	Hypothetical protein

Table S3 (continued)

slr0093, dnaJ	137 bp	Chromosome	+	heat shock protein 40, molecular chaperone
slr0626	76 bp	Chromosome	+	probable glycosyltransferase
slr0302	177 bp	Chromosome	+	two-component sensor activity, regulation of transcription
slr1459, apcF	99 bp	Chromosome	+	phycobilisome core component, photosynthesis
slr1657	105 bp	Chromosome	+	Hypothetical protein
slr1660	300 bp	Chromosome	+	Hypothetical protein
slr0606	166 bp	Chromosome	+	Probable glycosyltansferase
sll0735	185 bp	Chromosome	-	Glycoside hydrolase, carbohydrate metabolic process
sll0630	226 bp	Chromosome	-	Hypothetical protein
sll0026	321 bp	Chromosome	-	NADH dehydrogenase subunit 5 (involved in constitutive, low affinity CO2 uptake)
sll0784, merR	295 bp	Chromosome	-	Nitrilase, Glutamate family / Nitrogen assimilation, intracellular signaling cascade, lipid metabolic process, hydrolase activity, acting on carbon-nitrogen bonds (not peptide)
sll0283	304 bp	Chromosome	-	Hypothetical protein
sll0290, ppK	45 bp	Chromosome	-	polyphosphate kinase
sll0611	228 bp	Chromosome	-	Hypothetical protein
sll0322, hypF	234 bp	Chromosome	-	transcription regulator activity, putative hydrogenase expression/formation protein HypF
sll0364	181 bp	Chromosome	-	Hypothetical protein
sll1531	323 bp	Chromosome	-	Hypothetical protein
sll0914	284 bp	Chromosome	-	hydrolase activity, acting on ester bonds, lipid metabolic process
sll0921	76 bp	Chromosome	-	two-component response regulator NarL subfamily, Regulatory functions
sll1095	325 bp	Chromosome	-	Hypothetical protein
sll1435, pet112	163 bp	Chromosome	-	glutamyl-tRNA(Gln) amidotransferase subunit B, Aminoacyl tRNA synthetases and tRNA modification, carbon-nitrogen ligase activity, with glutamine as amido-N-donor
sll1167, pbp	132 bp	Chromosome	-	Penicillin binding protein, unknown function
sll1254	269 bp	Chromosome	-	Hypothetical protein
sll0815	190 bp	Chromosome	-	Hypothetical protein
sll1418	42 bp	Chromosome	-	photosystem II oxygen-evolving complex 23K protein PsbP, Photosystem II
sll1426	12 bp	Chromosome	-	Hypothetical protein
sll0244, galE	235 bp	Chromosome	-	UDP-glucose 4-epimerase, Sugars
sll0249	262 bp	Chromosome	-	Hypothetical protein
sll0837	50 bp	Chromosome	-	periplasmic protein, function unknown
sll1621	257 bp	Chromosome	-	AhpC/TSA family protein, cell redox homeostasis, oxidoreductase activity
sll1694, hofG	62 bp	Chromosome	-	pilin polypeptide PilA1, type II protein secretion system complex
sll1708	217 bp	Chromosome	-	two-component response regulator NarL subfamily, Regulatory functions
ssl2598, psbH	80 bp	Chromosome	-	photosystem II PsbH protein, protein stabilization
sll1358	283 bp	Chromosome	-	oxalate decarboxylase, periplasmic protein, nutrient reservoir activity
sll1127, menB	25 bp	Chromosome	-	1,4-dihydroxy-2-naphthoate synthase, Menaquinone and ubiquinone
sll1129, todF	269 bp	Chromosome	-	2-hydroxy-6-oxohepta-2,4-dienoate hydrolase

Table S3 (continued)

sll1812, rps5	165 bp	Chromosome	-	30S ribosomal protein S5, Ribosomal proteins: synthesis and modification
ssl3093, cpcD	180 bp	Chromosome	-	phycobilisome small rod linker polypeptide
sll1831, glcF	44 bp	Chromosome	-	glycolate oxidase subunit, oxidoreductase activity, glycolate pathway
sll1837	83 bp	Chromosome	-	periplasmic protein, function unknown
sll1942	104 bp	Chromosome	-	Hypothetical protein
sll1654	320 bp	Chromosome	-	Universal stress protein (usp), response to stress
sll1672	338 bp	Chromosome	-	two-component hybrid sensor and regulator, regulatory functions
sgl0002	105 bp	Chromosome	-	Hypothetical protein
sll0222, phoA	325 bp	Chromosome	-	putative purple acid phosphatase, hydrolase activity
sll1063	251 bp	Chromosome	-	Proteolysis, metalloendopeptidase activity
sll1209, lig	31 bp	Chromosome	-	DNA ligase, DNA replication, restriction, modification, recombination, and repair
MYO_4470 (*slr7049*)	310 bp	pSYSA	+	resolvase, Transposon-related functions
MYO_5300 (*slr8029*)	314 bp	pSYSG	+	resolvase, Transposon-related functions
MYO_ 5370 (*slr8036*)	57 bp	pSYSG	+	probable acetyltransferase
MYO_250 (*sll5004*)	78 bp	pSYSM	-	Hypothetical protein
MYO_3580 (*slr6057*)	256 bp	pSYSX	+	Hypothetical protein
MYO_3630 (*ssr6062*)	346 bp	pSYSX	+	Hypothetical protein

Binding motif: 5'- [C/T]AGGC [N10-30] GGGT[A/G][A/G][A/G] - 3'

Gene	Motif distance	Location	Strand	Encoded protein / protein function
slr0479	73 bp	Chromosome	+	Hypothetical protein
slr1288	104 bp	Chromosome	+	Hypothetical protein
slr0721, me	334 bp	Chromosome	+	malic enzyme, oxidoreductase activity, Pyruvate and acetyl-CoA metabolism
slr1930	348 bp	Chromosome	+	type 4 pilin-like protein, pilA7
slr1338	134 bp	Chromosome	+	Hypothetical protein
slr2026, flrP	204 bp	Chromosome	+	dihydropteroate synthase, folic acid and derivative biosynthetic process
slr1159, purD	136 bp	Chromosome	+	glycinamide ribonucleotide synthetase, Purine ribonucleotide biosynthesis
sll1770	175 bp	Chromosome	-	spkI, protein kinase activity, protein phosphorylation
sll2015	137 bp	Chromosome	-	Hypothetical protein
sll0394	122 bp	Chromosome	-	Hypothetical protein
sll0364	278 bp	Chromosome	-	Hypothetical protein
sll0171, gcvT	252 bp	Chromosome	-	probable aminomethyltransferase, Amino acids and amines
sll1694, hofG	62 bp	Chromosome	-	pilin polypeptide PilA1, type II protein secretion system complex
sll0055	327 bp	Chromosome	-	processing protease, Degradation of proteins, peptides, and glycopeptides
sll0869, aat	0 bp	Chromosome	-	Leu/Phe-tRNA-protein transferase, Protein modification and translation factors
sll1942	109 bp	Chromosome	-	Hypothetical protein
sll1675	114 bp	Chromosome	-	lactoylglutathione lyase activity

Table S3 (continued)

sll0716, lepB	211 bp	Chromosome	-	leader peptidase I (signal peptidase I, Protein and peptide secretion
sll0737	179 bp	Chromosome	-	Hypothetical protein
sll0756	0 bp	Chromosome	-	Hypothetical protein
sll0699	268 bp	Chromosome	-	transposase
ssl0738	122 bp	Chromosome	-	Hypothetical protein
sll0888	239 bp	Chromosome	-	Hypothetical protein
sll0634, btpA	317 bp	Chromosome	-	photosystem I biogenesis protein, Photosystem I, thiamin biosynthetic process
sll0082	83 bp	Chromosome	-	Hypothetical protein
sll1525, prK	56 bp	Chromosome	-	Phosphoribulokinase, CO2 fixation, carbohydrate metabolic process
sll0997	199 bp	Chromosome	-	Hypothetical protein
sll0832	354 bp	Chromosome	-	Hypothetical protein
MYO_710	280 bp	pCA2.4	+	Hypothetical protein
MYO_2580 (*sll5057*)	81 bp	pSYSM	-	glycosyltransferase

Table S4. Distribution by functional categories of the proteins quantified in the two iTRAQ analysis (A and B) with significant fold changes in *Synechocystis* Δ*sigF vs.* wild-type.

Protein name	Uniprot ID	Description	Fold changes (mt : wt) A	B
Carbon metabolism				
Sll1525, Prk, Ptk	P37101	Phosphoribulokinase (PRKase)	2,00	2,16
Sll1931, GlyA	P77962	Serine hydroxymethyltransferase	1,67	1,67
Sll0807, Rpe	P74061	Ribulose-phosphate 3-epimerase (R5P3E)	1,41	-
Sll1070, TktA	P73282	Transketolase	1,22	1,28
Sll0018, FbaA, Fda	Q55664	Fructose-bisphosphate aldolase class 2	1,22	1,23
Sll1342, Gap2	P80505	Glyceraldehyde-3-phosphate dehydrogenase 2 (GAPDH 2)	1,20	1,21
Slr0952, Fbp	P74324	Fructose-1,6-bisphosphatase class 1	1,19	1,20
Sll1275, Pyk2	P73534	Pyruvate kinase 2	1,18	1,16
Sll0945, GlgA1, GlgA	P74521	Glycogen synthase 1	1,11	-
Sll1138, PgmB	P73470	Beta-phosphoglucomutase	-	1,72
Sll0019, Dxr	Q55663	1-deoxy-D-xylulose 5-phosphate reductoisomerase	-	1,21
Sll1721, PdhB	P73405	Pyruvate dehydrogenase E1 beta subunit	-	1,20
Slr1934, PdhA	P74490	Pyruvate dehydrogenase E1 component subunit alpha	-	1,18
Slr1124, GpmB	P72649	Phosphoglycerate mutase	-	1,10
Ssl2501, PhaP	P73545	Phasin	1,59	1,39
Sll0576, HrEpiB	P74729	Putative sugar-nucleotide epimerase	1,13	1,18
Sll1625, SdhB	P73723	Succinate dehydrogenase iron-sulfur subunit	-	-1,19
Sll0741, NifJ	P52965	Putative pyruvate-flavodoxin oxidoreductase	-	-1,41
Slr0370, GabD	Q55585	Probable succinate-semialdehyde dehydrogenase	-1,11	-
Sll0990, FrmA	P73138	S-(hydroxymethyl)glutathione dehydrogenase	-1,13	-
Slr0009, CbbL, RbcL	P54205	Ribulose bisphosphate carboxylase large chain (RuBisCO large subunit)	-1,13	-1,12
Slr0012, CbbS, RbcS	P54206	Ribulose bisphosphate carboxylase small chain (RuBisCO small subunit)	-1,27	-1,30
Sll0726, Pgm	P74643	Phosphoglucomutase	-1,15	-1,13
Sll1641, Gad	P73043	Glutamate decarboxylase	-1,17	-
Slr1843, Zwf	P73411	Glucose-6-phosphate 1-dehydrogenase	-1,20	-1,17
Sll0329, Gnd	P52208	6-phosphogluconate dehydrogenase	-1,24	-1,16
Slr0194, RpiA	Q55766	Ribose-5-phosphate isomerase A	-1,26	-1,17
Sll1356, GlgP	P73511	Glycogen phosphorylase	-1,27	-1,26
Sll1502, GltB	P55037	Ferredoxin-dependent glutamate synthase 1	-1,27	-1,27
Slr0623, TrxA	P52231	Thioredoxin	-1,28	-1,25
Slr1857, GlgX	P73608	Glycogen operon protein	-1,35	-1,39
Slr0884, Gap1	P49433	Glyceraldehyde-3-phosphate dehydrogenase 1 (GAPDH 1)	-1,50	-1,60
Slr0006	Q55667	Ci sequester under CO_2 limitation (induced under carbon limitation)	-	-1,35
Sll1735, CupS	P73392	Part of a complex for CO_2 uptake	-	-1,46
Sll1734	P73393	Part of a complex for CO_2 uptake	-1,71	-1,73
Slr1513	P73954	Part of the SbtA/B Ci uptake system	-1,78	-1,79
Photosynthesis				
Sll1796, PetJ	P46445	Cytochrome c6 (Cytochrome c553)	2,26	2,79
Sll1579, CpcC2	P73204	Phycobilisome, phycocyanin-associated, rod 2	1,36	1,40
Sll1471, CpcG	P74625	Phycobilisome rod-core linker polypeptide	1,29	1,24
Sll1578, CpcA	Q54715	C-phycocyanin alpha chain	1,23	1,25
Sll1252	P74082	PSI synthesis related protein, redox sensing and electron flow	1,24	1,23

Table S4 (continued)

		balancing		
Sll1577, CpcB	Q54714	C-phycocyanin beta chain	1,17	1,20
Sll0634, BtpA	P72966	Photosystem I biogenesis protein	1,20	1,18
Sll0550, Dfa1	Q55393	Diflavin flavoprotein A1 (NADH:oxygen oxidoreductase)	1,10	-
Ssr2831, PsaE	P12975	Photosystem I reaction center subunit IV	-	-1,18
Sll0819, PsaF	P29256	Photosystem I reaction center subunit III (PSI-F)	-	-1,24
Sml0008, PsaJ	Q55329	Photosystem I reaction center subunit IX	-	-1,46
Slr2051, CpcG, CpcG1	P73093	Phycobilisome rod-core linker polypeptide	-1,14	-1,13
Slr0737, PsaD	P19569	Photosystem I reaction center subunit II (PSI-D)	-1,24	-
Ssl3093, CpcD	P73202	Phycobilisome (Rod-capping linker protein)	-1,34	-1,40
Ssr3383, ApcC	Q01950	Phycobilisome, allophycocyanin-associated	-1,49	-1,47
Sll0199, PetE	P21697	Plastocyanin	-1,71	-1,63
Slr1796	P72804	Thylakoid membrane protein	-1,26	-
Slr1128	P72655	Stabilizer of PSI trimers, part of high-light carotenoid complex binding protein	-1,14	-1,16
Sll1638, PsbQ	P73048	Lipoprotein (essential for PSII activity)	-1,25	-1,19
Oxidative phosphorylation				
Slr1622, Ppa, IpyR	P80507	Inorganic pyrophosphatase	1,14	-
Slr1623, NdhM	P74338	NAD(P)H dehydrogenase I subunit M	-1,24	-
Sll0520 NdhI	P26525	NAD(P)H dehydrogenase I subunit I	-1,25	-1,36
Slr0261 NdhH	P27724	NAD(P)H dehydrogenase I subunit H	-1,26	-1,30
Slr1280, NdhK1, PsbG	P19050	NAD(P)H dehydrogenase I subunit K1	-1,31	-1,34
Sll0223, NdhB	P72714	NAD(P)H dehydrogenase I subunit 2	-1,40	-
Sll1262, NdhN	P74069	NAD(P)H dehydrogenase I subunit N	-1,41	-
Sll0521, NdhG	P26523	NAD(P)H dehydrogenase I subunit chain 6	-1,65	-1,72
Ssl1690, NdhO	P74771	NAD(P)H dehydrogenase I subunit O	-1,44	-1,48
Sll0272, NdhV	P74394	NAD(P)H dehydrogenase I subunit M	-1,44	-1,49
Ssl0352, NdhS	P74795	NAD(P)H dehydrogenase I subunit M	-1,50	-1,48
Sll1220	P74025	Potential NAD-reducing hydrogenase subunit	-1,40	-
Sll1326, AtpA	P27179	ATP synthase subunit alpha	-1,12	-1,08
Sll1327, AtpG, AtpC	P17253	ATP synthase gamma chain	-1,13	-1,20
Sll1324, AtpF	P27181	ATP synthase subunit b	-1,09	-1,15
Slr1329, AtpD, AtpB	P26527	ATP synthase subunit beta	-1,14	-1,14
Slr1233, FrdA	P73479	Succinate dehydrogenase flavoprotein subunit	-1,09	-1,14
Protein / RNA folding & degradation				
Sll1514, Hsp17	P72977	Small heat shock protein, molecular chaperon	2,21	2,28
Slr2075, GroS, GroES	Q05971	Chaperonin	1,51	1,68
Sll0416, GroL2, Cpn60-2, GroEL2	P22034	Chaperonin 2	1,33	1,35
Sll0020, ClpC	Q55662	ATP-dependent Clp protease regulatory subunit	1,30	1,23
Slr0156, ClpB1	P74459	Chaperone protein ClpB 1	1,30	1,65
Sll0430, HtpG	P74702	Heat shock protein	1,25	1,22
Slr1653, Ama	P74654	N-acyl-L-amino acid amidohydrolase / metallopeptidase	1,25	-
Slr2076, GroL1, Cpn60-1, GroEL1	Q05972	Chaperonin 1	1,24	1,29
Slr0164, ClpR	P74466	ATP-dependent Clp protease proteolytic subunit-like	1,23	1,23
Sll0535, ClpX	Q55510	ATP-dependent Clp protease ATP-binding subunit	1,23	-
Slr0165, ClpP3	P74467	ATP-dependent Clp protease proteolytic subunit 3	1,21	1,17
Sll0534, ClpP2	Q59993	ATP-dependent Clp protease proteolytic subunit 2	1,20	-
Sll1663	P72807	NblB1 protein for the correct phycobilissome assembly	-	1,19
Slr1390, FtsH1	P73179	ATP-dependent zinc metalloprotease FtsH 1	-	1,23
Slr0083, CrhR, DeaD	Q55804	RNA helicase CrhR (mRNA degradation)	-	1,27
Slr1097	P72741	CRR6 protein (maturation/assembly of NdhI)	1,21	1,14
Slr1751, Prc	P73458	Carboxyl-terminal protease	-	-1,31
Sll1463, FtsH4	P73437	ATP-dependent zinc metalloprotease FtsH 4	-1,17	-
Sll0057, GrpE	Q59978	Protein GrpE (HSP-70 cofactor)	-1,30	-1,34

Table S4 (continued)

Slr1761, YtfC	P73037	Peptidyl-prolyl cis-trans isomerase	-1,14	-
Slr1854	P73605	Putative intracellular protease	-	-1,22
Sll1679, HhoA	P72780	Putative serine protease	-1,13	-1,10
Translation				
Sll1096, RpsL, Rps12	P74230	30S ribosomal protein S12	1,48	1,33
Sll0947, Hpf, lrtA	P74518	Ribosome hibernation promotion factor (HPF) (Light-repressed protein A)	1,41	1,43
Sll1804, RpsC, Rps3	P73314	30S ribosomal protein S3	1,41	1,44
Slr0628, RpsN, Rps14	P48944	30S ribosomal protein S14	1,37	1,39
Slr0974, InfC	P72874	Translation initiation factor IF-3	1,31	1,37
Sll1260, RpsB, Rps2	P74071	30S ribosomal protein S2	1,29	1,33
Sll1767, RpsF, Rps6	P73636	30S ribosomal protein S6	1,28	1,28
Slr0469, RpsD, Rps4	P48939	30S ribosomal protein S4	1,28	1,32
Sll1812, RpsE, Rps5	P73304	30S ribosomal protein S5	1,28	1,23
Sll1802, RplB, Rpl2	P73317	50S ribosomal protein L2	1,27	1,26
Sll1817, RpsK, Rps11	P73298	30S ribosomal protein S11	1,27	1,24
Sll1822, RpsI, Rps9	P73293	30S ribosomal protein S9	1,26	1,32
Sll1740, RplS, Rpl19	P36239	50S ribosomal protein L19	1,26	1,28
Sll1807, RplX, Rpl24	P73309	50S ribosomal protein L24	1,25	1,28
Ssr1399, RpsR, Rps18	P48946	30S ribosomal protein S18	1,25	-
Sll1800, RplD, Rpl4	P73319	50S ribosomal protein L4	1,24	1,24
Sll1809, RpsH, Rps8	P73307	30S ribosomal protein S8	1,24	-
Sll1101, RpsJ, Rps10	P74226	30S ribosomal protein S10	1,23	-
Ssr1604, RpmB, Rpl28	P72851	50S ribosomal protein L28	1,23	1,20
Sll1801, RplW, Rpl23	P73318	50S ribosomal protein L23	1,22	1,21
Sll1799, RplC, Rpl3	P73320	50S ribosomal protein L3	1,20	1,26
Sll1813, RplO, Rpl15	P73303	50S ribosomal protein L15	1,20	1,20
Sll1808, RplE, Rpl5	P73308	50S ribosomal protein L5	1,20	1,16
Ssr2799, RpmA, Rpl27	P74267	50S ribosomal protein L27	1,19	1,20
Slr0923	Q55385	Probable 30S ribosomal protein PSRP-3 (Ycf65-like protein)	1,19	1,18
Sll1097, RpsG, Rps7	P74229	30S ribosomal protein S7	1,18	1,23
Sll1745, RplJ, Rpl10	P23350	50S ribosomal protein L10	1,18	1,15
Sll1821, RplM, Rpl13	P73294	50S ribosomal protein L13	1,16	1,13
Sll1244, RplI, Rpl9	P42352	50S ribosomal protein L9	1,16	-
Slr1974, Der, EngA	P74120	GTPase Der (GTP-binding protein EngA)	1,15	1,16
Sll1811, RplR, Rpl18	P73305	50S ribosomal protein L18	1,14	1,16
Sll1810, RplF, Rpl6	P73306	50S ribosomal protein L6	1,13	1,13
Slr1356, Rps1A	P73530	30S ribosomal protein S1 homolog A	1,13	1,11
Slr0434, Efp	Q55119	Elongation factor P (EF-P)	1,13	-
Sll1744, RplA, Rpl1	P36236	50S ribosomal protein L1	1,13	1,15
Sll1816, RpsM, Rps13	P73299	30S ribosomal protein S13	1,12	1,14
Sll0454, PheS	Q55187	Phenylalanine--tRNA ligase alpha subunit (PheRS)	1,12	-
Sll1743, RplK, Rpl11	P36237	50S ribosomal protein L11	1,12	-
Sll0767, RplT, Rpl20	P48957	50S ribosomal protein L20	1,11	1,16
Sll1806, RplN, Rpl14	P73310	50S ribosomal protein L14	1,10	1,11
Sll1435, GatB	P74215	Aspartyl/glutamyl-tRNA(Asn/Gln) amidotransferase subunit B (Asp/Glu-ADT subunit B)	1,08	-
Sll1805, RplP, Rpl16	P73313	50S ribosomal protein L16	-	1,58
Sll1746, RplL, Rpl12	P23349	50S ribosomal protein L7/L12	-	1,22
Sll1144, RsmH, MraW	P73460	Ribosomal RNA small subunit methyltransferase H (16S rRNA m(4)C1402 methyltransferase)	-	1,22
Sll1261, Tsf	P74070	Elongation factor Ts (EF-Ts)	-	1,16
Slr1678, RplU, Rpl21	P74266	50S ribosomal protein L21	-	1,13
Slr0557, ValS	Q55522	Valine--tRNA ligase (Valyl-tRNA synthetase) (ValRS)	-	1,08
Sll0204, TrmFO, Gid	Q55692	Methylenetetrahydrofolate--tRNA-(uracil-5-)-methyltransferase	-	1,27

Table S4 (continued)

		TrmFO (Folate-dependent tRNA (uracil-5-)-methyltransferase)		
Slr1105, TypA	P72749	GTP-binding protein TypA/BipA homolog	1,46	1,37
Sll0362, AlaS	P74423	Alanine--tRNA ligase (Alanyl-tRNA synthetase) (AlaRS)	-1,11	-1,10
Slr0220, GlyS	Q55690	Glycine--tRNA ligase beta subunit (GlyRS)	-1,12	-1,12
Sll0830	Q55421	Elongation factor G-like protein	-1,15	-
DNA repair				
Sll0377, Mfd	Q55750	Transcription-repair-coupling factor (TRCF)	1,32	1,34
Sll1143, UvrD	P73465	ATP-dependent DNA helicase	1,19	-
Sll0569, RecA	P74737	Protein RecA (Recombinase A)	1,14	-
Slr0417, GyrA	Q55738	DNA gyrase subunit A	-	1,12
Slr7011	Q6ZEI7	Protein from prokaryotic defense mechanism / probably involved in CRISPR-Cas system	-	1,19
Nucleotide metabolism				
Sll1054	P72646	Hydrolase involved in purine metabolism	1,16	-
Sll1823, PurA	P73290	Adenylosuccinate synthetase (AMPSase) (AdSS) (IMP--aspartate ligase)	1,13	1,16
Slr1418, PyrD	P74782	Dihydroorotate dehydrogenase (quinone) (DHOdehase)	-	-1,39
Sll0368, PyrR	Q55758	Bifunctional protein PyrR [Includes: Pyrimidine operon regulatory protein; Uracil phosphoribosyltransferase (UPRTase)	-1,23	-1,19
Ssll0420, UreB	P74386	Urease subunit beta (Urea amidohydrolase subunit beta)	-1,30	-1,25
Slr1256, UreA	P73796	Urease subunit gamma (Urea amidohydrolase subunit gamma)	-1,35	-
Slr0477, PurN	Q55172	Phosphoribosylglycinamide formyltransferase (GAR transformylase) (GART)	-1,40	-1,46
Secretion & Membrane transporters				
Sll1481	P74617	HlyD family secretion protein	1,32	-
Sll0616, SecA	Q55709	Protein translocase subunit SecA	1,23	1,20
Sll1180, HlyB	P74176	ABC transporter	-	1,18
Sll0533, Tig	Q55511	Trigger factor (TF)(PPIase)	1,18	1,13
Sll1053	P72647	Putative periplasmic adaptor protein (AcrA-like)	1,16	1,15
Sll1453, NrtD	P73449	Nitrate transport protein	-	1,32
Sll1545, Gst1	P74665	Glutathione S-transferase (pore ion channel)	-	1,12
Sll0771, Gtr, GlcP	P15729	Glucose transport protein	1,76	1,74
Slr2011	P73231	Putative multicomponent Na+:H+ antiporter subunit B	1,32	-
Slr0875, MscL	P73553	Large-conductance mechanosensitive channel	1,20	-
Sll0689, NhaS3	Q55190	High-affinity Na(+)/H(+) antiporter	-1,42	-
Sll0374, BraG, LivF	Q55753	High-affinity branched-chain amino acid transport ATP-binding protein	-1,34	-
Slr0447, AmiC	P74390	Negative aliphatic amidase regulator (Urea transporter)	-1,17	-1,25
Sll0103	Q55874	Pore ion channel	-	-1,18
Sll1762	P73643	ABC amino acid transporter	-1,40	-1,37
Motility				
Slr1044, McpA	P73008	Methyl-accepting chemotaxis protein	-	1,13
Slr0073	Q55788	Sensory transduction histidine kinase	1,11	-
Sll0039	Q55447	CheY subfamily	-1,24	-
Sll1694, HofG	P73704	General secretion pathway protein G	-2,27	-2,39
Sll0041	Q55445	Putative methyl-accepting chemotaxis protein	-	-1,11
Sll1830	P73120	Possible methyl-accepting chemotaxis protein	-1,26	-1,32
Slr1694	P74295	Activator of photopigment (phototaxis photoreceptor)	-1,71	-1,54
Sll1384	P74157	DNAJ-like chaperone responding to PSI (involved in phototaxis)	-2,33	-1,99

Table S4 (continued)

Cell envelope & Lipid metabolism				
Sll1069, FabF	P73283	Beta-ketoacyl-ACP synthase II (KAS II)	1,20	1,31
Slr1874, Ddl, DdlA	P73632	D-alanylalanine synthetase	1,12	-
Sll0083, GmhA	Q55797	Phosphoheptose isomerase	1,66	1,67
Slr1167	P74246	Oxireductase involved in glicerolipid metabolism	1,63	1,16
Slr1020, SqdB	P73128	Sulfolipid biosynthesis protein SqdB	1,13	1,10
Sll0053, AccC	Q55160	Biotin carboxylase	1,13	1,15
Slr0776, LpxD	Q55612	UDP-3-O-acylglucosamine N-acyltransferase	-1,27	-
Slr1609	P73004	Long-chain-fatty-acid CoA ligase	-1,14	-
Slr1744, AmiA	P73736	N-acetylmuramoyl-L-alanine amidase	-	-1,29
Slr0193	Q55765	RNA-binding protein (involved in lipid peroxidation and change of degree of lipid unsaturation)	-1,29	-1,25
Cofactors & vitamins metabolism				
Slr1777, ChlD	P72772	Magnesium-chelatase subunit ChlD (Mg-protoporphyrin IX chelatase)	1,34	1,33
Slr1808, HemA	P28463	Glutamyl-tRNA reductase (GluTR)	1,30	1,24
Sll1994, HemB	P77969	Delta-aminolevulinic acid dehydratase (ALAD) (ALADH) (Porphobilinogen synthase)	1,23	1,28
Slr1030, ChlI	P51634	Magnesium-chelatase subunit ChlI (Mg-protoporphyrin IX chelatase)	1,18	1,19
Sll1127, MenB	P73495	1,4-dihydroxy-2-naphthoyl-CoA synthase (DHNA-CoA synthase)	1,12	-
Slr1780	P72777	Ycf54-like protein	1,32	1,43
Sll1214, AcsF1	P72584	Magnesium-protoporphyrin IX monomethyl ester [oxidative] cyclase 1	-1,16	-
Sll1185, HemF	P72848	Oxygen-dependent coproporphyrinogen-III oxidase (CPO) (Coprogen oxidase) (Coproporphyrinogenase)	-1,22	-1,18
Slr0917, BioF	P74770	Putative 8-amino-7-oxononanoate synthase (AONS) (7-keto-8-amino-pelargonic acid synthase) (7-KAP synthase)	-1,24	-1,36
Sll1091, ChlP	Q55087	Geranylgeranyl diphosphate reductase	-1,25	-1,25
Slr0506, Por, Pcr	Q59987	Light-dependent protochlorophyllide reductase (PCR) (NADPH-protochlorophyllide oxidoreductase) (LPOR) (POR)	-1,27	-1,29
Sll1242	P42349	Uncharacterized methyltransferase sll1242 (ORF N)	-	-1,21
Aminoacid metabolism				
Sll1234, AhcY	P74008	Adenosylhomocysteinase (S-adenosyl-L-homocysteine hydrolase) (AdoHcyase)	1,70	1,73
Sll0934, CcmA	P72864	Carboxysome formation protein	1,29	1,31
Sll0373, ProA1, ProA	P54902	Gamma-glutamyl phosphate reductase 1 (GPR 1) (Glutamate-5-semialdehyde dehydrogenase 1)	1,25	1,25
Sll0927, MetX	P72871	S-adenosylmethionine synthase (AdoMet synthase) (MAT) (Methionine adenosyltransferase)	1,23	1,24
Sll0422	P74383	Isoaspartyl peptidase/L-asparaginase (Beta-aspartyl-peptidase) (Isoaspartyl dipeptidase)	1,10	-
Slr0049	Q55131	Oxireductase	-	1,45
Sll1172, ThrC	P74193	Threonine synthase (TS)	-	1,30
Slr0293, GcvP	P74416	Glycine dehydrogenase (decarboxylating) (Glycine cleavage system P-protein)	-	1,24
Slr0077, Csd, SufS	Q55793	Probable cysteine desulfurase	-	1,23
Sll0480, DapL	Q55828	LL-diaminopimelate aminotransferase (DAP-AT)	-	1,19
Slr1560, HisZ, HisS2	P74592	ATP phosphoribosyltransferase regulatory subunit	-	1,15
Slr0032, IlvE	P54691	Probable branched-chain-amino-acid aminotransferase (BCAT)	-	1,24
Slr0186, LeuA	P48576	2-isopropylmalate synthase (Alpha-IPM synthase)	1,32	1,35
Slr2088, IlvG	P73913	Acetolactate synthase	1,16	1,13

Table S4 (continued)

Sll1908, SerA	P73821	D-3-phosphoglycerate dehydrogenase (PGDH) (2-oxoglutarate reductase)	1,13	1,14
Sll1559	P74281	Soluble hydrogenase 42 kD subunit	-	1,16
Slr0212, MetH	Q55786	Methionine synthase (vitamin-B12 dependent) (5-methyltetrahydrofolate--homocysteine methyltransferase)	-1,12	-1,10
Sll1682	P72775	Alanine dehydrogenase	-1,15	-1,10
Sll0461, ProA2	Q55167	Gamma-glutamyl phosphate reductase 2 (GPR 2) (Glutamate-5-semialdehyde dehydrogenase 2)	-1,16	-
Sll1750, UreC	P73061	Urease subunit alpha (Urea amidohydrolase subunit alpha)	-1,17	-1,12
Sll0902, ArgF	Q55497	Ornithine carbamoyltransferase (OTCase)	-1,17	-
Sll0828	Q55424	Putative amidase	-1,21	-
Sll1987, KatG	P73911	Catalase-peroxidase (CP) (Peroxidase/catalase)	-1,21	-1,20
Sll1027, GltD	P72762	NADH-glutamate synthase small subunit	-1,21	-1,26
Other				
Slr1963	P74102	Orange carotenoid-binding protein (OCP)	1,15	1,16
Sll1626, LexA	P73722	Transcription regulator LexA	-1,13	-1,14
Sll5059	Q6ZES1	Two-component response regulator	-	-1,30
Sll0822	Q55432	cyAbrBs, bidirectional hydrogenase modulator	-	-1,17
Sll0359	P74426	cyAbrB, bidirectional hydrogenase modulator	-1,16	-
Sll1783	P73602	Monooxygenase (associated to polysaccharide processing)	-1,70	-1,58
Slr0605	P74752	Oxireductase (quinone as aceptor), putative glutathione S-transferase	-1,16	-
Slr1205	P73355	Ferredoxin component	-1,35	-1,40
Slr1719, DrgA	Q55233	Flavoprotein with quinone reductase and nitroreductase acitivity, NAD(P)H as donor	-1,27	-1,27
Ssr0330, FtrV	Q55781	Ferredoxin-thioredoxin reductase, variable chain (FTR-V) (Ferredoxin- thioredoxin subunit A) (FTR-A)	-1,26	-
Ssl0546, MinE	Q55899	Cell division protein	-	-1,31
Sll1226, HoxH	P74018	Oxireductase (hydrogen as donor), NIFe bidirectional hydrogenase	-	-1,33
Slr0757, KaiB	P74645	Circadian clock protein KaiB	-	-1,14
Slr1192	P74721	Alcohol dehydrogenase (NADPH dependent)	-1,23	-
Slr6037, ArsI2	Q6YRW7	arsenate reductase - glutaredoxin-dependent family (use the GSH/glutaredoxin system)	-1,23	-1,21
Sll5104, ArsI1	Q6ZEM6	arsenate reductase - glutaredoxin-dependent family (use the GSH/glutaredoxin system)	-1,23	-1,21
Slr2097, GlbN	P73925	Cyanoglobolin	-1,30	-
Unknown				
Sll1060	P72637	Membrane protein (UPF0182 protein)	1,30	1,27
Slr1301	P72839		2,05	2,06
Slr2032	P73066	Ycf23 protein	1,66	1,76
Slr0106	Q55877		1,66	1,90
Sll1239	P74001		1,63	1,64
Ssl3364	P73654		1,58	1,39
Slr0374	Q55589	Possible aaa protease	1,42	1,45
Slr0105	Q55876		1,33	1,15
Slr1338	P74074		1,30	1,22
Sll1367	P74544		1,29	1,23
Slr1915	P73113		1,20	1,19
Sll1186	P72847		1,19	1,30
Sll1766	P73639		1,22	-
Sll1201	P72822		1,52	-
Sll6017	Q6YRS8		1,52	-
Slr5119	Q6ZEL1		1,52	-

Table S4 (continued)

Slr5077	Q6ZEQ3		1,52	-
Sll1774	P73620		1,52	-
Slr1789	P72789	Encoding gene part of the heat-responsive frpC operon	1,28	-
Slr0654	P74566		1,28	-
Slr1603	P72990		1,27	-
Slr1127	P72654		1,21	-
Slr1590	P72968		1,18	-
Slr1240	P73497		1,17	-
Sll1336	P74535		1,15	-
Slr1411	P72725	UPF0272 protein	-	1,26
Sll1654	P72817	Universal stress protein (USP)	-	1,22
Slr0013	Q55671		-	1,17
Sll1837	P73107		-	1,16
Slr1949	P74511	Thylakoid membrane protein	-	1,15
Sll1891	P74109	Secreted protein (related to stress conditions)	-	1,11
Sll0102	Q55875		-	1,11
Slr7024	Q6ZEH4		-	1,10
Sll0529	Q55517		-1,12	-1,11
Slr1734	P73720	Putative OxPP cycle protein OpcA	-1,13	-1,11
Sll0314	Q55648		-1,15	-1,23
Slr0729	P72673	Thylakoid-associated protein	-1,16	-1,14
Slr0670	P72937		-1,19	-1,14
Sll1665	P72805		-1,19	-1,15
Sll1306	P73597		-1,24	-1,32
Slr7061	Q6ZED7		-1,32	-1,34
Ssr1853	P72639		-1,39	-1,35
Slr0376	Q55590	Encoding gene is part of responsive operon to stress	-1,39	-1,16
Sll0335	Q55587		-1,40	-1,49
Slr0058	Q55149		-1,41	-1,28
Sll0553	Q55390		-1,47	-1,43
Slr0226	Q55698		-2,34	-2,36
Slr1768	P73049	SPHF homologue (essential for thylakoid maintenance and high-light acclimation)	-1,16	-
Slr0476	Q55171		-1,18	-
Slr0001	Q55660		-1,22	-
Sll1873	P74135		-1,24	-
Slr0384	Q55598	Homologue of *Synechococcus* sp. sulfolipd synthase (SqdX) (required for biosynthesis of sulfoquinovosyldiacylglycerol)	-1,26	-
Sll0837	P73762	Periplasmic protein (encoding gene regulated by SigF)	-1,35	-
Sll0172	Q55558		-1,36	-
Sll0319	P74789		-1,63	-
Slr1704	P73207		-2,16	-
Sll0858	P73742		-2,21	-
Sll0173	Q55557	lyase (similar to virginiamycin b hydrolase)	-1,32	-
Slr1103	P72747		-	-1,10
Sll1305	P73598		-	-1,17
Sll0274	P74392		-	-1,18
Slr1444	P73516		-	-1,19
Slr1438	P73504		-	-1,20
Slr1970	P74113		-	-1,21
Sll0230	P72699	UPF0045 protein	-	-1,22
Sll0827	Q55425		-	-1,25
Slr0929	Q55501		-	-1,26
Slr1220	P73463		-	-1,28
Slr7094	Q6ZEA4		-	-1,36

Supporting Figures

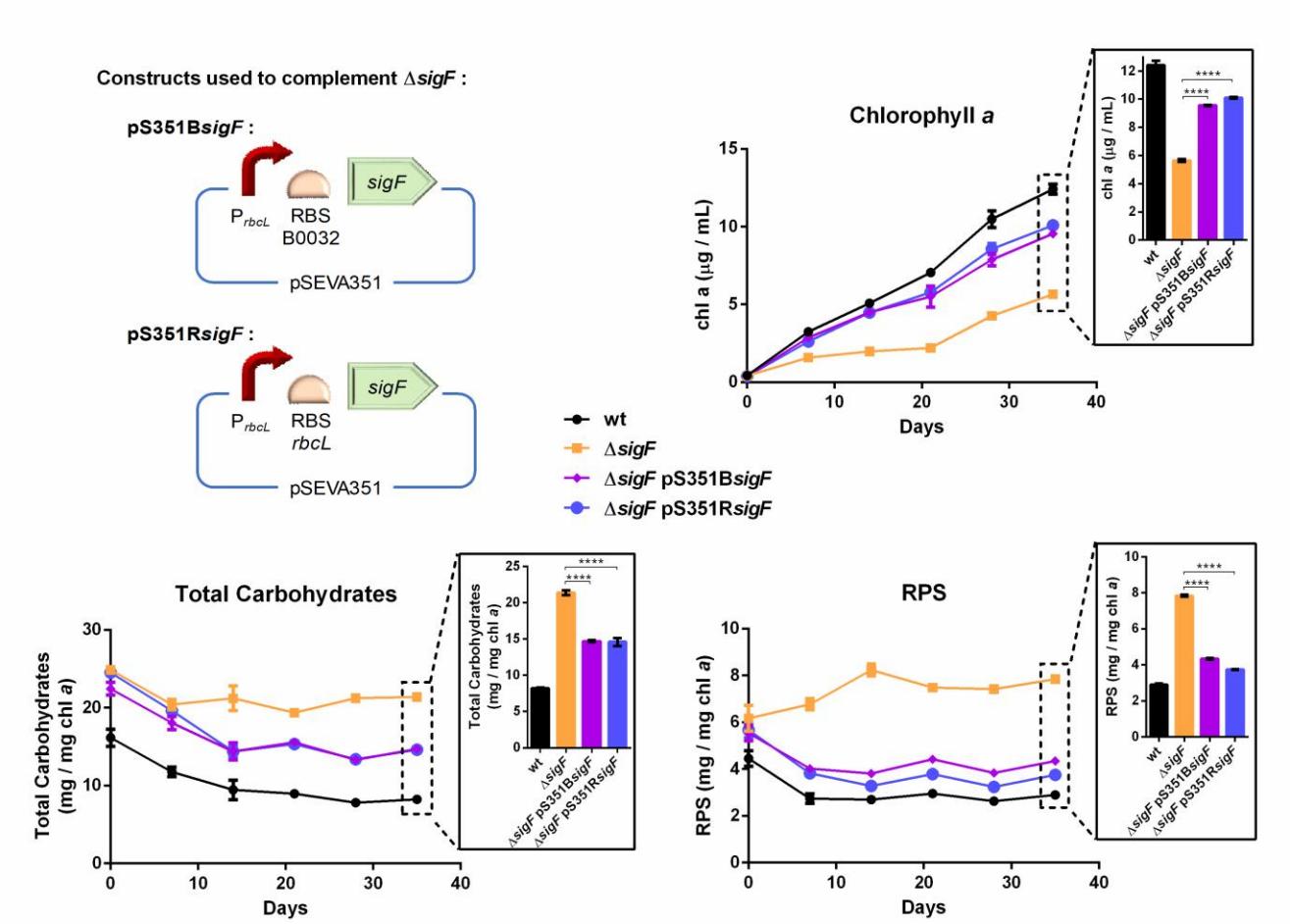

Figure S1. Characterization of *Synechocystis* sp. PCC 6803 wild-type (wt), Δ*sigF* and complementation mutants Δ*sigF* pS351B*sigF* and Δ*sigF* pS351R*sigF* in terms of growth (chlorophyll *a*), total carbohydrates content, and production of released polysaccharides (RPS). Cultures were grown in BG11, at 30 ºC under a 12h light (50 µE m^{-2} s^{-1}) / 12h dark regimen, with orbital shaking at 150 rpm. Experiments were made in triplicate and the statistical analysis is presented for the last time point comparing Δ*sigF* to the complemented mutants (**** *p* value ≤ 0.0001).

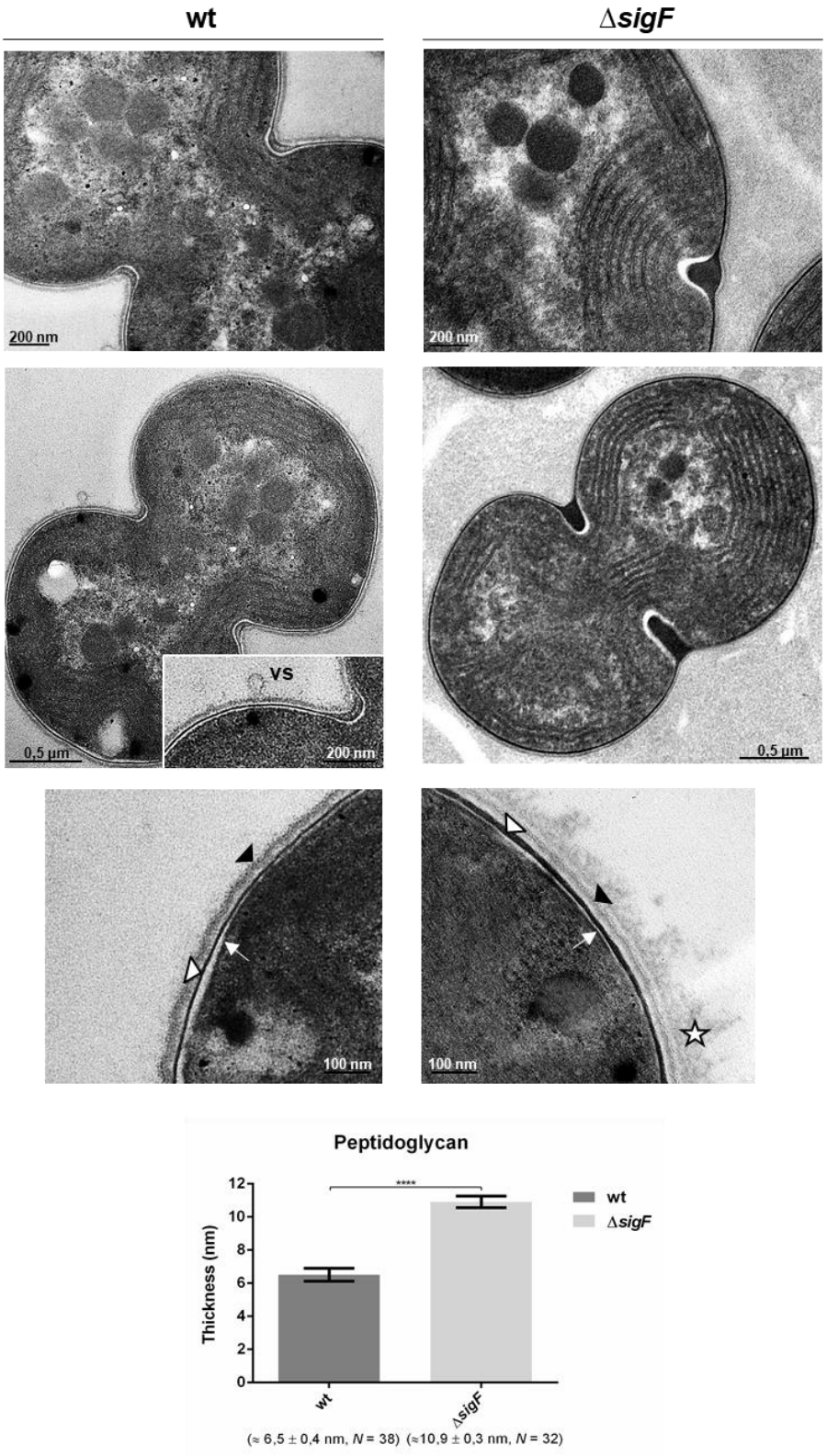

Figure S2. Transmission electron micrographs of *Synechocystis* sp. PCC 6803 wild-type (wt) and Δ*sigF* mutant highlighting differences in the cell envelope. In the left panel, it is possible to observe the vesiculation capacity of the wt (vs), while in the right panel the ticker peptidoglycan layer and the presence of amorphous material surrounding the cells of Δ*sigF* can be noticed. ☆, amorphous layer; ◗, outer membrane; ▷, peptidoglycan; →, cytoplasmic membrane. The measurements of the peptidoglycan thickness are presented below the micrographs (**** p value ≤ 0.0001).

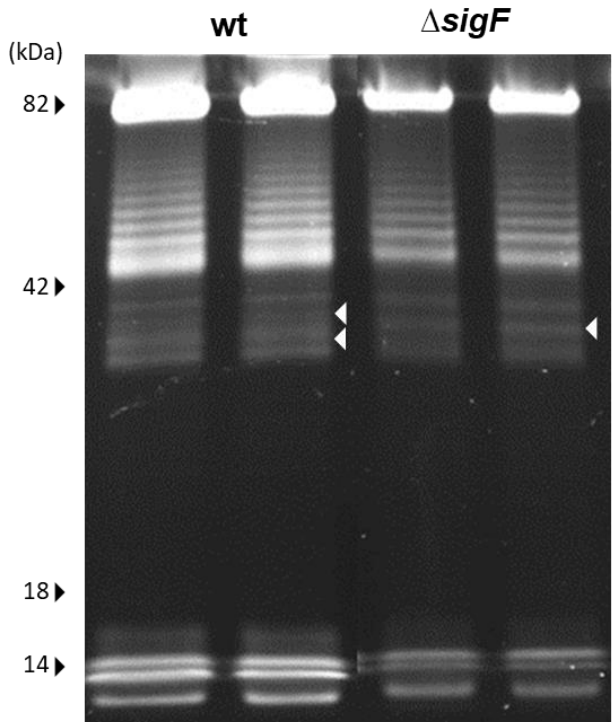

Figure S3. Lipopolysaccharides profile from outer membrane preparations of *Synechocystis* sp. PCC 6803 wild-type (wt) and Δ*sigF*. Samples were resolved in SDS-polyacrylamide gels and visualized using Pro-Q® Emerald 300 Lipopolysaccharide Gel Stain Kit (Life Technologies). White arrowheads highlight the differences between the profiles.

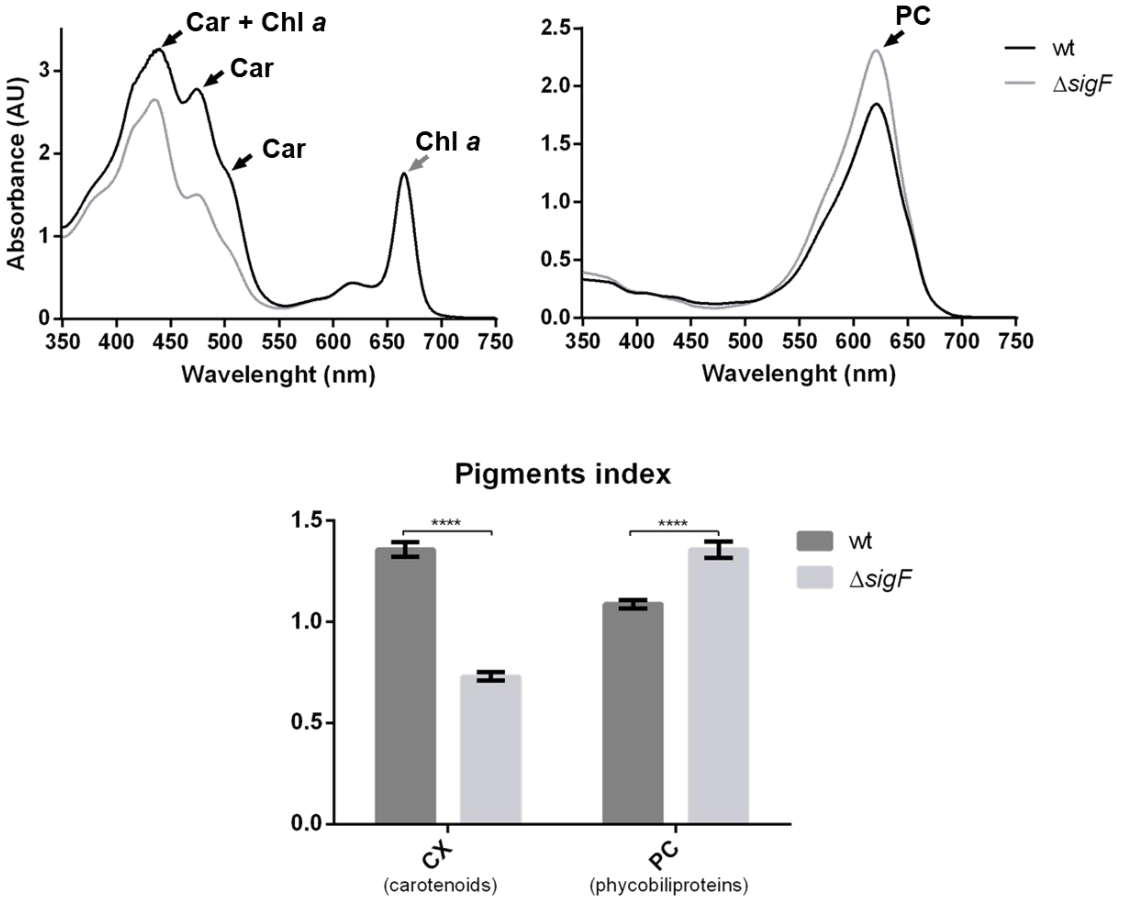

Figure S4. Absorption spectra of cell-free extracts of *Synechocystis* PCC 6803 wild-type (wt) and Δ*sigF* mutant (upper panel). Arrows indicate the characteristic absorption peaks of the different pigments – Car, carotenoids; Chl *a*, chlorophyll *a*; PC, phycocyanin. Quantification of the relative abundance of carotenoids – CX index and phycocyanin – PC index (lower panel) (**** p value ≤ 0.0001).

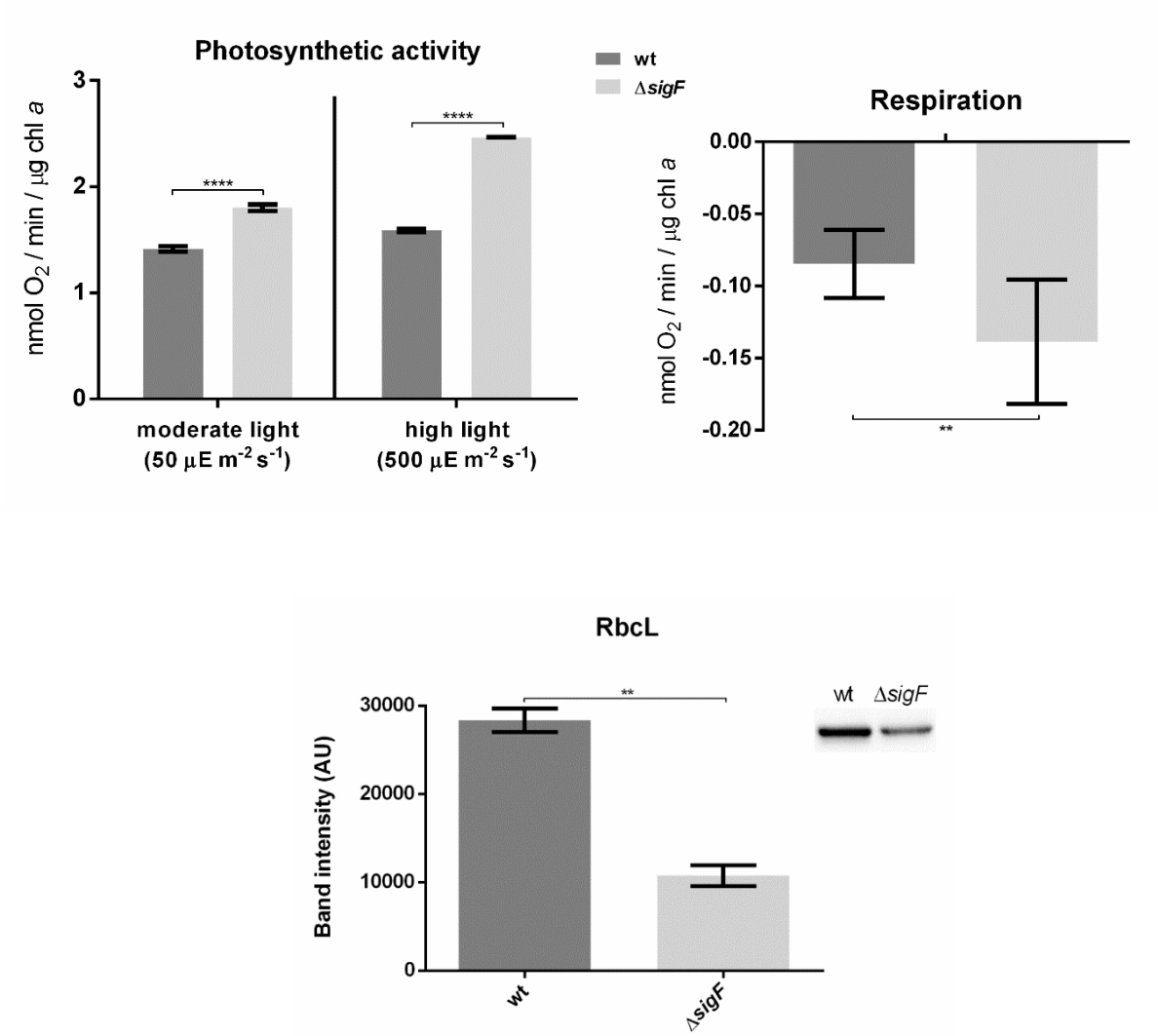

Figure S5. A. Oxygen evolution rates from cultures of *Synechocystis* sp. strain PCC 6803 wild-type (wt) and Δ*sigF*. The photosynthetic activity was measured during the light period, and the respiration rate during the dark period of the 12h light / 12h dark growth regimen as described at the Experimental procedures section (** p value ≤ 0.01; **** p value ≤ 0.0001). **B.** Western blot analysis of the relative amounts of RuBisCO – RbcL. Quantification of the bands intensity according to the Image J software (Rueden *et al.*, 2017) (** p value ≤ 0.01).

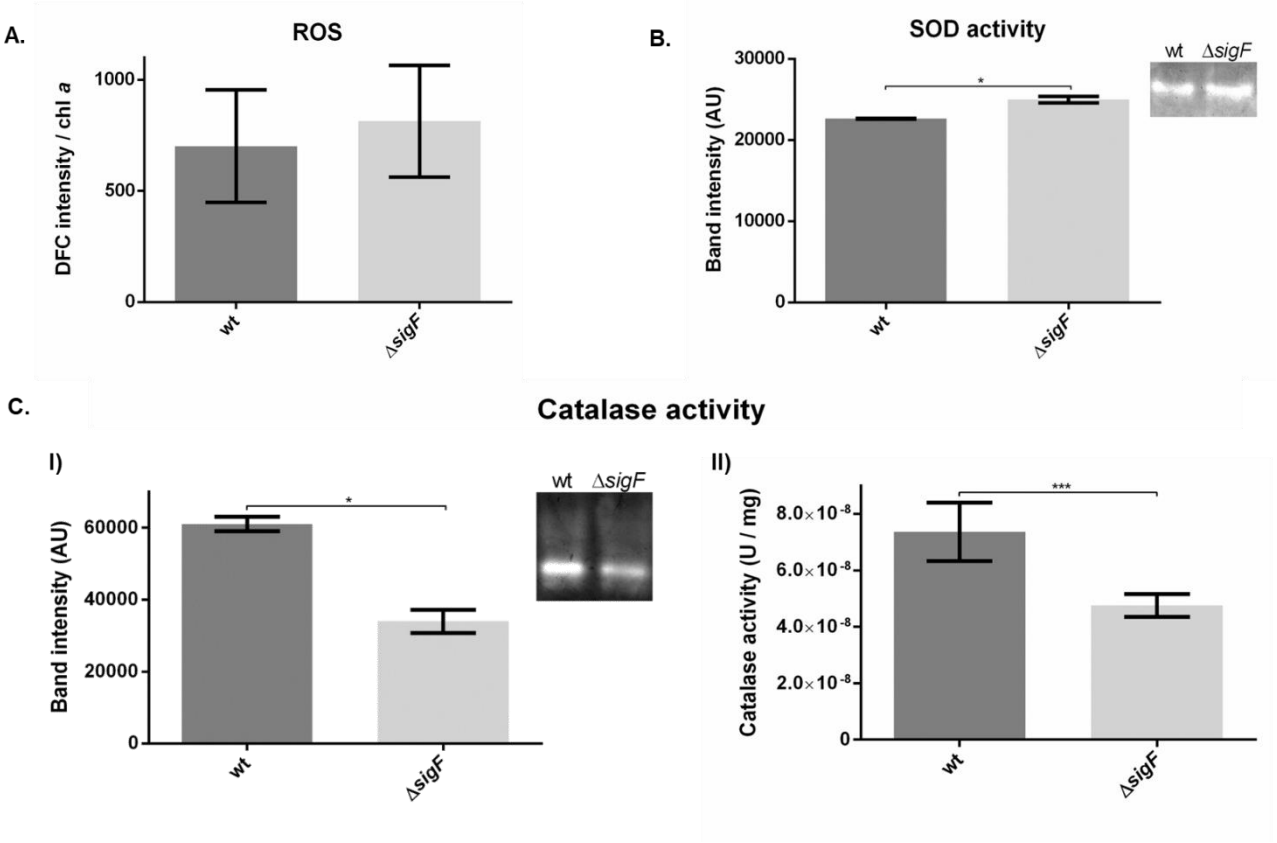

Figure S6. *In vivo* detection of reactive oxygen species (ROS) and assessment of superoxide dismutase and catalase activities from *Synechocystis* sp. PCC 6803 wild-type (wt) and Δ*sigF*. **A**. Relative levels of ROS are expressed as intensity of the fluorescent probe H2DCF-DA per amount of chlorophyll *a*. **B.** and **C.** Protein extracts from *Synechocystis* wt and Δ*sigF* were separated by electrophoresis on native-polyacrylamide gels and stained for specific detection of SOD (**B**) or catalase activities (C**I**). Total catalase activity was further quantified *in vitro* by spectrophotometry (C**II**), measuring absorbance at 240 nm as an indication of H2O2 dissociation. Catalase activity is expressed as units per mg of total protein, defining a unit as the amount of enzyme that catalyzes the dissociation of 1 μmol of H_2O_2 per minute at pH 7.0 at 25 ^{o}C. (* p value ≤ 0.05; *** $p \leq 0.001$).

Supporting Experimental Procedures

*Generation of Synechocystis Δ*sigF* complemented mutants*

The complementation of Δ*sigF* was achieved using the replicative shuttle vector pSEVA351 (SEVA database, Silva-Rocha *et al.*, 2012). The design of the constructs is shown in Fig. S1 and the complete list of the constructs and oligonucleotides is in Table S1. Briefly, a fragment covering *sigF* and either the native RBS from *rbcL* gene or the synthetic RBS BBa_B0032 was amplified and purified from agarose gel using the NZYGelpure purification (NZYTech). The *rbcL* promoter (P_{rbcL}) was also amplified and cloned in the psb1A3 plasmid after digestion with EcoRI and SpeI ($psbP_{rbcL}$). The fragments with *sigF* and the RBS were digested with XbaI and SpeI, and cloned in the $psbP_{rbcL}$ plasmid digested with SpeI. Subsequently, the plasmid was digested with XbaI and SpeI and the fragment containing the P_{rbcL}, RBS and *sigF* gene was purified from agarose gel (as described above) and cloned in pSEVA351 digested with XbaI. Plasmids were isolated from overnight grown *E. coli* DH5α cultures, using the GenElute™ Plasmid Miniprep Kit (Sigma-Aldrich), according to the manufacturer's instructions and verified by sequencing (StabVida). The constructs obtained were used to transform *Synechocystis* Δ*sigF* by electroporation, as previously described (Ludwig *et al.*, 2008). Increasing concentrations of chloramphenicol were used to select the transformants.

Pigment analysis

Cell-free extracts were performed as described by Meeks and Castenholz (1971) for chl *a* and carotenoids extraction, or by Brito *et al.* (2017) for phycobiliproteins extraction. Absorption spectra in the visible light range of the extracts were measured at room temperature from 350 to 750 nm using Shimadzu UV-2401 PC spectrophotometer (Shimadzu Corporation). The relative abundance of phycobiliproteins (PC index) or carotenoids (CX index) was determined using the phycobilin absorbance at 624 nm or carotenoids absorbance at 487 nm to the maximum chl *a* absorbance ratio (Yang *et al.*, 2010).

O_2 evolution measurements

O_2 evolution was measured using a Clark type O_2 electrode (Oxygraph, Hansatech Ltd.). Calibration was performed using sodium bisulfite and air saturated water at 30 °C. Assays were carried out using 1 ml of culture, at 30 °C and 100 rpm. Photosynthetic activity of cells

collected in the light period of the 12h light / 12h dark growth regimen was assessed under two different continuous irradiances: 50 or 500 µE m^{-2} s^{-1}. Respiration was assessed in samples collected in the dark period of the same growth regimen, but the chamber was kept in dark conditions.

Protein extraction

The cells were harvested by centrifugation at 3857 *g* for 10 min at room temperature and washed in phosphate buffer (50 mM K2HPO4, 50mM KH2PO4, pH 6.9). The cells were resuspended in protein extraction buffer (50 mM Tris-HCl, 1 mM EDTA, 0,5% Triton-X, 10% Glicerol, 2 mM DTT and 1 tablet of cOmplete™ EDTA-free Protease Inhibitor Cocktail, Roche per 10 mL of buffer) and proteins were extracted by mechanical cell disruption using FastPrepR-24 cell disruptor, output 6.5 m/s, 5 cycles of 30 s (MP Biomedicals) with glass beads (425–600 µm, Sigma-Aldrich), followed by centrifugation at 16 100 *g* for 15 min at 4 °C. The supernatant containing the proteins was stored at −80 °C until further use. Protein concentration was quantified and samples were separated by electrophoresis as described above.

Analysis of RuBisCO large subunit abundance by Western blot

The relative abundance of the large subunit of ribulose-1,5-bisphosphate carboxylase/oxygenase (RuBisCO) — RbcL was determined after Western immunoblot analysis. For that, 100 ug of protein samples obtained as described above were separated on 4-15 % SDS-PAGE gels (Bio-Rad) and transferred onto nitrocellulose membranes as previously described (Leitão *et al.,* 2005). Membranes were first incubated with rabbit polyclonal antibody anti-RbcL at a 1:5000 dilution (Agrisera Antibodies) and then with the secondary antibody goat anti-rat immunoglobulin G linked to horseradish peroxidase (Amersham Biosciences) at a 1:5000 dilution. The relative signal intensity of the bands obtained by immunodetection (Bio-Rad) was quantified using the Image J software (Rueden *et al.*, 2017).

Catalase-peroxidase (CAT) and Superoxide dismutase (SOD) activity

Protein extracts were obtained as described above, and subsequent analysis of CAT and SOD activities was performed as described by Oliveira *et al.* (2016), using 100 ug of total protein for gel-zymography and 200 μg for evaluation of CAT activity *in vitro*.

In vivo detection of reactive oxygen species (ROS) production

For detection of total ROS, samples were collected in the light period of the 12h light / 12h dark growth regimen. For each replicate, 4 mL of culture was sampled and incubated with 4 μL of 5 mM 2′,7′-dichlorofluorescein diacetate (H_2DCF-DA, Molecular Probes) for 1 h in the dark at 30 °C. The fluorescence of the samples was measured by a spectrofluorometer at 30 °C (FluoroMax-4®, Horiba Scientific), with an excitation wavelength of 485 nm and emission wavelengths between 500 and 600 nm.

Detailed description of iTRAQ experiment

The proteomes of *Synechocystis* wild type and Δ*sigF* were analyzed by 8-plex isobaric tags for relative and absolute quantification (iTRAQ), using two biological and two technical replicates. Cultures were grown in the conditions described at the Experimental procedures section until reaching a chlorophyll *a* content of 12 μg mL^{-1}. At that point, 100 mL of each culture was centrifuged at 3850 *g* for 5 min at room temperature, and cells were washed with K phosphate buffer (50 mM K_2HPO_4, 50 mM KH_2PO_4, pH 6.9) before saved at -80ºC. For protein extraction, cell pellets were re-suspended in 500 μL of lysis buffer (200 mM triethylammonium bicarbonate (TEAB), 0.1 % (v/v) Nonidet™ P40 (NP40), 10 mM dithiothreitol (DTT) and 0.1 % (v/v) plant protease inhibitor cocktail), and approximately 400 mg of 200 μm Zirconium beads were added to the re-suspended cells. Lysis was promoted using a cell disruptor (Genie) with 10 cycles of 1 min vortexing followed by 1 min incubation on ice. Unbroken cells and cell debris were pelleted by centrifugation at 21000 *g* for 10 min at 4°C and the supernatants were transferred to clean tubes. Pellets were further re-suspended in 200 μL of lysis buffer and 5 cycles on the bead-beater followed by centrifugation were performed before combining the supernatants. The combined supernatants were further clarified by centrifugation at 21000 *g* for 10 min at 4°C to ensure the complete removal of cell debris. The clarified extracts were incubated with 2 μL of benzonase nuclease (Novagene) for

2 min on ice. Protein content was estimated using the modified Lowry method as described (Bensadoun and Weinstein, 1976). In total, 100 µg of protein extract were collected from each sample for further processing. Cysteines were reduced with tris(2-carboxyethyl)phosphine (20 mM TCEP) for 45 min at 60ºC and alkylated with 40 mM MMTS (s-methyl methanethiosulfonate) for 30 min at room temperature. Subsequently, the proteins were digested overnight at 37°C, using trypsin 1:25 (w/w) (Promega). The quality of the protein extracts, the efficiency of the lysis method and the efficiency of the trypsin digestion were evaluated by 12% sodium dodecyl sulfate polyacrylamide gel. After digestion, iTRAQ labelling was performed according the manufacturer's protocols (iTRAQ® Reagents – 8plex, AB SCIEX™). Labels were assigned to a specific sample as follows: WTA1, WTB1, MA1, MA2, WTA2, WTB2, MA2 and MB2 were labelled with 113, 114, 115, 116, 117, 118, 119 and 121 respectively. After 2 h incubation period, labelled peptide samples were combined in one sample mixture which was dried using a vacuum concentrator and stored at −20°C before further analysis.

The first chromatographic separation was performed using a porous graphitic column (Hypercarb) with the following specifications: 7 µm particle size, 50 mm length, 2.1 mm diameter and 250 Å pore size, (ThermoScientific). Just before fractionation, iTRAQ-labelled peptide mixture was re-suspended in 100 µL of Hypercarb buffer A (97% (v/v) HPLC water, 3% (v/v) HPLC acetonitrile, 0.1% (v/v) trifluoroacetic acid (TFA)) and injected on a UHPLC Ultimate 3000 RS (Dionex, ThermoFisher Scientific) at a flow rate of 0.2 mL min^{-1}. A set of binary gradient buffers was used to perform peptide separation starting with 2 % buffer B (97 % (v/v) HPLC acetonitrile, 3% (v/v) HPLC water, 0.1% (v/v) TFA) for 5 min, 2-10% B for 5 min, 10-60% for 50 min, 60-90% B for 1 min, 90% B for 6 min, 90-2% B for 1 min and 2% B for 7 min, in a total of 75 min. The chromatographic separation was monitored at the wavelength of 240 nm through Chromeleon software (ThermoFisher Scientific). Fractions were collected every 2 min from 10 min until 50 min (20 fractions) using a Foxy Jr. Fraction Collector (Dionex). Collected fractions were then dried in a vacuum concentrator and stored at -20ºC until further analysis. Just prior the second chromatographic separation, each fraction was re-suspended in 10 µL reverse phase (RP) buffer A (97% (v/v) HPLC water, 3% (v/v) HPLC acetonitrile, 0.1% (v/v) FA) and combined to obtain in total 10 fractions for LC MS analysis. From each fraction, 2 µL were injected twice on a UHPLC Ultimate 3000 (Dionex,

ThermoFisher Scientific) online connected to a Q Exactive™ Hybrid Quadrupole-Orbitrap™ mass spectrometer (Thermo Scientific). Peptide separation was performed using a PepMap RSLC C18 analytical column (2 µm, 100Å, 75 µm x 50 cm) (ThermoFisher Scientific) preceded by a C18 trap column (Dionex, LC Packings) at a constant flow rate of 300 nL min^{-1}. Peptides were eluted using an 135 min automated gradient using RP buffer B (97% (v/v) HPLC acetonitrile, 3% (v/v) HPLC water, 0.1% (v/v) FA) as follows: 4% B for 5 min, 4-40% of B for 100 min, 40-90% of B for 1 min, 90 % B for 14 min, 90-4% for 1 min and finally 4% of buffer B for 14 min.

Data acquisition in the mass spectrometer was set to acquire in the positive ion mode. MS scans were acquired with 60,000 resolution, automatic gain control (AGC) target $3e^6$, maximum injection time (IT) 100 ms. The MS mass range was set to be in the range 100-1500 m/z. Tandem mass spectrometry (MS/MS) scans were acquired using high-energy collision dissociation (HCD), 30,000 resolution, AGC target $5e^4$, maximum IT 120 ms. In total, 15 MS/MS were acquired per MS scan using normalised collision energy (NCE) of 34% and isolation window of 1.2 m/z. Protein identification and quantification was carried out using the MaxQuant software. The reference proteome of *Synechocystis* sp. (strain PCC 6803 / Kazusa) (Strain: PCC 6803 / Kazusa) containing 3507 proteins was download from UniProt on May 2017 (fasta) and uploaded on MaxQuant. MS2 and 8-plex iTRAQ were selected as "type the experimental set" with reporter mass tolerant 0.01 Da. Trypsin was selected as proteolysis and two missed cleavages were allowed. Fixed peptide modifications included methyl-thiol of cysteines, and variable modifications included the oxidation of methionine and deamidation of asparagine and glutamine. The false discovery rate (FDR) at the peptide spectrum match/protein level was set at 1%. The reporter ions intensities were used for quantification proposes. Isotopic and median corrections were applied using an in-house automated method by which protein quantifications were obtained by computing the geometric means of the reporters' intensities. Median correction was subsequently applied to every reporter in order to compensate for systematic errors. These factors, estimated at the protein level, were used in subsequent analysis. The reporters' intensities, in each individual MS/MS scan, were then themselves median corrected using the same factors (Ow *et al.*, 2009). Further, these data were analyzed using a method previously described with significant

changes ($\alpha = 0.05$) (Pham *et al.*, 2010). Only proteins satisfying a 1% FDR and identified with at least two peptides unique were considered for further quantitative analysis.

References

Bensadoun, A., and Weinstein, D. (1976) Assay of proteins in the presence of interfering materials. Anal Biochem 70: 241-250.

Brito, Â., Ramos, V., Mota, R., Lima, S., Santos, A., Vieira, J., *et al.* (2017) Description of new genera and species of marine cyanobacteria from the Portuguese Atlantic coast. Mol Phylogenet Evol 111: 18-34.

Cheregi, O., Miranda, H., Gröbner, G., and Funk, C. (2015) Inactivation of the Deg protease family in the cyanobacterium *Synechocystis* sp. PCC 6803 has impact on the outer cell layers. J Photochem Photobiol B 152: 383-394.

Gao, L., Huang, X., Ge, H., Zhang, Y., Kang, Y., Fang, L., *et al.* (2014) Profiling and Compositional Analysis of the Exoproteome of *Synechocystis* Sp. PCC 6803. J Metabol Sys Biol 1: 8.

Huckauf, J., Nomura, C., Forchhammer, K., and Hagemann, M. (2000) Stress responses of *Synechocystis* sp. strain PCC 6803 mutants impaired in genes encoding putative alternative sigma factors. Microbiology 146: 2877-2889.

Leitao, E., Oxelfelt, F., Oliveira, P., Moradas-Ferreira, P., and Tamagnini, P. (2005) Analysis of the hupSL operon of the nonheterocystous cyanobacterium *Lyngbya majuscula* CCAP 1446/4: Regulation of transcription and expression under a light-dark regimen. Appl Environ Microbiol 71:4567-4576.

Ludwig, A., Heimbucher, T., Gregor, W., Czerny, T., and Schmetterer, G. (2008) Transformation and gene replacement in the facultatively chemoheterotrophic, unicellular cyanobacterium *Synechocystis* sp. PCC 6714 by electroporation. Appl Microbiol Biotechnol 78: 729-735.

Meeks, J.C., and Castenholz, R.W. (1971) Growth and photosynthesis in an extreme thermophile, *Synechococcus lividus* (Cyanophyta). Arch Mikrobiol 78: 25-41.

Oliveira, P., Martins, N.M., Santos, M., Pinto, F., Büttel, Z., Couto, N.A., *et al.* (2016) The versatile TolC-like Slr1270 in the cyanobacterium *Synechocystis* sp. PCC 6803. Environ Microbiol 18: 486-502.

Ow, S.Y., Salim, M., Noirel, J., Evans, C., Rehman, I., and Wright, P.C. (2009) iTRAQ underestimation in simple and complex mixtures: "the good, the bad and the ugly". J Proteome Res 8: 5347–55.

Pham, T.K., Roy, S., Noirel, J., Douglas, I., Wright, P.C., and Stafford, G.P. (2010) A quantitative proteomic analysis of biofilm adaptation by the periodontal pathogen *Tannerella forsythia*. Proteomics 10: 3130–41.

Rueden, C.T., Schindelin, J., Hiner, M.C., DeZonia, B.E., Walter, A.E., Arena, E.T., and Eliceiri, K.W. (2017) ImageJ2: ImageJ for the next generation of scientific image data. BMC Bioinformatics 18: 529.

Sergeyenko, T.V., and Los, D.A. (2000) Identification of secreted proteins of the cyanobacterium *Synechocystis* sp. strain PCC 6803. FEMS Microbiol Lett 193: 213-216.

Silva-Rocha, R., Martínez-García, E., Calles, B., Chavarría, M., Arce-Rodríguez, A., de Las Heras, A., *et al.* (2012) The Standard European Vector Architecture (SEVA): a coherent platform for the analysis and deployment of complex prokaryotic phenotypes. Nucleic Acids Res 41: D666-D675.

Yang, D., Qing, Y., and Min, C. (2010) Incorporation of the chlorophyll d-binding light-harvesting protein from *Acaryochloris marina* and its localization within the photosynthetic apparatus of *Synechocystis* sp. PCC6803. Biochim Biophys Acta 1797: 204-211.

CHAPTER IV

Looking outwards: Isolation of cyanobacterial released carbohydrate polymers and proteins

Work published in: ***FLORES, C.***, *& Tamagnini, P. (2019). Looking Outwards: Isolation of Cyanobacterial Released Carbohydrate Polymers and Proteins. JoVE - Journal of visualized experiments, 147: e59590.*

jove Journal of Visualized Experiments www.jove.com

Video Article

Looking Outwards: Isolation of Cyanobacterial Released Carbohydrate Polymers and Proteins

Carlos Flores[1,2,3], Paula Tamagnini[1,2,4]

[1]Bioengineering and Synthetic Microbiology Group, Instituto de Investigação e Inovação em Saude, Universidade do Porto

[2]Instituto de Biologia Celular e Molecular, Universidade do Porto

[3]Instituto de Ciências Biomédicas Abel Salazar

[4]Departamento de Biologia, Faculdade de Ciências, Universidade do Porto

Correspondence to: Paula Tamagnini at pmtamagn@ibmc.up.pt

URL: https://www.jove.com/video/59590
DOI: doi:10.3791/59590

Keywords: Biochemistry, Issue 147, extracellular carbohydrate polymers, released polysaccharides, exoproteome, secretion, cyanobacteria, Synechocystis

Date Published: 5/27/2019

Citation: Flores, C., Tamagnini, P. Looking Outwards: Isolation of Cyanobacterial Released Carbohydrate Polymers and Proteins. *J. Vis. Exp.* (147), e59590, doi:10.3791/59590 (2019).

Abstract

Cyanobacteria can actively secrete a wide range of biomolecules into the extracellular environment, such as heteropolysaccharides and proteins. The identification and characterization of these biomolecules can improve knowledge about their secretion pathways and help to manipulate them. Furthermore, some of these biomolecules are also interesting in terms of biotechnological applications. Described here are two protocols for easy and rapid isolation of cyanobacterial released carbohydrate polymers and proteins. The method for isolation of released carbohydrate polymers is based on conventional precipitation techniques of polysaccharides in aqueous solutions using organic solvents. This method preserves the characteristics of the polymer and simultaneously avoids the presence of contaminants from cell debris and culture medium. At the end of the process, the lyophilized polymer is ready to be used or characterized or can be subjected to further rounds of purification, depending on the final intended use. Regarding the isolation of the cyanobacterial exoproteome, the technique is based on the concentration of the cell-free medium after removal of the major contaminants by centrifugation and filtration. This strategy allows for reliable isolation of proteins that reach the extracellular milieu via membrane transporters or outer membrane vesicles. These proteins can be subsequently identified using standard mass spectrometry techniques. The protocols presented here can be applied not only to a wide range of cyanobacteria, but also to other bacterial strains. Furthermore, these procedures can be easily tailored according to the final use of the products, purity degree required, and bacterial strain.

Video Link

The video component of this article can be found at https://www.jove.com/video/59590/

Introduction

Cyanobacteria are widely recognized as prolific sources of natural products with promising biotechnological/biomedical applications. Therefore, understanding cyanobacterial secretion mechanisms and optimization of the extraction/recovery methods are essential to implement cyanobacteria as efficient microbial cell factories.

Many cyanobacterial strains are able to produce extracellular polymeric substances (EPS), mainly formed by heteropolysaccharides, that remain associated to the cell surface or are released into the medium[1]. These released carbohydrate polymers have distinct features compared to those from other bacteria, which make them suitable for a wide range of applications (e.g., antivirals[2], immunostimulatory[3], antioxidant[4], metal-chelating[5], emulsifying[6], and drug delivery agents[7,8]). Methodology for the isolation of these polymers largely contributes not only to improved yield but also to increased purity and the specific physical properties of the polymer obtained[9]. A vast majority of these methods for isolation of the polymers rely on precipitation strategies from the culture medium that are easily accomplished due to the polymer's strong anionic nature[9,10]. In addition, removal of the solvents used in the precipitation step can be rapidly achieved by evaporation and/or lyophilization. Depending on the foreseen application, different steps can be coupled either after or before polymer precipitation in order to tailor the final product, which include trichloroacetic acid (TCA) treatment, filtration, or size exclusion chromatography (SEC) column purification[10].

Cyanobacteria are also able to secrete a wide range of proteins through pathways dependent on membrane transporters (classical)[11] or mediated by vesicles (non-classical)[12]. Therefore, analysis of the cyanobacterial exoproteome constitutes an essential tool, both to understand/manipulate cyanobacterial protein secretion mechanisms and understand the specific extracellular function of these proteins. Reliable isolation and analysis of exoproteomes require the concentration of the extracellular milieu, since the abundance of secreted proteins is relatively low. In addition, other physical or chemical steps (e.g., centrifugation, filtration, or protein precipitation) may optimize the quality of the exoproteome obtained, enriching the protein content[13], and avoiding the presence of contaminants (e.g., pigments, carbohydrates, etc.)[14,15]

or the predominance of intracellular proteins in the samples. However, some of these steps may also restrict the set of proteins that can be detected, leading to a biased analysis.

This work describes efficient protocols for the isolation of released carbohydrate polymers and exoproteomes from cyanobacteria culture media. These protocols can be easily adapted to the study's specific objectives and user needs, while maintaining the basic steps presented here.

Protocol

1. Cyanobacterial released carbohydrate polymer isolation

1. **Polymer isolation and removal of contaminants**
    1. Cultivate the cyanobacterial strain under standard conditions [e.g., 30 °C under a 12 h light (50 µE $m^{-2}s^{-1}$)/12 h dark regimen, with orbital shaking at 150 rpm]. Measure growth using standard protocols [e.g., optical density at 730 nm (OD_{730nm}), chlorophyll *a*, dry-weight, etc.], then measure the production of released polysaccharides according to the phenol-sulfuric acid method[16].
    2. Transfer the culture into dialysis membranes (12-14 kDa of molecular weight cut-off) and dialyze against a minimum of 10 volumes of deionized water for 24 h with continuous stirring.
    NOTE: Depending on the volume of culture to dialyze and medium composition, it may be necessary to change the dialysis water.
    3. Centrifuge the culture at 15,000 x *g* for 15 min at 4 °C. Transfer the supernatant to a new vial and discard the pellet (cells).
    4. Centrifuge again at 20,000 x *g* for 15 min at 4 °C to remove contaminants such as cell wall debris or lipopolysaccharides (LPS).
    5. Transfer the supernatant to a glass beaker and discard the pellet.

2. **Precipitation of the polymer**
    1. Add 2 volumes of 96% ethanol to the supernatant.
    2. Incubate the suspension at 4 °C, at least overnight.
    3. Polymer recovery
        1. For small or not visible amounts of precipitated polymer: centrifuge the suspension at 13,000 x *g* for 25 min at 4 °C. Discard the supernatant and resuspend the pellet in 1 mL or 2 mL of autoclaved deionized water. Transfer the aqueous suspension to a vial.
        CAUTION: The supernatant should be discarded gently, as it can become easily resuspended.
        2. For visible/large amounts of precipitated polymer: collect the precipitated polymer with sterile metal forceps to a vial. Squeeze the polymer and discard the excess ethanol.
    4. Optional: depending on the degree of polymer purification required, repeat the precipitation step with 96% ethanol after resuspension of the polymers in deionized water.

3. **Lyophilization of the polymer**
    1. Keep the vials with the precipitated polymer at -80 °C, at least overnight.
    2. Freeze-dry (lyophilize) the polymer for at least 48 h (do not let the suspension defrost before freeze-drying).
    3. Store the dried polymer at room temperature (RT) until further use.
    NOTE: Storing the polymer in a desiccator is advisable, as it can absorb water over time.

2. Cyanobacterial exoproteome isolation

1. **Medium concentration**
    1. Cultivate cyanobacteria under standard conditions [e.g., 30 °C under a 12 h light (50 µE $m^{-2}s^{-1}$)/12 h dark regimen, with orbital shaking at 150 rpm]. Monitor the cyanobacterium growth using standard procedures (e.g., OD_{730nm}, chlorophyll *a*, dry-weight, etc.).
    2. Centrifuge the cultures at 4,000 x *g,* for 10 min at RT.
    3. Transfer the supernatant to a flask and discard the cell pellet.
    4. Filter the decanted medium through a 0.2 µm pore size filter.
    NOTE: The protocol can be paused here for a short time period, if the medium is kept at 4 °C.
    5. Concentrate the medium approximately 500x (considering the initial volume of filtered medium), using centrifugal concentrators with a nominal molecular weight cut-off of 3 kDa. Centrifugation should be operated at 4,000 x *g* (maximum 1 h per centrifugation round) at 15 °C.
    CAUTION: For the majority of concentrator brands, the filter device needs to be rinsed by centrifugation with ultrapure water before use. Once the filter is wet, do not let it dry out. Leave enough fluid on the reservoir when the device is not being used.
    NOTE: Reducing the centrifugation temperature to 4 °C may be helpful if the aim is to study protein activity, though it will increase the time necessary for sample concentration. The protocol can be paused between centrifugation steps for short time periods if the medium is kept at 4 °C.
    6. Rinse the walls of the filter device sample reservoir with the concentrated sample and transfer the content to a microcentrifuge tube.
    7. Perform an additional washing step of the filter device sample reservoir with autoclaved culture medium to ensure maximal exoproteome recovery.
    NOTE: To quantify the percentage of recovery, follow the specific manufacturer's instructions.
    8. Store the exoproteome samples at -20 °C until further use.
    NOTE: Addition of protease inhibitors is recommended for long-term storage.

2. **Analysis of the exoproteome**
    1. Quantify the protein content by BCA protein assay in 96-well plate according to the manufacturer's instructions.

2. Separate the proteins by sodium dodecyl sulfate-polyacrylamide gel electrophoresis (SDS-PAGE), using standard staining protocols (e.g., Coomassie blue, silver staining).
3. Cut out the bands/gel regions of interest and collect them in different microcentrifuge tubes containing appropriate volumes of ultra-pure water.
4. Proceed with identification and analysis of the proteins by mass spectrometry.

Representative Results

A schematic representation of the method described to extract released carbohydrate polymers from cyanobacterial cultures is depicted in **Figure 1**. Precipitated polymers from the moderate EPS producer cyanobacterium *Synechocystis* sp. PCC 6803 and the efficient EPS producer *Cyanothece* sp. CCY 0110 are shown in **Figure 2**. In **Figure 3**, lyophilized polymers with different degrees of contamination are shown, highlighting the importance of the centrifugation steps for the final product purity. **Figure 4** depicts the isolation method for the cyanobacterial exoproteome. Distinct cell-free medium concentrated samples (i.e., obtained from cultures in different growth phases and from a cyanobacterial strain with lower carotenoid production) are shown in **Figure 5**. Exoproteome samples from two morphologically distinct cyanobacterial strains, the unicellular cyanobacteria *Synechocystis* sp. PCC 6803 and the filamentous cyanobacteria *Anabaena* sp. PCC 7120, separated by SDS-PAGE, are shown in **Figure 6**.

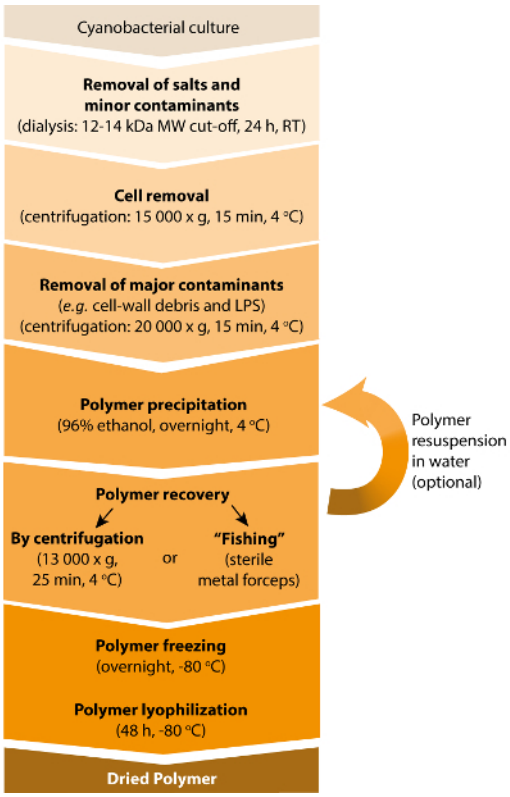

Figure 1: Workflow for the isolation of cyanobacterial released carbohydrate polymers. Starting from the cyanobacterial culture and removal of contaminants and ending with polymer isolation and lyophilization. Please click here to view a larger version of this figure.

jove Journal of Visualized Experiments www.jove.com

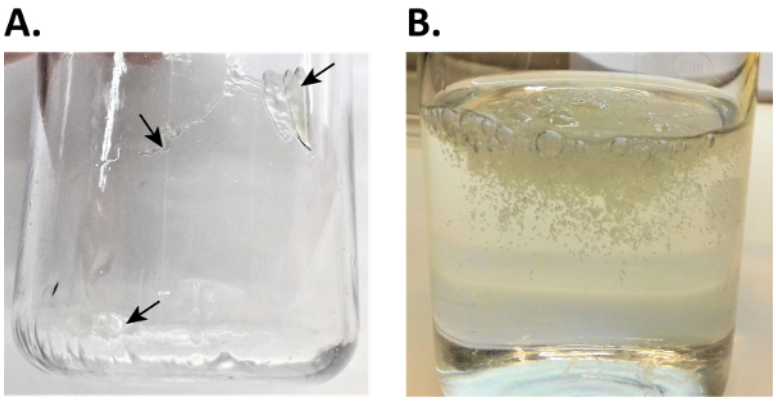

Figure 2: Cyanobacterial polymers after precipitation. (A) Polymer from the moderate EPS producer *Synechocystis* sp. PCC 6803 on the wall of the centrifuge flask after precipitation and centrifugation (arrows). **(B)** Polymer clumps from the efficient EPS producer *Cyanothece* sp. CCY 0110 floating in the glass beaker after precipitation. Please click here to view a larger version of this figure.

Figure 3: Lyophilized cyanobacterial polymers. (A) Three independent batches of polymers isolated from *Synechocystis* sp. PCC 6803: without visible contamination **(AI)**, and with pigmentation indicative of contamination with carotenoids **(AII)** or cell debris **(AIII)**. **(B)** Lyophilized polymer from *Cyanothece* sp. CCY 0110. Please click here to view a larger version of this figure.

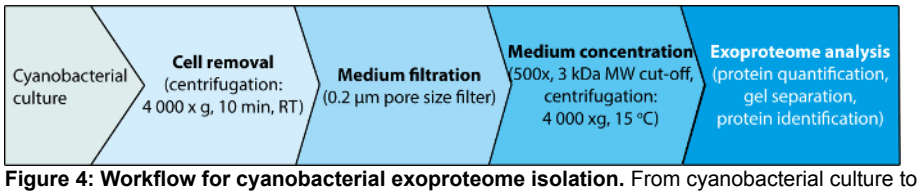

Figure 4: Workflow for cyanobacterial exoproteome isolation. From cyanobacterial culture to medium separation and concentration, ending with exoproteome analysis. Please click here to view a larger version of this figure.

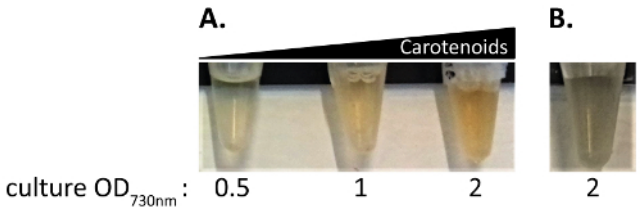

Figure 5: Microcentrifuge tubes with concentrated cell-free medium samples. (A) Concentrated medium samples from *Synechocystis* sp. PCC 6803 wild-type, collected at different OD_{730nm} (0.5, 1, and 2). **(B)** Concentrated medium sample from *Synechocystis* Δ*sigF*, a mutant with impaired carotenoids production[15]. Please click here to view a larger version of this figure.

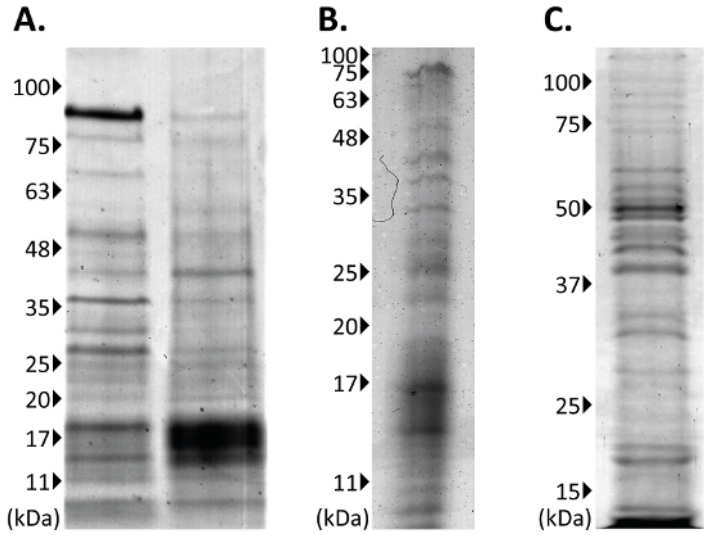

Figure 6: Coomassie blue-stained SDS-PAGE gels showing the proteins accumulated in cyanobacterial cell-free concentrated medium. (A) Exoproteome from the unicellular cyanobacteria *Synechocystis* sp. PCC 6803 wild-type and Δ*sigF* mutant. **(B)** Exoproteome from *Synechocystis* Δ*sigF* contaminated with high levels of polysaccharides. **(C)** Exoproteome from the filamentous cyanobacterium *Anabaena* sp. PCC 7120. Please click here to view a larger version of this figure.

Discussion

To better understand bacterial secretion mechanisms and study the released products, it is of extreme importance to demonstrate the efficient isolation and analysis of the biomolecules present in the extracellular bacterial environment (such as released carbohydrate polymers and proteins).

Cyanobacterial extracellular carbohydrate polymers are extremely complex, mainly due to the number and proportion of different monosaccharides that constitute their composition[1]. The conventional methods used for isolation of these polymeric substances rely on the simple concept that these sugar-rich substances are soluble in aqueous solutions and can be precipitated by the addition of organic solvents (such as acetone or ethanol)[9,17,18]. This occurs due to the extraction of water molecules from the polymers' hydration shells, and efficiency of the process depends intrinsically on the polymer's molecular weight (more efficient at higher molecular weight fractions), chemical structure, and concentration[9,18]. In addition to the precipitation step, the method described here includes the critical steps of dialysis and centrifugation. Dialysis will efficiently remove salts and other compounds from the medium, which may appear after lyophilization as powder-like structures, while the centrifugation steps will remove major contaminants and cell debris.

Failures during these steps may lead to polymers with high contamination levels and different characteristics, depending on the isolation batch. Some contaminations can be easily detected macroscopically after polymer lyophilization, since they will alter the polymer pigmentation (usually white or light brown). For example, lyophilized polymers that are green or orange are generally highly contaminated with cell debris/chlorophyll or carotenoids. This is related to insufficient time or *g* force in centrifugation steps. However, some cyanobacterial strains can release pigments and secrete proteins that remain naturally associated with the polymers, and this needs to be considered when analyzing the final product[19]. Additional steps can be added to further purify the polymers (e.g., TCA treatments)[10]. Nevertheless, these purification steps could also have a negative impact in the final product, as removing proteins and other components can alter the polymer properties (e.g., viscosity, hydrophobicity, etc.)[1,20]. Even repeating the precipitation/lyophilization steps can negatively affect polymers, mainly due to the freeze-thawing cycles that easily modify their physicochemical properties[21]. To improve the polymer yields, heating treatments can be applied to whole cultures prior to precipitation. This extra step releases the polymer associated with the cell surface, but it may also lead to depolymerization[18,20]. In summary, it is important to notice that the choice of protocol will influence both the amount and quality of isolated polymers[9,20].

Regarding the cyanobacterial proteins identified in the extracellular milieu, they display a wide range of molecular weights and isoelectric points and can be either soluble or membrane-associated. This diversity of physicochemical properties represents an issue for the selection of the most suitable method for exoproteome isolation. The method presented here depends heavily on the concentration of the biomolecules in the extracellular milieu. This method isolates not only proteins that are secreted into the medium but also proteins present in outer membrane

vesicles (OMVs) and derived from cell lysis. Therefore, centrifugation steps should be gently performed in order to avoid cell disruption, but at the same time collect OMVs. In cyanobacterial strains that are efficient OMVs producers, the exoproteome preparations are usually orange due to the presence of carotenoids associated with these lipidic structures[14,15]. However, this feature can vary considerably depending on the cyanobacterial strain and growth phase. In order to assess the contribution of proteins by OMVs, ultracentrifugation steps should be added to the procedure[22]. Furthermore, proteins that reach the extracellular space due to cell lysis may be detected by collecting samples in different growth phases and increasing the number of replicates.

As aforementioned, since many cyanobacterial strains produce extracellular carbohydrate polymers (EPS), the exoproteome preparations could also have EPS in their composition. The filtration step should retain more complex and large EPS, but simpler EPS fractions may eventually pass through. Consequently, contamination with large amounts of carbohydrates can interfere with exoproteome analysis. For example, this contamination may cause a delay in protein separation in polyacrylamide gels, as well as mask less abundant proteins. Alternative protocols have been proposed for exoproteome isolation aiming to remove contaminating biomolecules present in the extracellular medium, but they have been shown to be very selective, which may lead to biased exoproteome profiles[13]. On the other hand, a certain amount of proteins may be trapped in more complex EPS fractions if they are stuck in the filter. In this case, analyzing exoproteome preparations from different growth phases/experimental conditions as well as analysis of the proteins in EPS fractions may help identify the entrapped proteins.

Overall, the protocols described here embody the crucial steps for efficient isolation of cyanobacterial released carbohydrate polymers and exoproteomes. Most importantly, they can be easily tailored according to specific user needs and include other bacterial strains.

Disclosures

The authors have nothing to disclose.

Acknowledgments

This work was financed by Fundo Europeu de Desenvolvimento Regional (FEDER) funds through the COMPETE 2020 - Operacional Programme for Competitiveness and Internationalisation (POCI), Portugal 2020, and by Portuguese funds through FCT - Fundação para a Ciência e a Tecnologia/Ministério da Ciência, Tecnologia e Ensino Superior in the framework of the project POCI-01-0145-FEDER-028779 and the grant SFRH/BD/99715/2014 (CF).

References

1. Pereira, S. et al. Complexity of cyanobacterial exopolysaccharides: composition, structures, inducing factors and putative genes involved in their biosynthesis and assembly. *FEMS Microbiology Reviews.* **33** (5), 917–941 (2009).
2. Kanekiyo, K. et al. Isolation of an Antiviral Polysaccharide, Nostoflan, from a Terrestrial Cyanobacterium, Nostoc flagelliforme. *Journal of Natural Products.* **68** (7), 1037-1041 (2005).
3. Løbner, M., Walsted, A., Larsen, R., Bendtzen, K., Nielsen, C. H. Enhancement of human adaptive immune responses by administration of a high-molecular-weight polysaccharide extract from the cyanobacterium Arthrospira platensis. *Journal of Medicinal Food.* **11** (2), 313-322 (2008).
4. Wang, H. B., Wu, S. J., Liu, D. Preparation of polysaccharides from cyanobacteria *Nostoc commune* and their antioxidant activities. *Carbohydrate Polymers.* **99**, 553-555 (2014).
5. Ozturk, S., Aslim, B., Suludere, Z., Tan, S. Metal removal of cyanobacterial exopolysaccharides by uronic acid content and monosaccharide composition. *Carbohydrate Polymers.* **101**, 265-271 (2014).
6. Han, P. P. et al. Emulsifying, flocculating, and physicochemical properties of exopolysaccharide produced by cyanobacterium Nostoc flagelliforme. *Applied Biochemistry and Biotechnology.* **172** (1), 36-49 (2014).
7. Leite, J. P. et al. Cyanobacterium#Derived Extracellular Carbohydrate Polymer for the Controlled Delivery of Functional Proteins. *Macromolecular Bioscience.* **17** (2), 1600206 (2017).
8. Estevinho, B. N. et al. Application of a cyanobacterial extracellular polymeric substance in the microencapsulation of vitamin B12. *Powder Technology.* **343**, 644-651 (2019).
9. Klock, J. H., Wieland, A., Seifert, R., Michaelis, W. Extracellular polymeric substances (EPS) from cyanobacterial mats: characterisation and isolation method optimisation. *Marine Biology.* **152** (5), 1077-1085 (2007).
10. Delattre, C., Pierre, G., Laroche, C., Michaud, P. Production, extraction and characterization of microalgal and cyanobacterial exopolysaccharides. *Biotechnology Advances.* **34** (7), 1159-1179 (2016).
11. Costa, T. R. et al. Secretion systems in gram-negative bacteria: structural and mechanistic insights. *Nature Reviews Microbiology.* **13** (6), 343–359 (2015).
12. Roier, S., Zingl, F. G., Cakar, F., Schild, S. Bacterial outer membrane vesicle biogenesis: a new mechanism and its implications. *Microbial Cell.* **3** (6), 257–259 (2016).
13. Sergeyenko, T. V., Los, D. A. Identification of secreted proteins of the cyanobacterium Synechocystis sp. strain PCC 6803. *FEMS Microbiology Letters.* **193** (2), 213–216 (2000).
14. Oliveira, P. et al. The versatile TolC-like Slr1270 in the cyanobacterium Synechocystis sp. PCC 6803. *Environmental Microbiology.* **18** (2), 486–502 (2016).
15. Flores, C. et al. The alternative sigma factor SigF is a key player in the control of secretion mechanisms in Synechocystis sp. PCC 6803. *Environmental Microbiology.* **21** (1), 343-359 (2018).
16. Dubois, M., Gilles, K. A., Hamilton, J. K., Rebers, P. A., Smith, F. Colorimetric method for determination of sugars and related substances. *Analytical Chemistry.* **28** (3), 350–356 (1956).
17. Parikh, A., Madamwar, D. Partial characterization of extracellular polysaccharides from cyanobacteria. *Bioresource Technology.* **97** (15), 1822-1827 (2006).

18. Rühmann, B., Schmid, J., Sieber, V. Methods to identify the unexplored diversity of microbial exopolysaccharides. *Frontiers in Microbiology.* **6**, 565 (2015).
19. Pathak, J., Rajneesh, R., Sonker, A. S., Kannaujiya, V. K., Sinha, R. P. Cyanobacterial extracellular polysaccharide sheath pigment, scytonemin: A novel multipurpose pharmacophore. *Marine Glycobiology.* CRC Press, 343-358 (2016).
20. Nguyen, A. T. B. et al. Performances of different protocols for exocellular polysaccharides extraction from milk acid gels: Application to yogurt. *Food Chemistry.* **239**, 742-750 (2018).
21. Jamshidian, H., Shojaosadati, S. A., Mousavi, S. M., Soudi, M. R., Vilaplana, F. Implications of recovery procedures on structural and rheological properties of schizophyllan produced from date syrup. *International Journal of Biological Macromolecules.* **105**, 36-44 (2017).
22. Couto, N., Schooling, S. R., Dutcher, J. R., Barber, J. Proteome profiles of outer membrane vesicles and extracellular matrix of Pseudomonas aeruginosa biofilms. *Journal of Proteome Research.* **14** (10), 4207-4222 (2015).

CHAPTER V

Characterization and antitumor activity of the extracellular carbohydrate polymer from the cyanobacterium *Synechocystis* Δ*sigF* mutant

Work published in: ***FLORES, C.***, *Lima, R. T., Adessi, A., Sousa, A., Pereira, S. B., Granja, P. L., De Philippis, R., Soares, P., & Tamagnini, P. (2019). Characterization and antitumor activity of the extracellular carbohydrate polymer from the cyanobacterium* Synechocystis *Δ*sigF *mutant. International Journal of Biological Macromolecules, 136: 1219-1227.*

International Journal of Biological Macromolecules 136 (2019) 1219–1227

Contents lists available at ScienceDirect

International Journal of Biological Macromolecules

journal homepage: http://www.elsevier.com/locate/ijbiomac

Characterization and antitumor activity of the extracellular carbohydrate polymer from the cyanobacterium *Synechocystis* Δ*sigF* mutant

Carlos Flores [a,b,c], Raquel T. Lima [a,d,e], Alessandra Adessi [f], Aureliana Sousa [a,g], Sara B. Pereira [a,b], Pedro L. Granja [a,g,h], Roberto De Philippis [f], Paula Soares [a,d,e], Paula Tamagnini [a,b,i,*]

[a] *i3S - Instituto de Investigação e Inovação em Saúde, Universidade do Porto, Rua Alfredo Allen, 208, 4200-135 Porto, Portugal*
[b] *IBMC - Instituto de Biologia Celular e Molecular, Universidade do Porto, Rua Alfredo Allen, 208, 4200-135 Porto, Portugal*
[c] *ICBAS - Instituto de Ciências Biomédicas Abel Salazar, Rua de Jorge Viterbo Ferreira 228, 4050-313 Porto, Portugal*
[d] *IPATIMUP - Institute of Molecular Pathology and Immunology of the University of Porto, Rua Alfredo Allen, 208, 4200-135 Porto, Portugal*
[e] *FMUP - Faculty of Medicine, Department of Pathology, University of Porto, Alameda Prof. Hernâni Monteiro, 4200-319 Porto, Portugal*
[f] *DAGRI - Department of Agriculture, Food, Environment and Forestry, University of Florence, Via Maragliano 77, 50144 Firenze, Italy*
[g] *INEB - Instituto de Engenharia Biomédica, Universidade do Porto, Rua Alfredo Allen, 208, 4200-135 Porto, Portugal*
[h] *FEUP - Faculdade de Engenharia, Departamento de Engenharia Metalúrgica e Materiais, Universidade do Porto, Rua Dr. Roberto Frias, 4200-465 Porto, Portugal*
[i] *FCUP - Faculdade de Ciências, Departamento de Biologia, Universidade do Porto, Rua do Campo Alegre, Edifício FC4, 4169-007 Porto, Portugal*

ARTICLE INFO

Article history:
Received 26 March 2019
Received in revised form 12 June 2019
Accepted 20 June 2019
Available online 21 June 2019

Keywords:
Released polysaccharides (RPS)
Sulfated polymer
Synechocystis
Antitumor activity
Apoptosis

ABSTRACT

Cyanobacterial extracellular carbohydrate polymers are particularly attractive for biotechnological applications. Previously, we determined the monosaccharidic composition of the polymer of a *Synechocystis* Δ*sigF* overproducing mutant. Here, we further characterized this polymer, demonstrated that it is possible to recover it in high yields, and successfully use it for biomedical research. This amorphous polymer is formed by a mesh of fibrils/lamellar structures with high porosity, is constituted by high molecular mass fractions, is highly sulfated and displays low viscosity, even in highly concentrated aqueous solutions. FTIR analysis confirmed the presence of several functional groups. We demonstrated that the Δ*sigF* polymer has strong biological activity, decreasing the viability of melanoma, thyroid and ovary carcinoma cells by inducing high levels of apoptosis, through p53 and caspase-3 activation. Therefore, the Δ*sigF Synechocystis* mutant is a promising platform for the sustainable production of biological active carbohydrate polymer(s) with the desired characteristics for biomedical applications.

1. Introduction

Bacterial extracellular polymeric substances (EPS) are mainly composed by polysaccharides that play crucial physiological roles in cell protection, cell-cell communication and/or biofilm formation [1]. Many cyanobacteria are able to produce EPS that can remain attached to the cell surface (as sheaths, capsules or slimes) or be released into the extracellular environment (RPS - released polysaccharides) [2]. Cyanobacterial RPS display distinct features in comparison to the ones from other bacterial sources, for example: i) high number of different monosaccharides (up to 15), which allows a wide range of conformational possibilities to the polymers and contribute to their complex structures; ii) presence of two uronic acids and sulfate groups, which are rare in bacterial EPS and confer anionic charge to the polymers; iii) presence of peptides and deoxysugars that confer hydrophobicity, and vi) presence of uncommon sugars such as acetylated or amino-sugars, that may be involved in polymers' biological activity [3]. In addition, cyanobacteria have simple nutritional requirements and can grow much faster than other profitable EPS producers (e.g. algae and plants), decreasing the polymer production costs. Therefore, the industrial interest on cyanobacterial extracellular carbohydrate polymers has been rising, namely for biomedical and pharmaceutical applications, due to their antiviral [4], antioxidant [5] or immunomodulatory [6] activities. Recently, a few studies have also reported the antitumor activity of cyanobacterial EPS from *Nostoc sphaeroides* [7] and *Aphanothece halophytica* [8]. In contrast to the anticancer properties of other natural carbohydrate polymers (mainly from eukaryotic sources) that have been extensively evaluated [9,10], the mode of action of cyanobacterial polymers is still unknown. The majority of the studies correlate the EPS biological activities with the sulfate content, but there are also references to the presence of unusual sugars [10,11].

* Corresponding author at: i3S - Instituto de Investigação e Inovação em Saúde, Universidade do Porto, Rua Alfredo Allen, 208, 4200-135 Porto, Portugal.
E-mail addresses: carlos.flores@ibmc.up.pt (C. Flores), rlima@ipatimup.pt (R.T. Lima), alessandra.adessi@unifi.it (A. Adessi), filipa@ineb.up.pt (A. Sousa), sarap@ibmc.up.pt (S.B. Pereira), pgranja@i3s.up.pt (P.L. Granja), roberto.dephilippis@unifi.it (R. De Philippis), psoares@ipatimup.pt (P. Soares), pmtamagn@ibmc.up.pt (P. Tamagnini).

https://doi.org/10.1016/j.ijbiomac.2019.06.152
0141-8130/

The model cyanobacterium *Synechocystis* sp. PCC 6803 produces both capsular and released polysaccharides [12] and, since it is naturally transformable, several studies aiming to study/manipulate RPS production have been performed in this organism [12–14]. Recently, we reported that a *Synechocystis* knockout mutant in the Group 3 alternative sigma factor F (Δ*sigF*) exhibits considerable changes in its secretion mechanisms, producing 3 to 4-fold more RPS than the wild-type [15]. Moreover, this mutant displays a particular interesting phenotype for biotechnological applications since its faster spontaneous cell sedimentation facilitates the harvesting of the biomass and RPS isolation. Therefore, in the present study, the polymer produced by the Δ*sigF* mutant was further characterized, and its antitumor activity towards well-established human cancer cell lines was evaluated.

2. Material and methods

2.1. Cyanobacterial strains and culture conditions

The cultures of *Synechocystis* sp. PCC 6803 sub-strain PCC-M, henceforth referred to as *Synechocystis* wild-type, and the respective knockout mutant Δ*sigF* [16] were grown at 30 °C under a 12 h light (50 μE/m^2/s^1)/12 h dark regimen, with orbital shaking at 150 r.p.m. as previously reported by Flores et al. [15].

2.2. Determination of cell culture dry weight and polymer yield

To determine the dry weight, 5 mL of culture were centrifuged and the cell pellets were dried overnight at 60 °C. The yields of isolated polymer were expressed as the amount of lyophilized polymer obtained per dry weight of cell culture. All the measurements were performed with biological triplicates.

2.3. Determination of total carbohydrate content and released polysaccharides (RPS)

The amount of total carbohydrates and RPS in cyanobacterial cultures was determined using the phenol-sulfuric acid method [17], as reported in Mota et al. [18].

2.4. Polymer isolation and quantification of the protein and sulfate contents

Polymers were isolated as described in Flores and Tamagnini [19]. Lyophilized polymers were resuspended in deionized water and the protein content was determined using the Lowry method [20]. For sulfate quantification, lyophilized RPS were hydrolyzed in 2 M HCl at 100 °C for 2 h, centrifuged after cooling, and the supernatant was analyzed by ion-exchange chromatography. The analysis was performed using a Dionex ICS-2500 system chromatograph equipped with a continuously regenerated anion-trap column, a continuous anionic self-regenerating suppressor, a conductivity detector (ED50), an IonPac PA11 4 × 250 mm column (Dionex, USA), and a reagent-free Dionex system producing high-purity 50 mM KOH at a flow rate of 2 mL/min. Sulfate solutions (1 to 10 mg/L; Fluka, Switzerland) were used as standards.

2.5. Molecular mass analysis

The apparent molecular weight, hereafter referred to as molecular mass, of the RPS from *Synechocystis* wild-type and Δ*sigF* was determined according to a previously reported method [21], with some modifications. Briefly, samples were dissolved in HPLC grade water at a concentration of 5 mg/mL and analyzed using a Varian ProStar HPLC chromatograph (Varian, USA) equipped with a 355 RI (refractive index) detector and two columns for Size Exclusion Chromatography (SEC), Polysep-GFC-P 6000 and 4000 (Phenomenex, USA) connected in series. The analyses were performed with runs of 70 min and with HPLC grade water as eluent at a flow rate of 0.4 mL/min, using Pullulan at different molecular weights (800 kDa, 400 kDa, 200 kDa, 110 kDa, 50 kDa and 320 Da) and Dextran (at 2 MDa and 1.1 MDa) as standards (Sigma–Aldrich, USA).

2.6. Scanning electron microscopy (SEM)

For SEM, the lyophilized polymer was mounted on metal stubs using double sided carbon tape and coated with a gold/palladium thin film by sputtering, using the SPI module sputter coater equipment (Structure Probe Inc., USA), for 100 s and with an electric current of 15 mA. The analysis was performed using a high-resolution environmental SEM combined with x-ray microanalysis and electron backscattered diffraction analysis (Quanta 400 FEG ESEM/EDAX Genesis X4M).

2.7. Rheological behavior

The rheological behavior of the polymer in aqueous solutions (from 0.1% to 5% w/v) were determined using a Kinexus Pro rheometer (Malvern Instruments, Malvern, UK), at 37 °C in a water-vapor saturated environment ensured by the rheometer chamber. A cone-plate combination geometry was used.

2.8. Fourier transformed infrared (FTIR) spectrum

For FTIR analysis, 2 mg of polymer were mixed with 198 mg of KBr and the powders pressed at 9 tons for 30 s, using an automatic press. FTIR spectra of the polymer were acquired using a PerkinElmer Frontier FTIR spectrometer from 4000 to 400 cm^{-1} and with 4 cm^{-1} resolution.

2.9. Human tumor cell lines and culture conditions

The human melanoma cell line Mewo (kindly given by Prof. Marc Mareel, Department of Radiotherapy and Nuclear Medicine, Ghent University Hospital, Belgium) [22] was maintained in DMEM culture medium with stable glutamine (Capricorn Scientific), whereas the human thyroid carcinoma cell line, 8505C (also given by Prof. Mareel) [23] and human ovarian carcinoma A2780 (kind gift of Prof. Etel Gimba, INCA, Brazil) were maintained in RPMI-1640 culture medium with stable glutamine (Capricorn Scientific). Both culture media were supplemented with 10% of fetal bovine serum (FBS, GIBCO, Invitrogen, UK), 1× penicillin/streptomycin (Biowest) and 1.25 μg/mL amphotericin B (Corning). Cells were maintained in a humidified incubator at 37 °C with 5% CO_2. All cell lines were authenticated following genotyping at i3S Genomics Core Facility (Porto, Portugal) using the PowerPlex® 16 HS System (Promega, USA) and according to DNA profiles available at ATCC and ECACC STR profiles database.

2.10. Cell viability assays

Cells were plated on 96-well plates (5×10^3 cells/well for 8505C and A2780 cells and 1×10^4 cells/well for Mewo cells) and allowed to adhere for 24 h at 37 °C. Cells were then treated for 24, 48 and 72 h with supplemented media (Blank), the *Synechocystis* wild-type and Δ*sigF* polymers (both resuspended in non-supplemented media) at concentrations ranging from 0.02 to 5 mg/mL, or with polymer vehicle (supplemented media containing the equivalent amount of non-supplemented medium used in the polymer treatments). To assess cell viability after treatment, PrestoBlue™ cell viability assay was carried out as previously described [22]. Briefly, cells were washed three times with the respective non-supplemented medium and then further incubated for 45 min with PrestoBlue™ reagent (Life Technologies). Fluorescence was measured (excitation 560 nm; emission 590 nm) on a Synergy HT Multi-Mode Microplate Reader (BioTek Instruments Inc.). All samples and controls were analyzed with four biological and five technical replicates. Cellular viability was determined by analyzing the fluorescence

values of each sample as percentage in relation to control wells (after removing the background values).

2.11. Cell cycle profile

Mewo cells were plated on 6-well plates (1×10^5 cells/well), allowed to adhere for 24 h and then treated for 24 or 48 h with complete media (Blank), polymer vehicle or with 0.7 mg/mL Δ*sigF* polymer. Cells were pelleted, fixed in 70% ice-cold ethanol for at least 12 h and subsequently incubated with 0.1 mg/mL RNase A (Ambion) and 5 μg/mL propidium iodide (Sigma) in PBS for 40 min in the dark. Cellular DNA content, for cell cycle distribution analysis and the presence of sub-G1 peak, was determined by flow cytometry using a FACSCalibur flow cytometer (BD Biosciences, Belgium), plotting at least 20,000 events per sample. The percentage of cells in the different phases of the cell cycle (including in the sub-G1 peak) was determined using FlowJo 7.6.5 software (Tree Star, Inc., USA), after exclusion of cell debris and aggregates [24].

2.12. Apoptotic cell death

Mewo cells were plated on 6-well plates and treated as abovementioned for *Cell cycle profile* analysis. For analysis of the levels of apoptosis, flow cytometry was carried out following Annexin V-FITC/PI double staining [22]. Briefly, cell pellets were resuspended in ApoAlert Binding buffer 1× (Clontech), incubated with 250 μg/mL FITC-conjugated Annexin V (Immunotools) for 10 min at room temperature in the dark and then further incubated with 10 μL propidium iodide (PI) (Sigma, Germany). Flow cytometry was performed using a FACS Calibur Flow Cytometer (Becton-Dickinson, USA), plotting at least 20,000 events after debris exclusion [25]. Data was analyzed using FlowJo 7.6.5 software (Tree Star, Inc., USA).

2.13. Protein expression analysis by Western blot

Mewo cells were plated on 6-well plates and treated as aforementioned in *Cell cycle profile*. Following treatment, cells were lysed in RIPA buffer (1% NP-40, 0.05 M Tris-HCl pH 7.5, 0.15 M NaCl, and 2 mM EDTA) complemented with 1× EDTA-free protease inhibitor cocktail (Roche, Germany) and 1× Phosphatase Inhibitor Cocktail (Sigma, Germany). Protein lysates were quantified using a DC™ Protein Assay kit (Bio-Rad, USA), according to the manufacturer's instructions, and 25 μg of protein was loaded and run in 10% SDS-polyacrylamide gel. After transfer into nitrocellulose membranes (Amersham, USA), the membranes were incubated with the following primary antibodies: monoclonal anti-p53 (1:1000, Leica, USA), anti-p21 (Ab-1) mouse mAb (EA10) (1:1000, Merck, Germany), monoclonal anti-α-tubulin (clone DM1A; 1:8000, Sigma-Aldrich, Germany), or mouse anti-caspase 3 antibody (1:1000; Cell Signaling Technology®, Netherlands) and subsequently with the corresponding HRP-conjugated secondary antibody (1:3000, GE Healthcare). Signals were detected using Western Lightning Plus-ECL reagent (PerkinElmer, USA), Amersham Hyperfilm ECL (GE Healthcare) and Kodak GBX developer and fixer (Sigma-Aldrich, Germany) [26].

2.14. Statistical analysis

Data were plotted and statistically analyzed using GraphPad Prism version 7.0 (GraphPad Software) using an analysis of variance (ANOVA), followed by Bonferroni's multiple comparisons test.

3. Results and discussion

3.1. Yield, sulfate and protein contents, and molecular mass of the polymers

Previously, we isolated and determined the monosaccharide composition of the released carbohydrate polymers from *Synechocystis* sp. PCC 6803 wild-type and its knockout mutant Δ*sigF* [15]. In the present work, we further characterized these polymers regarding the sulfate and protein content, and molecular mass distribution (Fig. 1). Remarkably, the yield of isolated polymer (i.e. the amount of lyophilized polymer obtained per dry weight of cell culture) from Δ*sigF* (80.7 ± 10.8 mg/g DW) is approximately 4-fold higher than that from the wild-type (17.5 ± 3.2 mg/g DW). These results are in agreement with the quantification of RPS by the phenol-sulfuric acid method performed here (Fig. S1) and by Flores et al. [15]. Although a previous study also described a *Synechocystis* mutant (Δ*sll1783* – a monooxygenase) that produces a higher amount of RPS than the wild-type [27], the yields reported here are the highest for a *Synechocystis* strain (Fig. 1A).

Both the wild-type and the Δ*sigF* polymers are highly sulfated (≈12% w/w), again among the highest values found for cyanobacterial polymers [2,3]. Moreover, the polymer produced by Δ*sigF* mutant has higher protein content (27.4 ± 2.2% w/w) compared to the wild-type (18.3 ± 1.1% w/w), which can be associated with the remarkable differences in protein secretion reported for these two strains [15]. It is known that the protein content influences the physical-chemical properties of this type of polymers, namely conferring them hydrophobicity which can be useful for some industrial applications [28].

Concerning the molecular mass distribution (Figs. 1B and S2), four main different fractions were detected for both polymers, with the

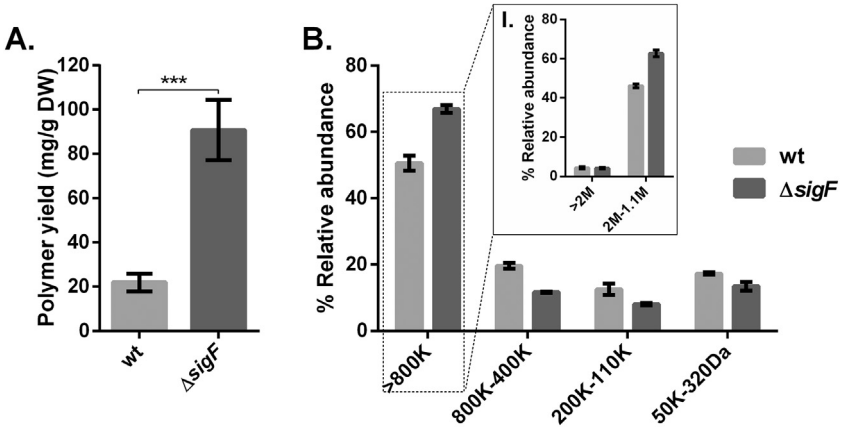

Fig. 1. Isolated polymer yields obtained from cultures of *Synechocystis* sp. PCC 6803 wild-type (wt) and Δ*sigF* (expressed as mg of lyophilized polymer per g of cell culture dry weight) (A) and molecular mass distribution of the polymers obtained by size exclusion chromatography using pullulan standards (B), and dextran standards for discrimination of high molecular mass fractions (I). Measurements were made with three biological and three technical replicates (***$p \leq 0.001$).

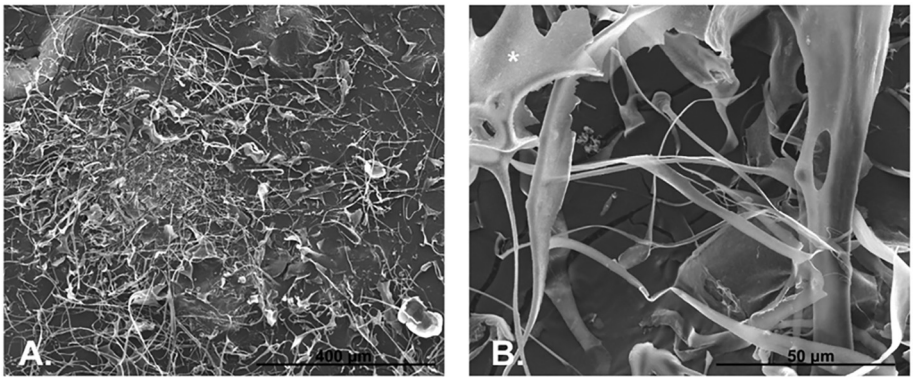

Fig. 2. Scanning electron micrographs of the released carbohydrate polymer isolated from *Synechocystis* Δ*sigF* cultures. * Lamellar structures. Scale bars = 400 μm (A), 50 μm (B).

fraction >800 kDa being the most abundant. The distribution of the fractions is also similar for both strains. These results show that the complexity of the polymers from *Synechocystis* wild-type and Δ*sigF* is not restricted to their monosaccharidic composition, but also extended to their molecular mass distribution. High molecular mass fractions are commonly detected in cyanobacterial extracellular carbohydrate polymers. However, the number of total fractions can vary significantly depending on the strain, ranging from a single fraction e.g. *Nostoc* strains polymers to several e.g. *Cyanospira* [3,4,7].

3.2. Morphological and physical features of the ΔsigF polymer

As the yield of the isolated polymer obtained from Δ*sigF* was remarkably higher and its biological activity was slightly higher compared to the wild-type (see Section 3.3 below), we pursued the characterization only for the mutants' polymer. Macroscopically, the Δ*sigF* polymer displays high porosity and exhibits scaly veins. Additionally, the surface morphological analysis performed using scanning electron microscopy, revealed its amorphous nature and a heterogeneous distribution of fibrils mixed with lamellar structures (Fig. 2). Although the majority of natural carbohydrate polymers have a more homogeneous and fibrillar aspect, lamellar and granular structures are also commonly found (including in cyanobacterial polymers) [7,29,30]. This heterogeneity may indicate the presence of more than one polymeric species. Recently, Li et al. [7] showed that the cyanobacterial polymer Nostoglycan (from *Nostoc sphaeroides*) has a multilayered flaky morphology, and Jia et al. [30] observed that the polymer from *Nostoc flagelliforme* was formed by "loose flaky curly aggregations" with scaly veins.

The rheological properties were evaluated by measuring the apparent viscosity of the polymer in aqueous solutions (from 0.1% to 5% w/v) over a range of different shear rates and stresses. In all cases, the viscosity decreased significantly with the increase of the shear rate. Representative results for the 1% (w/v) solution are depicted in Fig. 3A. This rheological behavior is characteristic of non-Newtonian fluids with shear-thinning or pseudoplastic properties, which can be explained by the disentanglement of polymer chains during flow and it is commonly observed for natural polymer solutions including cyanobacterial ones [31–34]. Nevertheless, increasing the polymer concentration did not increase significantly the viscosity (Figs. 3B and S3). These results suggest that, despite the abundance of RPS fractions with higher molecular mass (see above), the fiber net of the polymer has a relatively simple arrangement in solution. The rheological behavior of a polymer is intimately related to its structure and molecular mass, providing important data to determine the most appropriate polymer biotechnological application. The possibility to obtain highly concentrated polymer solutions with low viscosity is an interesting feature for a bioactive compound, as less viscous solutions allow higher interaction of the polymer chains with biological targets (e.g. cell receptors).

The FTIR spectra of the polymer produced by Δ*sigF* (Fig. S4) confirmed the presence of a polysaccharide backbone, with the band at 1043.13 cm^{-1} corresponding to the vibration absorptions of C-O-C ring of polysaccharides [35–37]. Other polysaccharide characteristic bands include those ranging from 2926.60 to 2856.12 cm^{-1} that can be assigned to the symmetrical or asymmetrical stretching vibrations of C—H, –CH3, and >CH_2 functional groups [38]. The band at 1402.78 cm^{-1} can be attributed to the C—H bending of aliphatic CH_2, although the stretching of C═O from carboxylates may also contribute to the spectral features in this region [37,38]. The absorption band at 622.92 cm^{-1} is indicative of the pyranose ring of glucose [35], that it was previously shown to be the most abundant monosaccharide in this polymer [15]. The absorption band at 3368.96 cm^{-1} is due to the stretching vibration of –OH [35,36,38]. Bands at 1653.57 and 1550.68 cm^{-1} are related to the C═O stretching vibrations of peptide

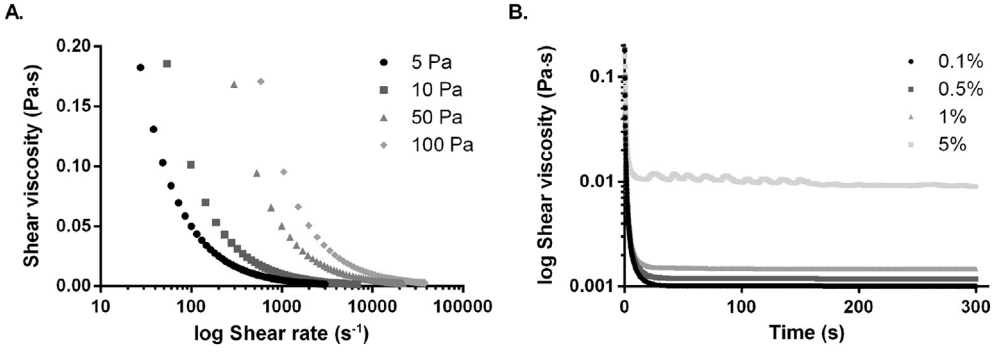

Fig. 3. Rheological properties of the polymer isolated from *Synechocystis* Δ*sigF* cultures. Shear viscosity of polymer solution at 1% (w/v) subjected to different shear stresses: 5, 10, 50 or 100 Pa (A) and shear viscosity of polymer solutions at 0.1%, 0.5%, 1% and 5% (w/v) under a shear stress of 10 Pa (B). Experiments were made in triplicate.

groups (amide I) or to the N—H bending and C—H stretching vibrations (amide II), respectively [37], thus corroborating the existence of a significant peptide/protein fraction in the polymer produced by Δ*sigF* (see above). Likewise, the band at 1245.29 cm^{-1} is indicative of the S═O stretching vibration of ester sulfate groups [31,39] consistent with the presence of sulfate groups.

3.3. Synechocystis wild-type and ΔsigF polymers reduce the viability of human tumor cell lines

The effect of the polymers from *Synechocystis* wild-type and Δ*sigF* mutant on the cell viability of three different human tumor cell lines: 8505C (human thyroid carcinoma), Mewo (human melanoma) and A2780 (human ovarian carcinoma) was analyzed *in vitro* (Fig. S5). A wide range of polymer concentrations was used (from 0 to 5 mg/mL), and for all the cell lines studied, both polymers induced a strong decrease in tumor cell viability, being this effect more evident in 8505C and Mewo cells. The 0% of cell viability was achieved for concentrations above 1.5 mg/mL. Therefore, the effect of the polymers was further analyzed over time in the 8505C and Mewo cell lines using lower polymer concentrations (0.7, 1 or 1.5 mg/mL) (Fig. 4). Both polymers decreased cell viability in dose- and time-dependent manner, being the Δ*sigF* polymer more potent than the wild-type. Several factors related to the mutant's polymer composition may contribute to the differences observed, namely the amount/exposure of the two uronic acids and the two amino sugars present in this polymer [15] or the higher protein content mentioned above. These constituents are frequently reported as biological active components in natural carbohydrate polymers [3,40,41].

The effect of both polymers was also tested towards a non-tumoral human thyroid cell line, Nthy-ori 3-1, and none of the concentrations tested decrease significantly cell viability (Fig. S6).

As mentioned above since *Synechocystis* Δ*sigF* produces larger amounts of polymer, and here we verified that is the one having stronger biological activity, the following studies were carried out only with this polymer.

3.4. Effect of Synechocystis ΔsigF polymer in the cell cycle of tumor cell lines

In order to understand the mechanism(s) involved in the decrease of human tumor cell viability caused by *Synechocystis* Δ*sigF* polymer, the cell cycle of Mewo cells was investigated after 24 and 48 h of treatment with this polymer at 0.7 mg/mL (Fig. 5). Overall there were no major alterations in Mewo cell cycle profile, only a slight reduction in the percentage of cells in G2/M was detected after treatment. Remarkably, a significant increase in the percentage of cells in sub-G1 peak was observed, and this percentage rose over time. This effect is suggestive of induction of cell death by apoptosis [25,42].

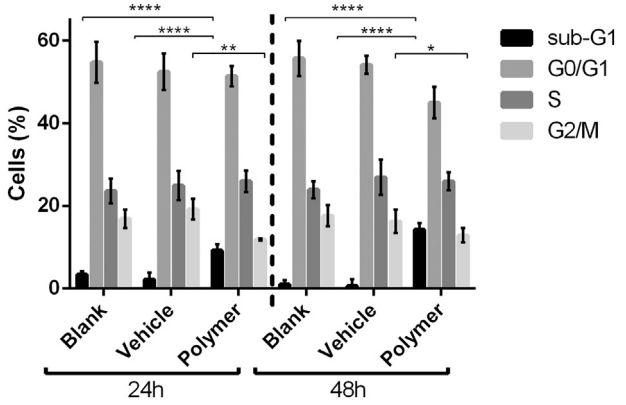

Fig. 5. Percentage of Mewo cells in the different cell cycle phases after treatment with complete medium (Blank), vehicle or 0.7 mg/mL of *Synechocystis* Δ*sigF* polymer for 24 h and 48 h. Results are expressed as mean ± STD of three independent experiments (*p value ≤0.05; **p value ≤0.01; ****p value ≤0.0001).

3.5. Synechocystis ΔsigF polymer induces tumor cell death by apoptosis

Since the high percentage of Mewo cells in sub-G1 strongly suggested an effect of *Synechocystis* Δ*sigF* polymer in the induction of apoptosis, the participation of this mechanism of cell death was studied by flow cytometry using the Annexin-V-FITC/PI double staining assay [43,44]. Our results confirmed that the effect of the polymer in apoptosis increased in a time-dependent manner, with levels of apoptosis reaching 34.6 ± 4.6% after 48 h treatment (Fig. 6). Previously, two studies reported the induction of apoptosis in tumor cell lines after treatment with other cyanobacterial extracellular carbohydrate polymers isolated from the colonial *Aphanothece halophytica* [8] and the filamentous *Nostoc sphaeroides* [7]. In the later study, similar levels of apoptosis (≈40%) were detected after treatment of human lung adenocarcinoma cells with 1 mg/mL Nostoglycan. It is important to notice that these results were obtained with a different cell line, different polymer and with a higher polymer concentration. However, Nostoglycan shares also some features with the Δ*sigF* polymer, namely the macroscopically observed lamellar structures, presence of galacturonic acid and some functional groups e.g. hydroxyl [7].

Overall, the Δ*sigF* polymer seems to be among the most potent natural carbohydrate polymers regarding induction of apoptosis in human tumor cells, even when compared to polymers from eukaryotic organisms. For example, similar levels of apoptosis (40 and 45%) to the ones reached by us, were obtained with higher concentrations of EPS from the halophilic bacterium *Halomonas stenophila* (at 1.5 mg/mL) [45] or from the brown algae *Padina tetrastromatica* (at 1.2 mg/mL) [46], while lower levels of apoptosis (22.7%) were detected using

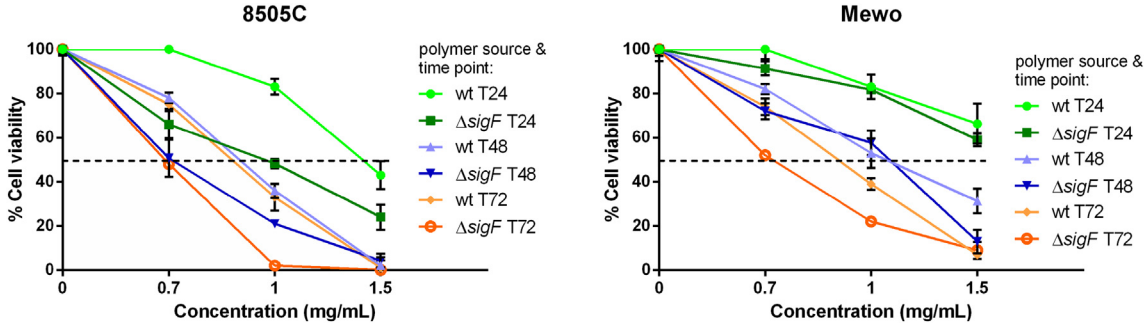

Fig. 4. Effect of the polymers produced by *Synechocystis* wild-type (wt) and mutant (Δ*sigF*) on cell viability of human thyroid carcinoma (8505C) and human melanoma (Mewo) cells, analyzed using PrestoBlue™ viability assay. Cells were treated with 0.7, 1 or 1.5 mg/mL of polymer and the dose-response curves after 24, 48 or 72 h of cell treatment (T24, T48, T72, respectively) are presented. Results are expressed in relation to Blank and are represented as mean ± STD of three independent experiments. Cells treated with polymer vehicle were used as controls, showing no differences to Blank (*data not shown*).

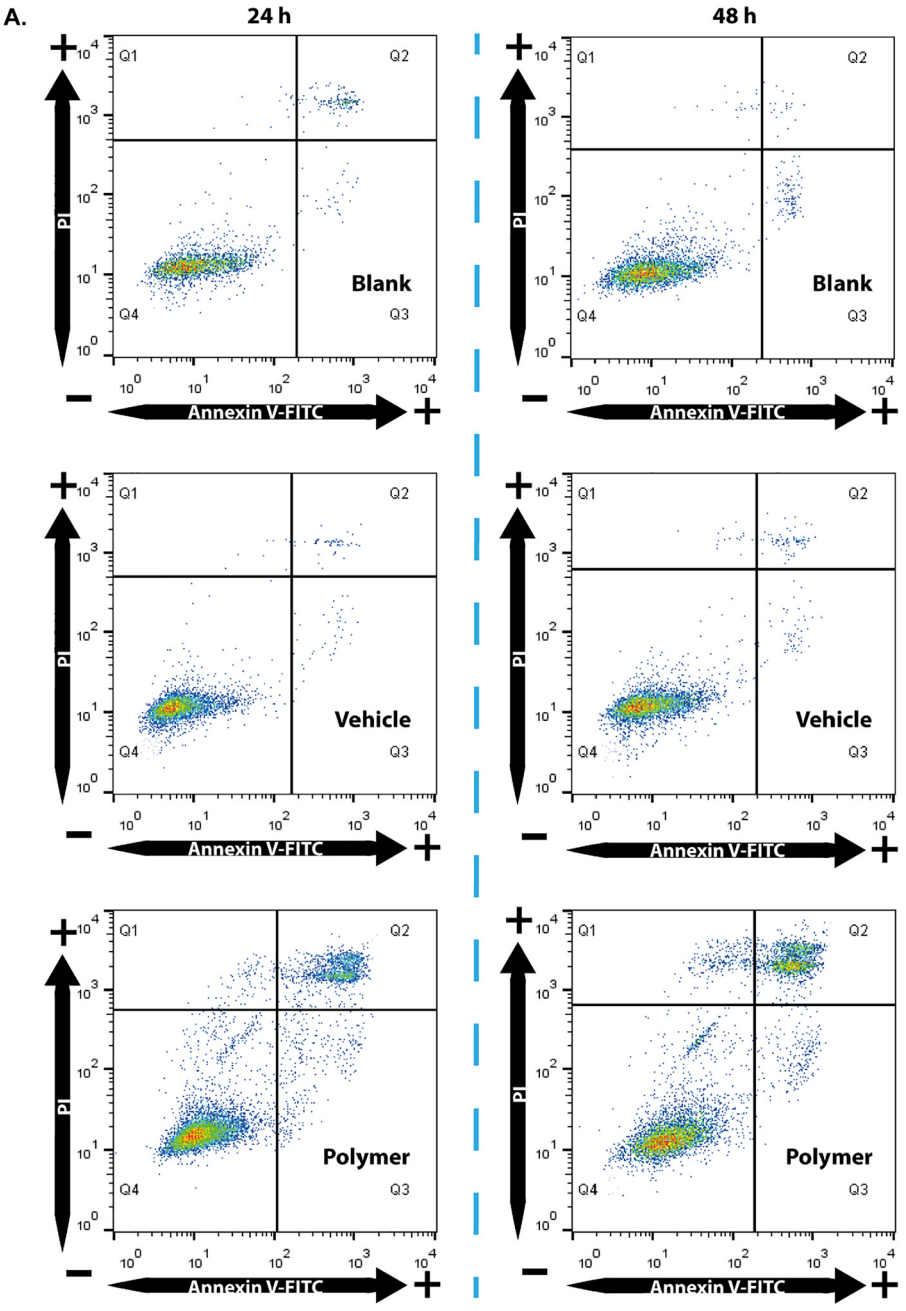
A.
24 h
48 h
Q1
Q2
Q3
Q4
PI
Annexin V-FITC
Blank
Vehicle
Polymer

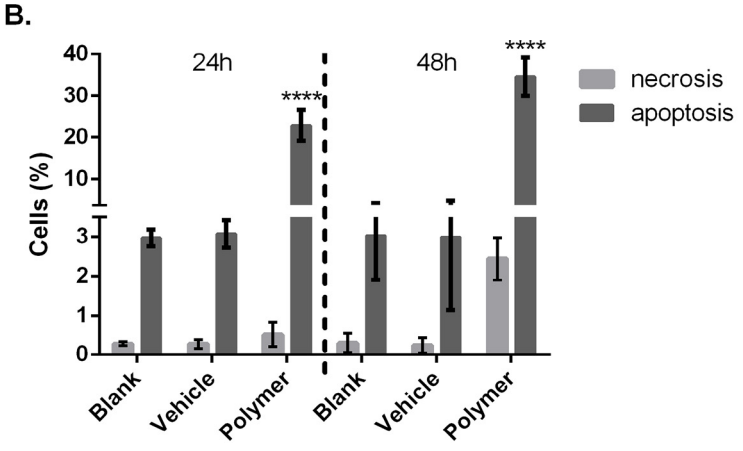
B.
24h
48h
****
****
Cells (%)
necrosis
apoptosis
Blank
Vehicle
Polymer
Blank
Vehicle
Polymer

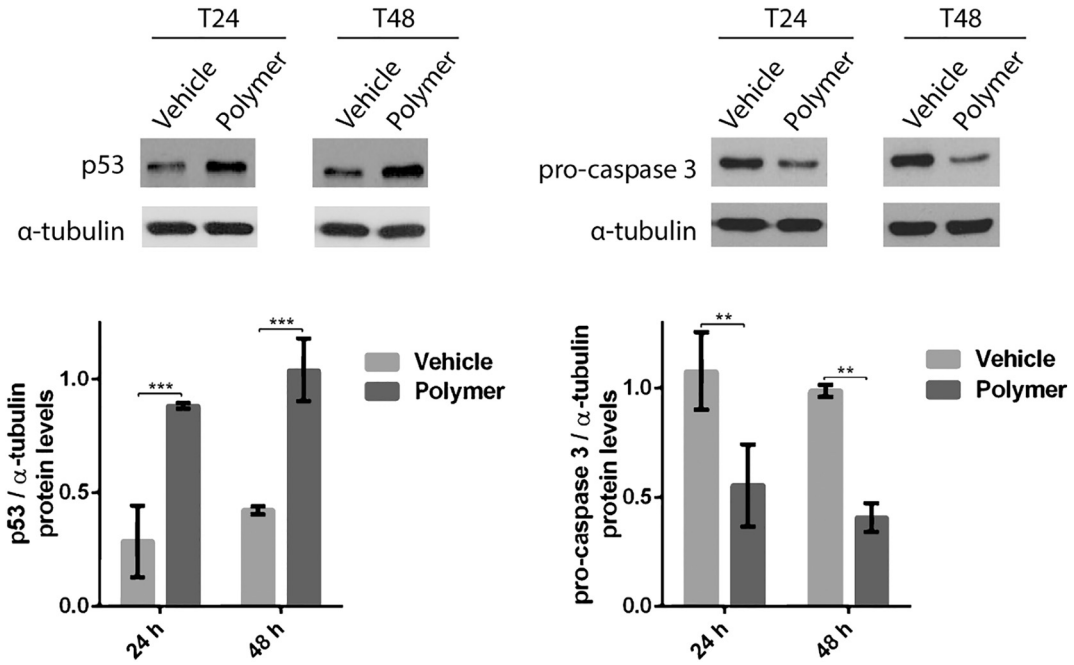

Fig. 7. Western blot analysis of p53 and pro-caspase 3 protein levels in Mewo cells after 24 and 48 h of treatment with vehicle or 0.7 mg/mL of *Synechocystis* Δ*sigF* polymer. Images are representative of at least 3 independent experiments and α-tubulin was used as loading control (upper panels). The values obtained from densitometry analysis of the band's intensity were normalized with the values obtained for α-tubulin bands and were represented as mean ± STD of three independent experiments.

polysaccharides extracted from the mushroom *Morchella esculenta* at a similar concentration (0.8 mg/mL) [47].

The involvement of apoptosis in the mechanism of action of the Δ*sigF* polymer in Mewo cells was further corroborated by the analysis of the levels of proteins related to apoptosis. Our results clearly showed an effect in the levels of the executioner caspase-3, one of the most important players in apoptotic signaling [48]. A clear decrease in the levels of pro-caspase 3 was observed after cell treatment with Δ*sigF* polymer (Fig. 7), which indicates an increase in caspase-3 cleaved and active form [26,49]. Furthermore, Δ*sigF* polymer increased the levels of p53 (Fig. 7), a well-known tumor suppressor which may delay cell cycle progression and trigger apoptotic pathways [48]. Similarly, the pro-apoptotic effect of the extracellular carbohydrate polymer from the cyanobacterium *Aphanothece halophytica* on HeLa cells was shown to be dependent on p53 and caspase-3 [8]. Furthermore, p53 may also promote apoptosis via cell cycle arrest, particularly through the overexpression of its downstream target p21, which is involved in cell cycle arrest at G1/S and G2/M [50]. Therefore, the effect of the Δ*sigF* polymer on p21 protein levels was also analyzed in the present study. Although our results showed that the p21 protein levels were slightly higher after treatment with Δ*sigF* polymer, a significant effect was not observed (Fig. S7). Accordingly, our previous analysis of the Mewo cell cycle profile showed no evident effect of the Δ*sigF* polymer treatment, which suggest that this polymer may act preferentially through apoptosis induction. Future studies will help to further unravel the players involved in the pro-apoptotic effect induced by the Δ*sigF* polymer.

4. Conclusions

In brief, the comprehensive characterization of the extracellular carbohydrate polymer from the *Synechocystis* Δ*sigF* mutant revealed its amorphous nature, that it is formed mainly by polysaccharidic fractions with high molecular mass, and organized in a highly porous heterogeneous mesh of fibrils with lamellar structures. The polymer contains high amount of peptides and possesses several functional groups, e.g. sulfate, carboxyl and hydroxyl. Notably, this natural highly sulfated polymer showed a strong biological activity towards different human tumor cell lines, reducing their viability even in low concentrations. The antitumor effect of Δ*sigF* polymer was associated with the induction of apoptotic pathways via p53 protein increased levels and caspase-3 activation. These results, together with the possibility of obtaining concentrated solutions with low viscosity, highlight the potential of this polymer for biomedical research.

Declaration of Competing Interest

None.

Acknowledgments

This work was financed by FEDER - Fundo Europeu de Desenvolvimento Regional funds through the COMPETE 2020 - Operacional Programme for Competitiveness and Internationalisation (POCI), Portugal 2020, and by Portuguese funds through FCT - Fundação para a Ciência e a Tecnologia/Ministério da Ciência, Tecnologia e Ensino Superior in the framework of the projects POCI-01-0145-FEDER-028779 (PTDC/BIA-MIC/28779/2017) and POCI-01-0145-FEDER-031520 (PTDC/MEC-ONC/31520/2017), and the grant SFRH/BD/99715/2014 (CF). Further funding was obtained from the projects "Structured Programme on Bioengeneering Therapies for Infectious Diseases and Tissue Regeneration", NORTE-01-0145-FEDER-000012 and "Advancing cancer research: from basic knowledge to application", NORTE-01- 0145-FEDER-000029: "Projetos Estruturados de I & D & I", funded by Norte 2020 – Programa Operacional Regional do Norte. The authors thank the staff of the Materials Centre of University of Porto (CEMUP) for the technical assistance in the SEM analysis.

Fig. 6. Flow cytometry analysis of apoptotic cell death in Mewo cells after treatment with *Synechocystis* Δ*sigF* polymer, using Annexin V-FITC/PI staining. Cells were treated with complete medium (Blank), vehicle (Vehicle) or 0.7 mg/mL of Δ*sigF* polymer (Polymer) for 24 h (left panel) and 48 h (right panel), and representative images of four independent experiments are shown (A). Percentage of cells in apoptosis and necrosis expressed as mean ± STD (B) of four independent experiments (****p value ≤0.0001).

Appendix A. Supplementary data

Supplementary data to this article can be found online at https://doi.org/10.1016/j.ijbiomac.2019.06.152.

References

[1] R.S. Wotton, The utiquity and many roles of exopolymers (EPS) in aquatic systems, Sci. Mar. 68 (2004) 13–21, https://doi.org/10.3989/scimar.2004.68s113.
[2] F. Rossi, R. De Philippis, Exocellular polysaccharides in microalgae and cyanobacteria: chemical features, role and enzymes and genes involved in their biosynthesis, Physiol. Microalgae, Springer International Publishing, Cham 2016, pp. 565–590, https://doi.org/10.1007/978-3-319-24945-2_21.
[3] S. Pereira, A. Zille, E. Micheletti, P. Moradas-Ferreira, R. De Philippis, P. Tamagnini, Complexity of cyanobacterial exopolysaccharides: composition, structures, inducing factors and putative genes involved in their biosynthesis and assembly, FEMS Microbiol. Rev. 33 (2009) 917–941, https://doi.org/10.1111/j.1574-6976.2009.00183.x.
[4] K. Kanekiyo, J.B. Lee, K. Hayashi, H. Takenaka, Y. Hayakawa, S. Endo, et al., Isolation of an antiviral polysaccharide, nostoflan, from a terrestrial cyanobacterium *Nostoc flagelliforme*, J. Nat. Prod. 68 (2005) 1037–1041, https://doi.org/10.1021/NP050056C.
[5] L. Parwani, M. Bhatnagar, A. Bhatnagar, V. Sharma, Antioxidant and iron-chelating activities of cyanobacterial exopolymers with potential for wound healing, J. Appl. Phycol. 26 (2014) 1473–1482, https://doi.org/10.1007/s10811-013-0180-7.
[6] A.B. Gudmundsdottir, S. Omarsdottir, A. Brynjolfsdottir, B.S. Paulsen, E.S. Olafsdottir, J. Freysdottir, Exopolysaccharides from *Cyanobacterium aponinum* from the Blue Lagoon in Iceland increase IL-10 secretion by human dendritic cells and their ability to reduce the IL-17+RORγt+/IL-10+FoxP3+ ratio in CD4+ T cells, Immunol. Lett. 163 (2015) 157–162, https://doi.org/10.1016/J.IMLET.2014.11.008.
[7] H. Li, L. Su, S. Chen, L. Zhao, H. Wang, F. Ding, H. Chen, R. Shi, Y. Wang, Z. Huang, Physicochemical characterization and functional analysis of the polysaccharide from the edible microalga *Nostoc sphaeroides*, Molecules 23 (2018) 508, https://doi.org/10.3390/molecules23020508.
[8] Y. Ou, S. Xu, D. Zhu, X. Yang, Molecular mechanisms of exopolysaccharide from *Aphanothece halaphytica* (EPSAH) induced apoptosis in HeLa cells, PLoS One 9 (2014), e87223. https://doi.org/10.1371/journal.pone.0087223.
[9] A. Zong, H. Cao, F. Wang, Anticancer polysaccharides from natural resources: a review of recent research, Carbohydr. Polym. 90 (2012) 1395–1410, https://doi.org/10.1016/J.CARBPOL.2012.07.026.
[10] I. Wijesekara, R. Pangestuti, S.-K. Kim, Biological activities and potential health benefits of sulfated polysaccharides derived from marine algae, Carbohydr. Polym. 84 (2011) 14–21, https://doi.org/10.1016/J.CARBPOL.2010.10.062.
[11] S. Raveendran, Y. Yoshida, T. Maekawa, D.S. Kumar, Pharmaceutically versatile sulfated polysaccharide based bionano platforms, Nanomed. Nanotechnol. Biol. Med. 9 (2013) 605–626, https://doi.org/10.1016/J.NANO.2012.12.006.
[12] T. Jittawuttipoka, M. Planchon, O. Spalla, K. Benzerara, F. Guyot, C. Cassier-Chauvat, F. Chauvat, Multidisciplinary evidences that *Synechocystis* PCC6803 exopolysaccharides operate in cell sedimentation and protection against salt and metal stresses, PLoS One 8 (2013), e55564. https://doi.org/10.1371/journal.pone.0055564.
[13] S.B. Pereira, M. Santos, J.P. Leite, C. Flores, C. Eisfeld, Z. Büttel, R. Mota, F. Rossi, R. De Philippis, L. Gales, J.H. Morais-Cabral, P. Tamagnini, The role of the tyrosine kinase Wzc (Sll0923) and the phosphatase Wzb (Slr0328) in the production of extracellular polymeric substances (EPS) by *Synechocystis* PCC 6803, Microbiologyopen (2019), e753. https://doi.org/10.1002/mbo3.753.
[14] M.L. Fisher, R. Allen, Y. Luo, R. Curtiss, Export of extracellular polysaccharides modulates adherence of the cyanobacterium *Synechocystis*, PLoS One 8 (2013), e74514. https://doi.org/10.1371/journal.pone.0074514.
[15] C. Flores, M. Santos, S.B. Pereira, R. Mota, F. Rossi, R. De Philippis, N. Couto, E. Karunakaran, P.C. Wright, P. Oliveira, P. Tamagnini, The alternative sigma factor SigF is a key player in the control of secretion mechanisms in *Synechocystis* sp. PCC 6803, Environ. Microbiol. 21 (2019) 343–359, https://doi.org/10.1111/1462-2920.14465.
[16] J. Huckauf, C. Nomura, K. Forchhammer, M. Hagemann, Stress responses of *Synechocystis* sp. strain PCC 6803 mutants impaired in genes encoding putative alternative sigma factors, Microbiology 146 (2000) 2877–2889, https://doi.org/10.1111/1462-2920.14465.
[17] M. Dubois, K.A. Gilles, J.K. Hamilton, P.T. Rebers, F. Smith, Colorimetric method for determination of sugars and related substances, Anal. Chem. 28 (1956) 350–356, https://doi.org/10.1021/ac60111a017.
[18] R. Mota, R. Guimarães, Z. Büttel, F. Rossi, G. Colica, C.J. Silva, C. Santos, L. Gales, A. Zille, R. De Philippis, S.B. Pereira, P. Tamagnini, Production and characterization of extracellular carbohydrate polymer from *Cyanothece* sp. CCY 0110, Carbohydr. Polym. 92 (2013) 1408–1415, https://doi.org/10.1016/J.CARBPOL.2012.10.070.
[19] C. Flores, P. Tamagnini, Looking outwards: isolation of cyanobacterial released carbohydrate polymers and proteins, J. Vis. Exp. 147 (2019), e59590. https://doi.org/10.3791/59590.
[20] O.H. Lowry, N.J. Rosebrough, A.L. Farr, R.J. Randall, Protein measurement with folin phenol reagent, J. Biol. Chem. 193 (1951) 265–275.
[21] L. Chen, F. Rossi, S. Deng, Y. Liu, G. Wang, A. Adessi, R. De Philippis, Macromolecular and chemical features of the excreted extracellular polysaccharides in induced biological soil crusts of different ages, Soil Biol. Biochem. 78 (2014) 1–9, https://doi.org/10.1016/J.SOILBIO.2014.07.004.
[22] H. Pópulo, R. Caldas, J.M. Lopes, J. Pardal, V. Máximo, P. Soares, Overexpression of pyruvate dehydrogenase kinase supports dichloroacetate as a candidate for cutaneous melanoma therapy, Expert Opin. Ther. Targets 19 (2015) 733–745, https://doi.org/10.1517/14728222.2015.1045416.
[23] A.M. Meireles, A. Preto, A.S. Rocha, A.P. Rebocho, V. Máximo, I. Pereira-Castro, S. Moreira, T. Feijão, T. Botelho, R. Marques, V. Trovisco, L. Cirnes, C. Alves, S. Velho, P. Soares, M. Sobrinho-Simões, Molecular and genotypic characterization of human thyroid follicular cell carcinoma–derived cell lines, Thyroid 17 (2007) 707–715, https://doi.org/10.1089/thy.2007.0097.
[24] M.J.R.P. Queiroz, D. Peixoto, R.C. Calhelha, P. Soares, T. dos Santos, R.T. Lima, J.F. Campos, R.M.V. Abreu, I.C.F.R. Ferreira, M.H. Vasconcelos, New di(hetero)arylethers and di(hetero)arylamines in the thieno[3,2-b]pyridine series: synthesis, growth inhibitory activity on human tumor cell lines and non-tumor cells, effects on cell cycle and on programmed cell death, Eur. J. Med. Chem. 69 (2013) 855–862, https://doi.org/10.1016/J.EJMECH.2013.09.023.
[25] R.T. Lima, D. Sousa, A.M. Paiva, A. Palmeira, J. Barbosa, M. Pedro, M.M. Pinto, E. Sousa, M.H. Vasconcelos, Modulation of autophagy by a thioxanthone decreases the viability of melanoma cells, Molecules 21 (2016) 1343, https://doi.org/10.3390/molecules21101343.
[26] V. Lopes-Rodrigues, A. Oliveira, M. Correia-da-Silva, M. Pinto, R.T. Lima, E. Sousa, M.H. Vasconcelos, A novel curcumin derivative which inhibits P-glycoprotein, arrests cell cycle and induces apoptosis in multidrug resistance cells, Bioorg. Med. Chem. 25 (2017) 581–596, https://doi.org/10.1016/J.BMC.2016.11.023.
[27] H. Miranda, P. Immerzeel, L. Gerber, K. Hörnaeus, S.B. Lind, B. Pattanaik, P. Lindberg, F. Mamedov, P. Lindblad, Sll1783, a monooxygenase associated with polysaccharide processing in the unicellular cyanobacterium *Synechocystis* PCC 6803, Physiol. Plant. 161 (2017) 182–195, https://doi.org/10.1111/ppl.12582.
[28] L. Zhang, X. Feng, N. Zhu, J. Chen, Role of extracellular protein in the formation and stability of aerobic granules, Enzym. Microb. Technol. 41 (2007) 551–557, https://doi.org/10.1016/J.ENZMICTEC.2007.05.001.
[29] C. Cassier-Chauvat, F. Chauvat, C. Cassier-Chauvat, F. Chauvat, Responses to oxidative and heavy metal stresses in cyanobacteria: recent advances, Int. J. Mol. Sci. 16 (2014) 871–886, https://doi.org/10.3390/ijms16010871.
[30] S. Jia, H. Yu, Y. Lin, Y. Dai, Characterization of extracellular polysaccharides from *Nostoc flagelliforme* cells in liquid suspension culture, Biotechnol. Bioprocess Eng. 12 (2007) 271–275, https://doi.org/10.1007/BF02931103.
[31] B. Bhunia, U.S. Prasad Uday, G. Oinam, A. Mondal, T.K. Bandyopadhyay, O.N. Tiwari, Characterization, genetic regulation and production of cyanobacterial exopolysaccharides and its applicability for heavy metal removal, Carbohydr. Polym. 179 (2018) 228–243, https://doi.org/10.1016/J.CARBPOL.2017.09.091.
[32] M.H. Hussein, G.S. Abou-Elwafa, S.A. Shaaban-Dessuuki, N.I. Hassan, Characterization and antioxidant activity of exopolysaccharide secreted by *Nostoc carneum*, Int. J. Pharmacol. 11 (2015) 432–439, https://doi.org/10.3923/ijp.2015.432.439.
[33] P. Han, Y. Sun, X. Wu, Y. Yuan, Y. Dai, S. Jia, Emulsifying, flocculating, and physicochemical properties of exopolysaccharide produced by cyanobacterium Nostoc flagelliforme, Appl. Biochem. Biotechnol. 172 (2014) 36–49, https://doi.org/10.1007/s12010-013-0505-7.
[34] M. Bhatnagar, S. Pareek, J. Ganguly, A. Bhatnagar, Rheology and composition of a multi-utility exopolymer from a desert borne cyanobacterium *Anabaena variabilis*, J. Appl. Phycol. 24 (2012) 1387–1394, https://doi.org/10.1007/s10811-012-9791-7.
[35] H. Li, X. Gong, Z. Wang, C. Pan, Y. Zhao, X. Gao, W. Liu, Multiple fingerprint profiles and chemometrics analysis of polysaccharides from *Sarcandra glabra*, Int. J. Biol. Macromol. 123 (2019) 957–967, https://doi.org/10.1016/J.IJBIOMAC.2018.11.103.
[36] I.P.S. Fernando, K.K.A. Sanjeewa, K.W. Samarakoon, W.W. Lee, H.-S. Kim, E.-A. Kim, U.K.D.S.S. Gunasekara, D.T.U. Abeytunga, C. Nanayakkara, E.D. de Silva, H.-S. Lee, Y.-J. Jeon, FTIR characterization and antioxidant activity of water soluble crude polysaccharides of Sri Lankan marine algae, Algae 32 (2017) 75–86, https://doi.org/10.4490/algae.2017.32.12.1.
[37] N. Yee, L.G. Benning, V.R. Phoenix, F.G. Ferris, Characterization of metal—cyanobacteria sorption reactions: a combined macroscopic and infrared spectroscopic investigation, Environ. Sci. Technol. 38 (2004) 775–782, https://doi.org/10.1021/ES0346680.
[38] A. Parikh, D. Madamwar, Partial characterization of extracellular polysaccharides from cyanobacteria, Bioresour. Technol. 97 (2006) 1822–1827, https://doi.org/10.1016/J.BIORTECH.2005.09.008.
[39] Y. Cai, P. Chen, C. Wu, J. Duan, H. Bai, Sulfated modification and biological activities of polysaccharides derived from *Zizyphus jujuba cv*. Jinchangzao, Int. J. Biol. Macromol. 120 ((2018) 1149–1155, https://doi.org/10.1016/J.IJBIOMAC.2018.08.141.
[40] C. Roca, V.D. Alves, F. Freitas, M.A.M. Reis, Exopolysaccharides enriched in rare sugars: bacterial sources, production, and applications, Front. Microbiol. 6 (2015), 288. https://doi.org/10.3389/fmicb.2015.00288.
[41] P. Laurienzo, Laurienzo, Paola, Marine polysaccharides in pharmaceutical applications: an overview, Mar. Drugs. 8 (2010) 2435–2465, doi:https://doi.org/10.3390/md8092435.
[42] C. Riccardi, I. Nicoletti, Analysis of apoptosis by propidium iodide staining and flow cytometry, Nat. Protoc. 1 (2006) 1458–1461, https://doi.org/10.1038/nprot.2006.238.
[43] J. Barbosa, R.T. Lima, D. Sousa, A.S. Gomes, A. Palmeira, H. Seca, K. Choosang, P. Pakkong, H. Bousbaa, M.M. Pinto, E. Sousa, M.H. Vasconcelos, M. Pedro, Screening a small library of xanthones for antitumor activity and identification of a hit compound which induces apoptosis, Molecules 21 (2016) 81, https://doi.org/10.3390/molecules21010081.
[44] I. Vermes, C. Haanen, H. Steffens-Nakken, C. Reutellingsperger, A novel assay for apoptosis flow cytometric detection of phosphatidylserine expression on early apoptotic cells using fluorescein labelled Annexin V, J. Immunol. Methods 184 (1995) 39–51, https://doi.org/10.1016/0022-1759(95)00072-I.

[45] C. Ruiz-Ruiz, G.K. Srivastava, D. Carranza, J.A. Mata, I. Llamas, M. Santamaría, E. Quesada, I.J. Molina, An exopolysaccharide produced by the novel halophilic bacterium *Halomonas stenophila* strain B100 selectively induces apoptosis in human T leukaemia cells, Appl. Microbiol. Biotechnol. 89 (2011) 345–355, https://doi.org/10.1007/s00253-010-2886-7.

[46] G.M. Jose, M. Raghavankutty, G.M. Kurup, Sulfated polysaccharides from *Padina tetrastromatica* induce apoptosis in HeLa cells through ROS triggered mitochondrial pathway, Process Biochem. 68 (2018) 197–204, https://doi.org/10.1016/J.PROCBIO.2018.02.014.

[47] C. Liu, Y. Sun, Q. Mao, X. Guo, P. Li, Y. Liu, N. Xu, C. Liu, Y. Sun, Q. Mao, X. Guo, P. Li, Y. Liu, N. Xu, Characteristics and antitumor activity of *Morchella esculenta* polysaccharide extracted by pulsed electric field, Int. J. Mol. Sci. 17 (2016) 986, https://doi.org/10.3390/ijms17060986.

[48] J. Chen, The cell-cycle arrest and apoptotic functions of p53 in tumor initiation and progression, Cold Spring Harb. Perspect. Med. 6 (2016) a026104, https://doi.org/10.1101/cshperspect.a026104.

[49] R. T. Lima, G. A. Barron, J. A. Grabowska, G. Bermano, S. Kaur, N. Roy, M. Helena Vasconcelos, P. K.T. Lin, Cytotoxicity and cell death mechanisms induced by a novel bisnaphthalimidopropyl derivative against the NCI-H460 non-small lung cancer cell line, Anti Cancer Agents Med. Chem. 13 (2013) 414–421, https://doi.org/10.2174/187152013804910488.

[50] A. Karimian, Y. Ahmadi, B. Yousefi, Multiple functions of p21 in cell cycle, apoptosis and transcriptional regulation after DNA damage, DNA Repair (Amst) 42 (2016) 63–71, https://doi.org/10.1016/J.DNAREP.2016.04.008.

Supplementary data

Characterization and antitumor activity of the extracellular carbohydrate polymer from the cyanobacterium *Synechocystis* Δ*sigF* mutant

Carlos Flores[a,b,c], Raquel T. Lima[a,d,e], Alessandra Adessi[f], Aureliana Sousa[a,g], Sara B. Pereira[a,b], Pedro L. Granja[a,g,h], Roberto De Philippis[f], Paula Soares[a,d,e], Paula Tamagnini[a,b,i,*]

[*] Corresponding author. Tel.: +351 220 408 800. E-mail address: pmtamagn@ibmc.up.pt.

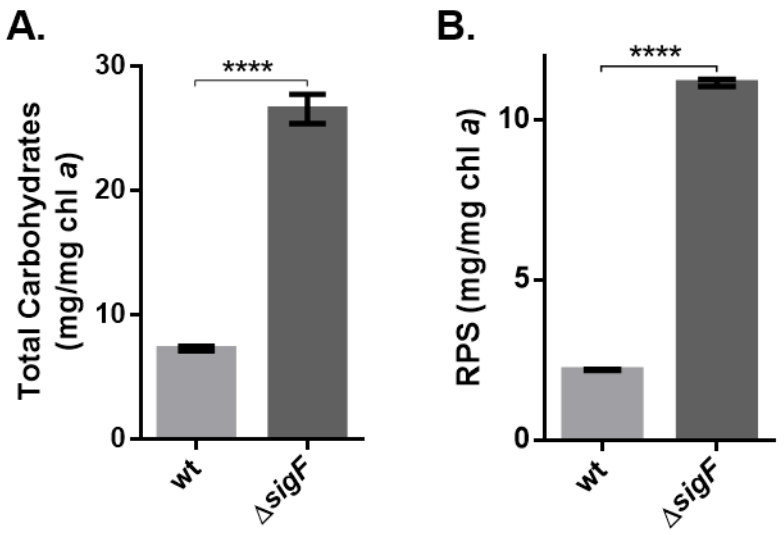

Fig. S1. Total carbohydrates (A) and released polysaccharides - RPS (B) from *Synechocystis* wild-type and Δ*sigF* cultures. Cultures were grown in BG11 at 30 ^{o}C under a 12 h light (50 µE m^{-2} s^{-1})/12 h dark regimen, with orbital shaking at 150 r.p.m. Results are expressed as mg of polymer per mg of chlorophyll *a* (chl *a*). Experiments were made in triplicate (**** *p* value ≤ 0.0001).

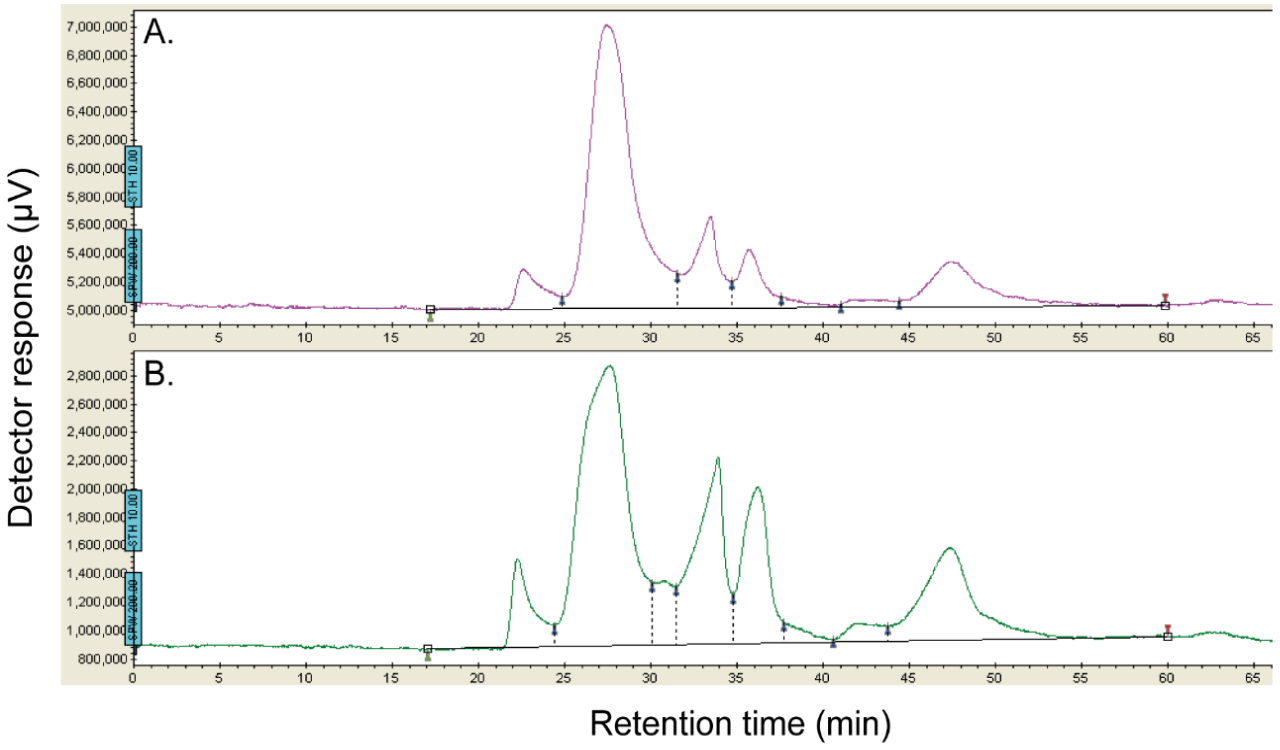

Fig. S2. Size exclusion chromatographic profiles of *Synechocystis* Δ*sigF* (A) and wild-type (B) polymers. Experiments were made in triplicate and a representative chromatogram is shown.

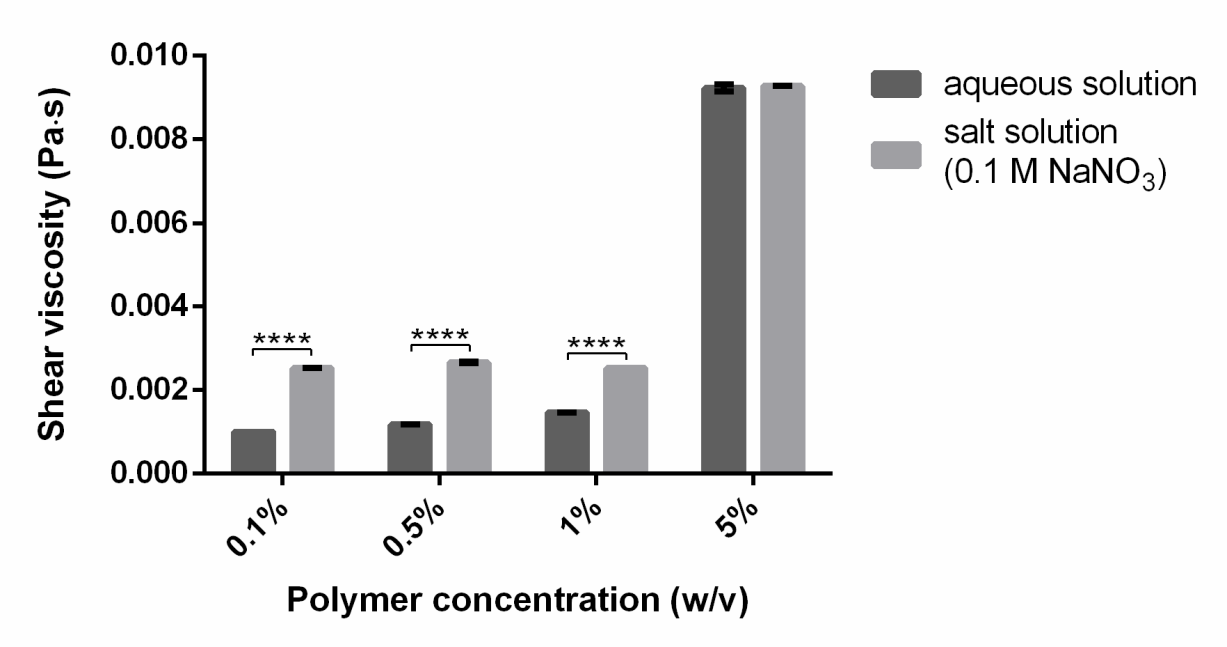

Fig. S3. Shear viscosity of Δ*sigF* polymer solutions at 0.1%, 0.5%, 1.0% and 5% (w/v) under a shear stress of 10 Pa. Polymer was dissolved in water or salt solution (0.1 M $NaNO_3$). Experiments were made in triplicate (**** p value ≤ 0.0001).

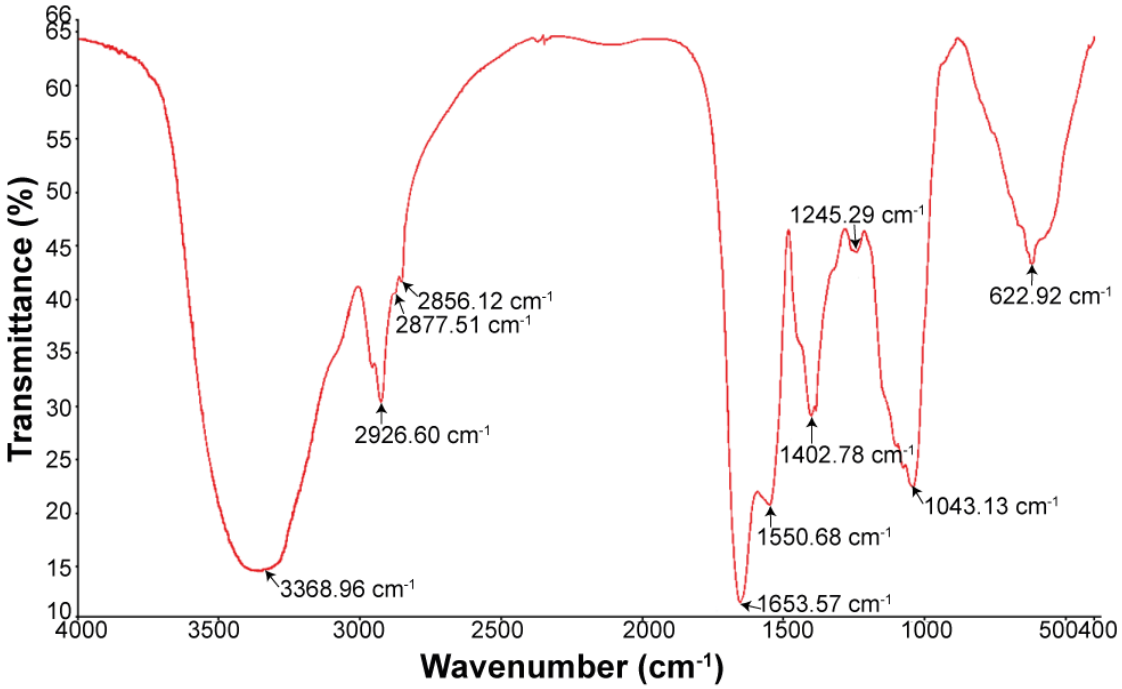

Fig. S4. Fourier transformed infrared (FTIR) spectrum of the polymer isolated from *Synechocystis* Δ*sigF* cultures. Arrows indicate the major absorptions bands and the corresponding wavenumbers. Experiments were made in triplicate and a representative spectrum is shown.

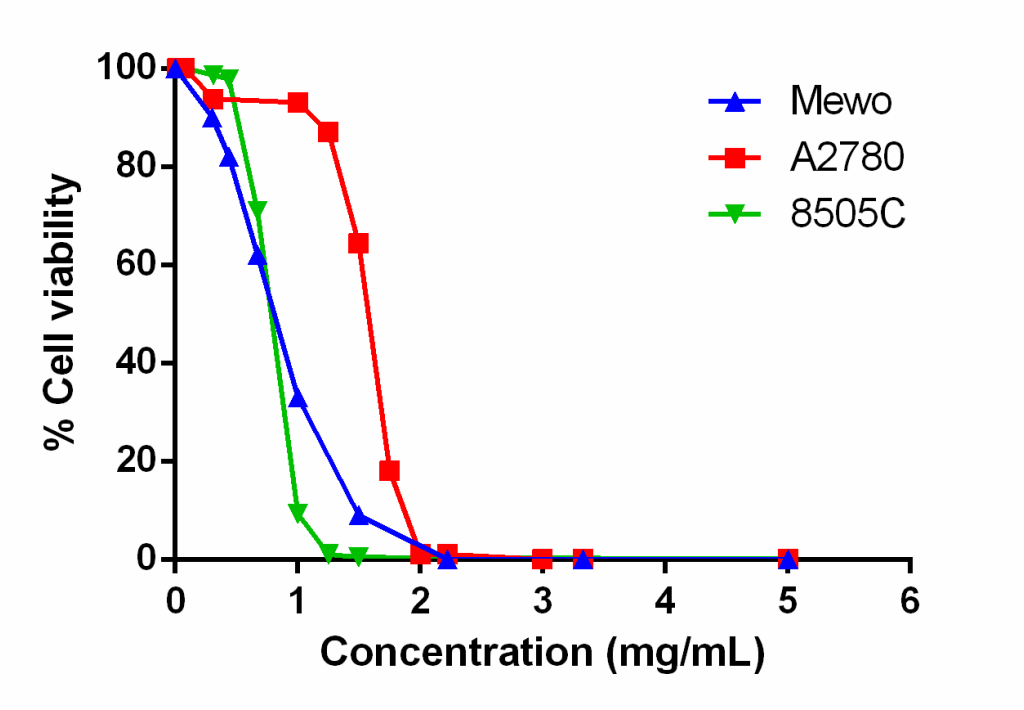

Fig. S5. Effect of the polymer produced by *Synechocystis* wild-type (wt) and Δ*sigF* on the viability of human melanoma (Mewo), human ovarian carcinoma (A2780) and human thyroid carcinoma (8505C) cells, analyzed using PrestoBlue™ viability assay. Cells were treated with a range of concentrations of polymer (from 0 to 5 mg/mL) and the dose-response curves after 72 hours of cell treatment are presented. Results are expressed in relation to Blank (cells treated with supplemented medium) and are represented as mean ± STD of three independent experiments. Cells treated with the polymer vehicle were used as controls, showing no differences to Blank (*data not shown*).

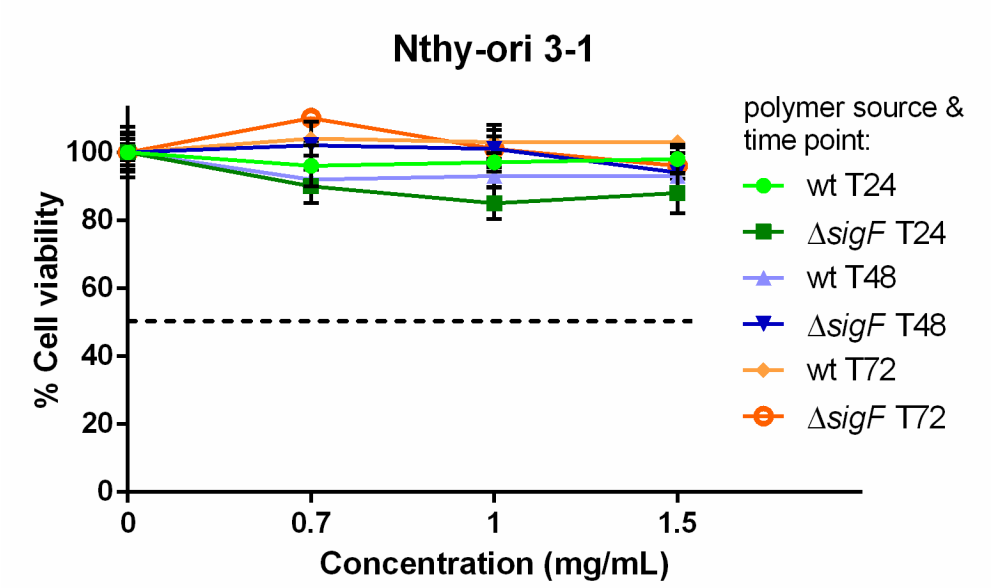

Fig. S6. Effect of the polymers produced by *Synechocystis* wild-type (wt) and mutant (Δ*sigF*) on cell viability of human thyroid cell line (Nthy-ori 3-1), analyzed using PrestoBlue™ viability assay. Cells were treated with 0.7, 1 or 1.5 mg/mL of polymer and the dose-response curves after 24, 48 or 72 hours of cell treatment (T24, T48, T72, respectively) are presented. Results are expressed in relation to Blank and are represented as mean ± STD of three independent experiments. Cells treated with polymer vehicle were used as controls, showing no differences to Blank (*data not shown*).

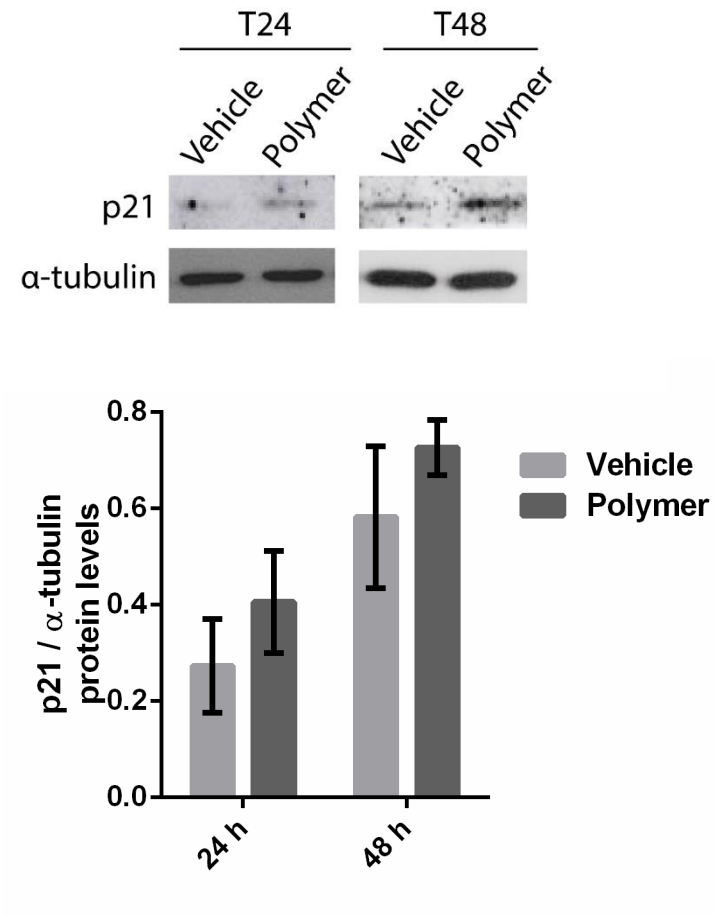

Fig. S7. Western blot analysis of p21 protein levels in Mewo cells after 24 and 48 h of treatment with vehicle or 0.7 mg/mL of *Synechocystis* Δ*sigF* polymer. Images are representative of at least 3 independent experiments and α-tubulin was used as loading control (upper panel). The values obtained from densitometry analysis of the band's intensity were normalized with the values obtained for the α-tubulin bands and were represented as mean ± STD of three independent experiments.

CHAPTER VI

Manipulation of the Δ*sigF* polymer and its effect in the antitumor activity

Manipulation of the Δ*sigF* polymer and its effect in the antitumor activity

Abstract

It was previously shown that the extracellular carbohydrate polymer from *Synechocystis* Δ*sigF* mutant has a strong antitumor activity (Flores et al., 2019, Chapter V). In order to understand which characteristics of the polymer contribute most to the bioactivity, its molecular weight (MW) and sulfate content were manipulated. Preliminary results indicated that the high MW polysaccharide fractions are essential for polymer's bioactivity. Currently, more studies are underway.

1. Introduction

Several studies have described polysaccharidic polymers with antitumor activity, mainly derived from macroalgae, fungi, mammals and bacteria (Zong et al., 2012). A wide range of polymer features was associated to their activity, such as the presence of uronic acids, amino-sugars, sulfate, non-carbohydrate constituents, or specific structural conformations. In contrast, there are very few studies reporting antitumor activity for cyanobacterial extracellular polymeric substances (EPS) (Li et al., 2018; Ou et al., 2014; Li et al., 2011b; Yue et al., 2011; Zheng et al. 1994), and only two proposed a possible association between specific polymer features and their activity, but still without conclusive experimental data (Gacheva et al., 2013; Mishima et al., 1998). Mishima et al., 1998 showed that Calcium-Spirulan (from *Arthrospira platensis*) inhibits the cell adhesion of lung-metastasizing tumors to the tissue extracellular matrix components. Since these tumor cells have specific surface receptors capable of recognizing rhamnose, the authors mentioned that the high rhamnose content of the polymer may be the main contributing factor for its bioactivity. Regarding Gacheva et al., 2013, they associated the protein content of *Gloeocapsa* sp. EPS with its antiproliferative activity towards HeLa cells. Therefore, the lack of information about the features that play a key role in cyanobacterial EPS antitumor activity impairs not only the better understanding of their mode of action, but also their effective application. In addition, the manipulation of these features is advantageous for industrial applications, since it allows the optimization of polymer bioactivity and reduction of production costs (Schmid, 2018).

Previously, we reported a strong antitumor activity of the EPS isolated from a *Synehcocystis* overproducing mutant, Δ*sigF*, towards human melanoma, ovary and thyroid carcinoma cells (Chapter V). Currently, we are aiming at correlating the polymer features with

its bioactivity. For this purpose, and to start with, the sulfate content and molecular weight of the Δ*sigF* polymer was manipulated, and the effect of the modified polymer was evaluated on the viability of human melanoma cell lines.

2. Material and Methods

2.1. Cyanobacterial culture conditions

Synechocystis sp. PCC 6803 Δ*sigF* (Huckauf et al., 2000) was grown in Erlenmeyer flasks with BG11 (Rippka et al., 1979). Cultures were incubated at 30 ºC under a 12h light (50 µE m^{-2} s^{-1}) / 12h dark regimen, with orbital shaking at 150 r.p.m.

2.2. Polymer isolation and chemical desulfation

Polymers were isolated as described in Chapter IV (Flores & Tamagnini, 2019). For chemical desulfation of the polymer, two distinct methodologies were followed. Lyophilized polymers were hydrolyzed in 2 M HCl at 100 ºC for 10 min, 25 min, 45 min, 1 h or 2 h. The hydrolysates were centrifuged at 14 100 *g* for 10 min, after cooling at 4 ºC for 10 min. Pellets were resuspended in ultrapure water, dialyzed overnight against deionized water (membranes with 12–14 kDa of molecular weight cut-off; Medicell International) and lyophilized. In parallel, solvolytic desulfation of the polymers in hot DMSO was also performed, following different procedures: i) DMSO (10% water) at 120 ºC for 3 h; ii) DMSO (5% water) at 50 ºC for 2 h; iii) DMSO (10% water) at 80 ºC for 5 h. Suspensions were cooled at 4 ºC and dialyzed overnight against deionized water.

2.3. Quantification of the sulfate content

For sulfate quantification, the polymers were treated as described in *step 2.2.*, and after centrifugation, the supernatant was analyzed by ion-exchange chromatography. The analysis was performed using a Dionex ICS-2500 system chromatograph equipped with a continuously regenerated anion-trap column, a continuous anionic self-regenerating suppressor, a conductivity detector (ED50), an IonPac PA11 4 x 250 mm column (Dionex), and a reagent-free Dionex system producing high-purity 50 mM KOH at a flow rate of 2 mL/min. Sulfate solutions (1 to 10 mg/L, Fluka) were used as standards.

2.4. Modifications of molecular weight

Molecular weight alterations were achieved through hydrolysis of the polymers either in 2 M HCl at 100 ºC, or in 2 M trifluoroacetic acid (TFA) at 120 ºC, for 10 min, 25 min, 45 min, 1

h or 2 h. After hydrolysis, the samples were evaporated 2 times and the polymers resuspended in ultrapure water, before being analyzed by Size Exclusion Chromatography (SEC).

2.5. Molecular weight analysis

The apparent molecular weight, hereafter referred to as molecular weight (MW) was determined according to a previously reported method (Chen et al., 2014), with some modifications. Briefly, samples were dissolved in HPLC grade water at a concentration of 5 mg/mL and analyzed using a Varian ProStar HPLC chromatograph (Varian) equipped with a 355 RI (refractive index) detector and two columns for Size Exclusion Chromatography (SEC), Polysep-GFC-P 6000 and 4000 (Phenomenex) connected in series. The analyses were performed with runs of 70 min and with HPLC grade water as eluent at a flow rate of 0.4 mL/min, using Dextran (Sigma–Aldrich) at different MWs (2000 kDa, 1100 kDa, 410 kDa, 150 kDa and 50 kDa) and saccharose (MW 0.34 kDa) as standards.

2.6. Human tumor cell lines and culture conditions

The human melanoma cell line Mewo (kindly given by Prof. Marc Mareel, Department of Radiotherapy and Nuclear Medicine, Ghent University Hospital, Belgium) (Pópulo et al., 2015) was maintained in DMEM culture medium with stable glutamine (Capricorn Scientific), supplemented with 10% fetal bovine serum (FBS, GIBCO, Invitrogen), 1x penicillin/streptomycin (Biowest) and 1.25 µg/mL amphotericin B (Corning). Cells were maintained in a humidified incubator at 37 ºC with 5% CO_2. Cell lines were authenticated following genotyping at i3S Genomics Core Facility (Porto, Portugal) using the PowerPlex® 16 HS System (Promega) and confirmation with the DNA profiles available at ATCC and ECACC STR profiles database.

2.7. Cell viability assays

Mewo cells were plated on 96-well plates at 1 x 10^4 cells/well and allowed to adhere for 24 h at 37 ºC. Cells were then treated for 24 and 48 h with supplemented media (Blank), Δ*sigF* polymer (resuspended in non-supplemented media) at 0.7, 1 and 1.5 mg/mL or with polymer vehicle (supplemented media containing the equivalent amount of non-supplemented medium used in the polymer treatments). To assess cell viability after treatment, PrestoBlue™ cell viability assay was carried out as previously described (Pópulo et al., 2015). Briefly, cells were washed three times with the respective non-supplemented medium and further incubated for 45 min with PrestoBlue™ reagent (Life Technologies). Fluorescence was measured (excitation

560 nm; emission 590 nm) on a Synergy HT Multi-Mode Microplate Reader (BioTek Instruments Inc.). All samples and controls were analyzed with three biological and five technical replicates. Cellular viability was determined by analyzing the fluorescence values of each sample as percentage in relation to control wells (after removing the background values).

2.8. Statistical analysis

Data were plotted and statistically analyzed using GraphPad Prism version 7.0 (GraphPad Software) using an analysis of variance (ANOVA), followed by Bonferroni's multiple comparisons test.

3. Results and Discussion

3.1. Molecular weight distribution of TFA hydrolyzed polymer and its antitumor activity

Alteration of the molecular weight (MW) distribution of Δ*sigF* polymer was firstly achieved through trifluoroacetic acid (TFA) hydrolysis (Fig. 1). A gradual increase of the abundance of lower MW fractions was observed increasing the hydrolysis time. This stepwise effect was expected since TFA disrupts glycosidic bonds selectively, at different rates depending on the linked monosaccharide (Fengel & Wegener, 1979). For example, disruption of bonds from amino-sugars implies higher time of TFA hydrolysis, while pentoses are among the first monosaccharides to be released and even degraded under longer reaction times (> 2 h).

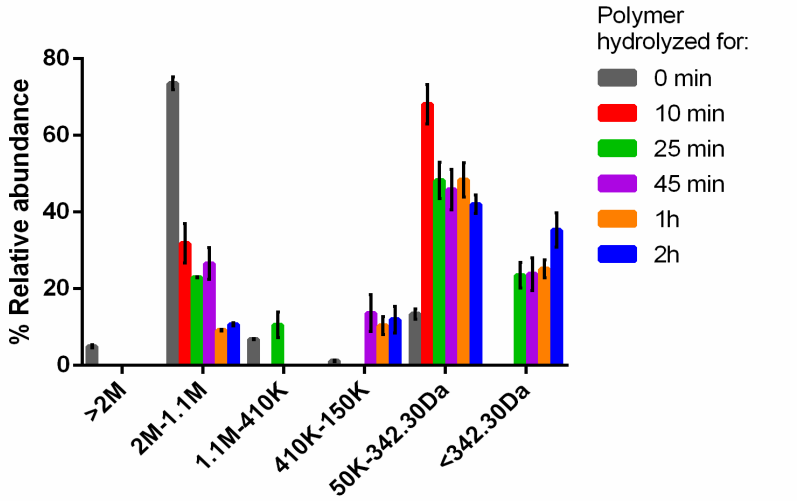

Figure 1. Modification of the molecular weight distribution of *Synechocystis* Δ*sigF* polymer after hydrolysis with TFA (from 10 min to 2 h). Measurements were made using size exclusion chromatography and results are represented as mean ± STD of three biological and three technical replicates.

Since previous studies associated the MW distribution of natural polysaccharides with their antitumor activity, the effect of the TFA hydrolyzed Δ*sigF* polymer is currently being evaluated on the viability of melanoma cell lines. So far, the two polymer variants tested (obtained after 25 min and 2 h of TFA hydrolysis) showed less pronounced antitumor activity compared to the original polymer. However, the decrease in polymer bioactivity could only be observed after 48 h of melanoma cell treatment, and not during the first 24 h (Fig. 2). Furthermore, the variant with lower abundance of high MW fractions (derived from polymer hydrolysis for 2 h), had the lowest bioactivity. These results indicate that the high MW fractions of Δ*sigF* polymer play a more important role in its antitumor activity.

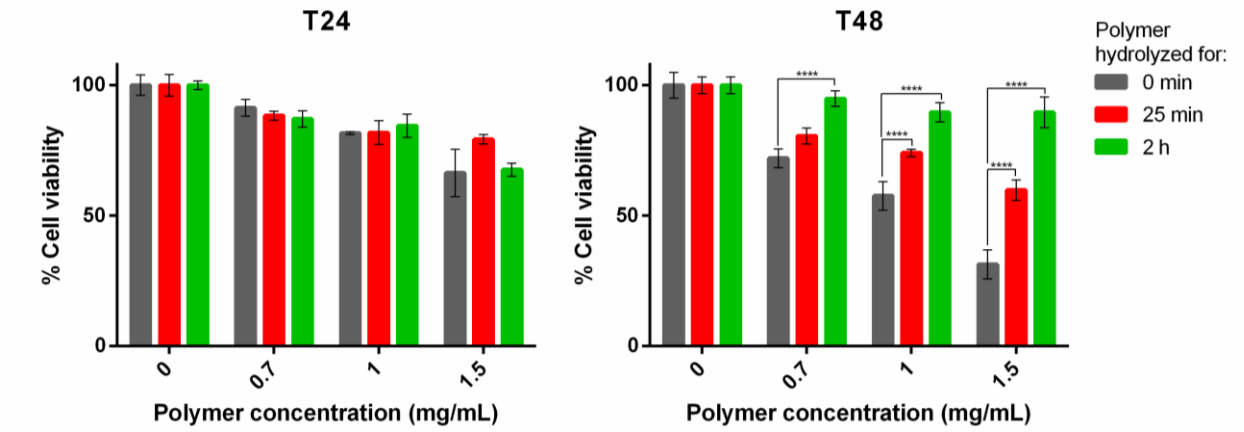

Figure 2. Effect of the *Synechocystis* Δ*sigF* polymer hydrolyzed with TFA on the viability of human melanoma (Mewo) cells, analyzed using PrestoBlue™ viability assay. Cells were treated with 0.7, 1 or 1.5 mg/mL of polymer for 24 or 48 hours (T24 and T48, respectively). Cells treated with polymer vehicle were used as controls, showing no differences to Blank (*data not shown*). Results are expressed in relation to Blank and are represented as mean ± STD of three independent experiments (**** $p \leq 0.0001$).

In agreement to our results, a previous study reported that the reduction of MW of a cyanobacterial EPS (from *Synechocystis aquatilis*) after TFA hydrolysis led to the loss of its bioactivity inhibiting the human complement system (Flamm & Blaschek, 2014b). Furthermore, recent studies showed that hydrolyzed algae polysaccharidic polymers, maintained or reduced their antitumor activity compared to the original polymer (Oliveira et al., 2017). Altogether, these findings contradict the perspective that polymer variants with lower MW fractions are expected to have higher antitumor activity, since they are easily internalized by the cells (Atashrazm et al., 2015; Kasai et al., 2015).

3.2. Molecular weight distribution and sulfate content of HCl hydrolyzed polymer and its antitumor activity

The MW distribution of the Δ*sigF* polymer was also modified using HCl hydrolysis, which led to the formation of polymer variants mainly composed by low MW fractions (<342.30 Da). Moreover, the polymer variants derived from 10, 25 and 45 min of hydrolysis presented a similar MW distribution, while the variants obtained after 1 or 2 h had a distinct one (Fig. 3). Altogether, these results indicate that the disruption of glycosidic bonds by HCl is extremely fast, and HCl has a stronger action than TFA in the hydrolysis of the high MW weight fractions. Nevertheless, both HCl and TFA hydrolysis allowed the development of polymer variants in a reliable and simple manner, being the acids easily evaporated afterwards.

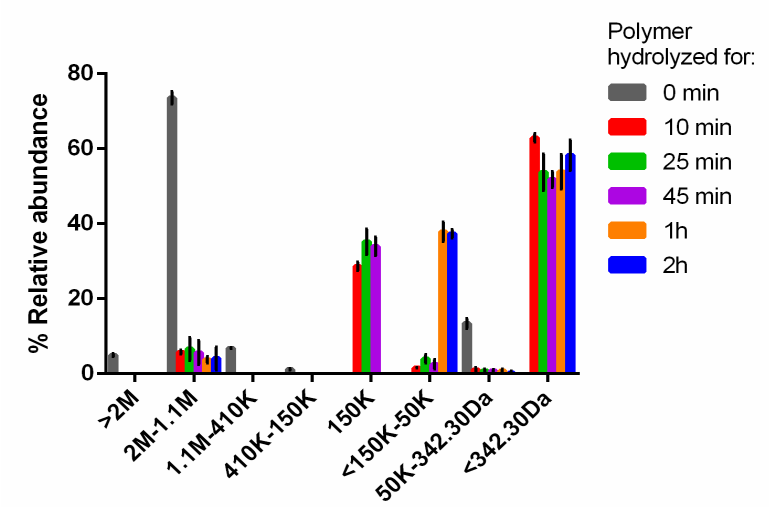

Figure 3. Modification of the molecular weight distribution of *Synechocystis* Δ*sigF* polymer after hydrolysis with HCl (from 10 min to 2 h). Measurements were made using size exclusion chromatography and results are represented as mean ± STD of three biological and three technical replicates.

The polymer variants obtained after HCl hydrolysis not only had alterations in their MW distribution, but had also different sulfate contents. In fact, this methodology was proven to be a valuable technique to obtain polymer variants with different degrees of desulfation in a reproducible way (Fig. 4), being the maximum of desulfation (100%) reached after 2 hours of hydrolysis. This is in agreement with the saturation point described for the HCl hydrolytic reaction at high temperatures using natural polysaccharides, which is frequently achieved after 2 / 3 hours (Dodgson & Price, 1962). At that point, it is expected that sulfate groups from all type of sugars have been released, from glucose, galactose or fucose, to uronic acids and amino-sugars. However, degradation of some sugars (e.g. uronic acids), alteration in the degree of polymerization and reduction of the polymer yield might also occur, as previously reported for natural polysaccharides hydrolyzed with HCl for long times (Takano, 2002; Dodgson & Price, 1962).

Although acid-catalyzed desulfation using HCl is widely used for determination of the sulfate content of polysaccharides due to the high speed of reaction and technical simplicity (Takano, 2002; Dodgson & Price, 1962), it is not frequently used to generate polymer variants with different desulfation degrees, due to the randomness of the process, and it has not been previously reported for cyanobacterial EPS.

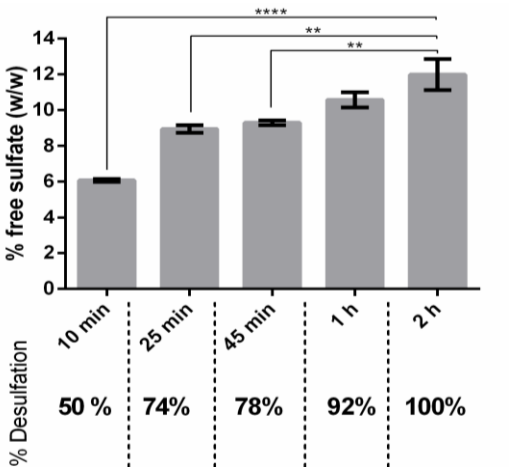

Figure 4. Quantification of the sulfate released from *Synechocystis* Δ*sigF* polymer after HCl hydrolysis (from 10 min to 2 h), and the respective percentage of desulfation obtained. Statistical analysis is presented in comparison to the maximum time of hydrolysis (** $p \leq 0.01$; **** $p \leq 0.0001$).

The Δ*sigF* polymer variants obtained after different times of HCl hydrolysis were also used in viability tests with human melanoma cell lines (Fig. 5). Similar to the results obtained using the TFA hydrolyzed polymer, all the variants derived from HCl hydrolysis had less antitumor activity compared to the original polymer. This could be observed during the first 24 h of cell treatment, although being more evident after 48 h of treatment. Since these variants have alterations in both MW and sulfate content, the contribution of each factor for polymer bioactivity cannot be distinguished.

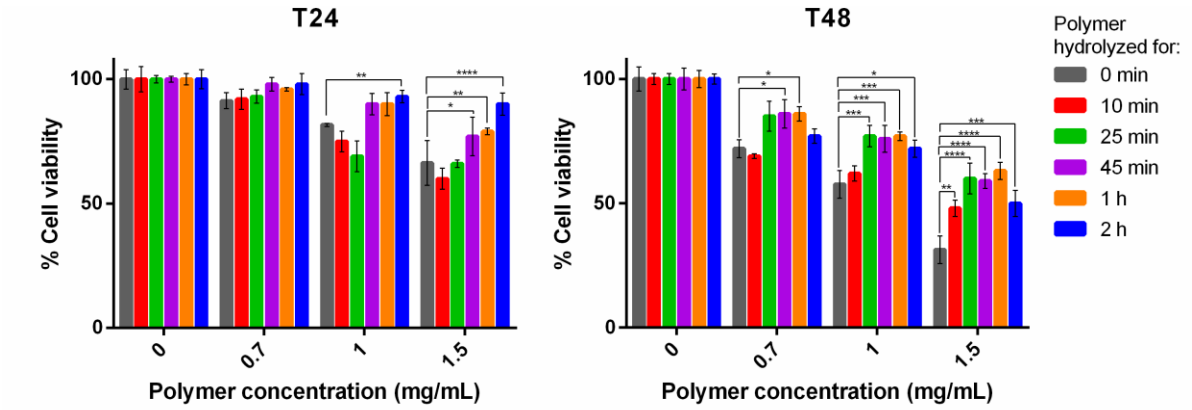

Figure 5. Effect of the *Synechocystis* Δ*sigF* polymer hydrolyzed with HCl on the viability of human melanoma (Mewo) cells, analyzed using PrestoBlue™ viability assay. Cells were treated with 0.7, 1 or 1.5 mg/mL of polymer for 24 or 48 hours (T24 and T48, respectively). Cells treated with polymer vehicle were used as controls, showing no differences to Blank (*data not shown*). Results are expressed in relation to Blank and are represented as mean ± STD of three independent experiments (* $p \leq 0.05$; ** $p \leq 0.01$; *** $p \leq 0.001$; **** $p \leq 0.0001$).

3.3. Desulfation of the polymer using solvolytic strategies

As desulfation under acidic conditions may cause several side effects in the polymer, we employed also different strategies of solvolytic desulfation (Table 1), which are not so deleterious for polymer structure and composition (Takano, 2002; Miller & Blunt, 1998). Three sets of optimal reaction conditions were used, as previously established for desulfation of polysaccharides from plants, animals and algae (Miller & Blunt, 1998; Nagasawa et al., 1979, 1977; Inoue & Nagasawa, 1976). In all cases, highly desulfated polymer variants were obtained (up to 79% of desulfation), and only in one situation desulfation was accompanied by alterations in the polymer MW distribution (see Table 1). These changes in MW distribution were observed for the Δ*sigF* polymer desulfated at 120 ºC, indicating that it has relatively low thermostability, which is not frequently observed for complex cyanobacterial polymers (Mota et al., 2013; Parikh & Madamwar, 2006). Melanoma cell viability tests using the polymer variants obtained after solvolysis (without MW alterations) are currently underway, which will allow us to discriminate the importance of each feature for polymer bioactivity.

Table 1. Desulfation of *Synechocystis* Δ*sigF* polymer using solvolytic strategies.

% water (in DMSO)	Temperature	Heating time	% Desulfation
5%	50 ºC	2 h	77%
10%	80 ºC	5 h	79%
10%	120 ºC	3 h	76%*

* Slight alterations in the molecular weight distribution were observed.

Being the high sulfate content of cyanobacterial EPS one of their most peculiar features, and frequently associated to different bioactivities (Chirasuwan et al., 2007; Lee et al., 2007), the simple solvolytic desulfation strategies presented here are of major importance to obtain tailor-made polymers with fined-tuned biological activities. For example, in our approaches, the complex step of conversion of the polymer into its pyridinium salt form prior to the reaction was not performed, in contrast to the conventional solvolytic desulfation methods described in the literature. This may explain the absence of completely desulfated polymers with the three solvolytic strategies used (Table 1), since carbohydrate-salt forms are expected to have higher solubility/stability in aprotic solvents, such as dimethyl sulfoxide (DMSO) or dimethyl formamide, and to optimize solvolysis (Usov et al., 1971). Moreover, the location of the sulfate groups in the Δ*sigF* polymer is still unknown, which may also influence the efficiency of the reaction. For example, *N*-sulfates are desulfated more efficiently than *O*-sulfates (Takano, 2002; Inoue & Nagasawa, 1976).

In the future, besides the formation of carbohydrate-salt forms, other alterations might be introduced in order to optimize the polymer solvolytic desulfation, such as the addition of methanol or water, that work as acceptors of sulfur trioxide derived from the sulfate groups. In fact, adding methanol to solvolysis allowed the successful desulfation of other cyanobacterial EPS, from *Arthrospira platensis* and *Phormidium* (Chirasuwan et al., 2007; Lee et al., 2007; Hayashi et al., 1996a, 1996b; Bar Or & Shilo, 1987). However, the high desulfation rates obtained were also accompanied by some side effects, such as the reduction of polymer MW and yield (Lee et al., 2007), or alterations in polymer components, such as carboxyl groups (Bar Or & Shilo, 1987). Moreover, a recent study using *Synechocystis aquatilis* EPS showed that solvolysis with the addition of methanol or water, led to massive polymer degradation and partial hydrolysis, causing a dramatic reduction of the polymer MW and yield, which hindered the sulfate quantification of the samples (Flamm & Blaschek, 2014a, 2014b). These authors could only desulfate the polymer efficiently (1.8% of residual sulfate) using a silylating agent, although accompanied by alterations in the linkage pattern of some fucose residues (Flamm & Blaschek, 2014b). However, desulfation using silylating agents are extremely complex and variable depending on the combination of polymer and reagent used (Takano, 2002), and therefore were not tried here.

4. Conclusions

Overall, the molecular weight distribution of *Synechocystis* Δ*sigF* polymer, namely the high molecular weight fractions, was shown to be important for its strong antitumor activity. Further studies are needed to unveil other key features that may be involved in polymer antitumor activity, such as the sulfate content or even the peptide fraction of the polymer.

5. References

Atashrazm, F., Lowenthal, R., Woods, G., Holloway, A., Dickinson, J., Atashrazm, F., et al. (2015). Fucoidan and Cancer: A Multifunctional Molecule with Anti-Tumor Potential. *Mar. Drugs* 13(4), 2327–2346.

Bar Or, Y., and Shilo, M. (1987). Characterization of macromolecular flocculants produced by *Phormidium* sp. strain J-1 and by *Anabaenopsis circularis* PCC 6720. *Appl. Environ. Microbiol.* 53(9), 2226–2230.

Chen, L., Rossi, F., Deng, S., Liu, Y., Wang, G., Adessi, A., et al. (2014). Macromolecular and chemical features of the excreted extracellular polysaccharides in induced biological soil crusts of different ages. *Soil Biol. Biochem.* 78, 1–9.

Chirasuwan, N., Chaiklahan, R., Ruengjitchatchawalya, M., Bunnag, B., and Tanticharoen, M. (2007). Anti HSV-1 activity of *Spirulina platensis* polysaccharide. *Kasetsart J. - Nat. Sci.* 41(2), 311–318.

Fengel, D., and Wegener, G. (1979). Hydrolysis of Polysaccharides with Trifluoroacetic Acid and its Application to Rapid Wood and Pulp Analysis. In *Hydrolysis of cellulose: mechanisms of enzymatic and acid catalysis* (Adv. Chem. Ser. No. 181 ACS), pp 145–158.

Flamm, D., and Blaschek, W. (2014a). A Sulfated Cyanobacterial Polysaccharide Proven as a Strong Inhibitor of Human Complement Activity in an In Vitro Assay. *Planta Med.* 80(12), 1009–1016.

Flamm, D., and Blaschek, W. (2014b). Exopolysaccharides of *Synechocystis aquatilis* are sulfated arabinofucans containing N-acetyl-fucosamine. *Carbohydr. Polym.* 101, 301–306.

Gacheva, G., Gigova, L., Ivanova, N., Iliev, I., Toshkova, R., Gardeva, E., et al. (2013). Suboptimal growth temperatures enhance the biological activity of cultured cyanobacterium *Gloeocapsa* sp. *J. Appl. Phycol.* 25(1), 183–194.

Hayashi, T., Hayashi, K., I Kojima - US Patent 5, 585,365, and 1996, undefined Antiviral polysaccharide. *Google Patents*.

Hayashi, K., Hayashi, T., and Kojima, I. (1996). A Natural Sulfated Polysaccharide, Calcium Spirulan, Isolated from *Spirulina platensis: In Vitro* and *Ex Vivo* Evaluation of Anti-Herpes Simplex Virus and Anti-Human Immunodeficiency Virus Activities. *AIDS Res. Hum. Retroviruses* 12(15), 1463–1471.

Inoue, Y., and Nagasawa, K. (1976). Selective N-desulfation of heparin with dimethyl sulfoxide containing water or methanol. *Carbohydr. Res.* 46(1), 87–95.

Kasai, A., Arafuka, S., Koshiba, N., Takahashi, D., and Toshima, K. (2015). Systematic synthesis of low-molecular weight fucoidan derivatives and their effect on cancer cells. *Org. Biomol. Chem.* 13(42), 10556–10568.

Lee, J.-B., Hou, X., Hayashi, K., and Hayashi, T. (2007). Effect of partial desulfation and oversulfation of sodium spirulan on the potency of anti-herpetic activities. *Carbohydr. Polym.* 69(4), 651–658.

Li, H., Su, L., Chen, S., Zhao, L., Wang, H., Ding, F., et al. (2018). Physicochemical Characterization and Functional Analysis of the Polysaccharide from the Edible Microalga *Nostoc sphaeroides*. *Molecules* 23(2), 508.

Miller, I.J., and Blunt, J.W. (1998). Desulfation of algal galactans. *Carbohydr. Res.* 309(1), 39–43.

Mishima, T., Murata, J., Toyoshima, M., Fujii, H., Nakajima, M., Hayashi, T., et al. (1998). Inhibition of tumor invasion and metastasis by calcium spirulan (Ca-SP), a novel sulfated polysaccharide derived from a blue-green alga, *Spirulina platensis*. *Clin. Exp. Metastasis* 16(6), 541–550.

Mota, R., Guimarães, R., Büttel, Z., Rossi, F., Colica, G., Silva, C.J., et al. (2013). Production and characterization of extracellular carbohydrate polymer from *Cyanothece* sp. CCY 0110. *Carbohydr. Polym.* 92(2), 1408–1415.

Nagasawa, K., Inoue, Y., and Kamata, T. (1977). Solvolytic desulfation of glycosaminoglycuronan sulfates with dimethyl sulfoxide containing water or methanol. *Carbohydr. Res.* 58(1), 47–55.

Oliveira, C., Ferreira, A.S., Novoa-carballal, R., Nunes, C., Pashkuleva, I., Neves, N.M., et al. (2016). The Key Role of Sulfation and Branching on Fucoidan Antitumor Activity. *Macromol. Biosci.* 17(5), 1–13.

Ou, Y., Xu, S., Zhu, D., and Yang, X. (2014). Molecular Mechanisms of Exopolysaccharide from *Aphanothece halaphytica* (EPSAH) Induced Apoptosis in HeLa Cells. *PLoS One* 9(1), e87223.

Parikh, A., and Madamwar, D. (2006). Partial characterization of extracellular polysaccharides from cyanobacteria. *Bioresour. Technol.* 97(15), 1822–1827.

Pópulo, H., Caldas, R., Lopes, J.M., Pardal, J., Máximo, V., and Soares, P. (2015). Overexpression of pyruvate dehydrogenase kinase supports dichloroacetate as a candidate for cutaneous melanoma therapy. *Expert Opin. Ther. Targets* 19(6), 733–745.

Schmid, J. (2018). Recent insights in microbial exopolysaccharide biosynthesis and engineering strategies. *Curr. Opin. Biotechnol.* 53, 130–136.

Takano, R. (2002). Desulfation of Sulfated Carbohydrates. *Trends Glycosci. Glycotechnol.* 14(80), 343–351.

Usov, A.I., Adamyants, K.S., Miroshnikova, L.I., Shaposhnikova, A.A., and Kochetkov, N.K. (1971). Solvolytic desulphation of sulphated carbohydrates. *Carbohydr. Res.* 18(2), 336–338.

Yue, S.J., Jia, S.R., Yao, J., and Dai, Y.J. (2011). Nutritional Analysis of the Wild and Liquid Suspension Cultured *Nostoc flagelliforme* and Antitumor Effects of the Extracellular Polysaccharides. *Adv. Mater. Res.* 345, 177–182.

Zong, A., Cao, H., and Wang, F. (2012). Anticancer polysaccharides from natural resources: A review of recent research. *Carbohydr. Polym.* 90(4), 1395–1410.

CHAPTER VII

Final Remarks

Final Remarks

This work contributes to a better knowledge on the mechanisms underlying EPS production in cyanobacteria, as well as on the polymers produced and their action as antitumor agents.

1. Putative key players in *Synechocystis* EPS production and in its regulation

Recent studies have reported that cyanobacterial EPS production relies on more complex mechanisms than those described for other bacteria (Pereira et al., 2015; 2013). Using *Synechocystis* sp. PCC 6803 as model organism, our extensive *in silico* analysis together with experimental data from the characterization of knockout mutants, not only supported these previous works, but also revealed promising candidate genes/proteins for further studies (Chapter II). Although several homologs of the genes involved in the 3 main bacterial EPS assembly/export pathways (EPS-related genes) were found in *Synechocystis* (Pereira et al., 2013), 9 of them are expected to play a more prominent role in EPS production (Chapter II). In agreement, a few studies showed that the knockout of some of these 9 genes affected EPS production, such as *sll1581* (*wza*/*kpsD*), *sll0923* (*wzc*/*kpsE*), *slr0982* (*kpsT*), *slr0977* (*kpsM*) and *slr1875* (*exoD*) (Pereira et al., 2019; Fisher et al., 2013; Jittawuttipoka et al., 2013a), while there is still no information available for the others, *slr1074* (*wzy*), *sll0575* (*kpsT*), *sll0574* (*kpsM*) and *sll1377* (*alg8*). The remaining 22 putative EPS-related genes may play a redundant role or be associated to the production of specific types of polysaccharides (e.g. O-antigen of LPS), such as *slr2115* (*kpsC*/*kpsS*), *slr2122* (*kpsU*) and *slr2111* (*kpsF*), or may even not be involved in EPS production, e.g. *slr0067* (*wzc*/*kpsE*) and *slr0946* (*wzb*) (Chapter II). From the *in silico* analyses, genes encoding carbohydrate activation/modification proteins emerged also as key players in *Synechocystis* EPS biosynthesis (Chapter II). More importantly, 3 EPS-related gene clusters were identified (2 in the chromosome and 1 in the plasmid pSYSM), containing a higher diversity of genes encoding this type of enzymes compared to what is usually found in other bacteria (Schmid et al., 2015a). Moreover, a total of 103 enzymes that can create, degrade or modify glycosidic bonds in *Synechocystis* polysaccharidic polymers were found, with the predominance of glycosyltransferases, followed by glycosyl hydrolases, and some carbohydrate esterases and carbohydrate-binding modules proteins. Remarkably, although the presence of uronic acids was previously described in *Synechocystis* EPS (Pereira et al., 2019; Miranda et al., 2017; Panoff et al., 1988), no polysaccharide lyases capable of degrading uronic acids glycosidic bonds were found in this cyanobacterium.

As observed for other bacterial strains (Schmid et al., 2015), our results also suggested that transcriptional regulation is an important step in the control of EPS production in *Synechocystis*, namely through the action of particular types of global transcriptional regulators (e.g. sigma factors, LexA and Crp). In agreement, the only cyanobacterial regulators previously associated to EPS production were the global transcriptional factors, SigJ and NtcA, in *Anabaena* sp. (López-Igual et al., 2012; Yoshimura et al., 2012). Nevertheless, further experimental studies are needed to reveal the impact of the putative *Synechocystis* EPS-related genes/proteins and regulators in EPS production.

2. Sigma factor F is a key regulator of *Synechocystis* EPS production and other secretion mechanisms

According to the *in silico* analysis presented in Chapter II and in agreement with the information available in the literature, RNA polymerase sigma factors are promising masterpieces in the control of EPS production in cyanobacteria. Since the *Synechocystis* Group 3 sigma factor SigF is the most similar protein to the only sigma factor associated to cyanobacterial EPS production, the *Anabaena'*s SigJ, the characterization of a knockout mutant on its encoding gene was carried out (Chapter III, Flores et al., 2019a). The results obtained showed that SigF is a key player in EPS biosynthesis, namely in the production of released polysaccharides (RPS), which is up to 4-fold higher in *Synechocystis* Δ*sigF* compared to the wild-type. Carbon and energy resources seem to be redirected to EPS production in this mutant, similarly to what occurs in other *Synechocystis* mutants that overproduce carbon-rich polymers (Carpine et al., 2017; Yoo et al., 2007). Moreover, the changes observed in the levels of proteins involved in carbohydrate metabolism and polysaccharide modification, as well as the presence of SigF binding motifs in some of their encoding genes, highlighted possible targets of this sigma factor and molecular players that may operate in EPS production (Chapter III, Flores et al., 2019a).

SigF was also shown to be involved in the control of other secretion pathways, both classical/transporter-mediated (e.g. protein secretion, pilin export) and non-classical (through vesiculation), which play an essential role in the cell envelope maintenance and cell acclimation to the environment (Chapter III, Flores et al., 2019a). Furthermore, *Synechocystis* Δ*sigF* displayed a conspicuous cell clumping phenotype, probably related to a mechanism of cell self-shading, as previously described for other *Synechocystis* mutants (Miranda et al., 2017).

3. *Synechocystis* Δ*sigF* mutant is a promising platform for the production of bioactive polymer(s)

The *Synechocystis* Δ*sigF* clumping phenotype and its fast spontaneous cell sedimentation, the fastest reported so far for a *Synechocystis* strain (Chapter III, Flores et al., 2019a), are particular interesting in terms of biotechnological application, since they facilitate the harvesting of biomass and recovery of secreted products (Depraetere et al., 2015). Therefore, and since *Synechocystis* Δ*sigF* is an efficient RPS overproducer, this mutant was used to optimize the isolation method of the polymer produced (Chapter IV, Flores & Tamagnini, 2019). This method allowed to obtain approximately 80 mg of polymer per g of Δ*sigF* culture dry-weight (≈2 mg/L/day), which is 4-fold higher than the wild-type polymer yield and the highest polymer yield reported for this genus (Chapter V, Flores et al., 2019b).

Both wild-type and Δ*sigF* isolated polymers have particular features that make them very attractive for biotechnological applications, such as the presence of amino-sugars and uronic acids, peptides, sulfate and other functional groups, high molecular mass fractions, and a non-Newtonian rheological behavior (Chapter V, Flores et al., 2019b). Moreover, they are easily dissolved in water, allowing highly concentrated solutions with low viscosity. However, there are some differences between the two polymers, e.g. the Δ*sigF* polymer has two uronic acids (in contrast with the one detected in the wild-type) and a higher peptide content. This last feature is probably related to the differences in protein secretion observed between the mutant and wild-type (Chapter III, Flores et al., 2019a). Since some of the features abovementioned were previously described as key factors for the interaction between polysaccharidic polymers and cells (e.g. with eukaryotic cell receptors) (Khan et al., 2019; Moscovici, 2015), the wild-type and Δ*sigF* polymers were tested towards different human tumor cell lines (melanoma, thyroid and ovarian carcinomas). Both polymers strongly reduced tumor cell viability in a dose- and time-dependent manner, being this effect more accentuated in cells treated with Δ*sigF* polymer (Chapter V, Flores et al., 2019b). In contrast, none of the polymers significantly decreased the viability of a non-tumor human thyroid cell line.

4. *Synechocystis* Δ*sigF* polymer as potent antitumor agent

As a strong effect on the human tumor cell viability was observed using the Δ*sigF* polymer, we pursued the study of the molecular mechanisms underlying its bioactivity. Our results revealed that after treatment with this polymer, the levels of apoptosis of the melanoma cell line dramatically increased (Chapter V, Flores et al., 2019b). Additionally, a minimal impact on its cell cycle was also detected, with a higher number of cells found in

the sub-G1 peak, which is also indicative of cells undergoing apoptosis (Riccardi & Nicoletti, 2006). The apoptotic rates induced by Δ*sigF* polymer (≈40%) are among the highest described for natural polysaccharides, even compared to polymers isolated from eukaryotic sources (Chapter V, Flores et al., 2019b).

A few studies mostly based on cell viability/growth assays have reported cyanobacterial EPS with antitumor activity (Table S1), however, without explaining the mechanism of action. In contrast, we showed that the potent Δ*sigF* polymer bioactivity relies on the stimulation of the mitochondrial-mediated apoptotic pathway (Chapter V, Flores et al., 2019b). This polymer triggers a signaling apoptotic pathway mediated by the tumor suppressor protein p53, that culminates with the activation of caspase-3, similarly to the mechanism proposed for the antitumor activity of the cyanobacterial EPS from *Aphanothece halophytica* (Ou et al., 2014), and for some polysaccharides from macroalgae (Jose et al., 2018; Wang et al., 2014).

5. Unveiling the properties underlying Δ*sigF* polymer antitumor activity

In order to unveil some of the Δ*sigF* polymer features that might be responsible for its potent antitumor activity, its molecular weight (MW) and sulfate content were successfully manipulated and the polymer variants obtained were tested towards human tumor cell lines (Chapter VI). The molecular weight of the Δ*sigF* polymer was modified through TFA hydrolysis. Overall, increasing the hydrolysis time resulted in an increase in the abundance of low MW fractions, and a decrease in the antitumor activity of the polymer variants. This indicates that high MW fractions are very important for Δ*sigF* polymer bioactivity, contradicting the conventional perception that lower MW fractions from polysaccharidic polymers have enhanced antitumor activity (Atashrazm et al., 2015; Kasai et al., 2015).

To modify the sulfate content, chemical desulfation of the Δ*sigF* polymer was performed using either HCl hydrolysis or solvolysis. Completely desulfated polymer variants were obtained only in the case of acidic hydrolysis, but it was accompanied by changes in the MW distribution. Once more, these polymer variants demonstrated lower antitumor activity compared to the original polymer. The evaluation of the antitumor activity of highly desulfated polymer variants obtained by solvolysis (without MW alterations) is currently underway. This will allow to fully understand the impact of the sulfate groups in the reduction of human tumor cell viability.

The polymer manipulation methodologies implemented here represent straightforward strategies for the creation of tailor-made cyanobacterial EPS in a reproducible way (Chapter VI), responding to the current demand for natural polymers that could be easily customized to fulfil specific biotechnological needs.

6. Future Perspectives

This work unveiled crucial aspects of cyanobacterial EPS production and about the antitumor activity of the produced polymers, but several other questions emerged and other paths are still waiting to be explored, such as the:

i) Experimental validation of the several putative EPS-related key players and respective redundant partners, e.g. generating mutants with multiple EPS-related genes repressed, using CRISPRi.

ii) Unveiling of SigF specific targets and the regulatory network underlying *Synechocystis* secretion mechanisms, e.g. through the overexpression and purification of *Synechocytis* SigF followed by CHIP-Seq.

iii) Assessment of the environmental factors that affect *Synechocystis* EPS production and the properties of the produced polymers.

iv) Fine-tuning of the amount of sulfate in the polymer, through optimization of polymer oversulfation and desulfation techniques, as well as the study and manipulation of the putative carbohydrate sulfotransferases identified in *Synechocystis*.

v) Manipulation of other polymer features (e.g. peptides, uronic acids, amino-sugars, structure).

vi) Recovery and characterization of the different *Synechocystis* polymer fractions (e.g. using HPLC), and evaluation of their specific antitumor activity.

vii) Evaluation *in vivo* of the antitumor activity of the *Synechocystis* polymers.

7. References

Angelis, S., Novak, A.C., Sydney, E.B., Soccol, V.T., Carvalho, J.C., Pandey, A., et al. (2012). Co-Culture of Microalgae, Cyanobacteria, and Macromycetes for Exopolysaccharides Production: Process Preliminary Optimization and Partial Characterization. *Appl. Biochem. Biotechnol.* 167(5), 1092–1106.

Archibald, J.M. (2009). The Puzzle of Plastid Evolution. *Curr. Biol.* 19(2), 81–88.

Arunkumar, M., Divya, S., Lewisoscar, F., Thajuddin, N., and Nithya, C. (2018). Cyanobacterial exopolysaccharides: A potent antibiofilm agent against *Pseudomonas aeruginosa*. *Int. J. Res. Anal. Ver.* 5(4), 31-38.

Atashrazm, F., Lowenthal, R., Woods, G., Holloway, A., Dickinson, J., Atashrazm, F., et al. (2015). Fucoidan and Cancer: A Multifunctional Molecule with Anti-Tumor Potential. *Mar. Drugs* 13(4), 2327–2346.

Bemal, S., and Anil, A.C. (2018). Effects of salinity on cellular growth and exopolysaccharide production of freshwater *Synechococcus* strain CCAP1405. *J. Plankton Res.* 40(1), 46–58.

Bhatnagar, M., Parwani, L., Sharma, V., Ganguly, J., and Bhatnagar, A. (2014). Exopolymers from *Tolypothrix tenuis* and three *Anabaena* sp. (Cyanobacteriaceae) as novel blood clotting agents for wound management. *Carbohydr. Polym.* 99, 692–699.

Borowitzka, M.A. (2013). Patents on cyanobacteria and cyanobacterial products and uses. In *Cyanobacteria* (Chichester, UK: John Wiley & Sons, Ltd), pp. 329–338.

Branco dos Santos, F., Du, W., and Hellingwerf, K.J. (2016). *Synechocystis*: not just a plug-bug for CO_2, but a green *E. coli*. *Front. Bioeng. Biotechnol.* 2, 36.

Brito, Â., Gaifem, J., Ramos, V., Glukhov, E., Dorrestein, P.C., Gerwick, W.H., et al. (2015). Bioprospecting Portuguese Atlantic coast cyanobacteria for bioactive secondary metabolites reveals untapped chemodiversity. *Algal Res.* 9, 218–226.

Brull, L.P., Huang, Z., Thomas-Oates, J.E., Paulsen, B.S., Cohen, E.H., and Michaelsen, T.E. (2000). Studies Of Polysaccharides From Three Edible Species Of *Nostoc* (Cyanobacteria) With Different Colony Morphologies: Structural Characterization And Effect On The Complement System Of Polysaccharides From *Nostoc Commune*. *J. Phycol.* 36(5), 871–881.

Cade-Menun, B.J., and Paytan, A. (2010). Nutrient temperature and light stress alter phosphorus and carbon forms in culture-grown algae. *Mar. Chem.* 121(1–4), 27–36.

Canfield, D.E., Glazer, A.N., and Falkowski, P.G. (2010). The evolution and future of Earth's nitrogen cycle. *Science* 330(6001), 192–196.

Carpine, R., Du, W., Olivieri, G., Pollio, A., Hellingwerf, K.J., Marzocchella, A., et al. (2017). Genetic engineering of *Synechocystis* sp. PCC6803 for poly-β-hydroxybutyrate overproduction. *Algal Res.* 25, 117–127.

Carroll, A.L., Case, A.E., Zhang, A., and Atsumi, S. (2018). Metabolic engineering tools in model cyanobacteria. *Metab. Eng.* 50, 47–56.

Castenholz, R.W., Wilmotte, A., Herdman, M., Rippka, R., Waterbury, J.B., Iteman, I., et al. (2001). Phylum BX. Cyanobacteria. In *Bergey's Manual of Systematic Bacteriology* (New York, NY: Springer New York), pp. 473–599.

Challouf, R., Trabelsi, L., Ben Dhieb, R., El Abed, O., Yahia, A., Ghozzi, K., et al. (2011). Evaluation of cytotoxicity and biological activities in extracellular polysaccharides released by cyanobacterium *Arthrospira platensis*. *Brazilian Arch. Biol. Technol.* 54(4), 831–838.

Chentir, I., Hamdi, M., Doumandji, A., HadjSadok, A., Ouada, H. Ben, and Nasri, M. (2017). Enhancement of extracellular polymeric substances (EPS) production in *Spirulina* (*Arthrospira* sp.) by two-step cultivation process and partial characterization of their polysaccharidic moiety. *Int. J. Biol. Macromol.* 105, 1412–1420.

Choi, K.Y., Min, K.H., Na, J.H., Choi, K., Kim, K., Park, J.H., et al. (2009). Self-assembled hyaluronic acid nanoparticles as a potential drug carrier for cancer therapy: synthesis, characterization, and in vivo biodistribution. *J. Mater. Chem.* 19(24), 4102-4107.

Collins, R.F., Beis, K., Dong, C., Botting, C.H., McDonnell, C., Ford, R.C., et al. (2007). The 3D structure of a periplasm-spanning platform required for assembly of group 1 capsular polysaccharides in *Escherichia coli*. *Proc. Natl. Acad. Sci.* 104(7), 2390–2395.

Cragg, G.M., and Newman, D.J. (2018). Natural Products as Sources of Anticancer Agents: Current Approaches and Perspectives. In *Natural Products as Source of Molecules with Therapeutic Potential* (Cham: Springer International Publishing), pp. 309–331.

Cuthbertson, L., Mainprize, I.L., Naismith, J.H., and Whitfield, C. (2009). Pivotal roles of the outer membrane polysaccharide export and polysaccharide copolymerase protein families in export of

extracellular polysaccharides in gram-negative bacteria. *Microbiol. Mol. Biol. Rev.* 73(1), 155–177.
Cuthbertson, L., Kos, V., and Whitfield, C. (2010). ABC transporters involved in export of cell surface glycoconjugates. *Microbiol. Mol. Biol. Rev.* 74(3), 341–362.
D'Arrigo, G., Navarro, G., Di Meo, C., Matricardi, P., and Torchilin, V. (2014). Gellan gum nanohydrogel containing anti-inflammatory and anti-cancer drugs: a multi-drug delivery system for a combination therapy in cancer treatment. *Eur. J. Pharm. Biopharm.* 87(1), 208–216.
Depraetere, O., Pierre, G., Deschoenmaeker, F., Badri, H., Foubert, I., Leys, N., et al. (2015). Harvesting carbohydrate-rich *Arthrospira platensis* by spontaneous settling. *Bioresour. Technol.* 180, 16–21.
Deschoenmaeker, F., Markou, G., Badri, H., Pierre, G., Wattiez, R., Michaud, P., et al. (2014). Harvesting carbohydrate-rich *Arthrospira platensis* by spontaneous settling. *Bioresour. Technol.* 180, 16–21.
Díez-Municio, M., Rivas, B. de las, Jimeno, M.L., Muñoz, R., Moreno, F.J., and Herrero, M. (2013). Enzymatic Synthesis and Characterization of Fructooligosaccharides and Novel Maltosylfructosides by Inulosucrase from *Lactobacillus gasseri* DSM 20604. *Appl. Environ. Microbiol.* 79(13), 4129–4140.
Dittmann, E., Gugger, M., Sivonen, K., and Fewer, D.P. (2015). Natural Product Biosynthetic Diversity and Comparative Genomics of the Cyanobacteria. *Trends Microbiol.* 23(10), 642–652.
Donot, F., Fontana, A., Baccou, J.C., and Schorr-Galindo, S. (2012). Microbial exopolysaccharides: Main examples of synthesis, excretion, genetics and extraction. *Carbohydr. Polym.* 87(2), 951–962.
Dyall, S.D., Brown, M.T., and Johnson, P.J. (2004). Ancient invasions: from endosymbionts to organelles. *Science* 304(5668), 253–257.
Ehling-Schulz, M., Bilger, W., and Scherer, S. (1997). UV-B-induced synthesis of photoprotective pigments and extracellular polysaccharides in the terrestrial cyanobacterium *Nostoc commune*. *J. Bacteriol.* 179(6), 1940–1945.
Estevinho, B.N., Mota, R., Leite, J.P., Tamagnini, P., Gales, L., and Rocha, F. (2019). Application of a cyanobacterial extracellular polymeric substance in the microencapsulation of vitamin B12. *Powder Technol.* 343, 644–651.
Fisher, M.L., Allen, R., Luo, Y., and Iii, R.C. (2013). Export of Extracellular Polysaccharides Modulates Adherence of the Cyanobacterium *Synechocystis*. *PloS one* 8(9), e74514.
Flamm, D., and Blaschek, W. (2014). Exopolysaccharides of *Synechocystis aquatilis* are sulfated arabinofucans containing N-acetyl-fucosamine. *Carbohydr. Polym.* 101, 301–306.
Flemming, H.-C. (2016). EPS—Then and Now. *Microorganisms* 4(4), 41.
Flemming, H.C., and Wingender, J. (2010). The biofilm matrix. *Nat. Rev. Microbiol.* 8(9), 623–633.
Freitas, F., Alves, V.D., and Reis, M.A.M. (2011). Advances in bacterial exopolysaccharides: From production to biotechnological applications. *Trends Biotechnol.* 29(8), 388–398.
Gacheva, G., Gigova, L., Ivanova, N., Iliev, I., Toshkova, R., Gardeva, E., et al. (2013). Suboptimal growth temperatures enhance the biological activity of cultured cyanobacterium *Gloeocapsa* sp. *J. Appl. Phycol.* 25(1), 183–194.
Galloway, J.N., Dentener, F.J., Capone, D.G., Boyer, E.W., Howarth, R.W., Seitzinger, S.P., et al. (2004). Nitrogen cycles: past, present, and future. *Biogeochemistry* 70(2), 153-226.
Gao, F., Li, L., Zhang, H., Yang, W., Chen, H., Zhou, J., et al. (2010). Deoxycholic acid modified-carboxymethyl curdlan conjugate as a novel carrier of epirubicin: *In vitro* and *in vivo* studies. *Int. J. Pharm.* 392(1–2), 254–260.
Gao, Y., Cheng, X., Wang, Z., Wang, J., Gao, T., Li, P., et al. (2014). Transdermal delivery of 10,11-methylenedioxycamptothecin by hyaluronic acid based nanoemulsion for inhibition of keloid fibroblast. *Carbohydr. Polym.* 112, 376–386.
Garbacki, N., Gloaguen, V., Damas, J., Hoffmann, L., Tits, M., and Angenot, L. (2000). Inhibition of croton oil-induced oedema in mice ear skin by capsular polysaccharides from Cyanobacteria. *Naunyn. Schmiedebergs. Arch. Pharmacol.* 361(4), 460–464.
Garozzo, D., Impallomeni, G., Spina, E., and Sturiale, L. (1998). The structure of the exocellular polysaccharide from the cyanobacterium *Cyanospira capsulata*. *Carbohydr. Res.* 307(1–2), 113–124.
Gloaguen, V., Morvan, H., Hoffmann, L., Plancke, Y., Wieruszeski, J.-M., Lippens, G., et al. (1999). Capsular polysaccharide produced by the thermophilic cyanobacterium *Mastigocladus laminosus*. *Eur. J. Biochem.* 266(3), 762–770.
Gunn, J.S., Bakaletz, L.O., and Wozniak, D.J. (2016). What's on the Outside Matters: The Role of the Extracellular Polymeric Substance of Gram-negative Biofilms in Evading Host Immunity and as

a Target for Therapeutic Intervention. *J. Biol. Chem.* 291(24), 12538–12546.
Hagemann, M., and Hess, W.R. (2018). Systems and synthetic biology for the biotechnological application of cyanobacteria. *Curr. Opin. Biotechnol.* 49, 94–99.
Han, P., Sun, Y., Jia, S., Zhong, C., and Tan, Z. (2014a). Effects of light wavelengths on extracellular and capsular polysaccharide production by *Nostoc flagelliforme*. *Carbohydr. Polym.* 105, 145–151.
Han, P., Sun, Y., Wu, X., Yuan, Y., Dai, Y., and Jia, S. (2014b). Emulsifying, Flocculating, and Physicochemical Properties of Exopolysaccharide Produced by Cyanobacterium *Nostoc flagelliforme*. *Appl. Biochem. Biotechnol.* 172(1), 36–49.
Han, P., Shen, S., Wang, H.-Y., Sun, Y., Dai, Y., and Jia, S. (2015). Comparative metabolomic analysis of the effects of light quality on polysaccharide production of cyanobacterium *Nostoc flagelliforme*. *Algal Res.* 9, 143–150.
Hartwell, J., Shear, M., Adams, J., and Perrault, A. (1943). Chemical Treatment of Tumors. VII. Nature of the Hemorrhage-Producing Fraction From *Serratia marcescens* (*Bacillus prodigiosus*) Culture Filtrate. *J. Natl. Cancer Inst.* 4(1), 107-122.
Hayakawa, Y., Hayashi, T., Hayashi, K., Hayashi, T., Ozawa, T., Niiya, K., et al. (1996). Heparin cofactor II-dependent antithrombin activity of calcium spirulan. *Blood Coagul. Fibrinolysis* 7(5), 554–560.
Hayakawa, Y., Hayashi, T., Hayashi, K., Ozawa, T., Niiya, K., and Sakuragawa, N. (1997). Calcium spirulan as an inducer of tissue-type plasminogen activator in human fetal lung fibroblasts. *Biochim. Biophys. Acta - Mol. Cell Res.* 1355(3), 241–247.
Hayakawa, Y., Hayashi, T., Lee, J.B., Ozawa, T., and Sakuragawa, N. (2000). Activation of heparin cofactor II by calcium spirulan. *J. Biol. Chem.* 275(15), 11379–11382.
Hayashi, O., Ono, S., Ishii, K., Shi, Y., Hirahashi, T., and Katoh, T. (2006). Enhancement of proliferation and differentiation in bone marrow hematopoietic cells by *Spirulina* (*Arthrospira*) platensis in mice. *J. Appl. Phycol.* 18(1), 47–56.
Hayashi, T., Hayashi, K., & Kojima, I. (1996). *U.S. Patent No. 5,585,365*. Washington, DC: U.S. Patent and Trademark Office.
Hayashi, K., Hayashi, T., and Kojima, I. (1996). A Natural Sulfated Polysaccharide, Calcium Spirulan, Isolated from *Spirulina platensis: In Vitro* and *ex Vivo* Evaluation of Anti-Herpes Simplex Virus and Anti-Human Immunodeficiency Virus Activities. *AIDS Res. Hum. Retroviruses* 12(15), 1463–1471.
Hays, S.G., and Ducat, D.C. (2015). Engineering cyanobacteria as photosynthetic feedstock factories. *Photosynth. Res.* 123(3), 285–295.
Helm, R.F., Huang, Z., Edwards, D., Leeson, H., Peery, W., and Potts, M. (2000). Structural characterization of the released polysaccharide of desiccation-tolerant *Nostoc commune* DRH-1. *J. Bacteriol.* 182(4), 974–982.
Hernández-Corona, A., Nieves, I., Meckes, M., Chamorro, G., and Barron, B.L. (2002). Antiviral activity of *Spirulina maxima* against herpes simplex virus type 2. *Antiviral Res.* 56(3), 279–285.
Huang, G., Fan, Q., Lechno-Yossef, S., Wojciuch, E., Wolk, C.P., Kaneko, T., et al. (2005). Clustered genes required for the synthesis of heterocyst envelope polysaccharide in *Anabaena* sp. strain PCC 7120. *J. Bacteriol.* 187(3), 1114–1123.
Huang, W.-J., Lai, C.-H., and Cheng, Y.-L. (2007). Evaluation of extracellular products and mutagenicity in cyanobacteria cultures separated from a eutrophic reservoir. *Sci. Total Environ.* 377(2–3), 214–223.
Imamura, S., and Asayama, M. (2009). Sigma factors for cyanobacterial transcription. *Gene Regul. Syst. Bio.* 3, 65–87.
Islam, S.T., and Lam, J.S. (2013). Wzx flippase-mediated membrane translocation of sugar polymer precursors in bacteria. *Environ. Microbiol.* 15(4), 1001–1015.
Jindal, N., Pal Singh, D., and Singh Khattar, J. (2013). Optimization, characterization, and flow properties of exopolysaccharides produced by the cyanobacterium *Lyngbya stagnina*. *J. Basic Microbiol.* 53(11), 902–912.
Jittawuttipoka, T., Planchon, M., Spalla, O., Benzerara, K., Guyot, F., Cassier-Chauvat, C., et al. (2013). Multidisciplinary Evidences that *Synechocystis* PCC6803 Exopolysaccharides Operate in Cell Sedimentation and Protection against Salt and Metal Stresses. *PLoS One* 8(2), e55564.
Jose, G.M., Raghavankutty, M., and Kurup, G.M. (2018). Sulfated polysaccharides from *Padina tetrastromatica* induce apoptosis in HeLa cells through ROS triggered mitochondrial pathway. *Process Biochem.* 68, 197–204.
Kaji, T., Shimada, S., Yamamoto, C., Fujiwara, Y., Jung-Bum, L., and Hayashi, T. (2002). Inhibition of the Association of Proteoglycans with Cultured Vascular Endothelial Cell Layers by Calcium and Sodium Spirulan. *J. Heal. Sci.* 48(3), 250–255.

Kawaharada, Y., Kelly, S., Nielsen, M.W., Hjuler, C.T., Gysel, K., Muszyński, A., et al. (2015). Receptor-mediated exopolysaccharide perception controls bacterial infection. *Nature* 523(7560), 308–312.

Kanekiyo, K., Lee, J.B., Hayashi, K., Takenaka, H., Hayakawa, Y., Endo, S., and Hayashi, T. (2005). Isolation of an Antiviral Polysaccharide, Nostoflan, from a Terrestrial Cyanobacterium, *Nostoc flagelliforme*. *J. Nat. Prod.* 68(7), 1037-1041.

Kasai, A., Arafuka, S., Koshiba, N., Takahashi, D., and Toshima, K. (2015). Systematic synthesis of low-molecular weight fucoidan derivatives and their effect on cancer cells. *Org. Biomol. Chem.* 13(42), 10556–10568.

Kehr, J.-C., and Dittmann, E. (2015). Biosynthesis and Function of Extracellular Glycans in Cyanobacteria. *Life* 5(1), 164–180.

Khan, T., Date, A., Chawda, H., and Patel, K. (2019). Polysaccharides as potential anticancer agents—A review of their progress. *Carbohydr. Polym.* 210, 412–428.

Khattar, J.I.S., Singh, D.P., Jindal, N., Kaur, N., Singh, Y., Rahi, P., et al. (2010). Isolation and Characterization of Exopolysaccharides Produced by the *Cyanobacterium Limnothrix* redekei PUPCCC 116. *Appl. Biochem. Biotechnol.* 162(5), 1327–1338.

Khayatan, B., Meeks, J.C., and Risser, D.D. (2015). Evidence that a modified type IV pilus-like system powers gliding motility and polysaccharide secretion in filamentous cyanobacteria. *Mol. Microbiol.* 98(6), 1021–1036.

Klemm, L.C., Czerwonka, E., Hall, M.L., Williams, P.G., and Mayer, A.M.S. (2018). Cyanobacteria *Scytonema javanicum* and *Scytonema ocellatum* Lipopolysaccharides Elicit Release of Superoxide Anion, Matrix-Metalloproteinase-9, Cytokines and Chemokines by Rat Microglia *In Vitro*. *Toxins* 10(4), 130.

Knoot, C.J., Ungerer, J., Wangikar, P.P., and Pakrasi, H.B. (2018). Cyanobacteria: Promising biocatalysts for sustainable chemical production. *J. Biol. Chem.* 293(14), 5044–5052.

Koop, H.S., de Freitas, R.A., de Souza, M.M., Savi-Jr., R., and Silveira, J.L.M. (2015). Topical curcumin-loaded hydrogels obtained using galactomannan from *Schizolobium parahybae* and xanthan. *Carbohydr. Polym.* 116, 229–236.

Kurd, F., and Samavati, V. (2015). Water soluble polysaccharides from *Spirulina platensis*: Extraction and *in vitro* anti-cancer activity. *Int. J. Biol. Macromol.* 74, 498–506.

Lama, L., Nicolaus, B., Calandrelli, V., Manca, M.C., Romano, I., and Gambacorta, A. (1996). Effect of growth conditions on endo- and exopolymer biosynthesis in *Anabaena cylindrica* 10 C. *Phytochemistry* 42(3), 655–659.

Leite, J.P., Mota, R., Durão, J., Neves, S.C., Barrias, C.C., Tamagnini, P., et al. (2016). Cyanobacterium-Derived Extracellular Carbohydrate Polymer for the Controlled Delivery of Functional Proteins. *Macromol. Biosci.* 17(2), 1600206.

Li, B., Lu, F., Wei, X., Zhao, R., Li, B., Lu, F., et al. (2008). Fucoidan: Structure and Bioactivity. *Molecules* 13(8), 1671–1695.

Li, H., Xu, J., Liu, Y., Ai, S., Qin, F., Li, Z., et al. (2011a). Antioxidant and moisture-retention activities of the polysaccharide from *Nostoc commune*. *Carbohydr. Polym.* 83(4), 1821–1827.

Li, H., Li, Z., Xiong, S., Zhang, H., Li, N., Zhou, S., et al. (2011b). Pilot-scale isolation of bioactive extracellular polymeric substances from cell-free media of mass microalgal cultures using tangential-flow ultrafiltration. *Process Biochem.* 46(5), 1104–1109.

Li, H., Su, L., Chen, S., Zhao, L., Wang, H., Ding, F., et al. (2018). Physicochemical Characterization and Functional Analysis of the Polysaccharide from the Edible Microalga *Nostoc sphaeroides*. *Molecules* 23(2), 508.

Li, P., Liu, Z., and Xu, R. (2001). Chemical characterisation of the released polysaccharide from the cyanobacterium *Aphanothece halophytica* GR02. *J. Appl. Phycol.* 13(1), 71–77.

Liu, D., and Pakrasi, H.B. (2018). Exploring native genetic elements as plug - in tools for synthetic biology in the cyanobacterium *Synechocystis* sp . PCC 6803. *Microb. Cell Fact.* 17(1), 48.

Liu, C., Sun, Y., Mao, Q., Guo, X., Li, P., Liu, Y., et al. (2016). Characteristics and Antitumor Activity of *Morchella esculenta* Polysaccharide Extracted by Pulsed Electric Field. *Int. J. Mol. Sci.* 17(6), 986.

Liu, H., and Buskey, E.J. (2000). The exopolymer secretions (EPS) layer surrounding *Aureoumbra lagunensis* cells affects growth, grazing, and behavior of protozoa. *Limnol. Oceanogr.* 45(5), 1187–1191.

Liu, K.S., Chen, J.-C., Lee, I.-T., Yang, T.-J., Chan, Y.-C., and Hwang, J.-H. (2012). Spirulina and C-phycocyanin reduce cytotoxicity and inflammation-related genes expression of microglial cells. *Nutr. Neurosci.* 15(6), 252–256.

Loke, M.F., Lui, S.Y., Ng, B.L., Gong, M., and Ho, B. (2007). Antiadhesive property of microalgal polysaccharide extract on the binding of *Helicobacter pylori* to gastric mucin. *FEMS Immunol. Med. Microbiol.* 50(2), 231–238.

Lombard, V., Golaconda Ramulu, H., Drula, E., Coutinho, P.M., and Henrissat, B. (2014). The carbohydrate-active enzymes database (CAZy) in 2013. *Nucleic Acids Res.* 42(1), 490–495.

López-Igual, R., Lechno-Yossef, S., Fan, Q., Herrero, A., Flores, E., and Wolk, C.P. (2012). A Major Facilitator Superfamily Protein, HepP, Is Involved in Formation of the Heterocyst Envelope Polysaccharide in the Cyanobacterium *Anabaena* sp. Strain PCC 7120. *J. Bacteriol.* 194(17), 4677–4687.

Low, K.E., and Howell, P.L. (2018). Gram-negative synthase-dependent exopolysaccharide biosynthetic machines. *Curr. Opin. Struct. Biol.* 53, 32–44.

Luan, G., and Lu, X. (2018). Tailoring cyanobacterial cell factory for improved industrial properties. *Biotechnol. Adv.* 36(2), 430-442.

Mader, J., Gallo, A., Schommartz, T., Handke, W., Nagel, C.-H., Günther, P., et al. (2016). Calcium spirulan derived from *Spirulina platensis* inhibits herpes simplex virus 1 attachment to human keratinocytes and protects against herpes labialis. *J. Allergy Clin. Immunol.* 137(1), 197–203.

Mager, D.M., and Thomas, A.D. (2011). Extracellular polysaccharides from cyanobacterial soil crusts: A review of their role in dryland soil processes. *J. Arid Environ.* 75(2), 91–97.

Majdoub, H., Mansour, M. Ben, Chaubet, F., Roudesli, M.S., and Maaroufi, R.M. (2009). Anticoagulant activity of a sulfated polysaccharide from the green alga *Arthrospira platensis*. *Biochim. Biophys. Acta - Gen. Subj.* 1790(10), 1377–1381.

Maréchal, E. (2018). Primary Endosymbiosis: Emergence of the Primary Chloroplast and the Chromatophore, Two Independent Events. In *Plastids* (Humana Press, New York, NY), pp. 3–16.

Markl, E., Grünbichler, H., and Lackner, M. (2018). Cyanobacteria for PHB Bioplastics Production: A Review. In *Algae* (IntechOpen), DOI: 10.5772/intechopen.81536.

Markou, G., Angelidaki, I., and Georgakakis, D. (2012). Microalgal carbohydrates: an overview of the factors influencing carbohydrates production, and of main bioconversion technologies for production of biofuels. *Appl. Microbiol. Biotechnol.* 96(3), 631–645.

Marles, R.J., Barrett, M.L., Barnes, J., Chavez, M.L., Gardiner, P., Ko, R., et al. (2011). United States Pharmacopeia Safety Evaluation of Spirulina. *Crit. Rev. Food Sci. Nutr.* 51(7), 593–604.

Miranda, H., Immerzeel, P., Gerber, L., Hörnaeus, K., Lind, S.B., Pattanaik, B., et al. (2017). Sll1783, a monooxygenase associated with polysaccharide processing in the unicellular cyanobacterium *Synechocystis* PCC 6803. *Physiol. Plant.* 161(2), 182–195.

Mishima, T., Murata, J., Toyoshima, M., Fujii, H., Nakajima, M., Hayashi, T., et al. (1998). Inhibition of tumor invasion and metastasis by calciumspirulan (Ca-SP), a novel sulfated polysaccharide derived from a blue-green alga, *Spirulina platensis*. *Clin. Exp. Metastasis* 16(6), 541–550.

Moreno, J., Vargas, M.A., Olivares, H., Rivas, J., and Guerrero, M.G. (1998). Exopolysaccharide production by the cyanobacterium *Anabaena* sp. ATCC 33047 in batch and continuous culture. *J. Biotechnol.* 60(3), 175–182.

Morsy, F.M., Nafady, N.A., Abd-Alla, M.H., and Elhady, D.A. (2014). Green Synthesis of Silver Nanoparticles by Water Soluble Fraction of the Extracellular Polysaccharides/Matrix of the Cyanobacterium *Nostoc Commune* and its Application as a Potent Fungal Surface Sterilizing Agent of Seed Crops. *Univers. J. Microbiol. Res.* 2(2), 36–43.

Moscovici, M. (2015). Present and future medical applications of microbial exopolysaccharides. *Front. Microbiol.* 6, 1012.

Mota, R., Guimarães, R., Büttel, Z., Rossi, F., Colica, G., Silva, C.J., et al. (2013). Production and characterization of extracellular carbohydrate polymer from from *Cyanothece* sp. CCY 0110. *Carbohydr. Polym.* 92(2), 1408–1415.

Muro-Pastor, A.M., and Hess, W.R. (2012). Heterocyst differentiation: from single mutants to global approaches. *Trends Microbiol.* 20(11), 548–557.

Najdenski, H.M., Gigova, L.G., Iliev, I.I., Pilarski, P.S., Lukavský, J., Tsvetkova, I. V., et al. (2013). Antibacterial and antifungal activities of selected microalgae and cyanobacteria. *Int. J. Food Sci. Technol.* 48(7), 1533–1540.

Nauts, H.C., Swift, W.E., and Coley, B.L. (1946). The treatment of malignant tumors by bacterial toxins as developed by the late William B. Coley, MD, reviewed in the light of modern research. *Cancer Res.* 6(4), 205-216

Nicolaus, B., Panico, A., Lama, L., Romano, I., Manca, M.C., De Giulio, A., et al. (1999). Chemical composition and production of exopolysaccharides from representative members of heterocystous and non-heterocystous cyanobacteria. *Phytochemistry* 52(4), 639–647.

Nobles, D.R., Romanovicz, D.K., and Brown, R.M. (2001). Cellulose in cyanobacteria. Origin of vascular plant cellulose synthase? *Plant Physiol.* 127(2), 529–542.

Oba, K., Kobayashi, M., Matsui, T., Kodera, Y., and Sakamoto, J. (2009). Individual patient based meta-analysis of lentinan for unresectable/recurrent gastric cancer. *Anticancer Res.* 29(7), 2739–2745.

Ochoa de Alda, J.A.G., Esteban, R., Diago, M.L., and Houmard, J. (2014). The plastid ancestor originated among one of the major cyanobacterial lineages. *Nat. Commun.* 5(1), 4937.

Okajima-kaneko, M., Ono, M., and Kabata, K. Extraction of novel sulfated polysaccharides from *Aphanothece sacrum* (Sur.) Okada, and its spectroscopic characterization. *Pure Appl. Chem.* 79(11), 2039-2046.

Okajima, M.K., Sornkamnerd, S., and Kaneko, T. (2018). Development of Functional Bionanocomposites Using Cyanobacterial Polysaccharides. *Chem. Rec.* 18(7–8), 1167–1177.

Otero, A., and Vincenzini, M. (2003). Extracellular polysaccharide synthesis by *Nostoc* strains as affected by N source and light intensity. *J. Biotechnol.* 102(2), 143–152.

Otero, A., and Vincenzini, M. (2004). *Nostoc* (Cyanophyceae) Goes Nude: Extracellular Polysaccharides Serve As A Sink For Reducing Power Under Unbalanced C/N Metabolism. *J. Phycol.* 40(1), 74–81.

Ou, Y., Xu, S., Zhu, D., and Yang, X. (2014). Molecular Mechanisms of Exopolysaccharide from *Aphanothece halaphytica* (EPSAH) Induced Apoptosis in HeLa Cells. *PLoS One* 9(1), e87223.

Ozturk, S., and Aslim, B. (2010). Modification of exopolysaccharide composition and production by three cyanobacterial isolates under salt stress. *Environ. Sci. Pollut. Res.* 17(3), 595–602.

Paiment, A., Hocking, J., and Whitfield, C. (2002). Impact of phosphorylation of specific residues in the tyrosine autokinase, Wzc, on its activity in assembly of group 1 capsules in *Escherichia coli*. *J. Bacteriol.* 184(23), 6437–6447.

Panoff, J.M., Priem, B., Morvan, H., and Joset, F. (1988). Sulphated exopolysaccharides produced by two unicellular strains of cyanobacteria, *Synechocystis* PCC 6803 and 6714. *Arch. Microbiol.* 150(6), 558–563.

Parages, M.L., Rico, R.M., Abdala-Díaz, R.T., Chabrillón, M., Sotiroudis, T.G., and Jiménez, C. (2012). Acidic polysaccharides of *Arthrospira* (*Spirulina*) *platensis* induce the synthesis of TNF-α in RAW macrophages. *J. Appl. Phycol.* 24(6), 1537–1546.

Parwani, L., Bhatnagar, M., Bhatnagar, A., and Sharma, V. (2014). Antioxidant and iron-chelating activities of cyanobacterial exopolymers with potential for wound healing. *J. Appl. Phycol.* 26(3), 1473–1482.

Pasteur, L. (1861). On the viscous fermentation and the butyrous fermentation. *Bull. Soc. Chim. Paris* 11, 30–31.

Pauli, C., Hopkins, B.D., Prandi, D., Shaw, R., Fedrizzi, T., Sboner, A., et al. (2017). Personalized *In Vitro* and *In Vivo* Cancer Models to Guide Precision Medicine. *Cancer Discov.* 7(5), 462–477.

Pavlova, N.N., and Thompson, C.B. (2016). The Emerging Hallmarks of Cancer Metabolism. *Cell Metab.* 23(1), 27–47.

Pereira, S., Zille, A., Micheletti, E., Moradas-Ferreira, P., De Philippis, R., and Tamagnini, P. (2009). Complexity of cyanobacterial exopolysaccharides: composition, structures, inducing factors and putative genes involved in their biosynthesis and assembly. *FEMS Microbiol. Rev.* 33(5), 917–941.

Pereira, S.B., Mota, R., Santos, C.L., De Philippis, R., and Tamagnini, P. (2013). Assembly and export of extracellular polymeric substances (EPS) in cyanobacteria: a phylogenomic approach. In *Advances in Botanical Research* (Academic Press), pp. 235-279.

Pereira, S.B., Mota, R., Vieira, C.P., Vieira, J., and Tamagnini, P. (2015). Phylum-wide analysis of genes/proteins related to the last steps of assembly and export of extracellular polymeric substances (EPS) in cyanobacteria. *Sci. Rep.* 5, 14835.

Phélippé, M., Gonçalves, O., Thouand, G., Cogne, G., and Laroche, C. (2019). Characterization of the polysaccharides chemical diversity of the cyanobacteria *Arthrospira platensis*. *Algal Res.* 38, 101426.

De Philippis, R., and Vincenzini, M. (1998). Exocellular polysaccharides from cyanobacteria and their possible applications. *FEMS Microbiol. Rev.* 22(3), 151–175.

De Philippis, R., Margheri, M.C., Pelosi, E., and Ventura, S. (1993). Exopolysaccharide production by a unicellular cyanobacterium isolated from a hypersaline habitat. *J. Appl. Phycol.* 5(4), 387–394.

De Philippis, R., Sili, C., and Vincenzini, M. (1996). Response of an exopolysaccharide-producing heterocystous cyanobacterium to changes in metabolic carbon flux. *J. Appl. Phycol.* 8(4–5), 275–281.

De Philippis, R., Margheri, M.C., Materassi, R., and Vincenzini, M. (1998). Potential of unicellular

cyanobacteria from saline environments as exopolysaccharide producers. *Appl. Environ. Microbiol.* 64(3), 1130–1132.

De Philippis, R., Ena, A., Paperi, R., Sili, C., and Vincenzini, M. (2000). Assessment of the potential of Nostoc strains from the Pasteur Culture Collection for the production of polysaccharides of applied interest. *J. Appl. Phycol.* 12(3/5), 401–407.

Di Pippo, F., Ellwood, N.T.W., Guzzon, A., Siliato, L., Micheletti, E., De Philippis, R., et al. (2012). Effect of light and temperature on biomass, photosynthesis and capsular polysaccharides in cultured phototrophic biofilms. *J. Appl. Phycol.* 24(2), 211–220.

Ponce-Toledo, R.I., Deschamps, P., López-García, P., Zivanovic, Y., Benzerara, K., and Moreira, D. (2017). An Early-Branching Freshwater Cyanobacterium at the Origin of Plastids. *Curr. Biol.* 27(3), 386–391.

Pugh, N., Ross, S., ElSohly, H., ElSohly, M., and Pasco, D. (2001). Isolation of Three High Molecular Weight Polysaccharide Preparations with Potent Immunostimulatory Activity from *Spirulina platensis* , *Aphanizomenon flos-aquae* and *Chlorella pyrenoidosa*. *Planta Med.* 67(08), 737–742.

Radonić, A., Thulke, S., Achenbach, J., and Kurth, A. (2011). Anionic polysaccharides from phototrophic microorganisms exhibit antiviral activities to Vaccinia virus. *J. Antivir. Antiretrovir.* 2, 051-055.

Rachid, S., Ohlsen, K., Wallner, U., Hacker, J., Hecker, M., and Ziebuhr, W. (2000). Alternative Transcription Factor δ^B is Involved in Regulation of Biofilm Expression in a *Staphylococcus aureus* Mucosal Isolate. *J. Bacteriol.* 182(23), 6824-6826.

Raposo, M., de Morais, R., Bernardo de Morais, A., Raposo, M.F. de J., De Morais, R.M.S.C., and Bernardo de Morais, A.M.M. (2013). Bioactivity and Applications of Sulphated Polysaccharides from Marine Microalgae. *Mar. Drugs* 11(12), 233–252.

Raven, J.A., Giordano, M., Beardall, J., and Maberly, S.C. (2012). Algal evolution in relation to atmospheric CO_2: carboxylases, carbon-concentrating mechanisms and carbon oxidation cycles. *Philos. Trans. R. Soc. B Biol. Sci.* 367(1588), 493–507.

Rehm, B.H.A. (2010). Bacterial polymers: Biosynthesis, modifications and applications. *Nat. Rev. Microbiol.* 8(8), 578–592.

Rehm, B.H.A. (2015). Synthetic biology towards the synthesis of custom-made polysaccharides. *Microb. Biotechnol.* 8(1), 19–20.

Reichert, M., Bergmann, S.M., Hwang, J., Buchholz, R., and Lindenberger, C. (2017). Antiviral activity of exopolysaccharides from *Arthrospira platensis* against koi herpesvirus. *J. Fish Dis.* 40(10), 1441–1450.

Rejdych, G., Chancelier, T., and Pasquet, T. (2014). Observation of operational disc brake system damping and measurement of brake squeal instability index in time and frequency-domains before and during squeal onset. *Preslia* 86(4), 295–335.

Riccardi, C., and Nicoletti, I. (2006). Analysis of apoptosis by propidium iodide staining and flow cytometry. *Nat. Protoc.* 1(3), 1458–1461.

Rippka, E., Deruelles, J., and Waterbury, N.B. (1979). Generic Assignments, Strain Histories and Properties of Pure Cultures of Cyanobacteria. *Microbiology* 111(1), 1-61.

Ristl, R., Steiner, K., Zarschler, K., Zayni, S., Messner, P., and Schäffer, C. (2011). The S-layer glycome-adding to the sugar coat of bacteria. *Int. J. Microbiol.* 2011, 127870.

Robyt, J.F., Yoon, S.-H., and Mukerjea, R. (2008). Dextransucrase and the mechanism for dextran biosynthesis. *Carbohydr. Res.* 343(18), 3039–3048.

Roca, C., Alves, V.D., Freitas, F., and Reis, M.A.M. (2015). Exopolysaccharides enriched in rare sugars: bacterial sources, production, and applications. *Front. Microbiol.* 6, 288.

Rodriguez, S., Torres, F.G., and López, D. (2017). Preparation and characterization of polysaccharide films from the cyanobacteria *Nostoc commune*. *Polym. from Renew. Resour.* 8(4), 133–150.

Rossi, F., and De Philippis, R. (2015). Role of Cyanobacterial Exopolysaccharides in Phototrophic Biofilms and in Complex Microbial Mats. *Life* 5(2), 1218–1238.

Rossi, F., and De Philippis, R. (2016). Exocellular Polysaccharides in Microalgae and Cyanobacteria: Chemical Features, Role and Enzymes and Genes Involved in Their Biosynthesis. In *The Physiology of Microalgae* (Cham: Springer International Publishing), pp. 565–590.

Ruiz-Ruiz, C., Srivastava, G.K., Carranza, D., Mata, J.A., Llamas, I., Santamaría, M., et al. (2011). An exopolysaccharide produced by the novel halophilic bacterium *Halomonas stenophila* strain B100 selectively induces apoptosis in human T leukaemia cells. *Appl. Microbiol. Biotechnol.* 89(2), 345–355.

Rütering, M., Schmid, J., Rühmann, B., Schilling, M., and Sieber, V. (2016). Controlled production of

polysaccharides-exploiting nutrient supply for levan and heteropolysaccharide formation in *Paenibacillus* sp. *Carbohydr. Polym.* 148, 326–334.
Sánchez-Baracaldo, P. (2015). Origin of marine planktonic cyanobacteria. *Sci. Rep. 5, 17418.*
Savage, D.F., Afonso, B., Chen, A.H., and Silver, P.A. (2010). Spatially ordered dynamics of the bacterial carbon fixation machinery. *Science* 327(5970), 1258–1261.
Schmid, J. (2018). Recent insights in microbial exopolysaccharide biosynthesis and engineering strategies. *Curr. Opin. Biotechnol.* 53, 130–136.
Schmid, J., Sieber, V., and Rehm, B. (2015). Bacterial exopolysaccharides: biosynthesis pathways and engineering strategies. *Front. Microbiol.* 6, 496.
Schopf, J.W. (2000). The Fossil Record: Tracing the Roots of the Cyanobacterial Lineage. In *The Ecology of Cyanobacteria* (Dordrecht: Kluwer Academic Publishers), pp. 13–35.
Schwab, C., Walter, J., Tannock, G.W., Vogel, R.F., and Gänzle, M.G. (2007). Sucrose utilization and impact of sucrose on glycosyltransferase expression in *Lactobacillus reuteri*. *Syst. Appl. Microbiol.* 30(6), 433–443.
Sekar, S., and Paulraj, P. (2007). Strategic mining of cyanobacterial patents from the USPTO patent database and analysis of their scope and implications. *J. Appl. Phycol.* 19(3), 277–292.
Shah, V., Garg, N., and Madamwar, D. (1999). Exopolysaccharide Production by a Marine Cyanobacterium *Cyanothece* sp.: Application in Dye Removal by Its Gelation Phenomenon. *Appl. Biochem. Biotechnol.* 82(2), 81–90.
Shah, V., Ray, A., Garg, N., and Madamwar, D. (2000). Characterization of the Extracellular Polysaccharide Produced by a Marine Cyanobacterium, *Cyanothece* sp. ATCC 51142, and Its Exploitation Toward Metal Removal from Solutions. *Curr. Microbiol.* 40(4), 274–278.
Shi, J.-Q., Wu, Z.-X., and Song, L.-R. (2013). Physiological and molecular responses to calcium supplementation in *Microcystis aeruginosa* (Cyanobacteria). *New Zeal. J. Mar. Freshw. Res.* 47(1), 51–61.
Simkovsky, R., Daniels, E.F., Tang, K., Huynh, S.C., Golden, S.S., and Brahamsha, B. (2012). Impairment of O-antigen production confers resistance to grazing in a model amoeba – cyanobacterium predator – prey system. *Proc. Natl. Acad. Sci. U. S. A.* 109(41), 16678-16683.
Singh, S., and Das, S. (2011). Screening, production, optimization and characterization of cyanobacterial polysaccharide. *World J. Microbiol. Biotechnol.* 27(9), 1971–1980.
Singh, S., Kant, C., Yadav, R.K., Reddy, Y.P., and Abraham, G. (2019). Cyanobacterial Exopolysaccharides: Composition, Biosynthesis, and Biotechnological Applications. In *Cyanobacteria* (Academic Press.), pp. 347-358.
Soo, R.M., Hemp, J., Parks, D.H., Fischer, W.W., and Hugenholtz, P. (2017). On the origins of oxygenic photosynthesis and aerobic respiration in Cyanobacteria. *Science* 355(6332), 1436–1440.
Su, C., Chi, Z., and Lu, W. (2007). Optimization of medium and cultivation conditions for enhanced exopolysaccharide yield by marine *Cyanothece* sp. 113. *Chinese J. Oceanol. Limnol.* 25(4), 411–417.
Su, J., Jia, S., Chen, X., and Yu, H. (2008). Morphology, cell growth, and polysaccharide production of Nostoc flagelliforme in liquid suspension culture at different agitation rates. *J. Appl. Phycol.* 20(3), 213–217.
Sznarkowska, A., Kostecka, A., Meller, K., and Bielawski, K.P. (2017). Inhibition of cancer antioxidant defense by natural compounds. *Oncotarget* 8(9), 15996–16016.
Tian, F., Karboune, S., and Hill, A. (2014). Synthesis of fructooligosaccharides and oligolevans by the combined use of levansucrase and endo-inulinase in one-step bi-enzymatic system. *Innov. Food Sci. Emerg. Technol.* 22, 230–238.
Tiwari, O.N., Khangembam, R., Shamjetshabam, M., Sharma, A.S., Oinam, G., and Brand, J.J. (2015). Characterization and Optimization of Bioflocculant Exopolysaccharide Production by Cyanobacteria *Nostoc* sp. BTA97 and *Anabaena* sp. BTA990 in Culture Conditions. *Appl. Biochem. Biotechnol.* 176(7), 1950–1963.
Tomitani, A., Knoll, A.H., Cavanaugh, C.M., and Ohno, T. (2006). The evolutionary diversification of cyanobacteria: Molecular-phylogenetic and paleontological perspectives. *Proc. Natl. Acad. Sci. U. S. A.* 103(14), 5442-5447.
Trabelsi, L., Ben Ouada, H., Bacha, H., and Ghoul, M. (2009). Combined effect of temperature and light intensity on growth and extracellular polymeric substance production by the cyanobacterium *Arthrospira platensis*. *J. Appl. Phycol.* 21(4), 405–412.
Tran, T.H., Choi, J.Y., Ramasamy, T., Truong, D.H., Nguyen, C.N., Choi, H.-G., et al. (2014). Hyaluronic acid-coated solid lipid nanoparticles for targeted delivery of vorinostat to CD44

overexpressing cancer cells. *Carbohydr. Polym.* 114, 407–415.
Ursell, T., Chau, R.M.W., Wisen, S., Bhaya, D., and Huang, K.C. (2013). Motility Enhancement through Surface Modification Is Sufficient for Cyanobacterial Community Organization during Phototaxis. *PLoS Comput. Biol.* 9(9), e1003205.
Vandamme, T., Lenourry, A., Charrueau, C., and Chaumeil, J.-C. (2002). The use of polysaccharides to target drugs to the colon. *Carbohydr. Polym.* 48(3), 219–231.
Volk, R.-B., Venzke, K., and Blaschek, W. (2007). Structural investigation of a polysaccharide released by the cyanobacterium *Nostoc insulare*. *J. Appl. Phycol.* 19(3), 255–262.
Vujicic-Zagar, A., Pijning, T., Kralj, S., López, C.A., Eeuwema, W., Dijkhuizen, L., et al. (2010). Crystal structure of a 117 kDa glucansucrase fragment provides insight into evolution and product specificity of GH70 enzymes. *Proc. Natl. Acad. Sci. U. S. A.* 107(50), 21406–21411.
Wallner, U., Ziebuhr, W., Hacker, J., Hecker, M., Ohlsen, K., and Rachid, S. (2002). Alternative Transcription Factor sigma B Is Involved in Regulation of Biofilm Expression in a *Staphylococcus aureus* Mucosal Isolate. *J. Bacteriol.* 182(23), 6824–6826.
Wang, H. Bin, Wu, S.J., and Liu, D. (2014). Preparation of polysaccharides from cyanobacteria *Nostoc commune* and their antioxidant activities. *Carbohydr. Polym.* 99, 553–555.
Wang, X., Chen, Y., Wang, J., Liu, Z., and Zhao, S. (2014). Antitumor activity of a sulfated polysaccharide from *Enteromorpha intestinalis* targeted against hepatoma through mitochondrial pathway. *Tumor Biol.* 35(2), 1641–1647.
Wang, X., and Zhao, Y. (2017). Molecular Actions of Marine Bioactive Compound Fucoidan. In *2nd International Conference on Biomedical and Biological Engineering 2017 (BBE 2017)* (Atlantis Press).
Whitfield, C., and Larue, K. (2008). Stop and go: regulation of chain length in the biosynthesis of bacterial polysaccharides. *Nat. Struct. Mol. Biol.* 15(2), 121–124.
Whitfield, C., and Trent, M.S. (2014). Biosynthesis and Export of Bacterial Lipopolysaccharides. *Annu. Rev. Biochem.* 83(1), 99–128.
Whitfield, G.B., Marmont, L.S., and Howell, P.L. (2015). Enzymatic modifications of exopolysaccharides enhance bacterial persistence. *Front. Microbiol.* 6, 471.
Whitney, J.C., and Howell, P.L. (2013). Synthase-dependent exopolysaccharide secretion in Gram-negative bacteria. *Trends Microbiol.* 21(2), 63–72.
Whitton, B.A. (2012). Ecology of cyanobacteria II : their diversity in space and time. (Springer Science & Business Media).
Wijesekara, I., Pangestuti, R., and Kim, S.-K. (2011). Biological activities and potential health benefits of sulfated polysaccharides derived from marine algae. *Carbohydr. Polym.* 84(1), 14–21.
Willis, L.M., and Whitfield, C. (2013). KpsC and KpsS are retaining 3-deoxy-D-manno-oct-2-ulosonic acid (Kdo) transferases involved in synthesis of bacterial capsules. *Proc. Natl. Acad. Sci. U. S. A.* 110(51), 20753–20758.
Xu, L., and Zhang, J. (2016). Bacterial glucans: production, properties, and applications. *Appl. Microbiol. Biotechnol.* 100(21), 9023–9036.
Yamamoto, C., Nakamura, A., Shimada, S., Kaji, T., Lee, J.B., and Hayashi, T. (2003). Differential effects of sodium spirulan on the secretion of fibrinolytic proteins from vascular endothelial cells: enhancement of plasminogen activator activity. *J. Health Sci. 49*(5), 405-409.
Yang, P., Liang, M., Zhang, Y., and Shen, B. (2008). Clinical application of a combination therapy of lentinan, multi-electrode RFA and TACE in HCC. *Adv. Ther.* 25(8), 787–794.
Yoo, S.H., Keppel, C., Spalding, M., and Jane, J. lin (2007). Effects of growth condition on the structure of glycogen produced in cyanobacterium *Synechocystis* sp. PCC6803. *Int. J. Biol. Macromol.* 40(5), 498–504.
Yoshimura, H., Okamoto, S., Tsumuraya, Y., and Ohmori, M. (2007). Group 3 sigma factor gene, sigJ, a key regulator of desiccation tolerance, regulates the synthesis of extracellular polysaccharide in cyanobacterium *Anabaena* sp. strain PCC 7120. *DNA Res.* 14(1), 13–24.
Yoshimura, H., Kotake, T., Aohara, T., Tsumuraya, Y., Ikeuchi, M., and Ohmori, M. (2012). The role of extracellular polysaccharides produced by the terrestrial cyanobacterium *Nostoc* sp. strain HK-01 in NaCl tolerance. *J. Appl. Phycol.* 24(2), 237–243.
Yu, H. (2012). Effect of mixed carbon substrate on exopolysaccharide production of cyanobacterium *Nostoc flagelliforme* in mixotrophic cultures. *J. Appl. Phycol.* 24(4), 669–673.
Yu, Y., You, L., Liu, D., Hollinshead, W., Tang, Y.J., and Zhang, F. (2013). Development of *Synechocystis* sp. PCC 6803 as a Phototrophic Cell Factory. *Mar. Drugs* 11(8), 2894–2916.
Yue, S.J., Jia, S.R., Yao, J., and Dai, Y.J. (2011). Nutritional Analysis of the Wild and Liquid Suspension Cultured *Nostoc flagelliforme* and Antitumor Effects of the Extracellular

Polysaccharides. *Adv. Mater. Res.* 345, 177–182.
Zhao, K., Liu, M., and Burgess, R.R. (2007). Adaptation in bacterial flagellar and motility systems: From regulon members to 'foraging'-like behavior in *E. coli. Nucleic Acids Res.* 35(13), 4441–4452.
Zheng, W., Chen, C., and Cheng, Q. (1994). Antitumor activity of exopolysaccharide from *Aphanothece halophytica*. *Chin. Tradit. Herbal Drugs* 36, 1026-1030.
Zong, A., Cao, H., and Wang, F. (2012). Anticancer polysaccharides from natural resources: A review of recent research. *Carbohydr. Polym.* 90(4), 1395–1410.

8. Supplementary Material

Table S1. Cyanobacterial EPS with antitumor activity.

Strain	Polymer	EPS relevant features	Tests	Cell lines	Antitumor activity	Ref.
Arthrospira platensis (*Spirulina*)	Calcium-spirulan (EPS)	• rhamnose and fructose are predominant sugars • 2 uronic acids (gluco and galacturonic). Other sugars: glucose, galactose, mannose, xylose, ribose. • sulfate (3.24% w/w). • 12.2% inorganic substance. • MW: ≈$3x10^5$ kDa. • calcium-chelating properties.	Invasion assays (Matrigel, laminin- or fibronectin-coated filters); Haptotactic migration assay; Heparanase assay; Collagenase IV secretion and activity (gel zymography); Assay of spontaneous lung tumor metastasis (co-injection or tumor inoculation + intravenous EPS administration); Growth measurement ($OD_{450\ nm}$)	metastatic mouse B16-BL6 melanoma and Colon 26 carcinoma, HT-1080 human fibrosarcoma *in vivo* metastasis assays with inbred 7-10-week-old female C57BL/6 mice	• anti-invasion of all cell lines (CDM). • anti haptotatic migration of B16-BL6 and Colon 26 to laminin (CDM). • antiadhesion of B16-BL6 to laminin and Matrigel (CDM). • inhibition of B16-BL6 hepanarase activity (CDM). • anti sponateous metastatic of B16-BL6 *in vivo* (CDM) (reduction of tumor colonies in lungs).	Mishima et al., 1998
			Cytotoxicity assay (MTT based); assessment of tumor growth (*in vivo* inoculation sarcoma cells + EPS)	mice sarcoma Smcc7721 and HeLa. *in vivo* test in ICR mice	• inhibition of tumor growth *in vivo*. • antiproliferative on all cell lines. (immunostimulatory activity)	Zheng et al., 1994
Aphanothece halophytica	EPSAH (EPS)	• carbonyl and hydroxyl groups. • aliphatic chains. • xanthan-like physical properties.	Cell viability assay (MTT based and Wright-Giemsa staining); DNA fragmentation assay (gel electrophoresis); Apoptosis assessment (AO/EB fluorescence); Mitochondrial transmembrane potential measurements (rhodamine 123 staining and flow cytometry); Western blot analysis of (pro)apoptotic protein levels	human cervical cancer HeLa	• antiproliferative (CDM and TDM). • Induction of nuclear and DNA fragmentation, chromatin condensation and/or margination (CDM). • reduction of mitochondrial transmembrane potential (CDM). • Pro-apoptotic (CDM): high levels of CHOP/GADD153, p53, cleaved caspase-3 and Bax; low levels of Bcl-2, Grp78/BiP and survivin.	Ou et al., 2014
Mastigocladus laminosus	CPS	• uronic acids (30% w/w). • neutral sugars (60% w/w). • proteins (10% w/w). • sugars: rhamnose, fucose, xylose, mannose, glucose, galactose, glucuronic and galacturonic acids. • sulfate (5% w/w). • highly ramified structure, with a minimal repeating unit of 15 monosaccharides.	Cell viability assay (MTT based); Cell migration (Boyden chamber) and invasion assays (Matrigel); Cell MMP gelatinase expression and activity (zymography)	human squamous vulvar epidermoid carcinoma A431	• antiproliferative (CDM). • anti migration. • anti-invasion. • Reduction of MMP expression and activity. • HCl hydrolyzed CPS have lower antiproliferative, anti-invasion and anti migration activities, no changes in MMP expression/activity. (anti-inflammatory activity)	Gloaguen et al., 2007

Nostoc flagelliforme	Nostoflan (EPS)	• two different EPS fractions • sugars: glucose, xylose, galactose and mannose. • one fraction has MW ≈2.6x10^5 kDa and carboxyl groups (no sulfate, nucleic acids or proteins).	Cell viability assay (MTT based)	human cervical cancer HeLa	• antiproliferative (CDM).	Yue et al., 2011
Nostoc sphaeroides	Nostoglycan (EPS)	• mannose is predominant. • 1 uronic acid (galacturonic). • other sugars: fructose, galactose, glucose, xylose, rhamnose. • hydroxyl and carboxyl groups. • amorphous nature with flaky morphology. • MW: ≈ 2 x 10^3 kDa. • strong moisture absorption and retention capacity. • high viscosity.	Cytotoxicity assay (MTT based)	human gastric carcinoma BGC-823, acute lymphoblastic MOLT-4, promyelocytic HL60 and K562 erythromyeloblastoid	• antiproliferative on all cell lines (CDM).	Li et al., 2011b
			Cell viability assay (MTT based); Apoptosis assessment (flow cytometry with Annexin V/PI staining); Caspase-3 activity (colorimetric assay)	human carcinomas: prostate PC3, lung A549, hepatocellular HepG2, breast MCF-7, promyelocytic leukemia HL-60, and leukemic T Jurkat	• antiproliferative on A549, HepG2, PC3, MCF-7, and Jurkat. • Induction of apoptosis in A549. • Stimulation of caspase-3 activity in A549. (antioxidant activity)	Li et al., 2018
Gloeocapsa sp.	EPS	• polymer aspect differs in SDS-PAGE, according to different cultivation conditions. • protein content varying from 1.9 to 29.5% (proteins with protease activity). • three different EPS fractions.	Cell viability assay (MTT based)	human cervical cancer HeLa	• antiproliferative (CDM), dependent on temperature and light cultivation conditions (were tested different polymers, extracted from cultures grown at different temperatures). (antibacterial and antifungal activity)	Gacheva et al., 2013

Legend: CDM, concentration-dependent manner; TDM, time-dependent manner; MW, molecular weight; MTT, 3-(4,5-dimethylthiazol-2-yl)-2,5-diphenyl tetrazolium bromide; PI, propidium iodide; AO/E, acridine orange/ethidium bromide; MMP, metalloproteases.